



DET NORSKE VERITAS

Final Report
for
**UNITED STATES DEPARTMENT
OF THE INTERIOR**
BUREAU OF OCEAN ENERGY MANAGEMENT,
REGULATION, AND ENFORCEMENT
WASHINGTON, DC 20240
**FORENSIC EXAMINATION OF DEEPWATER
HORIZON BLOWOUT PREVENTER**
CONTRACT AWARD No. M10PX00335

VOLUME I FINAL REPORT

Report No. EP030842
20 March 2011

**Exhibit No.
8855**

**Worldwide Court
Reporters, Inc.**

The view, opinions, and/or findings contained in this report are those of the author(s) and should not be construed as an official government position, policy or decision, unless so designated by other documentation.

DET NORSKE VERITAS

United States Department of the Interior, Bureau of Ocean Energy
Management, Regulation, and Enforcement
Forensic Examination of Deepwater Horizon Blowout Preventer
Volume I Main Report

**MANAGING RISK**

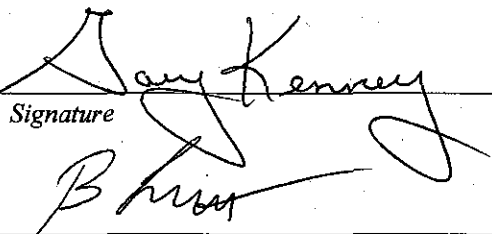
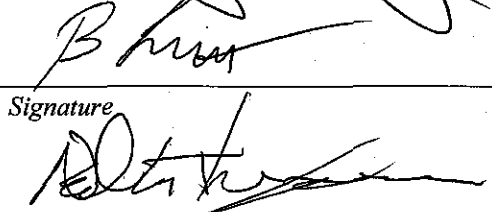
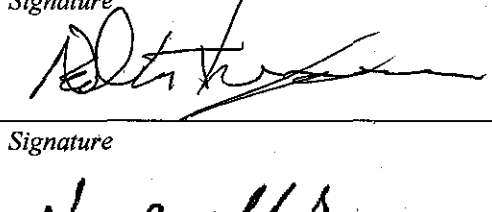
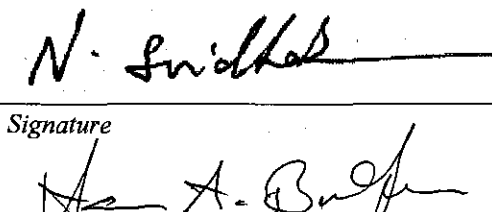
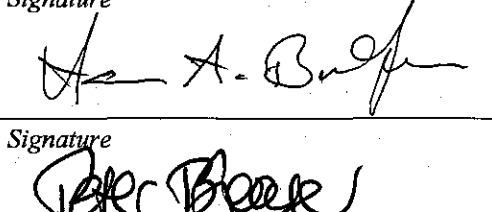
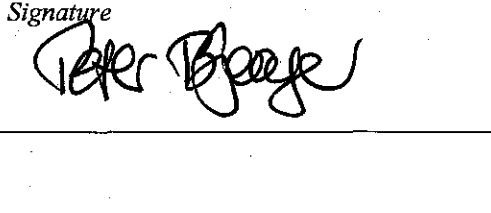
Forensic Examination of Deepwater Horizon
Blowout Preventer

For:

United States Department of the Interior
Bureau of Ocean Energy Management, Regulation,
and Enforcement
Washington, DC 20240

DET NORSKE VERITAS (U.S.A.), INC.
Materials & Corrosion Technology Center
5777 Frantz Road
Dublin, OH 43017-1386
United States
Tel: (614) 761-1214
Fax: (614) 761-1633
<http://www.dnv.com>
<http://www.dnvcolumbus.com>

Account Ref.: Award: M10PX00335

Date of Issue: 20 March 2011	Project No: EP030842
Prepared by: Gary D. Kenney, Ph.D. Lead Investigator	Signature 
Prepared by: Bryce A. Levett Principal Investigator	Signature 
Prepared by: Neil G. Thompson, Ph.D. Project Manager	Signature 
Verified by: Narasi Sridhar, Ph.D. Project Sponsor	Signature 
Verified by: Hans Axel Bratfos Director of Technology, Services and Quality	Signature 
Approved by: Peter Bjerager, Ph.D. Senior Vice President	Signature 

No distribution without permission

© 2011 Det Norske Veritas (U.S.A.), Inc.

All rights reserved. This publication or parts thereof may not be reproduced or transmitted in any form or by any means, including photocopying or recording, without the prior written consent of Det Norske Veritas (U.S.A.), Inc.

TABLE OF CONTENTS – VOLUME I

1 EXECUTIVE SUMMARY.....	1
1.1 The Equipment.....	1
1.2 The Accident.....	2
1.3 Forensic Tests	3
1.4 What is Considered to Have Happened	4
1.5 Primary Cause and Contributing Causes	5
1.6 Recommendations for Industry.....	5
1.6.1 Study of Elastic Buckling.....	6
1.6.2 Study of the Shear Blade Surfaces of Shear Rams.....	6
1.6.3 Study of Well Control Procedures or Practices	6
1.6.4 Status of the Back-Up Control Systems	7
1.6.5 Common Mode Failure of Back-Up Control Systems	7
1.6.6 Study the Indication of Functions in an Emergency.....	7
1.6.7 Study of the Effectiveness of Remotely Operated Vehicle Interventions	7
1.6.8 Stipulating Requirements for Back-Up Control System Performance	8
1.7 Recommendations for Further Testing	8
1.7.1 Additional Studies of Conditions Leading to Elastic Buckling.....	8
1.7.2 Additional Tests or Studies of the Performance of the Blowout Preventer Stack....	9
2 INTRODUCTION.....	10
3 BACKGROUND	14
4 OBJECTIVES AND SCOPE	18
5 METHODOLOGY.....	20
5.1 Evidence Collection and Control.....	20
5.2 Technical Working Group	20
5.3 Investigative Process.....	20
5.4 Forensic Testing Plan and Protocol Development.....	21
5.5 Site Preparation.....	21
5.6 Blowout Preventer Functionality	22
5.7 Materials Evaluation and Damage Assessment	23

5.8 Document Review.....	24
5.9 Remotely Operated Vehicle Intervention Operations Review.....	24
5.10 Failure Cause Analysis	25
6 FINDINGS	26
6.1 Blowout Preventer Function Testing	26
6.1.1 Video and Photographic Documentation.....	26
6.1.2 Visual Examination	26
6.1.3 Fluid Collection and Analysis	27
6.1.4 Drill Pipe Removal	28
6.1.5 ST Locks.....	30
6.1.6 Lower Choke and Kill Valves	31
6.1.7 Functioning and Removal of Ram Blocks.....	32
6.1.8 AMF/Deadman and Autoshear Testing – Hydraulic Circuits	34
6.1.9 Remotely Operated Vehicle Panel Testing.....	40
6.1.10 Solenoid 103 Bench Testing.....	41
6.1.11 Solenoid 3A Bench Testing.....	42
6.1.12 Blue and Yellow Pod Battery Voltage and Load Testing	42
6.1.13 Blue and Yellow Pod Function Testing.....	43
6.2 Materials Evaluation and Damage Assessment	50
6.2.2 Three Dimensional Laser Scanning of Ram Blocks.....	73
6.2.3 Visual Examination of Drill Pipe	78
6.2.4 Matching Drill Pipe Segments.....	93
6.2.5 Damage on Drill Pipe Segment in Variable Bore Rams	107
6.2.6 Damage to the Wellbore.....	108
6.2.7 Other Evidence Assessment	110
6.2.8 Metallurgical, Mechanical, Chemical Property Assessment	112
6.3 Document Review.....	131
6.4 Remotely Operated Vehicle Intervention Efforts	136
6.4.1 Activation of the Blind Shear Rams	137
6.4.2 Repair Efforts	144
6.5 Modeling	147

6.5.1 Buckling Model	148
6.5.2 Buckling Considerations	151
6.5.3 Cutting of the Drill Pipe in the Blind Shear Ram.....	152
6.6 Failure Cause Analysis	164
6.6.1 Manual Function Blind Shear Ram Close and High Pressure Shear Close.....	165
6.6.2 Manual Function of Emergency Disconnect Sequence	165
6.6.3 Automated Mode Function/Deadman	166
6.6.4 Autoshear.....	167
6.6.5 Manual Function via Remotely Operated Vehicle	167
6.6.6 Recovered Drill Pipe Segments.....	168
6.6.7 Other Considerations.....	169
7 CONCLUSIONS	171
7.1 The Accident.....	171
7.2 What is Considered to have Happened	171
7.3 Discussion of Causes	172
7.3.1 Primary Cause	172
7.3.2 Contributing Cause.....	173
7.3.3 Contributing Cause.....	173
7.3.4 Contributing Cause.....	173
7.3.5 Contributing Cause.....	173
7.3.6 Contributing Cause.....	173
7.3.7 Contributing Cause.....	174
8 RECOMMENDATIONS.....	175
8.1 Recommendations for Industry.....	175
8.1.1 Study of Elastic Buckling.....	175
8.1.2 Study of the Shear Blade Surfaces of Shear Rams.....	175
8.1.3 Study of Well Control Procedures or Practices	176
8.1.4 Status of the Back-Up Control Systems	176
8.1.5 Common Mode Failure of Back-Up Control Systems	176
8.1.6 Study the Indication of Functions in an Emergency.....	176
8.1.7 Study of the Effectiveness of Remotely Operated Vehicle Interventions	177

8.1.8 Stipulating Requirements for Back-Up Control System Performance	177
8.2 Recommendations for Further Testing	177
8.2.1 Additional Studies of Conditions Leading to Elastic Buckling.....	178
8.2.2 Additional Tests or Studies of the Performance of the Blowout Preventer Stack	178

TABLE OF CONTENTS – VOLUME II

APPENDIX A	FORENSIC TESTING PLAN
APPENDIX B	SCANNED DRAWINGS
APPENDIX C	DOCUMENTS REVIEWED
APPENDIX D	LIST OF EVIDENCE
APPENDIX E	SITE TEST RESULTS
APPENDIX F	COMPREHENSIVE TIMELINE
APPENDIX G	FAULT TREE

List of Tables

Table 1 Summary of Annular and Ram Positions As Received at Michoud Facility.....	27
Table 2 ST Lock Position Measurements	31
Table 3 Pressure Required to Function Rams.....	34
Table 4 ROV Panel BSR Close Function Test	41
Table 5 Blue and Yellow Pod Battery Voltages Measurements.....	42
Table 6 Blue and Yellow Pod Battery Load Test Results	43
Table 7 Analog Channel Current Values for AMF/Deadman	45
Table 8 Event Time Log - Yellow Pod Disconnect (Replacement 103Y)	45
Table 9 Event Time Log - Blue Pod Reconnect (Replacement 103 Y).....	46
Table 10 Battery Voltage Following First AMF/Deadman Test	46
Table 11 Event Time Log - Yellow Pod Disconnect (Original 103Y).....	47
Table 12 Event Time Log - Yellow Pod Disconnect Second Test (Original 103Y)	47
Table 13 Event Time Log - Yellow Pod Disconnect Final Test (Original 103Y).....	48
Table 14 Yellow Pod Voltages - Post Sequence Testing.....	48
Table 15 Voltage Testing - Solenoid 103	49
Table 16 Evidence Item Numbers for Blocks Recovered from BOP	50
Table 17 Evidence Item Numbers for Recovered Drill Pipe	78
Table 18 Detail for the Matching of the Drill Pipe Segment Ends.....	93
Table 19 Location and Identification of Types of Test Samples	112
Table 20 Summary of Diameter Measurements Taken at Bottom End of 1-A-1-Q, 1-B-1-Q, 39-Q, 83-Q, 94-Q, and 148-Q.....	116
Table 21 Wall Thickness Measurements Taken at Bottom End of 1-A-1-Q, 1-B-1-Q, 39-Q, 83-Q, 94-Q, 148-Q, and 1-B-2Q.....	117
Table 22 Results for Rockwell C hardness Tests Conducted on the External Surfaces on the Test Samples	118
Table 23 Results for Vickers Hardness Tests Conducted Through Thickness on the Longitudinal Cross-Sections (see Figure 90).....	118

Table 24 Summary of Tensile Test Data for 39-Q	126
Table 25 Summary of Tensile Test Data for 83-Q	127
Table 26 Results of Charpy V-Notch Testing for 39-Q.....	127
Table 27 Results of Charpy V-Notch Testing for 83-Q.....	129
Table 28 Results of Chemical Analysis Compared with Specification for API 5D Grade S135, Seamless Drill Pipe.....	130
Table 29 Summary of ROV Interventions for BSRs	137
Table 30 Comparison of Calculated BSR Pressures.....	157

List of Figures

Figure 1 NASA-Michoud West Dock Test Site	11
Figure 2 NASA-Michoud Test Facility Test Pads	12
Figure 3 Early Stages of Temporary Enclosure Construction	13
Figure 4 Temporary Enclosure	13
Figure 7 ST Lock Measurements	30
Figure 8 Starboard Side (Upper) BSR As-Recovered Condition	52
Figure 9 Port Side (Lower) BSR As-Recovered Condition	52
Figure 10 Starboard Side (Upper) BSR Following Cleaning	53
Figure 11 Port Side (Lower) BSR Following Cleaning	55
Figure 12 Starboard Side (Lower) CSR As-Recovered Condition	56
Figure 13 Port Side (Upper) CSR As-Recovered Condition	57
Figure 14 Starboard Side (Lower) CSR Following Cleaning	58
Figure 15 Port Side (Upper) CSR Following Cleaning	59
Figure 16 Starboard Side Upper VBR in the As-Recovered Condition	60
Figure 17 Port Side Upper VBR in the As Recovered Condition	61
Figure 18 Starboard Side Upper VBR Following Cleaning (Segments Removed)	62
Figure 19 Starboard Segments from Upper VBRs Following Cleaning	62
Figure 20 Port Side Upper VBR Following Cleaning	63
Figure 21 Port Segments from Upper VBRs Following Cleaning. (Segment 1 Remained in Ram)	63
Figure 22 Starboard Side Middle VBR As-Recovered Condition	64
Figure 23 Port Side Middle VBR As-Recovered Condition	65
Figure 24 Starboard Side Middle VBR Following Cleaning	66
Figure 25 Starboard Segments from the Middle VBRs Following Cleaning	67
Figure 26 Port Side Middle VBR Following Cleaning	67
Figure 27 Port Segments from the Upper VBRs Following Cleaning	68

Figure 28 Starboard Side Lower VBR in the As-Recovered Condition.....	69
Figure 29 Port Side Lower VBR in the As-Recovered Condition.....	70
Figure 30 Starboard Side Lower VBR Following Cleaning.....	71
Figure 31 Starboard Segment from the Lower VBR Following Cleaning	71
Figure 32 Port Side Lower VBR Following Cleaning.....	72
Figure 33 Three-Dimensional Laser Scan of Starboard-Side (Upper) BSR Block	74
Figure 34 Three-Dimensional Laser Scan of Port-Side (Lower) BSR Block.....	75
Figure 35 Three-Dimensional Laser Scan of BSRs Placed Together in the Closed Position	76
Figure 36 Three-Dimensional Laser Scan of Starboard-Side (Lower) CSR	77
Figure 37 Three-Dimensional Laser Scan of Port-Side (Upper) CSR.....	77
Figure 38 Schematic Diagram of Positions from which Drill Pipe was Recovered.....	79
Figure 39 Photograph of Drill Pipe 148.....	80
Figure 40 Three-Dimensional Laser Scan of Drill Pipe Segment 148	82
Figure 41 Photograph of Drill Pipe Segment 94.....	82
Figure 42 Three-Dimensional Laser Scan of Drill Pipe Segment 94	83
Figure 43 Photograph of Drill Pipe Segment 83.....	84
Figure 44 Three-Dimensional Laser Scan of Drill Pipe Segment 83	85
Figure 45 Photograph of Drill Pipe Segment 84.....	85
Figure 46 Three-Dimensional Laser Scan of Drill Pipe Segment 84	86
Figure 47 Photograph of Drill Pipe Segment 1-B-2	87
Figure 48 Three-Dimensional Laser Scan of Drill Pipe Segment 1-B-2.....	88
Figure 49 Photograph of Drill Pipe Segment 1-B-1	89
Figure 50 Three-Dimensional Laser Scan of Drill Pipe Segment 1-B-1	90
Figure 51 Photograph of Drill Pipe Segment 39.....	91
Figure 52 Three-Dimensional Laser Scan of Drill Pipe Segment 39	92
Figure 53 Photograph of Drill Pipe Segment 1-A-1	93

Figure 54 Three-Dimensional Laser Scan of Drill Pipe Segment 1-A-1-F	93
Figure 55 Schematic Diagram of Sequence of Drill Pipe Segment Movement	94
Figure 56 Three-Dimensional Laser Scan Comparing 148-A and 94-A	95
Figure 57 Three-Dimensional Laser Scan of 148-A and 94-A Following CSR Cutting ..	95
Figure 58 Photographs of 83-B	96
Figure 59 Photographs of 94-B	97
Figure 60 Laser Scans of 94-B and 83-B	98
Figure 61 Laser Scans of 94-B and 83-B Matched Against the Upper BSR Block	99
Figure 62 Laser Scans of 83-C and 84-C	100
Figure 63 Laser Scans of 84-D and 1-B-2-D	100
Figure 64 Laser Scans of 1-B-2-D2 and 1-B-1-D2	101
Figure 65 Photographs of 1-B-1-E	102
Figure 66 Photographs of 39-E	103
Figure 67 Photograph showing 1-B-1-E and 39-E	104
Figure 68 Laser Scans of 1-B-1-E and 39-E	105
Figure 69 Photographs of the Upper Annular Preventer	106
Figure 70 Laser Scans of 39-F and 1-A-1-F	107
Figure 71 Laser Scans of Drill Pipe Segment 148 passing through the Upper and Middle VBRs	107
Figure 72 Laser Scan of the Upper VBR matched to Drill Pipe Segment 148	108
Figure 73 Laser Scan of the Middle VBR matched to Drill Pipe Segment 148	108
Figure 74 Laser Scan Showing Overhead View of BSR and Wellbore	109
Figure 75 Laser Scan of Wellbore Damage	109
Figure 76 Laser Scan Deviation Plot of the Wellbore on the Kill Side of the BSR	110
Figure 77 Laser Scan Deviation Plot of the Wellbore on the Choke Side of the BSR ...	110
Figure 78 Photograph Illustrating Cementitious Pieces Discovered in Evidence	111
Figure 79 Photograph Illustrating Metal Discovered in Evidence	111

Figure 80 Photograph Illustrating Elastomeric Discovered in Evidence.....	111
Figure 81 Photograph Illustrating Polymeric Discovered in Evidence	112
Figure 82 Photograph of 1-A-1-Q.....	113
Figure 83 Photograph of 1-B-1-Q.....	113
Figure 84 Photograph of 1-B-2-Q.....	114
Figure 85 Photograph 39-Q	114
Figure 86 Photograph 83-Q	115
Figure 87 Photograph 94-Q	115
Figure 88 Photograph of 148-Q	116
Figure 89 Photograph of 148-Q Showing the Locations of Rockwell C Hardness Measurements on the External Surface.....	117
Figure 90 Photograph of Longitudinal Cross-Section of 39-Q.....	118
Figure 91 Photograph of 39-Q Showing the Locations for Metallurgical, Mechanical, and Chemical Coupons	119
Figure 92 Photograph of 148-Q Showing the Locations for Metallurgical and Chemical Coupons	120
Figure 93 Stereo Light Photograph of Longitudinal Cross-Section of 39-Q.....	121
Figure 94 Light Photomicrograph Showing the Typical Microstructure of the Pipe Steel in the Longitudinal Orientation for 39-Q.....	122
Figure 95 Light Photomicrograph Showing the Typical Microstructure of the Pipe Steel in the Transverse Orientation for 39-Q.....	122
Figure 96 Light Photomicrograph Showing the Typical Microstructure of the Pipe Steel in the Transverse Orientation for 1-B-1-Q.....	123
Figure 97 Light Photomicrograph Showing the Typical Microstructure of the Pipe Steel in the Longitudinal Orientation for 83-Q.....	124
Figure 98 Light Photomicrograph Showing the Typical Microstructure of the Pipe Steel in the Transverse Orientation for 83-Q.....	124
Figure 99 Photograph of 39-Q Showing the Locations for Mechanical Coupon Removal	125

Figure 100 Photograph of 83-Q Showing the Locations for Mechanical Coupon Removal	126
Figure 101 Charpy V-Notch Impact Energy Plot as a Function of Temperature for 39-Q (Plot of 3/4-size samples).....	128
Figure 102 Percent Shear Plot from Charpy V-Notch Tests as a Function of Temperature for 39-Q.....	128
Figure 103 Charpy V-Notch Impact Energy Plot as a Function of Temperature for 83-Q (Plot of 3/4-size samples).....	129
Figure 104 Percent Shear Plot from Charpy V-Notch Tests as a Function of Temperature for 83-Q.....	130
Figure 105 Timeline Process	132
Figure 106 Illustration of the Events Pertaining to BSRs - April 20, 2010 to April 29, 2010.....	133
Figure 107 Illustration of Events Pertaining to VBRs - April 20, 2010 to May 5, 2010.	134
Figure 108 Illustration of Events from the comprehensive timeline that pertain to the Annular Preventers which occurred between January 31, 2010 to May 5, 2010.....	135
Figure 109 ROV C-Innovation video footage of the failed attempt to cut the Autoshear hydraulic plunger at 23:30 on April 21, 2010.....	139
Figure 110 ROV C-Innovation video footage of the failed attempt to raise pressure during hot stab of the blind shear ram at 01:15 on April 22, 2010.....	139
Figure 111 ROV C-Innovation video footage of the successful attempt to sever the PBOF cables 02:45 on April 22, 2010. The severed cable is highlighted with a yellow dashed circle.....	140
Figure 112 ROV Millennium 37 video footage of the successful attempt to cut the Autoshear hydraulic plunger at 07:30 on April 22, 2010	140
Figure 113 ROV Millennium 37 video footage of the LMRP/BOP stack connection shortly after cutting of the Autoshear hydraulic plunger at 07:30 on April 22, 2010.....	141
Figure 114 ROV Millennium 37 video footage of the LMRP “LATCH/UNLATCH” indicator shortly after cutting of the Autoshear hydraulic plunger at 07:30 on April 22, 2010.....	141
Figure 115 ROV Millennium 36 video footage of the failed attempt to raise pressure during hot stab of the blind shear ram at 08:00 on April 22, 2010	142

Figure 116 ROV Millennium 36 video footage of the LMRP Flex Joint before and after the kinking of the riser at 10:22 on April 22, 2010.....	142
Figure 117 ROV Millennium 37 video footage of a successful attempt to raise pressure during the hot stab of the blind shear ram at 10:45 on April 26, 2010	143
Figure 118 ROV Millennium 37 video footage of a successful attempt to raise pressure during the hot stab of the blind shear ram at 21:45 on April 26, 2010	143
Figure 119 ROV Millennium 37 video footage of a successful attempt to maintain pressure during hot stab of the blind shear ram at 3:15 on April 27, 2010.....	144
Figure 120 ROV Millennium 36 video footage of a successful attempt to maintain pressure during the hot stab of the blind shear ram at 21:30 on April 29, 2010.....	144
Figure 121 ROV Millennium 37 video footage of an inspection of a fitting on the blind shear ram at 08:15 on April 22, 2010	145
Figure 122 ROV Millennium 37 video footage of a repair to a fitting on the blind shear ram at 08:20 on April 22, 2010.....	145
Figure 123 ROV Millennium 37 video footage of an inspection of the ST lock shuttle valve on the blind shear ram at 22:20 on April 25, 2010.....	146
Figure 124 ROV Millennium 37 video footage of a repair of the ST lock shuttle valve on the blind shear ram at 5:45 on April 26, 2010	146
Figure 125 ROV Millennium 36 video footage of a leak in the fittings behind the right side ST Lock on the blind shear rams	147
Figure 126 Laser Scan of Drill Pipe Segment 1-B-1 (Top End).....	148
Figure 127 General Layout of Drill Pipe and Wellbore Section	149
Figure 128 Progression of Pipe Displacement Under Buckling	150
Figure 129 Predicted Deformation and Resulting Stresses Due to Buckling	150
Figure 130 Calculated Loads as a Function of Drill Pipe Displacement.....	151
Figure 131 Alignment of Pipe Segments with BSR and Buckled Pipe Displacement Comparison	152
Figure 132 BSR Configuration	153
Figure 133 FEA Model of BSR Blade Surfaces and Drill Pipe.....	154
Figure 134 FEA Model of BSR Blade Surfaces and Off-Center Drill Pipe	154
Figure 135 Progression of Centered BSR Shear Model - Side View	155

Figure 136 Progression of Centered BSR Shear Model - Isometric View	156
Figure 137 Photographs of BSR Shear Samples.....	156
Figure 138 Final Deformed Configuration of Shear Cut Showing Strain Concentration at Inner Bend.....	158
Figure 139 Progression of Off-Center BSR Shear Model - Side View	159
Figure 140 Progression of Off-Center BSR Shear Model - Isometric View	159
Figure 141 Top View Showing Deformation of Drill Pipe Outside of Shearing Blade Surfaces.....	160
Figure 142 Final Deformed Configuration of Shear Cut Showing Strain Concentration at Inner Bend.....	160
Figure 143 Final Deformation of the Drill Pipe as Predicted by the Off-Centered Pipe Model; Upper BSR Block Shown on the Right.....	161
Figure 144 Comparison of Recovered Drill Pipe Segments and Final Model	161
Figure 145 Final Model Deformation Compared with Recovered Drill Pipe Laser Scans - 83-B and 94-B.....	162
Figure 146 Spacing of Upper and Lower BSR Blocks in Partially Closed Position	162
Figure 147 Alignment of Scan Models - 2 Inch Standoff Between Block	163
Figure 148 BSR CAD Models - 2 Inch Standoff Between Blocks.....	163
Figure 149 Erosion Damage - BSR Blocks and Wellbore.....	164

List of Abbreviations and Acronyms

AMF	Automated Mode Function
API	American Petroleum Institute
BOEMRE	Bureau of Ocean Energy Management, Regulation, and Enforcement
BOP	Blowout Preventer
BP	BP Exploration & Production Inc.
BSR	Blind Shear Ram
CAD	Computer Aided Design
CSR	Casing Shear Ram
DHS	Department of Homeland Security
DNV	Det Norske Veritas
DOI	Department of the Interior
EDS	Emergency Disconnect Sequence
EPA	Environmental Protection Agency
ERT	Evidence Response Team
FAT	Factory Acceptance Test
FBI	Federal Bureau of Investigation
FEA	Finite Element Analysis
HP	High Pressure
HPU	Hydraulic Pressure Unit
ID	Inside Diameter
JIT	Joint Investigation Team
LA	Lower Annular
LMRP	Lower Marine Riser Package
MIC	Microbiologically Influenced Corrosion
MMS	Minerals Management Service
MODU	Mobile Offshore Drilling Unit
MOEX	Mitsui Oil and Exploration Company
MUX	Multiplex cables
NACE	National Association of Corrosion Engineers
NASA	National Aeronautics and Space Administration
NPT	National Pipe Thread
OD	Outside Diameter
PBOF	Pressure Balance of Oil Filled
PETU	Portable Electronic Test Unit
PSIG	Pounds Per Square Inch Gauge
RCB	Rigid Conduit Box cable
ROV	Remotely Operated Vehicle
SCAT	Systematic Causal Analysis Technique
SEM	Subsea Electronic Modules
SMYS	Specified Minimum Yield Strength



STM	Subsea Transducer Module
TWG	Technical Working Group
UA	Upper Annular
USCG	United States Coast Guard
UTS	Ultimate Tensile Strength
VBR	Variable Bore Ram
YS	Yield Stress



1 EXECUTIVE SUMMARY

A Joint Investigation Team (JIT) of the Departments of the Interior (DOI) and Homeland Security (DHS) was charged with investigating the explosion, loss of life, and blowout associated with the Deepwater Horizon drilling rig failure. As a part of this overall investigation, Det Norske Veritas (DNV) was retained to undertake a forensic examination, investigation, testing and scientific evaluation of the blowout preventer stack (BOP), its components and associated equipment used by the Deepwater Horizon drilling operation.

The objectives of the proposed investigations and tests were to determine the performance of the BOP system during the well control event, any failures that may have occurred, the sequence of events leading to failure(s) of the BOP and the effects, if any, of a series of modifications to the BOP Stack that BP and Transocean officials implemented.

The set of activities undertaken by DNV included:

- Establishing a base of operations at the NASA Michoud facilities for receiving and testing the BOP stack and associated equipment
- Building a temporary enclosure to house the BOP Stack to facilitate the forensic examinations
- Recovery of and assessment of drill pipe, rams, fluids and other material from the BOP Stack and recovered drilling riser
- Function testing of the hydraulic circuits, mechanical components and control systems of the BOP Stack
- Visual examination of evidence and additional analysis using laser profilometry
- Mechanical and metallurgical testing of pieces of drill pipe
- Coordination of activities with other stakeholders through the JIT and the Technical Working Group (TWG)
- Review of documents and Remotely Operated Vehicle (ROV) videos
- Mathematical modeling of the mechanical damage and deformation of drill pipe
- Developing possible failure scenarios

1.1 The Equipment

The Deepwater Horizon was a semi-submersible, dynamically positioned, mobile offshore drilling unit (MODU) that could operate in waters up to 8,000 feet deep and drill down to a maximum depth of 30,000 feet. The rig was built in South Korea by Hyundai Heavy Industries. The rig was owned by Transocean, operated under the Republic Of The Marshall Islands flag, and was under lease to BP from March 2008 to September 2013.



The BOP Stack, built by Cameron, was in use on the Deepwater Horizon since the commissioning of the rig in 2001. The BOP Stack consisted of the following systems, sub-systems and components:

- A Lower Marine Riser Package (LMRP) containing two annular preventers and two Control Pods
- The lower section of the BOP Stack contains five sets of rams. These rams are referred to as the Blind Shear rams (BSR), the Casing Shear rams (CSR), Upper Variable Bore rams (VBR), Middle VBRs and Lower VBRs. The LMRP sits on top of the lower section of the BOP.
- Two electronic Control Pods are located or fitted to the LMRP. These control pods receive signals from the control panels that are located on the rig itself, and then activate various solenoids in turn functioning various hydraulic circuits and mechanical components on the BOP Stack.

At the time of the accident, the rig was drilling an exploratory well at a water depth of approximately 5,000 feet in the Macondo Prospect. The well is located in Mississippi Canyon Block 252 in the Gulf of Mexico.

1.2 The Accident

On the evening of April 20, 2010, control of the well was lost, allowing hydrocarbons to enter the drilling riser and reach the Deepwater Horizon, resulting in explosions and subsequent fires. The fires continued to burn for approximately 36 hours. The rig sank on April 22, 2010. From shortly before the explosions until May 20, 2010, when all ROV intervention ceased, several efforts were made to seal the well. The well was permanently plugged with cement and “killed” on September 19, 2010.

In the event of a loss of well control, various components of the BOP Stack are functioned in an attempt to seal the well and contain the situation. The most important of these components are the blind shear rams. These can be activated in several different ways:

- Activation from either of two control panels located on the Deepwater Horizon rig itself
- Through the Emergency Disconnect Sequence which is also activated from either of the two control panels on the rig itself
- By the Automated Mode Function (AMF)/Deadman circuits located in the Subsea Electronic Modules within either of two subsea control pods mounted on the LMRP
- By the Autoshear function located on the BOP Stack
- By ROV intervention through a panel on the BOP Stack



1.3 Forensic Tests

On September 4, 2010, the BOP Stack was raised from the sea floor. The BOP Stack was transferred by barge to the NASA-Michoud facility in New Orleans, LA.

On October 3, the BOP Stack and LMRP were lifted from the barge and placed on test pans that were constructed on the West Dock of the Michoud facility. Per contract requirements, DNV developed and submitted a draft test plan to the JIT for review, comment and approval. The JIT forwarded this plan to several Parties-In-Interest to the forensic examinations for their review and comment. These comments were, in turn, submitted to DNV for consideration and possible inclusion. Part of the forensic testing protocol was to establish a Technical Working Group consisting of technical representatives from BP, Transocean, Cameron, Department of Justice, Chemical Safety Board and the Multi-District Litigation. A final Forensic Testing Plan was approved on October 22, 2010. Forensic testing began on November 15, 2010 and was completed on March 4, 2011.

The Blind Shear, Casing Shear and three sets of Variable Bore Rams were removed from the lower section of the BOP, cleaned and examined visually and using laser profilometry. The wellbore was examined using high definition video cameras and the section of the wellbore at the Blind Shear Rams was also examined by laser profilometry. The wellbore and the upper and lower annulars in the LMRP were examined using a high definition video camera. Fluid samples were collected from the wellbore and various hydraulic circuits.

A total of eight segments of drill pipe were recovered, examined and tested. Two drill pipe segments were recovered from the BOP at Michoud. Three additional segments were recovered from the drilling riser at Michoud. Three other segments of drill pipe previously recovered were also examined. The segments were matched together using a combination of visual examination of the shear or fracture surfaces, laser profilometry, mechanical and metallurgical testing. A timeline sequence of the various failures in the drill pipe was developed. The results of the mechanical and metallurgical testing for the drill pipe were in accordance with industry standards.

Function testing included:

- ST Locks
- Choke and Kill valves
- The hydraulic operators and circuits of the five ram sets on the lower BOP
- The high pressure accumulators on the lower BOP
- The hydraulic circuits of the AMF/Deadman and Autoshear
- The electronic circuits of the AMF/Deadman and Autoshear

The hydraulic circuits of all the above functioned as intended when tested or operated. The tests of the electronic circuits of the AMF/Deadman demonstrated that the voltage of



the 27V battery in the Blue Pod was insufficient to activate the High Pressure Blind Shear Ram pilot solenoid mounted on the Blue Pod. The tests of the Yellow Pod High Pressure Blind Shear Ram pilot solenoid circuits were inconsistent.

1.4 What is Considered to Have Happened

Prior to the loss of well control on the evening of April 20, 2010, the Upper Annular (UA) was closed as part of a series of two negative or leak-off tests. Approximately 30 minutes after the conclusion of the second leak-off (negative pressure) test, fluids from the well began spilling onto the rig floor. At 21:47 the standpipe manifold pressure rapidly increased from 1200 psig to 5730 psig. The first explosion was noted as having occurred at 21:49. At 21:56 the Emergency Disconnect Sequence (EDS) was noted to have been activated from the bridge. This was the final recorded well control attempt from the surface before the rig was abandoned at 22:28.

The Upper VBRs were found in the closed position as-received at the Michoud facility. There was no documented means of ROV intervention to close the Upper VBRs. ROV gamma ray scans on May 10, 2010, confirmed that the ST Lock on the port side Upper VBR was closed. Scans of the starboard side ST Lock on the Upper VBRs were inconclusive. Measurements of the ST Lock positions performed at the Michoud facility confirmed that both ST Locks on the Upper VBRs were closed. Evidence supports that the Upper VBRs were closed prior to the EDS activation at 21:56 on April 20, 2010.

A drill pipe tool joint was located between the Upper Annular and the Upper VBRs. With both the Upper Annular and the Upper VBRs closed on the drill pipe, forces from the flow of the well pushed the tool joint into the Upper Annular element. This created a fixed point arresting further upward movement of the drill pipe. The drill pipe was then fixed but able to pivot at the Upper Annular, and horizontally constrained but able to move vertically at the Upper VBRs. Forces from the flow of the well induced a buckling condition on the portion of drill pipe between the Upper Annular and Upper VBRs. The drill pipe deflected until it contacted the wellbore just above the BSRs. This condition would have most likely occurred from the moment the well began flowing and would have remained until either the end conditions changed (change in Upper Annular or Upper VBR state) or the deflected drill pipe was physically altered (sheared). The portion of the drill pipe located between the shearing blade surfaces of the BSRs was off center and held in this position by buckling forces.

As the BSRs were closed, the drill pipe was positioned such that the outside corner of the upper BSR blade contacted the drill pipe slightly off center of the drill pipe cross section. A portion of the pipe cross section was outside of the intended BSR shearing surfaces and would not have sheared as intended. As the BSRs closed, a portion of the drill pipe cross section became trapped between the ram block faces, preventing the blocks from fully closing and sealing. Since the deflection of the drill pipe occurred from the moment the well began flowing, trapping of the drill pipe would have occurred regardless of which



means initiated the closure of the BSRs.

Of the means available to close the BSRs evidence indicates that the activation of the BSRs occurred when the hydraulic plunger to the Autoshear valve was successfully cut on the morning of April 22, 2010. However, on the evidence available, closing of the BSRs through activation of the AMF/Deadman circuits cannot be ruled out.

In the partially closed position, flow would have continued through the drill pipe trapped between the ram block faces and subsequently through the gaps between the ram blocks. When the drill pipe was sheared on April 29, 2010, using the CSRs, the well flow pattern changed to a new exit point. At this point, the flow expanded through the open drill pipe at the CSRs and up the entire wellbore to the BSRs and through the gaps along the entire length of the block faces and around the side packers.

1.5 Primary Cause and Contributing Causes

The failure cause analysis was organized and conducted around a single top event. For the purposes of this investigation, the top event was defined as the failure of the BSRs to close and seal the well.

The primary cause of failure was identified as the BSRs failing to fully close and seal due to a portion of drill pipe trapped between the blocks.

Contributing causes to the primary cause included:

- The BSRs were not able to move the entire pipe cross section into the shearing surfaces of the blades.
- Drill pipe in process of shearing was deformed outside the shearing blade surfaces.
- The drill pipe elastically buckled within the wellbore due to forces induced on the drill pipe during loss of well control.
- The position of the tool joint at or below the closed Upper Annular prevented upward movement of the drill pipe.
- The Upper VBRs were closed and sealed on the drill pipe.
- The flow of well fluids was uncontrolled from downhole of the Upper VBRs.

1.6 Recommendations for Industry

The primary cause of failure was identified as the BSRs failing to close completely and seal the well due to a portion of drill pipe becoming trapped between the ram blocks. The position of the drill pipe between the Upper Annular and the upper VBRs led to buckling and bowing of the drill pipe within the wellbore. Once buckling occurred the BSRs would not have been able to completely close and seal the well. The buckling most likely occurred on loss of well control.



The recommendations are based on conclusions from the primary and contributing causes or on observations that arose during the course of DNV's investigations.

1.6.1 Study of Elastic Buckling

The elastic buckling of the drill pipe was a direct factor that prevented the BSRs from closing and sealing the well.

It is recommended the Industry examine and study the potential conditions that could arise in the event of the loss of well control and the effects those conditions would have on the state of any tubulars that might be present in the wellbore. These studies should examine the following:

- The effects of the flow of the well fluids on BOP components and various tubulars that might be present,
- The effects that could arise from the tubulars being fixed or constrained within the components of a Blowout Preventer,
- The ability of the Blowout Preventer components to complete their intended design or function under these conditions.

The findings of these studies should be considered and addressed in the design of future Blowout Preventers and the need for modifying current Blowout Preventers.

1.6.2 Study of the Shear Blade Surfaces of Shear Rams

The inability of the BSRs to shear the off-center drill pipe contributed to the BSRs being unable to close and seal the well.

It is recommended the industry examine and study the ability of the shear rams to complete their intended function of completely cutting tubulars regardless of their position within the wellbore, and sealing the well. The findings of these studies should be considered and addressed in the design of future Blowout Preventers and the need for modifying current Blowout Preventers to address these findings.

1.6.3 Study of Well Control Procedures or Practices

The timing and sequence of closing of the UA and upper VBRs contributed to the drill pipe segment buckling and bowing between the two moving the drill pipe off center.

It is recommended the industry examine and study the potential effects or results that undertaking certain well control activities (e.g. closing of the annulars, or closing of the VBRs) could have on the BOP Stack. Examination and study should identify conditions, which could adversely affect the ability to regain control of the well (e.g. elastic buckling of tubulars). Industry practices, procedures and training should be reviewed and revised, as necessary, to address the prevention of these conditions.



1.6.4 Status of the Back-Up Control Systems

The BOP functionality testing indicated some back-up control system components did not perform as intended.

It is recommended the industry review and revise as necessary the practices, procedures and/or requirements for periodic testing and verification of the back-up control systems of a Blowout Preventer to assure they will function throughout the entire period of time the unit is required on a well.

1.6.5 Common Mode Failure of Back-Up Control Systems

The BOP functionality testing indicated not all back-up control systems had built in redundancy.

It is recommended the industry review and revise as necessary the practices, procedures and/or requirements for evaluating the vulnerability of the back-up control systems of a Blowout Preventer to assure they are not subject to an event or sequence of events that lead to common mode failure.

1.6.6 Study the Indication of Functions in an Emergency

The ROV intervention efforts reviewed indicated the ROVs were not capable of directly and rapidly determining the status of various ROV components.

It is recommended the industry examine and revise the current requirements for providing a means to verify the operation, state or position of various components of Blowout Preventers in the event of an emergency. The industry should require that it is possible to confirm positively the state or position of certain components such as the rams, annulars and choke and kill valves either with the use of Remotely Operated Vehicles or by other means.

1.6.7 Study of the Effectiveness of Remotely Operated Vehicle Interventions

The ROV intervention efforts reviewed indicated initial ROV efforts were not capable of performing key intervention functions at a level equivalent to the primary control systems.

It is recommended the industry examine and study the conditions and equipment necessary for Remotely Operated Vehicles to perform various functions (e.g. the BSRs) at a performance level equivalent to the primary control systems. Make adequate provision to mobilize such equipment in the event of a well control emergency.



1.6.8 Stipulating Requirements for Back-Up Control System Performance

A review of industry standards indicated they do not stipulate performance requirements for back-up systems (e.g. closing response times) as they do for primary control systems.

It is recommended the industry review and revise the requirements for back-up control system performance to be equivalent to the requirements stipulated for primary control systems.

1.7 Recommendations for Further Testing

DNV's forensic examinations and testing were organized and conducted around the top event of the failure of the Blind Shear Rams to close and seal the well.

The recovery and examination of the eight segments of drill pipe and the five sets of rams shifted the focus from the question of whether the blind shear rams were activated to that of identifying the factors that would have caused or contributed to the blind shear rams failing to seal the well. As described in this report, DNV is of the view that the primary cause for the blind shear rams failing to close arose from conditions that led to the drill pipe being forced to one side of the wellbore at a position immediately above the Blind Shear Rams. DNV has investigated the conditions that could lead to such a buckling scenario developing. However, even here DNV recognizes there are additional studies and tests that could be undertaken to examine this scenario further.

In addition, DNV has identified a number of areas or issues associated with the overall performance of the BOP Stack that should be examined, investigated or tested further. As a result, DNV puts forward the following recommendations.

1.7.1 Additional Studies of Conditions Leading to Elastic Buckling

- Supplement the Finite Element Analysis buckling model with a Computational Fluid Dynamic simulation of the flow through the drill pipe.
- Run the Finite Element Analysis drill pipe-cutting model to include the buckling stresses that would have existed in the drill pipe.
- Field test the blind shear rams shearing a section of off-centered (buckled) 5-1/2 inch drill pipe.
- Field test the ability of a closed annular to restrain the upward movement of a 5-1/2 inch drill pipe tool joint at the forces calculated for buckling.
- Field test the conditions required to push a 5-1/2 inch tool-joint through a closed annular element.



1.7.2 Additional Tests or Studies of the Performance of the Blowout Preventer Stack

- It is suggested that the static pressure tests undertaken at Michoud on the high-pressure shear hydraulic circuits of the lower section of the BOP be supplemented with additional tests of the circuits of the Casing Shear Rams and the Variable Bore Rams.
- The tests at Michoud performed on the high-pressure blind shear close solenoid removed from the Yellow Pod in May 2010 gave inconsistent results. It is suggested this solenoid be further tested and possibly disassembled to discern the reason for its performance and whether it was likely to have functioned at the time of the incident.
- On pressuring the high-pressure shear ram circuit, the high-pressure casing shear regulator leaked. It is suggested the high-pressure casing shear regulator be further tested and disassembled to try and discern its state at the time of the incident.
- It is suggested that the behavior of the elastomeric elements of the rams and annulars be tested to assess their performance when exposed to well fluids at the temperatures that existed at the time of the blowout.
- The tests of the Subsea Electronic Modules (SEMs) undertaken at Michoud should be supplemented by removing the SEMs from the Control Pods, venting and then opening the SEMs to understand better their possible state at the time of the incident. The following tests or activities are suggested:
 - Collect and analyze samples of the SEMs gas/atmosphere prior to or as part of venting the SEMs.
 - Remove the batteries and record part numbers, serial numbers, date of manufacture and any other pertinent manufacturing data,
 - In place of the batteries connect a voltage generator and conduct a series of tests on the AMF/Deadman circuits at various voltages and record the results.
- The lower and upper annulars are well control components of the BOP stack. As a result the following tests or examinations of the lower and upper annulars are suggested:
 - Laser scanning of the upper annular in-situ and “as-is” condition,
 - Remove and examine the upper and lower annular elements,
 - Static pressure tests of the annular operating systems,
 - Function testing of the open and close operating systems of both annulars.
- The evidence from eyewitnesses was that the Emergency Disconnect Sequence was activated approximately seven minutes after the first explosion. It is suggested the hydraulic circuits and functioning of the LMRP HC collet connector and the choke and kill collet connectors be tested as a means to try and assess their state at the time of the incident.
- It is suggested the wellbore pressure-temperature sensor at the base of the lower section of the BOP be removed and its accuracy checked or tested.
- It is suggested the industry perform field tests on the ability of the BSRs to shear and seal a section of 5-1/2 inch drill pipe under internal flow conditions that existed at the time of the incident.



2 INTRODUCTION

On April 27, 2010, the Departments of Interior and Homeland Security signed an order that made provision for the Departments to convene a Joint Investigation of the April 21-22 2010, explosion and sinking of the Deepwater Horizon Mobile Offshore Drilling Unit¹.

On August 10, 2010 the Bureau of Ocean Energy, Management, Regulation and Enforcement (BOEMRE) of the Department of Interior issued a competitive Request for Proposal to undertake a series of forensic investigations and tests on the Deepwater Horizon Blowout Preventer. The objectives of the proposed investigations and tests were to determine the performance of the BOP system during the well control event, any failures that may have occurred, the sequence of events leading to failure(s) of the BOP and the effects, if any, of a series of modifications to the BOP stack that BP and Transocean officials implemented. As part of the foregoing task, the examination was to determine:

- If leaks on the BOP were critical to the non-performance during the blowout and during the ROV intervention attempts;
- If any modification(s) made to the control logic and stack inhibited the performance;
- If any other relevant factors, including but not limited to manufacturing defects, deferral of necessary repairs affecting functionality, and maintenance history contributed to the BOP's failure to operate as intended.

DNV submitted a proposal to undertake the forensic examinations, investigations and tests in accordance with the RFP and was awarded a contract on September 1, 2010.

The set of activities undertaken by DNV included:

- Establishing a base of operations at the NASA-Michoud facilities for receiving and testing the BOP stack and associated equipment,
- Building a temporary enclosure to house the BOP stack to facilitate the forensic examinations,
- Recovery of and assessment of drill pipe, rams, fluids and other material from the BOP stack and recovered drilling riser,
- Function testing of the hydraulic circuits, mechanical components and control systems of the BOP stack,
- Visual examination of evidence and additional analysis using laser profilometry,
- Mechanical and metallurgical testing of pieces of drill pipe,

¹ Statement of Principles and Convening Order regarding an investigation into the Marine Casualty, Explosion, Fire, Pollution and Sinking of Mobile Offshore Drilling Unit Deepwater Horizon, With Loss of Life in the Gulf of Mexico 21-22 April 2010

- Coordination of activities with other stakeholders through the JIT and the technical working group,
- Review of documents and ROV videos,
- Mathematical modeling of the mechanical damage and deformation of drill pipe, and
- Developing possible failure scenarios

On September 4, 2010, the Deepwater Horizon Blowout Preventer was removed from the wellhead and raised from the sea floor by the multi-purpose intervention vessel Q-4000. A hazards search of the BOP stack was conducted. Initial stabilization activities were also performed on board the Q-4000. The Lower Marine Riser Package (LMRP) was separated from the lower BOP section prior to transferring the two units from the Q-4000 to a transport barge. The two units were then towed to the NASA-Michoud facility in New Orleans, LA.



Figure 1 NASA-Michoud West Dock Test Site

The NASA-Michoud facility constructed two test pans or pads on their West Dock as part of their preparations to receive the two units. On October 3, the BOP and LMRP were lifted from the transport barge and placed on the test pans.

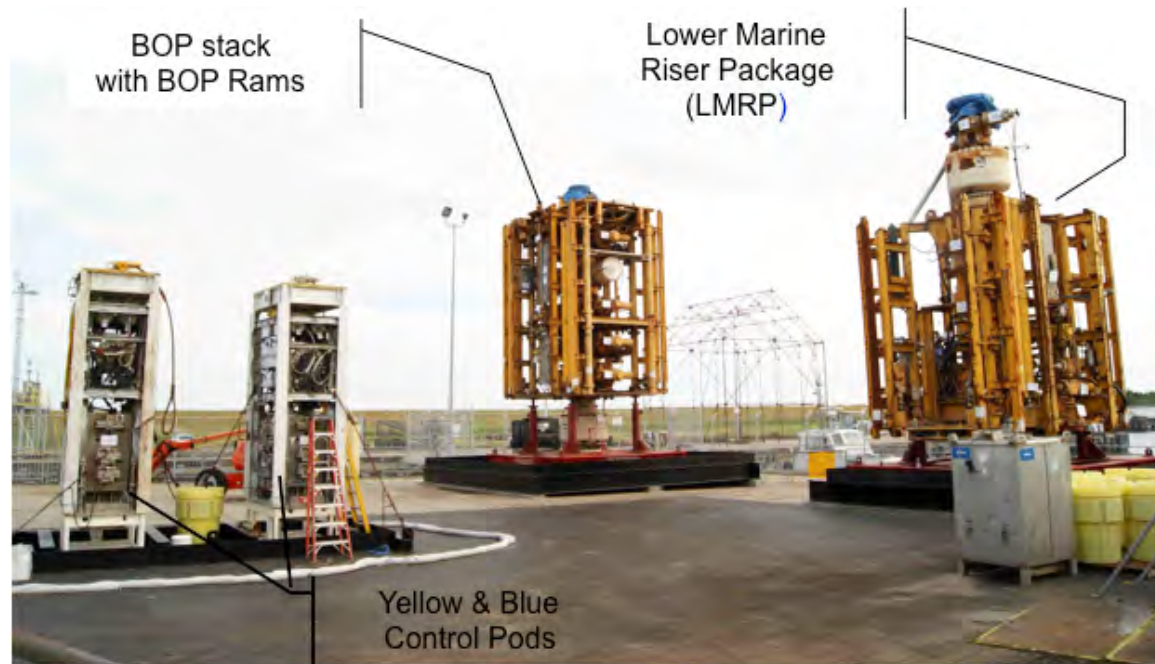


Figure 2 NASA-Michoud Test Facility Test Pads

Per contract requirements, DNV developed and submitted a draft test plan to the JIT for review, comment and approval. The JIT forwarded this plan to several Parties-In-Interest to the forensic examinations for their review and comment. These comments were returned to DNV for consideration and possible inclusion. Part of the forensic testing protocol was to establish a Technical Working Group (TWG) consisting of representatives from BP, Transocean, Cameron, Department of Justice, Chemical Safety Board and the Multi-District Litigation. A final test plan was approved by the JIT on October 27, 2010.

Forensic testing began on November 15, 2010. On December 23, 2010, the forensic investigations and testing on the West Dock stopped for enclosure construction. A temporary enclosure was constructed over and around the LMRP and BOP on the West Dock. Construction started on December 27 and continued on through January 28, 2011. During the enclosure construction period the drill pipe segments and rams were moved to Building 411 for cleaning and examination. Testing on the West Dock resumed on January 28 and continued through to March 4, 2011, when the last series of tests were completed.



Figure 3 Early Stages of Temporary Enclosure Construction



Figure 4 Temporary Enclosure

3 BACKGROUND

The rights to drill or explore the Macondo Prospect or well within the Mississippi Canyon are jointly owned by BP Exploration & Production (BP), Anadarko Petroleum and Mitsui Oil and Exploration Co (MOEX). The Mississippi Canyon is located approximately 40 miles off the coast of Louisiana.

The engineering and design of the well started in 2009. Drilling of the well began in October 2009 using the Mobile Offshore Drilling Unit "Marianas" which is owned by Transocean and was under contract to BP. Drilling was halted in November 2009 due to the passing of Hurricane Ida. Damage to the Marianas required it to be returned to dock for repairs and it subsequently went off contract. The Transocean Deepwater Horizon Mobile Offshore Drilling Unit was selected to continue drilling of the well.

The Deepwater Horizon started drilling in February and continued through to April 2010. On April 9, the well was drilled to its final depth of 18,360 feet.

During the afternoon and early evening hours of April 20, the crew performed two negative pressure or leak-off tests on the well. The second of these two tests was recorded as being completed at 21.10 hours. Approximately 30 minutes after having finished this test, the crew observed water and mud

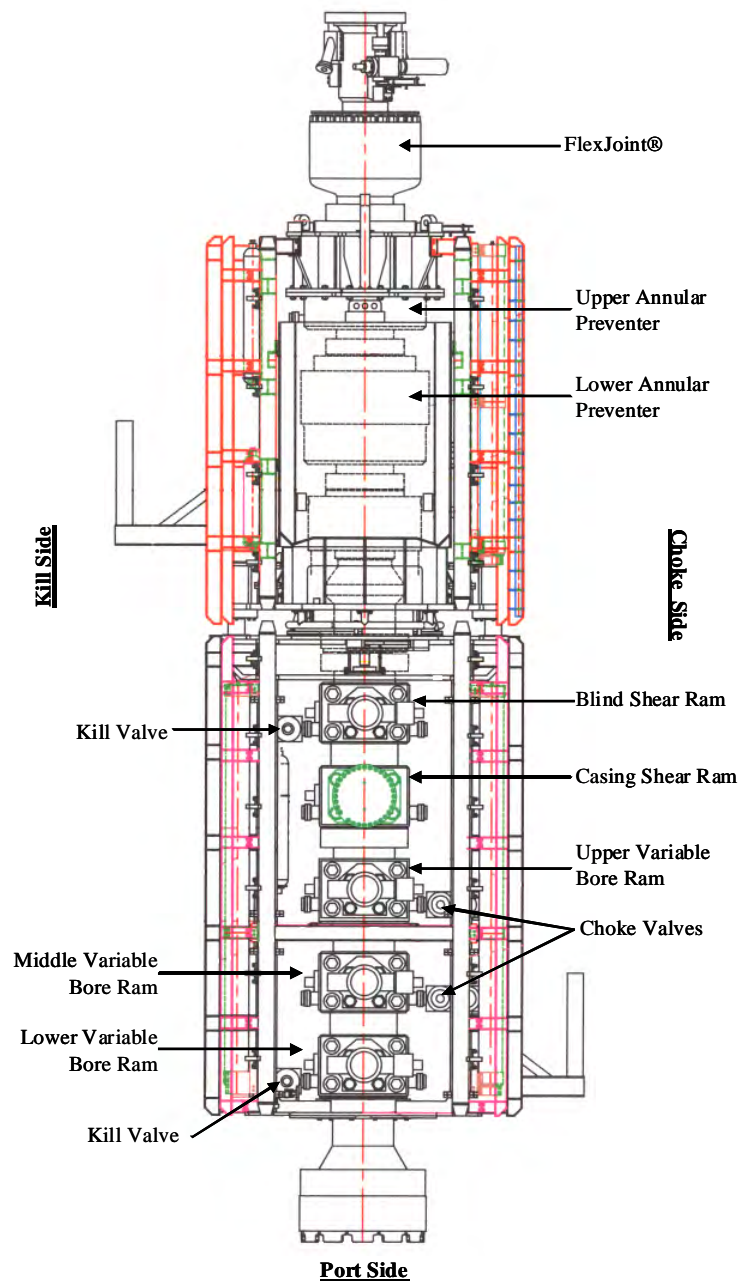
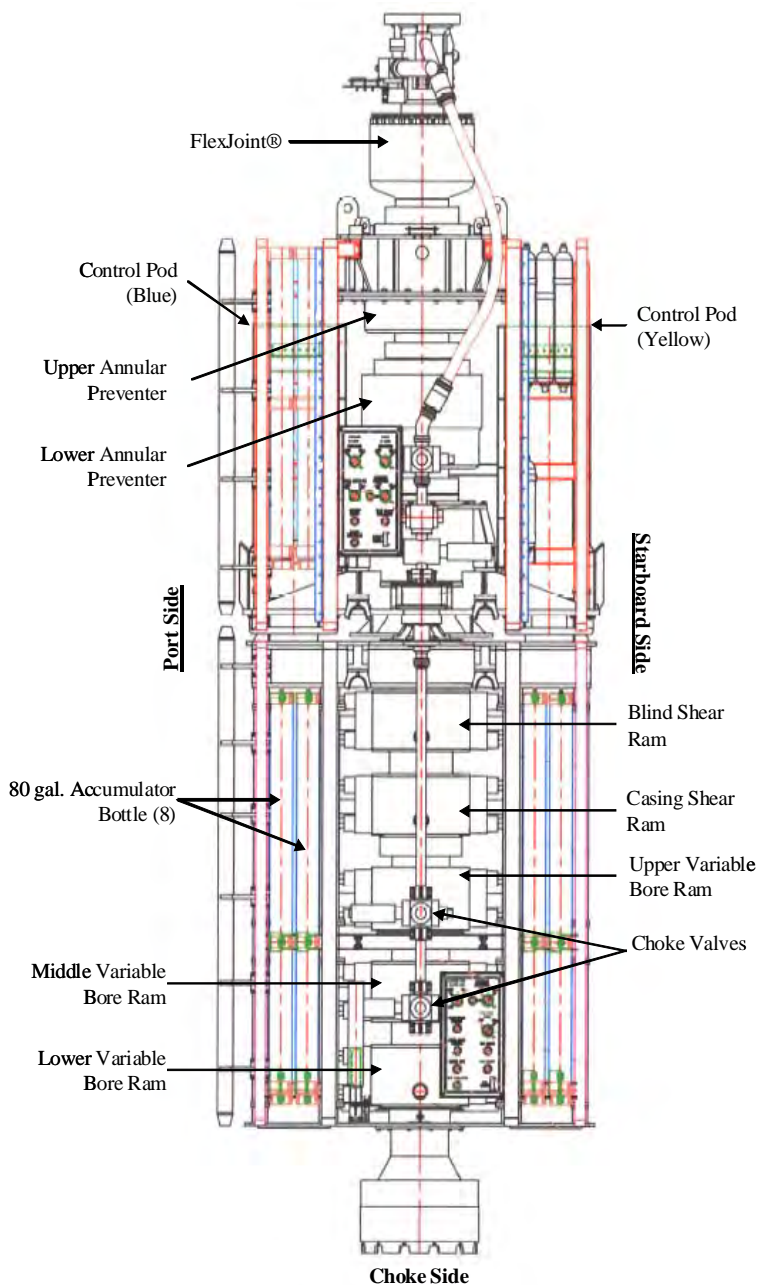


Figure 5 Deepwater Horizon BOP Port Side

on the floor of the drill rig. At 21:49 an explosion occurred on the rig followed immediately by fire. The Emergency Disconnect Sequence of the Blowout Preventer was reportedly activated just before 21:56. The rig was abandoned at 22:28.

Prior to, during and following the initial stages of the accident, numerous attempts were made to control the well by activating or functioning various components of the Deepwater Horizon's subsea Blowout Preventer (BOP). The Blowout Preventer is comprised of two primary packages or systems, the Lower Marine Riser Package and the lower section of the Blowout Preventer.



The lower section of the Blowout Preventer attaches to the subsea wellhead. The Lower Marine Riser Package attaches to the top of the lower section of the Blowout Preventer. When these two units are 'stacked' or attached they are generally referred to as the BOP 'Stack'. When stacked the two units are approximately 57 feet in overall height with a combined weight of approximately 400 tons.

The lower section of the Blowout Preventer consists of three sets of Variable Bore pipe Rams (VBRs), a set of Casing Shear Rams (CSRs), and a set of Blind Shear Rams (BSRs). The VBRs are designed to close and seal around drill pipe. The Casing Shear Rams are designed to sever casing (large diameter pipe). The Blind Shear Rams are designed to sever drill pipe that might be in the wellbore and seal the

Figure 6: Deepwater Horizon BOP Choke Side



wellbore in the event of the loss of well control. The BSRs are the only set of rams designed to cut drill pipe and seal the well in the event of a blowout. The lower section of the BOP also contains 8 x 80 gallon accumulators. These accumulators contain a bladder separating the accumulator into two sections or chambers. One chamber is filled with nitrogen gas; the other chamber with a hydraulic fluid. The chamber with nitrogen is pressured to a level that is established and dependent on the depth of water in which the BOP will be located (i.e., the 'pre-charge'). The second chamber is filled with hydraulic fluid which is then pressured to a level also dependent on the water depth in which the BOP will be located. It is this hydraulic fluid which is used to function the blind shear rams in the event of an emergency.

The LMRP contains two annular preventers, the Upper Annular (UA) and the Lower Annular (LA). The annular preventers consist of a set of hydraulically activated fingers and an elastomeric element that can be closed which will compress and seal around the drill pipe. The LMRP is also fitted with two control pods, one designated "blue" and the other "yellow". Each pod contains a Subsea Electronic Module (SEM), a hyperbaric cylinder or chamber in which the electronic control circuits for both the LMRP and BOP components are housed. Each control pod is connected to the control systems or panels on the drilling rig itself by Multiplex (MUX) cables. These cables transmit power from the rig to the Control Pods as well as send and receive communication signals between the control panels on the rig and SEMs in the Control Pods. In addition to the MUX cables, a hydraulic line from the rig to the LMRP charges the subsea accumulators to function the hydraulic circuits of various stack components.

A Flex Joint mounted to the top of the LMRP connects the LMRP to the subsea Riser.

In situations where events could lead to the loss of well control or well control is lost, the various rams and annulars can be functioned to regain control of the well. Of these functions, as noted earlier, the blind shear rams are the only component designed to shear drill pipe that might be in the wellbore (the situation that existed at the time of the accident) and then seal the well.

The Blind Shear Rams can be activated in several different ways.

- Activation from either of two control panels located on the Deepwater Horizon rig itself
- Through the Emergency Disconnect Sequence which is also activated from either of the two control panels on the rig itself
- By the AMF/Deadman circuits located in the Subsea Electronic Modules within either of two subsea control pods mounted on the LMRP
- By the Autoshear function located on the BOP stack
- By ROV intervention through a panel on the BOP stack



Normal or standard closing of the BSRs occurs at a pressure of 3,000 psig. The blind shear rams can also be closed through a high-pressure circuit of 4,000 psig. The two control panels on the rig have systems or buttons that provide for closing the rams in 'normal' or high-pressure mode. The Emergency Disconnect Sequence, Autoshear and AMF/Deadman all activate the high-pressure circuits to the BSRs. ROV intervention bypasses the accumulators on the lower BOP and uses pumps and systems ancillary to the BOP accumulators to function the BSRs. The pressure and flows to close the BSRs using an ROV are determined by the capability of the ROV and its ancillary systems, not those of the lower BOP. When activated, the time for the BSRs to close is approximately 25 seconds (other than by ROV).

As noted earlier, at 21:56/57 or approximately six minutes after the first explosion, the EDS was reported to have been pushed. This was the only recorded activation of a system on the rig, which would have functioned the high-pressure blind shear ram circuit. Despite having initiated the EDS, the LMRP did not unlatch from the lower BOP (one of several EDS functions). Unlatching of the LMRP would have provided the ability to disconnect the LMRP and riser from the source of well fluids and the move the MODU from over the well. In addition, the well continued to flow through the BOP stack feeding the fires on the rig indicating the BSRs had not closed and sealed. At 18.00 on April 21, the first of several ROV interventions to control the well was initiated. A number of these interventions were focused on satisfying the conditions required to initiate the AMF/Deadman or the Autoshear sequences to close the blind shear rams. Despite these attempts, flow through the BOP stack continued. This indicated the blind shear rams had either not functioned, or if they had functioned, they did not close fully and seal the well.

On July 16, the flow from the well was stopped after a method termed a 'top kill' was completed. On September 19, Admiral Thad Allen, USCG, announced the well was effectively dead after a relief well was completed and cement was pumped into the Macondo 252 well to seal it.



4 OBJECTIVES AND SCOPE

For this testing and analysis, DNV was asked to determine the performance of the BOP system during the well control event, any failures that may have occurred, the sequence of events leading to failure(s) of the BOP and the effects, if any, of a series of modifications to the BOP stack that BP and Transocean officials implemented. As part of the foregoing task, the examination sought to determine the following:

- If leaks on the BOP were critical to the non-performance during the blowout and during the ROV intervention attempts
- If any modification(s) made to the control logic and stack inhibited the performance
- If any other relevant factor, including but not limited to manufacturing defects, deferral of necessary repairs affecting functionality, and maintenance history contributed to the BOP's failure to operate as intended

The scope of the investigation included the following:

- Develop and submit for JIT approval a forensic testing plan consistent with the JIT-provided examination objectives and parameters that included (1) forensic testing procedures for the BOP stack and its components in accordance with established and accepted scientific protocols, methods, and techniques, and (2) processes and procedures DNV would implement to conform to the protection and preservation of evidence protocols also to be provided by the JIT
- Perform and manage the tests of the BOP stack and its components
- Document and record the testing and all related and supporting steps and procedures, including the video recording of the examination in its entirety
- Conform with the protocols established by the JIT for the proper custody and documentation of chain of custody of the BOP stack and its components
- Conform with the protocols established by the JIT for the proper protection and preservation of the evidence, which included all BOP stack components and preservation (and, as necessary, replication) of all pertinent physical conditions associated with those components on the sea floor and otherwise, to the maximum extent possible, avoid destructive testing
- Identify and provide for all specialized third-party (subcontractor) testing and ensure that this testing was performed in accordance with all established JIT approved protocols
- Execute all necessary agreements to review and utilize proprietary information
- Review video of remotely-operated underwater vehicle (ROV) intervention operations during pertinent times
- Review government provided records obtained from the commercial parties relevant to the BOP and its components, including design specifications, schematics, purchase orders, maintenance and operating manuals, service records, and other documents



-
- Produce a factual report of the testing of the BOP and its components including review of the ROV intervention operations, conclusions, and professional opinions; the final report shall include as an index the administrative record of the testing procedure, including but not limited to, all emails, other electronic media, videographic and photographic documentation, and other contractor work product
 - Testify in public hearings concerning the results of the testing and conclusions

5 METHODOLOGY

5.1 Evidence Collection and Control

Evidence was in the form of components removed from the BOP and LMRP during the investigation, items removed from the wellbore of the BOP and LMRP, or samples collected in the form of scrapings, particles, scale, coating samples, liquids, etc. All evidence was handled in accordance with the DNV Forensic Testing Plan.

US Coast Guard (USCG) personnel took possession of the evidence for secure storage. The FBI Evidence Response Team (ERT) recorded and documented all evidence.

The EPA National Environmental Investigations Center (NEIC) provided the primary support for all fluid samples collected during the investigation. The USCG personnel took initial custody of the fluid samples. The custody of the fluid samples was transferred from USCG control to the EPA NEIC for analysis.

5.2 Technical Working Group

The Parties In Interest Technical Working Group (TWG) was made up of technical representatives from interested parties including: Transocean, BP, Cameron, Chemical Safety and Hazard Investigation Board (CSB), Department of Justice, and two technical representatives from the Multi-District Litigation.

Meetings were held with the TWG on a daily basis to review site safety issues and the testing plan for the day. In addition, meetings were held on Wednesday afternoon to review the next week's work plan. Impromptu meetings were held with the TWG, or individual members of the TWG, to discuss issues as the DNV Investigation Team or the TWG deemed necessary.

5.3 Investigative Process

The investigative process was an iterative process that integrated the BOP and LMRP function testing, evidences collection, preservation of evidence (especially the drill pipe contained in the wellbores of the BOP and LMRP), materials examination and damage assessment, and video and photo documentation. In addition, as the testing proceeded, the findings dictated the sequence of steps required to balance further investigations and activities. Therefore, the protocols in the Forensic Testing Plan were not meant to be a step-by-step procedure, rather provided a roadmap for meeting the objectives. Additional protocols that were outside of the scope outlined in the original testing plan were submitted TWG for review and comment an to the JIT for approval. Detailed procedures to more fully describe a particular testing sequence were required on a routine basis. These detailed procedures were developed in cooperation between the DNV Investigation



Team and the TWG. In addition, the performance of these detailed procedures was documented through notes, photography, and videography.

5.4 Forensic Testing Plan and Protocol Development

The first activity was to develop and submit for JIT approval a Forensic Testing Plan consistent with the JIT objectives. The Forensic Testing Plan included forensic testing procedures for the BOP stack and its components in accordance with established and accepted protocols, methods, and techniques. The Forensic Testing Plan protocol and procedures conformed to the protection and preservation of evidence protocols agreed with the JIT. The protocols included professional video recording of the entire examination and complete photographic documentation.

DNV drafted a Forensic Testing Plan consistent with the examination objectives and parameters provided by the JIT, which included forensic testing procedures for the BOP stack and its components. The Forensic Testing Plan was presented in a meeting of the TWG for the purpose of review and comment.

As a result of the review and comment process, approximately 200 comments were received. The comments were reviewed by the DNV Team for technical viability, responses provided, and revisions made where appropriate to the Forensic Testing Plan. The revised Forensic Testing Plan was approved by the Joint Investigation Team on October 27, 2010. The approved Forensic Testing Plan is provided as Appendix A.

5.5 Site Preparation

As part of the preparations for receiving the Lower Marine Riser Package and the lower BOP, the NASA-Michoud facility constructed two test pans on the West Dock of the facility (see Figure 2). The test pans served two purposes, one to provide the necessary foundation for the receipt of the two units as they weigh approximately 190 tons each, the second to provide for secondary containment of any potential spills of hydraulic fluids or hydrocarbons contained within each of the units. With the removal of the rams and drill pipe segments, a second secure facility was necessary to carry out required evaluations. A building on the NASA-Michoud site (Building 411) was identified and prepared for this purpose.

Activities related to the mobilization included:

- Construction of security fencing around the test site and provision of guards for verification of permission to enter the test site
- Siting of a trailer to house an office for on-site technical staff and two additional trailers for evidence storage within the security fence
- Procurement of heavy lift equipment



- Construction of an enclosure around the BOP and LMRP stacks that was resistant to a wind loading of 105 mph
- Development and implementation of safety and environmental plans

5.6 Blowout Preventer Functionality

The forensic investigation as described in this report was both video and photo documented. This documentation was performed from multiple angles and included close-up documentation where details of specific activities or of specific component conditions dictated the need.

Video documentation was accomplished through J.A.M. Video Productions. J.A.M. used Sony A390 Digital Single Lens Reflex cameras with an aspect ratio of 3:2 and a density of 14 Megapixels per photograph. Each picture was recorded in a compressed jpg format in addition to a 'raw' uncompressed format. A variety of video cameras were used, including Sony DSR 570 cameras, with an aspect ratio of 16:9 and recording in High Aspect Definition. Other cameras of various sizes were required and used for examination and recording of information in areas such as the wellbore and ram cavities. The need for lighting was assessed and adjusted accordingly as each activity progressed.

Upon receipt of the BOP stack at the site, a visual examination was performed. Part and serial numbers that were visible were recorded. Internal components of the BOP stack were examined using a camera and video borescope.

The hydraulic circuits on the BOP stack were examined and compared to the most recent working drawings, dated 2004. Modifications and ROV interventions as observed were documented on the 2004 working drawings (Appendix B).

The forensic testing of the BOP stack was performed in accordance with the Forensic Testing Plan for the Forensic Investigation and Testing of the Blowout Preventer & Lower Marine Riser Package Ref – M10PS00234 (Appendix A) and commenced on November 15, 2010. In certain instances, decisions were made to deviate from the original test plan following discussions with the TWG and approval by the JIT where appropriate. From the period of November 15, 2010, to December 23, 2010, the following activities were undertaken:

- Determination of the final position of the annular preventers and rams
- Examination of the condition of the BOP and Lower Marine Riser Package (LMRP) wellbores, rams, and annulars
- Removal of drill pipe from the BOP and LMRP

On December 23, 2010, the forensic investigations and testing stopped for enclosure construction. A temporary enclosure was constructed over and around the LMRP and



BOP on the West Dock. Construction started on December 27 and continued on through January 28, 2011.

During the enclosure construction period the drill pipe segments and rams were moved to Building 411 for cleaning and examination. Following preliminary investigation of the drill pipe removed from the BOP, LMRP and Riser, prioritizations were discussed with the TWG members, agreed and then approved by the JIT. The purpose for prioritization was to focus the remaining function testing on certain critical functions and circuits that were involved in the attempts to control the well during the first two days following the blowout of the well and prior to the rig sinking. Testing at the West Dock test site restarted on January 28 and continued through to March 4, 2011, when the last series of tests were completed.

5.7 Materials Evaluation and Damage Assessment

Materials evaluation included (1) cleaning and examining the BOP rams, (2) cleaning and examining drill pipe segments removed from the BOP and LMRP, (3) cleaning and examining miscellaneous components extracted during the removal of the rams, and (4) sifting through viscous material(s) collected from different ram cavities and the wellbore and collecting and cleaning all solid objects found. Evidence collection included scale and debris from surfaces where appropriate. In addition, for the drill pipe recovered from the LMRP, swabs of the surface for microbiologically influenced corrosion (MIC) testing were performed.

Damage assessment was performed by several methods including (1) visual inspection and photo documentation, (2) dimensional measurements, and (3) three-dimensional laser scanning to characterize the as-received condition of the components. Laser scanning for the BSRs, CSRs, and VBRs recovered from the BOP and for all segments of drill pipe recovered from the BOP, LMRP, and Riser was performed with a FARO Laser ScanARM scanner. The ScanARM scanner is accurate up to ± 0.0014 inches. Laser scanning for select areas of the wellbore was performed with a Nextengine HD Scanner. The HD Scanner is accurate up to ± 0.005 .

Samples were removed from each recovered drill pipe segment to examine the metallurgical and chemical properties of the pipe. Samples were removed from two of the recovered drill pipe segments to examine the mechanical properties (tensile and toughness). The samples to test the mechanical properties were taken from areas representative of the two joints of drill pipe recovered.

Miscellaneous pieces of solid materials/objects were recovered at different stages of the investigation. These materials/objects were inspected, cleaned and entered into evidence indicating the area from which they were recovered. The viscous material collected from different locations was sifted using a 1/4-inch screen. Solid materials/objects were removed, inspected, cleaned, and entered into evidence.



Structural analysis and modeling was used to simulate drill pipe behavior within the wellbore. The modeling package used was ABAQUS™.

5.8 Document Review

The document investigation was implemented by reviewing documents from various information sources. Sources included publicly available information and Government-provided records. Information was available regarding the BOP stack, BOP components, and the events leading up to, during, and following the incident. A comprehensive list of the documents reviewed is provided in Appendix C.

All received documents were initially reviewed by the document investigation team for content and relevance. Documents considered of interest or key to the BOP forensic investigation were subsequently examined in further detail.

The document investigation had three objectives:

- To create a timeline of events prior to, during, and subsequent to the Deepwater Horizon incident that occurred on April 20, 2010
- To provide on-going specific document review support to efforts toward the BOP Functionality testing, the Materials Evaluation and Damage Assessment, and the Cause Analysis
- To identify relevant documents regarding the working configuration of the BOP stack at the time of the incident

5.9 Remotely Operated Vehicle Intervention Operations Review

Remotely Operated Vehicle intervention video footage and still photographs were provided from several ROVs; the Millennium 36 and Millennium 37 from the Boa Sub C, the C-Innovation from the C-Express, and the Hercules 6 and Hercules 14 ROVs from the Skandi Neptune. Other video footage was made available and reviewed on an “as requested” basis.

The ROV video footage was reviewed with two objectives:

- To confirm the times, dates and activities referenced by other sources for the purpose of substantiating and illustrating timeline events
- To provide on going ROV video review support to confirm observations related to the BOP condition, the origin of leaks and modifications to the hydraulic circuitry
- To assess the impact of various ROV interventions undertaken to try and control the well

The ROV footage of primary interest was from the C-Innovation, Millennium 36, and Millennium 37. These three ROVs performed significant interventions following the



incident. Dive logs were reviewed in detail and log entries of specific interest to the condition of the BOP were identified. Such log entries included monitoring of various BOP components, intervention efforts (cutting of the Autoshear pin, ROV hot stab, cutting of hoses, etc.) and identification and repair of leaks in the hydraulic systems. Specific successes/failures during the intervention efforts as well as general observations of BOP condition were noted.

The ROV intervention times and activities were cross-referenced to other supporting documentation where possible. Discrepancies identified were flagged for later confirmation. Times, dates and activities were then included in the “master” timeline that was developed as part of the document review task.

Information relevant to the BOP functionality testing task was relayed to project team members on site in New Orleans. As function testing evolved, requests were made by the project team members in New Orleans to review specific footage relating to the repair of leaks in the hydraulic system to assist in the testing program. In addition, the ROV intervention efforts were re-evaluated following retrieval and metallurgical analysis of the drill pipe, to support the overall effort of determining the sequence of key events that occurred both during and following the incident.

5.10 Failure Cause Analysis

The failure analysis approach used was based on the Systematic Causal Analysis Technique (SCATTM). The technique was developed by DNV to analyze the causes of failures and to assist in making recommendations to prevent future incidents.

The process involved development of a timeline, identification and investigation of key events, determination of both immediate and basic causes of failures, and rationalization and consolidation of causes.

The sequence of events allowed a list of possible contributing causes to be developed. BOP function testing results and information provided by the detailed timeline were then considered. Some possible contributing causes could then be eliminated. The nature of the evidence and the results of the examinations and testing allowed several conclusions to be considered.

6 FINDINGS

6.1 Blowout Preventer Function Testing

This section describes the testing performed on the BOP, LMRP, Yellow and Blue Control Pods and associated components.

6.1.1 Video and Photographic Documentation

In general, video cameras were set up to record ram movement, various pressure gauges, and other relevant features for specific BOP function tests. Still photography was used to document test results, rams, debris and drill pipe removed from the BOP and LMRP.

At the beginning of each day of testing, the schedule of planned activities was reviewed and the video and photo documentation plan for the day was established for the video teams. In addition to the video teams, individual investigators on the DNV Project Team requested and obtained photo documentation of activities on which they were working. All video and photo documentation was logged, backed up and stored in a secure location.

6.1.2 Visual Examination

Visual examination was performed of the external and internal surfaces of the BOP and the LMRP, in the as-received condition at the Michoud facility in New Orleans and as function testing progressed. The purpose of these examinations was to:

- Identify and record visible damage to the major elements and various components that comprise the BOP stack and LMRP
- Identify and record variations between the design of the BOP stack and LMRP as received at the Michoud facility and the original design as per various Cameron drawings
- Record externally visible serial/identification numbers on external components of the BOP and LMRP
- Identify and record the contents or materials that were located within the wellbore or central cavities of the BOP and the LMRP
- Identify and determine best method to extract the materials (including drill pipe) located within the wellbore or central cavities of the BOP and the LMRP
- Assist with planning the sequence of some of the subsequent inspections or tests that were completed as part of the forensic investigations

Table 1 details the ram and annular preventer positions as received and as function testing progressed for both the BOP and LMRP.

**Table 1 Summary of Annular and Ram Positions As Received at Michoud Facility**

Ram or Annular		Position
Upper Annular		Closed
Lower Annular		Open
BSRs	Starboard	Closed
	Port	Open
CSRs	Starboard	Open
	Port	Open
Upper VBRs	Starboard	Closed
	Port	Closed
Middle VBRs	Starboard	Closed
	Port	Closed
Lower VBRs	Starboard	Closed
	Port	Closed

Additional findings relevant to the forensic investigation are discussed in other sections of this report.

6.1.3 Fluid Collection and Analysis

Fluid sampling was performed throughout the BOP function testing. Samples were collected from hydraulic circuits, from debris found in the BOP and LMRP wellbore and during the removal of the ram blocks. The BOP and LMRP wellbores were both filled with StackGuard upon arrival at the Michoud Site to provide some protection against degradation of evidence. It was necessary to remove the StackGuard in order to perform visual examination, function testing and retrieval of drill pipe and debris from the wellbores.

Samples of the StackGuard from both the BOP and LMRP were collected during the draining of the wellbores. Samples were collected either directly into sterile containers or captured in sterile plastic lined trays and transferred to sterile containers. Samples were catalogued and sealed for further analysis before removal to a secured storage location. Samples were collected either under the supervision of the Environmental Protection Agency (EPA) or in accordance with EPA recommended sample protocols. A list of all samples collected is contained in Appendix D.

Twenty-three samples of fluids collected from the lower BOP and the LMRP were analyzed at the EPA's National Enforcement Investigations Laboratory in Denver, Colorado. The samples submitted for analysis were from the ST Lock operator and hoses, the open and close operators of the BSRs, CSRs and VBRs and one sample from the LMRP. The EPA also obtained, a representative sample of the ethylene glycol based



hydraulic fluids “Stack Guard” and “Aqualink 325-F” from the manufacturer and analyzed each of these to serve as a reference. Three ‘travel blanks’ all consisting of one liter of reagent grade water that were then shipped or transported to the Denver laboratory along with the other samples were also analyzed. All the samples were analyzed using the following techniques²:

- Water Content by Coulometric Karl Fischer Titration,
- Ethylene glycol and 2-butoxy ethanol by Gas Chromatography/Mass Spectrometry,
- Percent solids analysis by refractometer,
- Dissolved elemental constituent analysis by EPA Method 200.7,
- Dissolved bromine analysis by Inductively Coupled Plasma Mass Spectrometry,
- Dissolved anion analysis by EPA Method 300.0, Part A
- Monoethanol amine and triethanol amine by Liquid Chromatography/Mass Spectrometry,
- Organic constituent analysis by Nuclear Magnetic Resonance Spectrometry,
- Organic constituent analysis by Raman Spectrometry.

6.1.4 Drill Pipe Removal

Pieces of drill pipe were present upon arrival at the Michoud site in the BOP, LMRP (one piece in each) and Riser segment recovered prior to retrieval of the stack. Removal and preservation of these pieces of drill pipe was given priority in the forensic investigation.

6.1.4.1 Removal of Drill Pipe from LMRP

The drill pipe segment lodged in the Upper Annular was inspected following draining of the LMRP and removal of the flex joint from the UA. The upper portion of the drill pipe segment was deformed so that it was significantly out of round. An unsuccessful attempt had been made subsea prior to retrieval of the stack to remove this segment, resulting in the piece slipping down and wedging into the metal fingers of the UA packing element. There was insufficient length of the drill pipe segment above the packing element fingers to secure a safe hold for lifting the segment out of the LMRP. A tool was designed and fabricated such that it could be inserted into the flared end of the drill pipe segment, lowered past the deformed portion and rotated 90° to lock into place on the inside diameter (ID) of the pipe. Wood wedges were inserted between the tool and the drill pipe ID to prevent the tool from rotating during removal. The drill pipe was removed from the LMRP wellbore using a mobile crane. After removal it was moved to a secure storage facility for further examination.

² Analytical Results, Deep Water Horizon, New Orleans, Louisiana – NEICRP138R01



6.1.4.2 Removal of Drill Pipe from BOP

The drill pipe segment in the BOP wellbore was located just below the CSRs and was held in place by the closed Upper and Middle VBRs. The end of the drill pipe segment nearest the CSRs was packed with pieces of debris. An initial attempt was made to collect a sample of this debris first with a poly-vinyl chloride pole and then with an aluminum pole. Both attempts were unsuccessful. It was determined that the debris was tightly packed and would not become dislodged. The decision was taken to remove the drill pipe segment and collect a sample of the debris afterwards. The Upper and Middle VBRs had to be retracted and removed in order to secure a safe hold on the drill pipe segment. There was a significant amount of cementitious material in the wellbore between the Upper and Middle VBRs that had to be chiseled out and removed by hand before the Middle VBRs could be retracted. Extensive damage had occurred on the drill pipe segment where the Upper and Middle VBRs were closed around the drill pipe. It was necessary to use two lifting slings on the drill pipe to ensure that it would not be further damaged during removal. It was lifted from the BOP wellbore using a mobile crane. No debris fell from the drill pipe during removal from the BOP wellbore. After removal the drill pipe was moved to a secure storage facility in anticipation of further examination.

6.1.4.3 Removal of Drill Pipe from the Riser

One section of riser from the Deepwater Horizon was present that contained drill pipe that was relevant to the investigation. This section of riser came from the last riser joint in the drilling riser string that was connected to the Flex Joint atop the LMRP. This joint of riser “kinked” when the Deepwater Horizon sank. During ROV intervention this joint was saw cut and subsequently mechanically sheared just above the Flex Joint interface. The recovered riser section was from above the mechanical shear point and contained the “kink” and approximately 45-ft of riser above the “kink”. Prior to DNV’s involvement in the investigation, “windows” were cut into the riser such that some portions of the pieces of drill pipe were exposed. In the window nearest the bottom of the riser section (nearest to the BOP stack), two drill pipe sections were visible in the riser. For the window nearest the top of the riser section (farthest from the BOP stack), only one section of drill pipe was present.

A borescope was inserted into the riser section in order to examine the exterior surface of the drill pipe pieces and determine if any obstructions were present. Following the borescope inspection, a series of cuts was defined in order to remove the drill pipe pieces from the riser. All cuts with the exception of the final cut were made with an oxyacetylene torch. The final cut was made using a saw. Following completion of the cuts, the drill pipe pieces were removed from the riser sections using a mobile crane and lifting straps. The pieces were transported to a secure storage facility for further examination.

6.1.5 ST Locks

This section describes the testing performed on the ST Locks located on the hydraulic operators of the BSRs, Upper, Middle and Lower VBRs. ST Locks are designed to provide a mechanical lock and maintain the closed position of the ram blocks even if hydraulic pressure is bled off the operator. Fluid samples were collected from all of the ST Locks. The as received positions of all ST Locks were measured.

The position of each ST Lock was determined by measuring the position of the wedge lock piston through an inspection plug located on the opening chamber endcap of the ST Lock assembly. Prior to measurement, it was necessary to drain fluid from each ST Lock assembly. Fluid samples were collected during the draining process. Measurements were obtained by inserting a calibrated ruler through the inspection plug port until it contacted the flat face of the opening side of the wedge lock piston. ST Lock position measurement commenced on the starboard side Lower VBR and progressed up the starboard side to the BSR. Measurement then continued on the port side, beginning with the BSR and progressing down the port side to the Lower VBR. Two measurements were taken at each location.

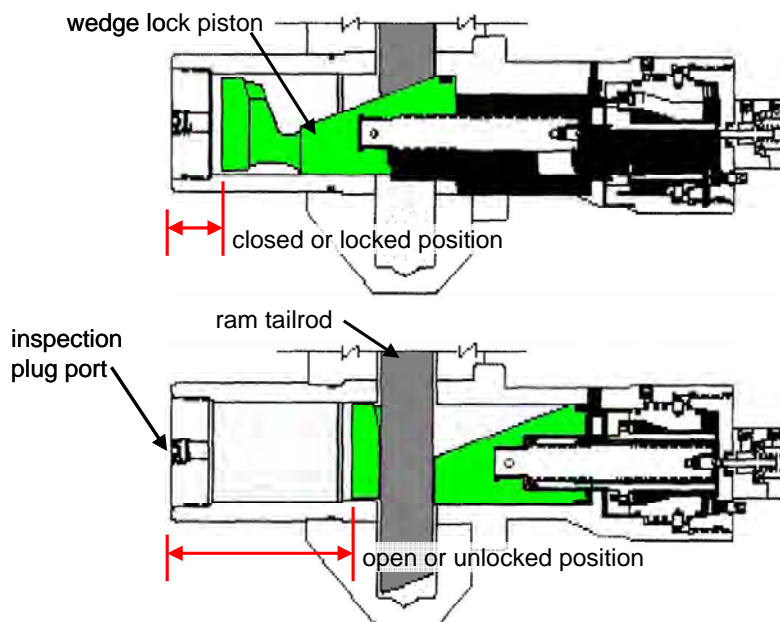


Figure 7 ST Lock Measurements

Figure 7 illustrates the measured features and reference point (inspection plug port). The length of the measurement indicates the position of the ST Lock and gives an indication of the ram block position. Measurements in the range of 14 inches indicate the wedge lock piston is in the open position. Measurements in the range of 3 to 5 inches indicate the wedge lock piston is in the closed position and the ram block is extended into the wellbore at or near the fully closed position. Variances in measurements are a result of



two effects: (1) different types of rams (BSRs or VBRs) have different close positions and (2) opposing ram blocks are not perfectly centered when closed. For the former effect, different types of rams have different stand-off or gaps between opposing ram blocks when in the closed position. This means that the hydraulic pistons in the ram operators end up at different positions when fully closed depending upon the ram type. For the latter effect, opposing ram blocks travel at slightly different rates when stroking closed. One ram block will always reach the wellbore center first and therefore will have stroked slightly further closed than its counterpart. These piston positions are rarely equal and subsequently it is not abnormal for the positions of the wedge lock pistons to be unequal. Table 2 shows the results of the ST Lock position measurements.

Table 2 ST Lock Position Measurements

Ram Type	Measurement of Wedge Lock Piston (inches)			
	Starboard		Port	
BSRs	14-5/8	14-5/8	14-5/8	14-5/8
Upper VBRs	4-15/16	4-15/16	3-3/8	3-3/8
Middle VBRs	3-7/16	3-7/16	4-1/2	4-1/2
Lower VBRs	5-3/8	5-3/8	14-3/16	14-3/16

The results of the measurements indicated that the ST Locks for the BSRs were fully open (unlocked). The ST Locks for the Upper and Middle VBRs were in the closed (locked) position. For the Lower VBRs, the port side ST Lock was closed (locked) and the starboard side ST Lock was in the open position (unlocked). Even though the starboard side ST Locks on both the BSRs and the Lower VBRs were unlocked, the ram blocks themselves were found in the closed position (reference Table 1).

Functioning of the ST Locks was performed in conjunction with ram block functioning. Discussion of pressures required to function the ST Locks can be found in Section 6.1.7.

6.1.6 Lower Choke and Kill Valves

The Lower Inner and Outer Choke and Kill Valves were functioned opened in order to access and drain wellbore fluid from the BOP stack. The Lower Choke Valves are connected to the BOP stack, intersecting the wellbore just below the Middle VBRs. The Lower Kill Valves are connected to the BOP stack, intersecting the wellbore just below the Lower VBRs. The Choke and Kill Valves are fail-safe close, meaning continuous hydraulic pressure is required to hold the valves open. A spring system in the hydraulic actuators closes the valve upon loss of hydraulics. The Inner and Outer Valves (both Choke and Kill) function as a pair with interconnected hydraulics. All of the Choke and Kill Valves were found in the closed position as received. The Lower Choke Valves were opened first on December 3, 2010. The maximum pressure applied was 500 psig. The Lower Kill Valves were opened on December 7, 2010. The maximum pressure applied

was 1,000 psig. No abnormalities were observed in the functioning of the Lower Choke and Kill Valves.

6.1.7 Functioning and Removal of Ram Blocks

As part of the process for visual examination and removal/extraction of materials (including drill pipe) located within the wellbore or central cavities, the ram blocks for the BSRs, CSRs, Upper, Middle and Lower VBRs were removed in sequence from top to bottom.

6.1.7.1 Ram Operator Fluid Sampling

Prior to any functioning, fluid samples were obtained from the ram operators. Samples were taken through fluid ports intersecting the opening and closing chambers by removal of National Pipe Thread (NPT) hex plugs. These locations were chosen deliberately as access points that were undisturbed since installation during the manufacture/assembly of the BOP. The NPT hex plugs were first visually examined for any indication of leakage. Due to the long-term undisturbed condition, the hex plugs required heating up with a MAPP® torch and break-out with an impact wrench.

Fluid sampling commenced with the starboard BSR. Sampling moved to the port BSR, and down the port side of the BOP on the Upper, Middle and Lower VBRs. Sampling continued with the starboard Upper VBR and continued down the starboard side concluding with the Lower VBR. Samples were obtained from the open and close sides of the port and starboard operators for the Upper, Middle, Lower VBRs. Only samples from the port open and close side and the starboard close side of the BSRs operators could be obtained. Attempts to draw a fluid sample from the open side of the starboard operator for the BSRs were unsuccessful.

6.1.7.2 Preparation for Ram Block Removal

Prior to the functioning of any of the rams, the bonnet cap nuts that connect the ram bonnets to the body of the BOP were first loosened and removed. The breakout torques required to loosen the bonnet cap nuts were recorded and are listed in Appendix E.

After the bonnet cap nuts were removed, extension sleeves were installed to act as both a guide and support for the bonnets. High pressure hoses were installed on both the open and close shuttle valves. A pressure chart, gauges, and flow meter were installed to monitor the pressure and volume used during the operating of the rams.

6.1.7.2.1 BSRs and CSRs

Since the starboard side BSR had not successfully opened when functioned on the Q-4000, it was decided to remove the port side BSR first and perform a visual inspection of the starboard side BSR to determine if there was any debris or damage causing the ram



not to move. In order to prevent the port side ram from extending into the wellbore and potentially contacting the starboard side ram, the port side bonnet had chain falls connected and tensioned to ensure that the port side bonnet would move back instead of the port side ram moving into the wellbore. The bonnet nuts were kept on the starboard side bonnet to keep it from opening. Hydraulic pressure was applied to the close shuttle valve of the BSRs and the port side bonnet opened. Debris was removed from the ram cavity as the bonnet opened, captured in a plastic lined tray, transferred to sterile containers and removed to a secured storage location. A sled was positioned between the port side bonnet and BOP to prevent the bonnet from closing while supplying open pressure. Open pressure was supplied through the open shuttle valve to retract the port side ram from the BOP cavity. The port side BSR was removed and lowered to the ground. It should be noted that when open pressure was supplied through the open shuttle valves, hydraulic pressure was applied to both BSRs. As with previously on the Q-4000, the starboard side BSR did not retract from the wellbore.

Following removal of the port side BSR, a visual inspection of the underside of the starboard side BSR did not reveal any damage which could explain the reason for not retracting. The starboard side bonnet bolts were removed and hydraulic pressure was applied to the close shuttle valve of the BSRs. The starboard side bonnet fully retracted. Debris was removed from the ram cavity as the bonnet opened, captured in a plastic lined tray, transferred to sterile containers and removed to a secured storage location. A sled was positioned between the starboard side bonnet and BOP to prevent the bonnet from closing while supplying open pressure. Open pressure was supplied through the open shuttle valve to retract the starboard side ram from the BOP cavity. After debris was removed from behind the ram block, the starboard side BSR was retracted, removed and lowered to the ground.

The CSR bonnets were opened manually using chain falls. Once the CSR bonnets are opened, the ram blocks are normally extracted by removing a pin that fastens the ram block to the operator connecting rod. This pin on the port CSR was bent. The pin on the starboard CSR was broken. The port CSR was lifted slightly with slings to remove the weight and binding on the connecting rod and the pin was able to be removed. Opening pressure was applied to retract the connecting rod from the ram block. It took less than 50 psig to retract the connecting rod. When opening pressure was applied to the starboard CSR (in an attempt to retract the connecting rod), the connecting rods seals leaked hydraulic fluid. In order to remove the starboard CSR, the block was first fully extended closed (using less than 50 psig). During extension, the entire wellbore-side connecting rod seal assembly came out of the bonnet. No retainer ring was present to hold the seal assembly in place. Once the block was fully extended, hydraulic bottle jacks were fitted between the back of the block and bonnet face using wood for spacers. The block was jacked forward away from the bonnet face, shearing the remainder of the broken pin and moving the block off the connecting rod. The connecting rod was retracted with less than 50 psig opening pressure. A damaged connecting rod seal was observed on the starboard CSR. Once free of the connecting rods, the rams were lowered to the ground.



6.1.7.2.2 Upper, Middle and Lower VBRs

The following procedure was used for all the VBRs. Pressure was first supplied to the close shuttle valve. Close pressure resulted in the bonnets moving open onto the extension sleeves. Debris found behind the blocks were removed from the ram cavity (as the bonnets opened) and captured in a plastic lined tray. After opening the bonnets, a sled was positioned between each bonnet and BOP to prevent the bonnet from closing while supplying open pressure. Open pressure was supplied through the open shuttle valve to retract the rams. Once retracted, lifting eye bolts were connected to each ram and the rams were moved off the connecting rods. Once free of the connecting rods, the rams were lowered to the ground.

After all ram blocks had been removed to ground level, they were cleaned and moved to Building 411 for further examination.

Table 3 details the pressures required to function the various rams. Pressures indicated with an asterisk were observed and recorded minimum pressures when the specific ram block began moving, otherwise the pressure indicated is the maximum pressure recorded during function.

Table 3 Pressure Required to Function Rams

Ram	Starboard Close (psig)	Starboard Open (psig)	Port Close (psig)	Port Open (psig)
BSR	800*	50*	300*	50*
CSR	less than 50	less than 50	No pressure applied	less than 50
Upper VBR	1,400	1,100	1,400	1,100
Middle VBR	700*	600	800*	600
Lower VBR	700*	800*	600*	800*

* Minimum pressure observed during the function.

6.1.8 AMF/Deadman and Autoshear Testing – Hydraulic Circuits

The automatic mode function (AMF)/Deadman and Autoshear function testing was designed to simulate two of the sequences that can automatically secure the well using the BOP stack during an emergency situation. The sequences are described below and discussed in additional detail later in this report. In accordance with API 16D, Section 5.2.1 ³Response Time (for subsea BOP stack control systems), the closing response time for each ram BOP must not exceed 45 seconds for the primary control system.

³ API SPEC 16D Specification for Control Systems for Drilling Well Control Equipment and Control Systems for Diverter Equipment, Second Edition



AMF/Deadman and Autoshear systems are considered by API 16D to be backup control systems and not subject to the response time requirement of the primary system. For purposes of these hydraulic circuit tests, the 45-second response was adopted as a comparison target for the closing of the BSR connecting rods,

The AMF/Deadman sequence is designed to be initiated when three forms of supply are all lost from the rig to the control pods; hydraulic pressure, electrical power, and communication from rig control systems. Additionally, these conditions (loss) must apply to both pods for AMF/Deadman to activate. Hydraulic pressure is supplied through the rigid conduit. Electrical power and control system communication are supplied through the MUX cables. Communication between the two pods to verify the status of hydraulic pressure and the MUX cables for each pod is accomplished through an RCB cable. AMF/Deadman is controlled through the subsea electronic modules (SEMs) on the Yellow and Blue pods. When the AMF/Deadman sequence is activated the BSRs are closed via the high pressure shear circuit with hydraulic fluid supplied by a dedicated bank of 8 x 80-gallon accumulators on the BOP.

The Autoshear sequence is designed to be initiated when the LMRP and BOP stack become unintentionally separated. A hydraulic plunger is fixed between the LMRP and BOP stack which maintains pressure and holds a control valve in closed position. When separation occurs, the plunger is released and relieves the hydraulic pressure on the control valve. A spring return on the control valve shifts, sending a pilot signal to open a high pressure shear control valve and send hydraulic supply from the high pressure shear circuit to the closing ports of the BSRs. The Autoshear function has to be intentionally armed; otherwise, the hydraulic supply from the high pressure shear circuit is blocked by another control valve. The unintentional separation between the LMRP and BOP stack also results in the Choke and Kill valves functioning close (fail-safe close).

6.1.8.1 Accumulator Functioning

The AMF/Deadman and Autoshear tests relied on the accumulator bottles (8 x 80 gallon) located on the BOP. The accumulator bottles consist of a nitrogen gas pre-charge side and a hydraulic chamber. The level of nitrogen pre-charge determines both the amount of hydraulic fluid (volume) and the average pressure the fluid can be delivered to a given function. There is a direct relationship between the nitrogen pre-charge level and the amount of hydraulic fluid that can be put into the hydraulic chamber. The pre-charge level is set to provide a balance between available volume at an average useable pressure.

The AMF/Deadman and Autoshear sequences were tested both in the as-received condition and in a reduced accumulator pre-charge condition. The as-received condition was tested first and then nitrogen was bled from the accumulator bottles to reduce the pre-charge pressure to compensate for lack of external hydrostatic pressure (subsea conditions at a water depth of approximately 5,000 feet).



6.1.8.1.1 As-Received Condition

The as-received pre-charge pressures in the high pressure shear circuit bank (8 x 80 gallons) on the BOP and the accumulator bank (4 x 60 gallons) on the LMRP were measured and recorded. Following the initial measurement, the accumulator dump function was performed for both banks in order to remove any hydraulic fluid that may have been present in the accumulators. There was no hydraulic fluid in the high pressure shear circuit bank. Hydraulic fluid present in the LMRP accumulator bank was sampled for further examination and the remainder collected for proper disposal. The existing pre-charges were then re-measured without any hydraulic fluid present. The pre-charge in the high pressure shear circuit bank (8 x 80 gallons) on the BOP ranged from 3425 to 3800 psig. For the accumulator bank (4 x 60 gallons) on the LMRP, the pre-charge in three of the accumulators ranged from 3400 to 3425 psig. The pre-charge in the fourth (labeled accumulator #1) was 1225 psig. The measured pre-charge was in proximity to levels set in accordance with the guidance provided in Transocean's Well Control Manual (i.e., 1500 psig [$\sim 1/3$ of the pressure for the high pressure shear circuit of 5000/4000 psig] plus the hydrostatic head of 2200 psig = 3700 psig). The only exception was accumulator #1 of the LMRP accumulator bank. The results are detailed in Appendix E.

6.1.8.1.2 Reduced Pre-Charge Condition

After completing measurements of the as-received pre-charge levels and performing AMF/Deadman and Autoshear sequence tests, the accumulator pre-charges were set to between 1,325 and 1,350 psig to compensate for operating at surface conditions (lack of external hydrostatic pressure from subsea conditions at a water depth of approximately 5,000 feet). The accumulator pre-charges were reduced by bleeding nitrogen from each accumulator. After the pre-charges were reduced, the accumulators were tested for leaks and pressure drop-off by checking the pre-charge levels after allowing the accumulators to settle for a period of approximately 12 hours. No leaks were observed.

6.1.8.1.3 BOP Accumulator Pressurization

The BOP accumulators (high pressure shear circuit bank) were hydraulically filled and pressurized in preparation for each AMF/Deadman and Autoshear function test. During the first pressurization of the BOP accumulators, a leak was discovered on the High Pressure (HP) Casing Shear Regulator. The pressure in the accumulators at the time of leak discovery was 3,500 psig.

It was decided to perform a static pressure test on the HP Casing Shear Regulator. Pressure was increased on the BOP accumulators and a leak containment device was installed below the HP Casing Shear Regulator. A video camera was used to monitor the leak rate of the HP Casing Shear Regulator during the entirety of the static pressure test.

At the conclusion of the test, the pressure in the BOP accumulators had dropped from 3,700 psig (start of test) to 400 psig. Approximately 1.5 gallons of fluid leaked from the



HP Casing Shear Regulator. The leak rate at the start of the test and was 144 drops per minute. The leak rate at the end of the test was 86 drops per minute. All leak rates were determined from review of video footage. The duration of the test was approximately 15 hours and 40 minutes.

The HP Casing Shear Regulator was removed in order to prevent the potential for damage that could occur during function testing. In the place of the regulator, a pressure gauge and plug were installed to permit continuation of the function testing.

The static pressure test of the BOP accumulators was re-run overnight. The starting pressure was approximately 4,000psig. The pressure did not change from the beginning to the end of the test. The duration of the test was approximately 14 hours and 22 minutes.

After completing the static pressure test, the BOP Accumulators were pressurized to 5,000 psig to prepare for function testing. A pressure gauge installed between the Autoshear panel and the Autoshear control read 0 psig during pressurization of the accumulators to 5,000 psig, confirming that the Autoshear function was in the disarmed state in the as-received condition. The Autoshear function was likely disarmed after the Control Pods were retrieved by the Q-4000.

Preceding each AMF/Deadman and Autoshear test, the BOP accumulators were drained of hydraulic fluid and then re-pressurized to 5,000 psig.

6.1.8.2 AMF/Deadman Testing

The hydraulic circuit portion of the AMF/Deadman function testing focused on the actual sequence of hydraulic functions that occur on the lower BOP during AMF/Deadman, not the electronics of the AMF/Deadman function. See Section 6.1.13.1 for detailed information regarding the electronic function testing. The AMF sequence of hydraulic functions is comprised of high pressure shear close (including ST Locks–lock), control pod LMRP and Stack Stingers extend and seals energized. These functions are initiated through the high pressure shear control valve on the high pressure shear circuit. The ST Locks–lock is integrated into the high pressure shear circuit and is supplied hydraulically when the AMF/Deadman activates through Solenoid 103. To simulate the initiation of an AMF/Deadman sequence, a high pressure hydraulic hose was connected to either the blue or yellow side of Solenoid 103. This was used to supply pilot pressure to high pressure shear control valve. Additional hoses and pressure gauges were installed on the connected hydraulic circuits to monitor and record the test results. In addition to the installed hoses and pressure gauges, video cameras were arranged to monitor the position of the connecting rods and the readings on the pressure gauges.

Pressure gauges were installed on the port and starboard ST Lock hoses, on the high pressure shear/BSR close hydraulic hose, at the removed casing shear regulator to monitor accumulator pressure, between the Autoshear panel and Autoshear control valve,



and at the manifold connected to the hydraulic pressure unit used to pressurize the accumulators and initiate the function.

The hydraulic fluid supplied from the BOP accumulators to close the BSRs is regulated to 4,000 psig through the high pressure shear regulator. The hydraulic fluid supplied from the BOP accumulators to function ST Locks–lock is regulated to 1,500 psig through the ST Locks pressure regulator. The maximum pressure that each hydraulic circuit received from the accumulators was recorded.

6.1.8.2.1 AMF/Deadman Testing – As-Received Pre-Charge

The AMF/Deadman sequence was initiated using the as-received pre-charge and the accumulators filled and pressurized to 5,000 psig hydraulic pressure. The maximum pressure shown on the BSR pressure was 3,850 psig. The BOP accumulator pressure after the function was 4,475 psig. The BSRs closed in 23 seconds. The maximum pressure shown on the pressure gauges for the starboard BSR ST Lock was 1,500 psig and 1,525 psig for the port BSR ST Lock. The starboard BSR ST Lock position was 3-5/8 inches and the port BSR ST Lock position was 3-3/8 inches. This confirmed that both BSR connecting rods were in the closed position. The volume to close was 26.4 gallons. The sequence test functioned as intended.³

6.1.8.2.2 AMF/Deadman Testing – Reduced Pre-Charge

The AMF/Deadman test using reduced pre-charge was run twice. During the first test a small leak was discovered between the test hydraulic supply line and AMF shuttle valve caused during test setup. The leak allowed the residual BOP accumulator pressure to vent to atmosphere after the test sequence was completed. The leak was corrected and a second test was run in order to capture an accurate residual pressure reading.

6.1.8.2.3 Test 1

The AMF/Deadman sequence was initiated using the reduced pre-charge and the accumulators filled and pressurized to 4,975 psig. The BSR connecting rods closed in 24 seconds. The maximum pressure shown on the BSR close pressure gauge was 3,900 psig. The BOP Accumulator pressure after the function was not able to be measured due to fluid being discharged from the high pressure blind shear vent. The maximum pressure shown on the starboard BSR ST Lock was 1,460 psig and 1,450 psig on the port BSR ST Lock. The BSRs were confirmed visually closed using a video camera in the wellbore. The volume to close was 25.3 gallons. The sequence test functioned as intended.³ The leak in the test hydraulic line/AMF shuttle valve interface was discovered after the sequence had completed.



6.1.8.2.4 Test 2

The AMF/Deadman sequence was initiated using the reduced pre-charge and the accumulators filled and pressurized to 5,000 psig. The maximum pressure shown on the BSR close pressure gauge was 3,800 psig. The BOP accumulator pressure after the function was 4,125 psig. The BSR connecting rods closed in 24 seconds. The maximum pressure shown on both the starboard and port BSR ST Locks was 1,400 psig. The BSR connecting rods were confirmed visually closed using a video camera in the wellbore. The volume to close was 24.4 gallons. The sequence test functioned as intended.³

6.1.8.3 Autoshear Testing

The Autoshear function was initiated by supplying pilot pressure through either the Blue or Yellow Pod side of Autoshear Arm shuttle valve 121. Since the hydraulic plunger was cut by ROV intervention, the spring return control valve was in the open position. By activating Autoshear Arm, pilot pressure was supplied through the control valve to the high pressure shear pilot valve.

6.1.8.3.1 Autoshear Function Testing – As-Received Pre-Charge

The Autoshear function was initiated using the existing pre-charge and the BOP accumulators filled and pressurized to 5,000 psig. The BSR connecting rods closed in 28 seconds. The highest pressure recorded on the Autoshear valve pressure gauge was 3,150 psig. The highest pressure recorded on the HP BSR close gauge was 3,800 psig. The maximum pressure on both the starboard and port BSR ST Lock pressure gauges was 1,500 psig. The starboard BSR ST Lock position was 3-5/8 inches and the port BSR ST Lock position was 3-5/16 inches. This confirmed that both connecting rods were in the closed position. The volume to close was 28.1 gallons. The sequence test functioned as intended.³

6.1.8.3.2 Autoshear Function Testing – Reduced Pre-Charge

The Autoshear test using reduced pre-charge was run twice. After the first test, during dump of the accumulator pressure, a return hose to a fluid tank became unsecured and an unknown volume of fluid was lost. A second test was run in order to obtain an accurate reading of fluid returned after sequence test and accumulator dump.

6.1.8.3.3 Test 1

The Autoshear function was initiated using the reduced pre-charge and the BOP accumulators filled and pressurized to 5,000 psig. The BSR connecting rods closed in 26 seconds. The highest pressure recorded on the Autoshear valve pressure gauge was 3,150 psig. The highest pressure recorded on the BSR close pressure gauge was 3,825 psig. The BOP accumulator pressure after the function was 4,000 psig. The maximum pressure on both the starboard and port ST Locks was 1,500 psig. The



starboard BSR ST Lock position was 3-1/2 inches and the port BSR ST Lock position was 3-5/16 inches. This confirmed that both connecting rods were in the closed position. The volume to close was 29.9 gallons. The sequence test functioned as intended.³

6.1.8.3.4 Test 2

The Autoshear function was initiated using the reduced pre-charge and the accumulators filled and pressurized to 4,900 psig. The BSR connecting rods closed in 26 seconds. The highest pressure recorded on the Autoshear valve pressure gauge was 3,300 psig. The highest pressure recorded on the BSR close pressure gauge was 3,850 psig. The BOP Accumulator pressure after the function was 3,900 psig. The maximum pressure on the starboard BSR ST Lock was 1,500 psig. The maximum pressure on the port BSR ST Lock was 1,475 psig. The BSR connecting rods were confirmed visually closed using a video camera in the wellbore. The volume to close was 24 gallons. The sequence test functioned as intended.³

After running the Autoshear system test using the reduced pre-charge, the BSR connecting rods failed to retract with an open pressure of 3,000 psig applied. A Cameron TWG member indicated that damage to the ST Lock bearings could cause unlocking problems and that repeated use of an ST Lock with a bad bearing could make the problems more severe. It was decided to replace the bearings on both the starboard and port ST Locks. Following replacement of the bearings, the ST Locks were opened and the BSR connecting rods were retracted. After the BSR connecting rods were opened, it was decided to bypass the ST Locks on the BSRs for future tests.

6.1.9 Remotely Operated Vehicle Panel Testing

The BSR close function on the ROV Panel was function tested using three different flow rates: 1, 2 and 7.5 gallons per minute (gpm). A hot stab supplied by a high pressure accumulator unit was used to supply hydraulic pressure to the ROV Panel BSR close port. The time needed for the BSRs to close when supplied with 3 different flow rates was measured and recorded. The initial setup used a high pressure pump to directly supply hydraulic pressure. The first test, using a flow rate of 1 gpm and the high pressure pump resulted in an inconsistent flow rate. The test setup was changed so that the hydraulic accumulators were used to supply pressure to the ROV panel.

The low flow rate test was re-run using the Hydraulic Pressure Unit (HPU) equipped with accumulators capable of supplying 3,000 psig. The accumulators were charged to 3,000 psig for the testing. Unlike previous BSR function tests, the hydraulic pressure supplied to the ST Locks is not separately regulated from the BSR closing pressure when functioned using the ROV Panel. After the BSR connecting rods were fully closed, a static leak test was performed for 15 minutes. There were no observable leaks for 1 gpm and 7.5 gpm flow rate static tests. For the 2 gpm flow rate test a leak was observed at a test setup fitting. It was corrected and the static test re-run for 15 minutes with no

observable leaks. Table 4 lists the recorded time to close and maximum applied pressures for each of the flow rates. There are no specific API or industry response time requirements for ram closure by ROV intervention.

Table 4 ROV Panel BSR Close Function Test

Flow Rate (gpm)	Time to Close BSRs (min:sec)	BSR ST Lock Max Pressure (psig)	
		Starboard	Port
1	72:28	2,850	2,750
2	13:34	2,850	2,775
7.5	3:15	2,900	2,875

6.1.10 Solenoid 103 Bench Testing

Solenoid 103 when activated supplies pilot pressure to the High Pressure Shear Ram Close shuttle valve, which is located on the High Pressure Shear Panel. Solenoid 103 is used for both EDS and AMF/Deadman sequences. Solenoid 103Y from the Yellow Pod was removed during intervention activities after the Yellow Pod was lifted to surface. The original Solenoid 103Y was removed, replaced with a new solenoid, and taken into evidence to allow for future testing.

The original Solenoid 103Y was tested for the resistance of both the A and B coils and for the voltage necessary to energize each coil. An initial voltage of 24 volts was applied. If the coil energized (indicated by an audible click), then the voltage was reduced until the coil de-energized (also indicated by an audible click). This determined the drop-out voltage. Starting voltage was then set at 0 volts and increased in one volt increments until the coil energized. This determined the coarse minimum voltage necessary to energize the coil. The minimum voltage was determined more precisely by setting the starting voltage to 2 volts lower than the coarse minimum voltage and manually increasing the voltage applied until the coil energized.

The resistance for coil A was 39.7 ohms. The resistance for coil B was 39.7 ohms. The resistance measurements between each of pins 1 through 4 and the solenoid chassis were greater than 20 megaohms. The minimum voltage at which coil A was energized was 14.6 volts. The dropout voltage for coil A was 1.9 volts. The minimum voltage at which coil B was energized was 14.5 volts. The dropout voltage was 1.8 volts. The bench testing of the original Solenoid 103Y functioned as intended in accordance with the manufacturer's specifications.⁴

As a result of functioning as intended, the original Solenoid 103Y was mounted back onto the Yellow Pod.

⁴ Refurbishment Procedure for Cameron Solenoid Valves Part No. 223290-15 and 223290-60; January 23, 2004 – CAMCG 00004025 to CAMCG 00004038



6.1.11 Solenoid 3A Bench Testing

Solenoid 3A when activated supplies hydraulic fluid to the Upper Annular Regulator Pilot – Increase, which is located on the LMRP. Solenoid 3A from the Yellow Pod was removed during intervention activities after the Yellow Pod was lifted to the surface. The original Solenoid 3A was removed, replaced with a new solenoid, and taken into evidence to allow for future testing.

The original Solenoid 3A was tested for the resistance of both the A and B coils and for the voltage necessary to energize each coil. An initial voltage of 24 volts was applied. If the coil energized (indicated by an audible click), then the voltage was reduced until the coil de-energized (also indicated by an audible click). This determined the drop-out voltage. Starting voltage was then set at 0 volts and increased in one volt increments until the coil energized. This determined the coarse minimum voltage necessary to energize the coil. The minimum voltage was determined more precisely by setting the starting voltage to 2 volts lower than the coarse minimum voltage and manually increasing the voltage applied until the coil energized.

The resistance for coil A was 40.0 ohms. The resistance for coil B was 40.0 ohms. The resistance measurements between each of pins 1 through 3 and the solenoid chassis were greater than 20 megaohms. The minimum voltage at which coil A was energized was 14.8 volts. The dropout voltage for coil A was 2.2 volts. The minimum voltage at which coil B was energized was 14.8 volts. The dropout voltage for coil B was 2.2 volts. The bench testing of the original Solenoid 3A functioned as intended in accordance with the manufacturer's specifications.⁴

6.1.12 Blue and Yellow Pod Battery Voltage and Load Testing

The as-received voltage of the SEM A and SEM B 9 volt batteries and the 27 volt battery was measured on both the Blue and Yellow Pods. The measured voltages are shown in Table 5. The 27V battery on the Blue Pod registered a low voltage. No abnormalities were noted with the voltages from the remaining batteries.

Table 5 Blue and Yellow Pod Battery Voltages Measurements

Battery	Blue Pod (Volts)		Yellow Pod (Volts)	
	Test 1	Test 2	Test 1	Test 2
SEM A (9V)	8.9	8.9	8.7	8.7
SEM B (9V)	8.7	8.7	8.4	8.4
Solenoid/Transducer (27V)	1.1	1.0	28.2	28.2

The Blue and Yellow Pod batteries are lithium-ion type. A load test was conducted to determine if the batteries would maintain their voltage after a current load was applied. The batteries were load tested with 100-ohm and 20-ohm resistors. The 100-ohm load was chosen as an initial low current load test. The 20-ohm was chosen to simulate the



demand seen by activation of the AMF/Deadman circuit. After load was applied, an initial reading was taken followed by a second reading after 2 minutes. Two minutes was chosen based on the fact that the AMF/Deadman sequence is active (and demanding power from the batteries) for approximately 90 seconds. The results are detailed in Table 6. Because the 27V battery on the Blue Pod registered a low voltage, it was not load tested.

Table 6 Blue and Yellow Pod Battery Load Test Results

	Yellow Pod				Blue Pod			
	Load				Load			
	100 Ohm		20 Ohm		100 Ohm		20 Ohm	
Battery	Voltage				Voltage			
	Initial	After 2 min	Initial	After 2 min	Initial	After 2 min	Initial	After 2 min
SEM A (9V)	8.3	8.3	8.0	8.0	8.6	8.6	8.3	8.2
SEM B (9V)	8.1	8.1	7.7	7.6	8.4	8.4	8.1	8.0
Sol/Trans (27V)	27.1	26.9	26.0	25.4	n/a	n/a	n/a	n/a

6.1.13 Blue and Yellow Pod Function Testing

The AMF/Deadman and the Autoshear functions can be initiated by either the Blue or the Yellow Pod. In order to test the two functions, one Cameron-supplied laptop equipped with testing software and one Portable Electronic Test Unit (PETU) were connected to each of the Blue and Yellow Pods.

6.1.13.1 AMF/Deadman Pod Function Testing

Individual component tests for the BOP and LMRP stingers on the Blue and Yellow Pods and Solenoids 103(Y&B) were run prior to full function testing of the AMF/Deadman sequence.

6.1.13.1.1 Control Pod Stingers

Retaining pins were removed from the BOP and LMRP stinger hydraulic actuators to disconnect the actuators and prevent the stingers from extending during the AMF/Deadman Pod function testing. This was done because the tests were carried out without a pod test stand with stinger receptacles. The Stinger Extend command was given for both the BOP and LMRP stingers on both the Blue and Yellow Pods. The Stinger Extend command functioned properly for all stingers. The Stinger Retract command was given for both the BOP and LMRP stingers on the Blue and Yellow pods. The Stinger Retract command functioned properly for all stingers. No abnormalities were noted during hydraulic actuator retraction and extension.



6.1.13.1.2 Solenoid 103Y and 103 B

Original Solenoids 103Y and 103B were activated using the laptop and PETU connected to the respective pods. Both SEM A and SEM B on each pod were used to activate the solenoid. The tests were run using 3,000 psig pod pilot supply pressure. Activation of a solenoid was confirmed by monitoring a pressure gauge connected to the ¼ inch flexible hose Swagelok connections just above the BOP Stack Junction Plate on each pod. Blue Pod original Solenoid 103B activated for both SEM A and SEM B, as confirmed by 3,000 psig observed on the pressure gauge. Yellow Pod original Solenoid 103Y did not activate regardless of which SEM was selected.

Pod pilot supply pressure was bled to 0 psig and further testing on Yellow Pod Solenoid 103Y was undertaken. Activation of the solenoid (coil energized) was confirmed by an audible click. The energize command was given multiple times through both SEM A and SEM B. There were no audible indications of the activation of Yellow Pod original Solenoid 103Y. The solenoid pie connector to the SEM was removed and the plugs and sockets cleaned, and the pie connector was reconnected. The energize command was given through SEM B multiple times. A faint audible indication of solenoid activation was heard once. 3,000 psig pod pilot supply pressure was supplied. The energize command was given to the solenoid using SEM B. No pressure was seen on the pressure gauge. The pod pilot supply pressure was bled off while the energize command continued to be given. No confirmation of solenoid activation was heard. The de-energize command was given.

The energize command was given through SEM B. No audible indication of solenoid activation was heard. The de-energize command was given. A faint audible indication of solenoid de-activation was heard. The energize command was given through SEM B again. No audible indication of solenoid activation was heard. The de-energize command was given. The second time, no audible indication of solenoid de-activation was heard.

The energize command was given through SEM A. No audible indication of solenoid activation was heard. The de-energize command was given. No audible indication of solenoid de-activation was heard.

Based on the testing results, the original Yellow Pod Solenoid 103Y was removed and the replacement Solenoid 103Y was installed.

The replacement Yellow Pod Solenoid 103Y was given the energize command using both SEM A and SEM B, without and with pod pilot supply pressure. The replacement solenoid activated for all tests.

6.1.13.1.3 AMF/Deadman Sequence Testing

Electrical power and communication was supplied via the two PETUs, simulating the MUX cables present during normal operation. A modified RCB cable was connected



between the Blue and Yellow pods. This cable allowed the pods to communicate and determine if the other pod has met all conditions necessary for AMF/Deadman to initiate. The AMF/Deadman conduit supply pressure sensing input (connection 24) for each pod was supplied with 1,000 psig hydraulic pressure. The pressure was blocked in. The Laptop/PETU showed a pressure of 1,099 psig on the conduit supply pressure sensing readout.

The baseline reading of the AMF/Deadman Arm analog channel was noted. The deactivate/disarm command was given and the analog values noted. The expected value was 900 ± 60 . The activate/arm command was given and the analog values noted. The expected value was 0-30. The results are shown in Table 7.

Table 7 Analog Channel Current Values for AMF/Deadman

Value	Yellow Pod		Blue Pod	
	SEM A (mA)	SEM B (mA)	SEM A (mA)	SEM B (mA)
Baseline	913	916	919	915
De-activate AMF/Deadman	917	915	918	915
Activate AMF/Deadman	18	16	14	16

The connection from the Laptop/PETU to the Blue Pod was removed to simulate loss of MUX communication to Blue Pod only. After one minute the AMF/Deadman function did not activate, as was expected since hydraulic pressure and MUX communication to the Yellow Pod were still present. The hydraulic pressure supplied to the AMF/Deadman conduit supply pressure sensing input (connection 24) for each pod was bled to 0 psig. After one minute the AMF/Deadman function did not activate, as was expected since MUX communication to the Yellow Pod was still present.

The connection from the Laptop/PETU to the Yellow Pod was removed to simulate loss of MUX communication (now to both Blue and Yellow Pods). The time (in seconds) after the connection was removed was monitored and the time at which various functions occurred was noted. Table 8 details the time at which each function occurred.

Table 8 Event Time Log - Yellow Pod Disconnect (Replacement 103Y)

Time (sec)	Event
0	Yellow Pod PETU connection removed
5	Laptop reading from PETU goes off
16	LMRP and BOP Stack stingers extend
18	LMRP and BOP Stack stingers energized
22	High Pressure (HP) BSR Gauge 103Y shows 3,000 psig
58	HP BSR Gauge 103Y shows 0 psig

The connection from the Laptop/PETU to the Blue Pod was re-established after more than three minutes had elapsed since removal. It was expected that due to the low voltage



of the 27V battery on the Blue Pod, the 9V supplied SEMs (A and B) would initiate but the sequence would not progress to the solenoids until an adequate power source was reapplied. This test was performed to determine if the Blue Pod had initiated and would complete the AMF/Deadman sequence. The time (in seconds) after the connection was re-established was monitored and the time at which various functions occurred was noted. The LMRP and BOP Stack stingers extend/energize events occurred and were confirmed visually; however, the times were not noted. The results are detailed in Table 9.

Table 9 Event Time Log - Blue Pod Reconnect (Replacement 103 Y)

Time (sec)	Event
0	Blue Pod PETU connection re-established
19	HP BSR Gauge 103B shows 3,000 psig.
55	HP BSR Gauge 103B shows 0 psig.

The voltage of all batteries was measured following the AMF/Deadman test. The results are detailed in Table 10.

Table 10 Battery Voltage Following First AMF/Deadman Test

Battery	Blue Pod (Volts)	Yellow Pod (Volts)
SEM A (9V)	8.9	8.6
SEM B (9V)	8.6	8.4
Solenoid/Transducer (27V)	0.7	27.7

The replacement Yellow Pod Solenoid 103Y was removed and the original Solenoid 103Y was installed. The AMF/Deadman test was repeated on the Yellow Pod only.

The AMF/Deadman function was activated/armed on both SEM A and SEM B. The analog channel value for SEM A was 17 and 15 for SEM B. The pressure on the AMF/Deadman conduit supply pressure sensing input (connection 24) for each pod was bled to 0 psig to simulate loss of hydraulics. The connection from the Laptop/PETU to the Yellow Pod was removed to simulate loss of MUX communication. The time (in seconds), after the connection was removed, was monitored and the time at which various functions occurred was noted. Pressure was observed on the HP BSR Gauge 103Y at 43 seconds and returned to 0 psig at 50 seconds. This was observed as a delay of Solenoid 103Y function, which in the previous test had occurred at around 20 seconds (energize) and de-energized at around 30 seconds later. This time the delayed function resulted in closing pressure only being applied for 7 seconds, which would be insufficient to fully close the BSRs. The LMRP and BOP Stack stingers extend/energize events occurred and were confirmed visually; however, the times were not noted. The results of the second test with the original Yellow Pod Solenoid 103Y are detailed in Table 11.

**Table 11 Event Time Log - Yellow Pod Disconnect (Original 103Y)**

Time (sec)	Event
0	Yellow Pod PETU connection removed
43	HP BSR Gauge 103Y shows 3,000 psig
50	HP BSR Gauge 103Y shows 0 psig
<180	Yellow Pod PETU reconnect, HP BSR Gauge 103Y shows 3,000 psig

The test was reset (i.e., BOP stack stinger seal retracted, BOP Stack stinger retracted) and re-run. There was no delayed function of Solenoid 103Y observed. The results of the second test with the original Yellow Pod Solenoid 103Y are detailed in Table 12.

Table 12 Event Time Log - Yellow Pod Disconnect Second Test (Original 103Y)

Time (sec)	Event
0	Yellow Pod PETU connection removed
16	LMRP and BOP Stack stingers extend
19	LMRP and BOP Stack stingers energized
21	HP BSR Gauge 103Y shows 3,000 psig
51	HP BSR Gauge 103Y shows 0 psig
~120	Yellow Pod PETU reconnect, HP BSR Gauge 103Y shows 3,000 psig

After the second test using the original Solenoid 103Y, an individual component function test was run on the solenoid. The energize command was given to the Yellow Pod original Solenoid 103Y through SEM A. The solenoid did not activate (confirmed through the HP BSR Gauge 103Y showing 0 psig). The energize command was then given to the Yellow Pod original Solenoid 103Y through SEM B. The solenoid did not activate (confirmed through the HP BSR Gauge 103Y showing 0 psig).

For the final AMF/Deadman test using the original Solenoid 103Y, a wait time of more than three minutes was used before re-establishing the Laptop/PETU connection to the Yellow Pod. The Yellow Pod was reset to re-run the AMF/Deadman test, as described previously. The AMF/Deadman function was activated/armed on both SEM A and SEM B. The analog channel value for SEM A was 17 and 16 for SEM B. The pressure on the AMF/Deadman conduit supply pressure sensing input (connection 24) for each pod was bled to 0 psig. The connection from the Laptop/PETU to the Yellow Pod was removed. The time (in seconds) after the connection was removed was monitored and the time at which various functions occurred was noted. The results are detailed in Table 13.

Table 13 Event Time Log - Yellow Pod Disconnect Final Test (Original 103Y)

Time (sec)	Event
0	Yellow Pod PETU connection removed
5	Laptop reading from PETU goes off
16	LMRP and BOP Stack stingers extend
19	LMRP and BOP Stack stingers energized.
21	HP BSR Gauge 103Y shows 3,000 psig.
51	HP BSR Gauge 103Y shows 0 psig.

Approximately six minutes after disconnecting the Laptop/PETU from the Yellow Pod, the connection was re-established. The HP BSR Gauge 103Y showed 3,000 psig. After approximately one minute, 0 psig was shown on the gauge.

An individual component function test was again run on the solenoid. The Laptop/PETU was then used to energize Yellow Pod Solenoid 103Y through both SEM A and SEM B. The solenoid did not activate using either SEM, confirmed through 0 psig being shown on the pressure gauge.

The voltage on the Yellow Pod batteries was measured at the end of sequence testing. The results are detailed in Table 14.

Table 14 Yellow Pod Voltages - Post Sequence Testing

Battery	(Volts)
SEM A (9V)	8.5
SEM B (9V)	8.1
Solenoid/Transducer (27V)	27.2

The analog channel values for AMF/Deadman Arm were checked for both SEM A and SEM B of the Blue and Yellow Pods at the end of sequence testing. Blue Pod SEM A showed an analog value of 15. Blue Pod SEM B showed an analog value of 918. SEM A and SEM B for the Yellow Pod were both greater than 900.

6.1.13.2 Post AMF/Deadman of Yellow Pod Solenoid 103

The most probable reason why the original Solenoid 103Y worked during two out of three sequence tests and failed during individual component testing was identified as being related to whether or not both solenoid coils energize simultaneously (sequence test) versus individually (component test). Energizing both coils simultaneously creates a greater coil armature force versus a single coil energizing. To validate this theory, additional testing was performed on the original Solenoid 103Y. The Yellow Pod was connected to the Laptop/PETU (designated PETU B) originally connected to the Blue



Pod, that was capable of activating SEM A and SEM B simultaneously. Pod pilot supply pressure of 3,000 psig was delivered to the Yellow Pod. The command to energize Solenoid 103Y was given via the Laptop/PETU with both SEM A and SEM B selected. A maximum pressure of 3,000 psig was observed on the pressure gauge.

After confirming the solenoid activated with both SEMs selected, the solenoid was tested with SEM A and SEM B selected individually. In both test conditions, the solenoid activated and 3,000 psig was observed on the pressure gauge.

PETU B connected to the Yellow Pod was replaced with the original Laptop/PETU (designated PETU Y) which was connected to the Yellow Pod during the AMF/Deadman testing. The command to energize Solenoid 103Y was given via PETU Y through SEM A. The solenoid activated and a maximum pressure of 3,000 psig was observed on the pressure gauge. SEM B was selected via PETU Y and the test was repeated. The solenoid did not activate as confirmed by 0 psig on the pressure gauge. This test was repeated two more times with SEM B. The command was given to de-energize Solenoid 103Y between each test. For both additional tests, the solenoid did not activate. SEM A was selected via PETU Y and the test was repeated. The solenoid did not activate as confirmed by 0-psig on the pressure gauge.

PETU Y connected to the Yellow Pod was replaced with PETU B. The command to energize Solenoid 103Y was given via PETU B through SEM A. The solenoid activated and a maximum pressure of 3,000 psig was observed on the pressure gauge. SEM B was selected via PETU B and the test was repeated. The solenoid activated as confirmed by 3,000-psig on the pressure gauge.

The pie end connector of the plug connecting Solenoid 103Y to the Yellow Pod was disconnected to measure the voltage delivered from the two PETUs (Y and B) to Solenoid 103Y via SEM A and SEM B. An approximate 4-foot jumper cable was connected to the pie receptacle to facilitate measurement of the voltage. The voltage was measured in both the energized and de-energized condition. The results of the voltage testing showed there was no appreciable difference in the voltage delivered to Solenoid 103Y by the two (see Table 15 for detailed results).

Table 15 Voltage Testing - Solenoid 103

PETU	SEM A			SEM B		
	De-energized	Energized		De-energized	Energized	
		Steady	Peak		Steady	Peak
Y	9.0	15.0	25.6	13.3	17.5	25.7
B	9.3	15.0	25.6	13.3	17.5	25.7

The Yellow Pod was reconnected to PETU B. Pod Pilot Supply pressure of 3,000 psig was delivered to the Yellow Pod. The command to energize Solenoid 103Y was given via



PETU B first with SEM A selected, second with SEM B selected, and third with SEM A and SEM B selected. Solenoid 103Y activated under each test condition, as confirmed by 3,000 psig observed on the pressure gauge.

6.1.13.3 Blue and Yellow Pod Autoshear Function Testing

The Autoshear Arm function was tested on both pods to verify that Solenoid 121 activates and allows hydraulic fluid to be supplied to the Autoshear Arm shuttle valve. Pod Pilot Supply pressure was delivered to each pod. The Pod Pilot Supply pressure was set to approximately 3,000 psig. This was confirmed via the Laptop/PETU as well as the pressure gauge connected to the hydraulic line used to supply the hydraulic fluid. The Autoshear Arm command, to activate Solenoid 121, was sent via the Laptop/PETU. Activation of the solenoid was confirmed by monitoring the pressure gauge connected to the ¼-inch flexible hose Swagelok connections just above the BOP Stack Junction Plate on each pod. A maximum of 2,950 psig was observed on the pressure gauge connected to the Yellow Pod. A maximum pressure of 2,700 psig was observed on the pressure gauge connected to the Blue Pod. The Blue and Yellow Pod Autoshear Arm solenoids (Solenoid 121) functioned as intended.

6.2 Materials Evaluation and Damage Assessment

Materials evaluation and damage assessment procedures followed protocols provided in:

- Forensic Testing Plan [October 22, 2010], Sections 5.13 - Materials Testing and Damage Evaluation and 5.14 - Cataloging and Examination of Recovered Evidence.
- Protocol for Metallurgical Examination and Testing of Drill Pipe [February 3, 2011]
- Test Procedure - Fractured/Sheared Recovered Drill Pipe Ends [February 21, 2011]
 Visual Examination of Blowout Preventer Ram Blocks

Visual assessment included photographic documentation, dimensional measurements, documentation of cleaning, and collection of any additional evidence from the ram blocks both as part of their removal and during cleaning. Samples of viscous materials cleaned from the ram blocks were collected and placed into evidence along with other solid evidence collected off of the ram blocks. Table 16 is a summary of the Federal Bureau of Investigation's (FBI) Evidence Recovery Team (ERT) Item Identifications that were used to label the rams. The location and date of recovery are indicated in the table.

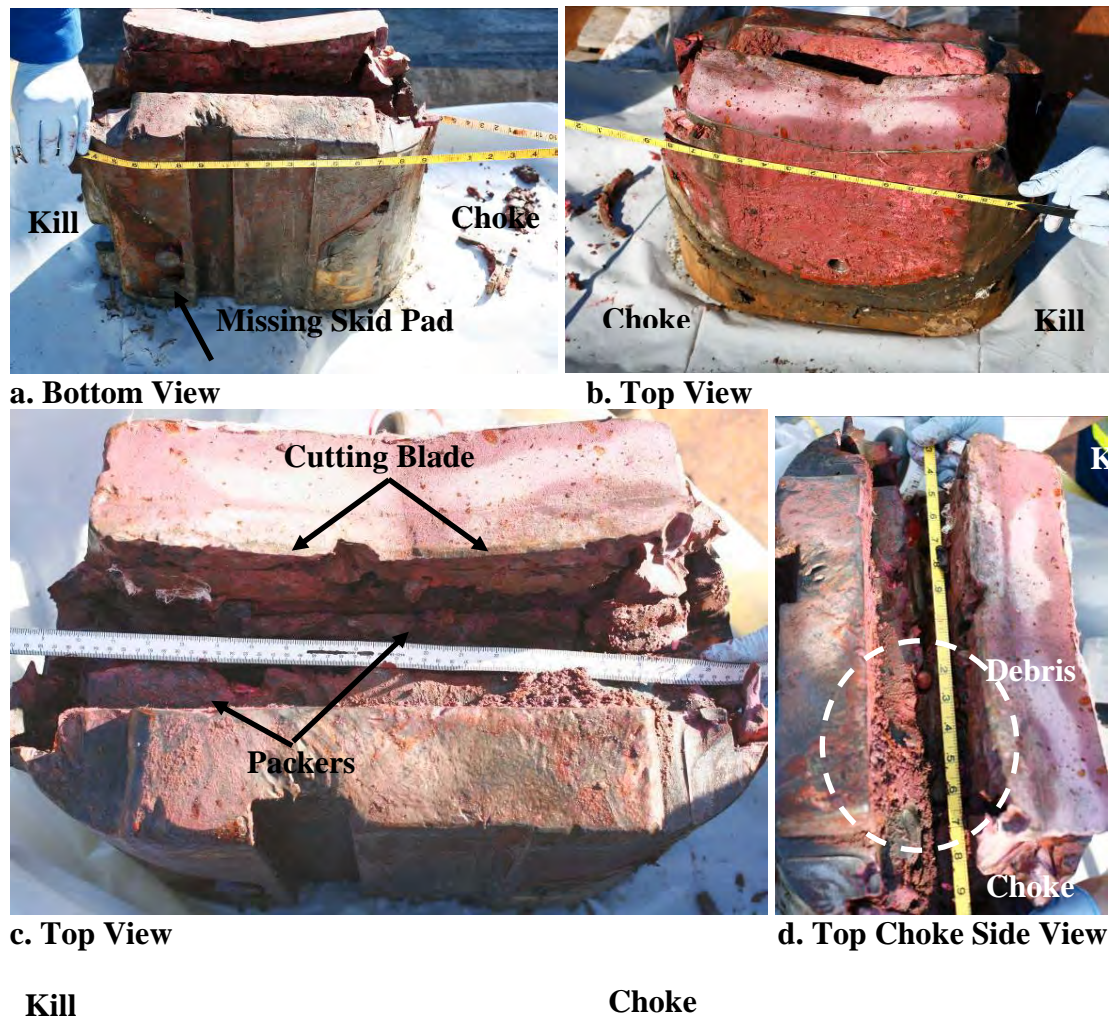
Table 16 Evidence Item Numbers for Blocks Recovered from BOP

Item ID	Description	Location of Recovery	Find Date
57	Port BSR	BOP	12/2/2010
68	Starboard BSR	BOP	12/3/2010
84	Port CSR	BOP	12/7/2010
104	Starboard CSR	BOP	12/9/2010
111	Port Upper VBR	BOP	12/10/2010

Item ID	Description	Location of Recovery	Find Date
112	Starboard Upper VBR	BOP	12/10/2010
139	Port Middle VBR	BOP	12/15/2010
140	Starboard Middle VBR	BOP	12/15/2010
158	Starboard Lower VBR	BOP	12/17/2010
159	Port Lower VBR	BOP	12/17/2010

6.2.1.1 Blind Shear Ram Blocks

The Blind Shear Ram Blocks (BSRs) in the as-recovered condition are shown in Figure 8 and Figure 9. Figure 10 and Figure 11 show the blocks following collection of viscous materials and any solid materials/objects and cleaning.

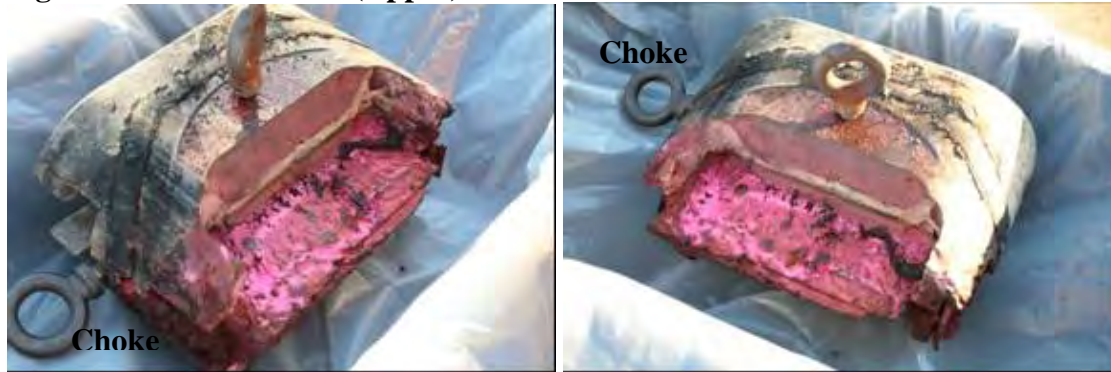




e. Kill Side View

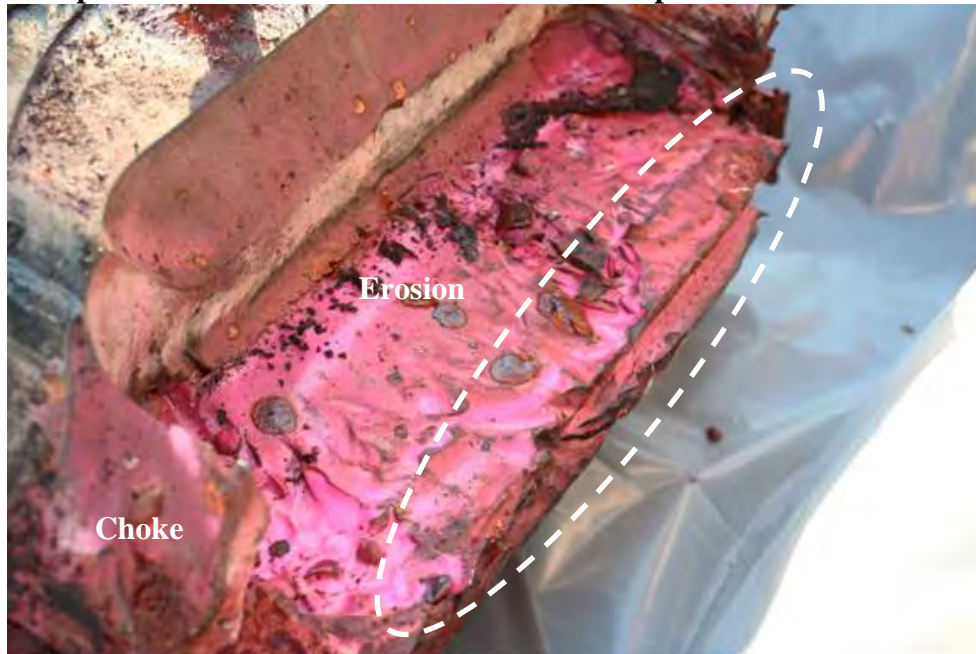
f. Choke Side View

Figure 8 Starboard Side (Upper) BSR As-Recovered Condition



a. Top View - Choke Side

b. Top View - Kill Side



c. Detail of Cutting Blade

Figure 9 Port Side (Lower) BSR As-Recovered Condition

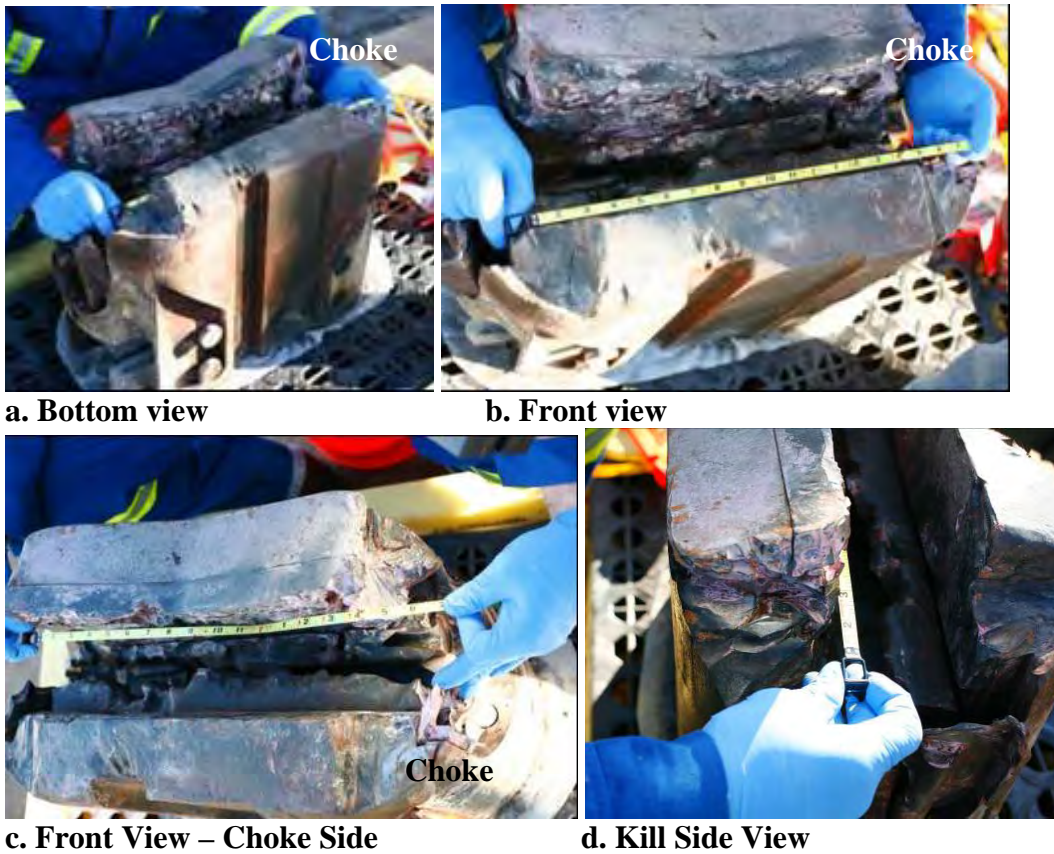


Figure 10 Starboard Side (Upper) BSR Following Cleaning



a. Choke Side View



b. Bottom View

Figure 11 Port Side (Lower) BSR Following Cleaning

After the ram blocks had been moved to ground level and prior to cleaning, indications of metal-to-metal contact between the two ram block faces were observed. Material was missing from both the starboard and port side BSRs due to erosion. The elastomer of side packers was totally missing and metallic components partially eroded. The elastomeric blade seal on the upper (starboard) ram block was missing except for approximately an inch of material pressed down beneath the metallic packer components which were also eroded. The skid pads on the bottom of the rams appeared to be slightly worn. The skid pad on the bottom of the kill side of starboard BSR was missing; however, the screws used for holding the pad in place were intact. The rubber insert on the top of the rams was slightly worn. Foreign material, which appears to be “junk shot” from the intervention effort, was found on both rams.

6.2.1.2 Casing Shear Ram Blocks

The Casing Shear Ram Blocks (CSRs) in the as-recovered condition are shown in Figure 12 and Figure 13. Figure 14 and Figure 15 show the CSRs following collection of viscous and any solid materials/objects and cleaning.



a. Top View

b. Bottom View



c. Front View - Cutting Blade

Figure 12 Starboard Side (Lower) CSR As-Recovered Condition

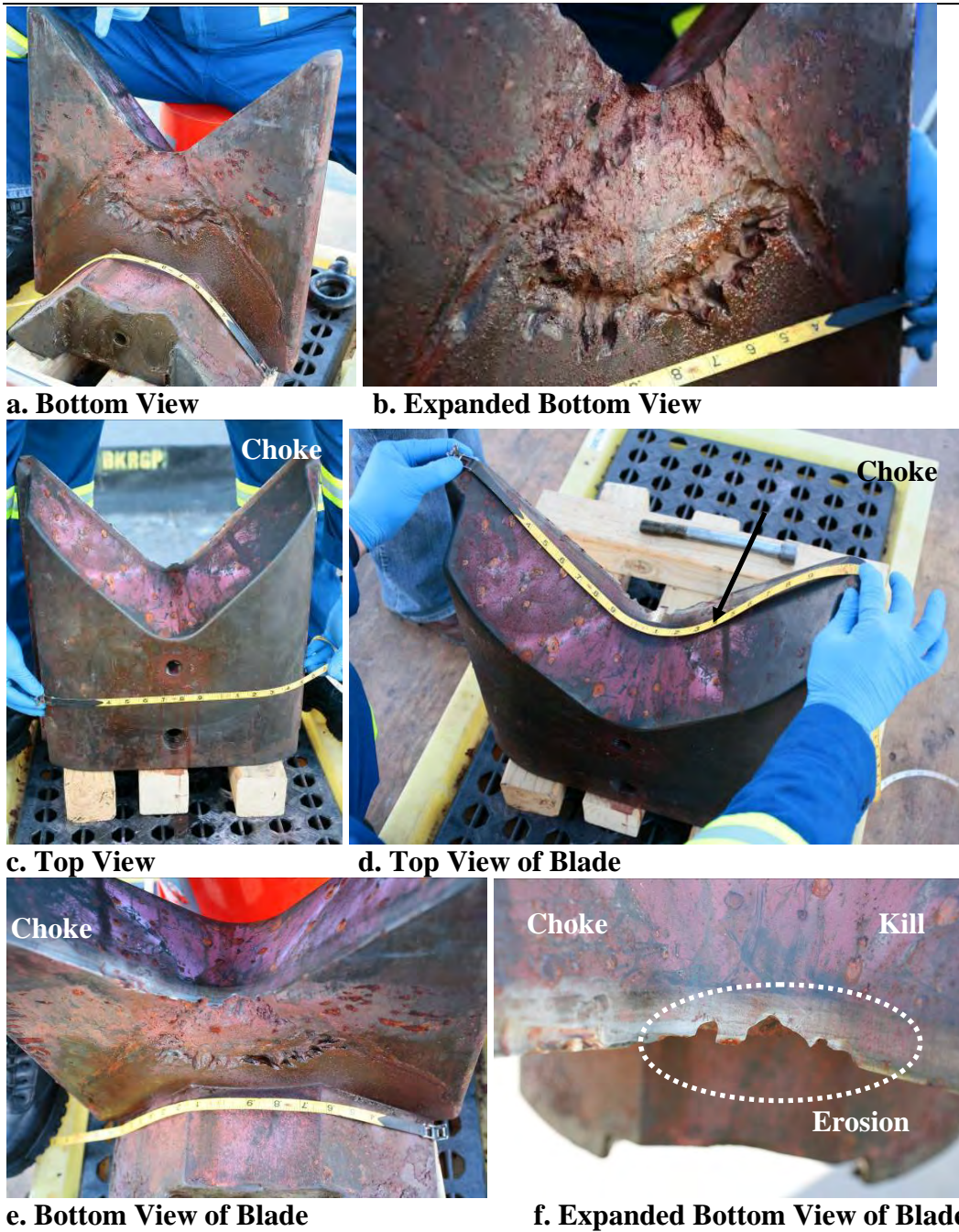


Figure 13 Port Side (Upper) CSR As-Recovered Condition

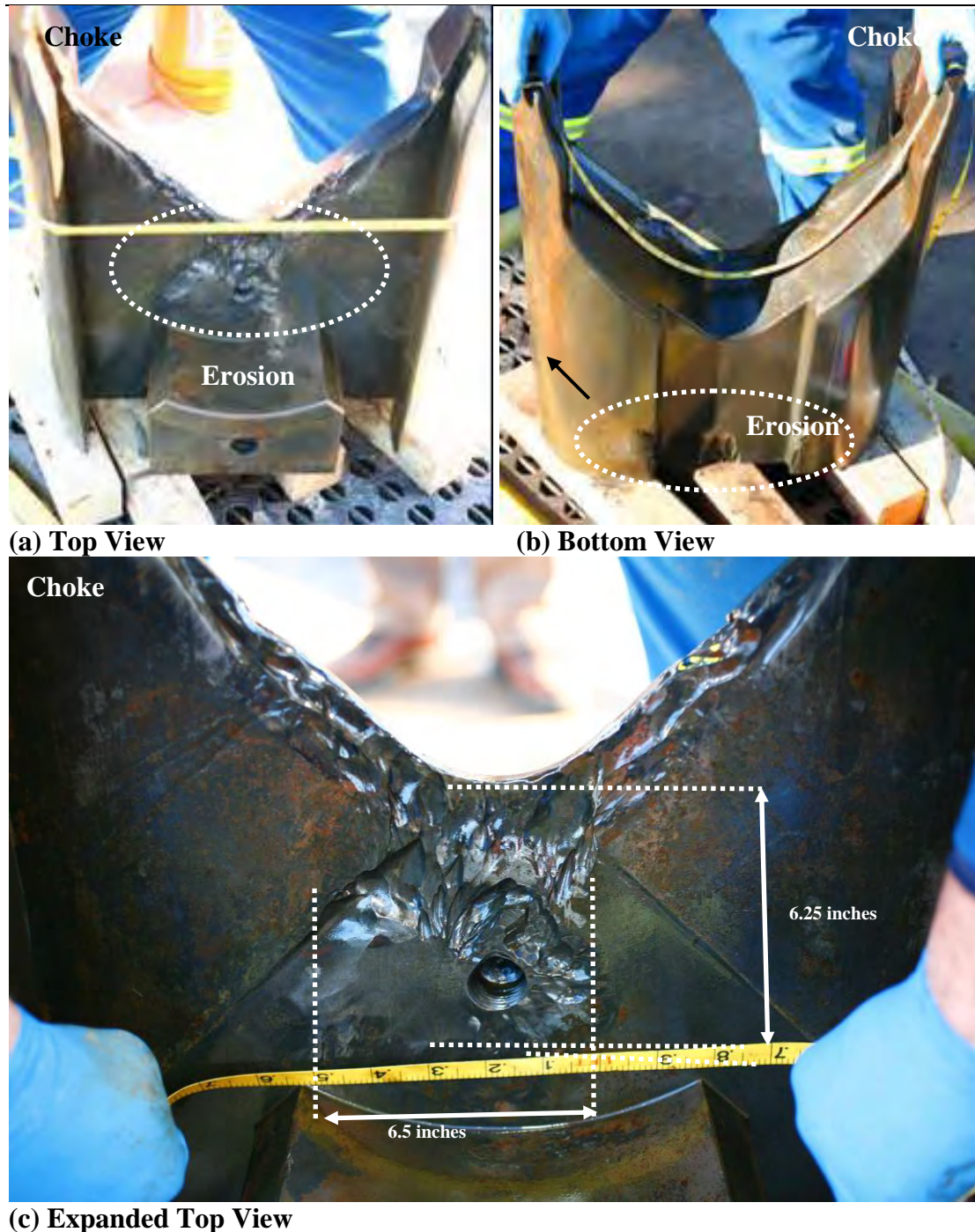


Figure 14 Starboard Side (Lower) CSR Following Cleaning



Figure 15 Port Side (Upper) CSR Following Cleaning

Erosion was present on both the starboard and port side ram blocks. The worn area on the port or upper block was approximately 6 inches by 8 inches in length. The shape and size of the erosion pattern is similar to the shape of the top end of Drill Pipe segment 148. The erosion on the top surface of the starboard or lower block indicated a flow path through the blades. Erosion patterns were also evident on the back surface of the starboard block.

These erosion markings indicate an additional flow path around the backside of the blocks (see Figure 14 (b)).

6.2.1.3 Upper Variable Bore Ram Blocks

The Upper Variable Bore Ram Blocks (VBRs) in the as-recovered condition are shown in Figure 16 and Figure 17. Figure 18 and Figure 20 show the Upper VBRs following collection of viscous materials and any solid materials/objects and cleaning. Figure 19 and Figure 21 show the segments from the starboard and port side upper VBR, respectively. All segments were eroded to some degree.

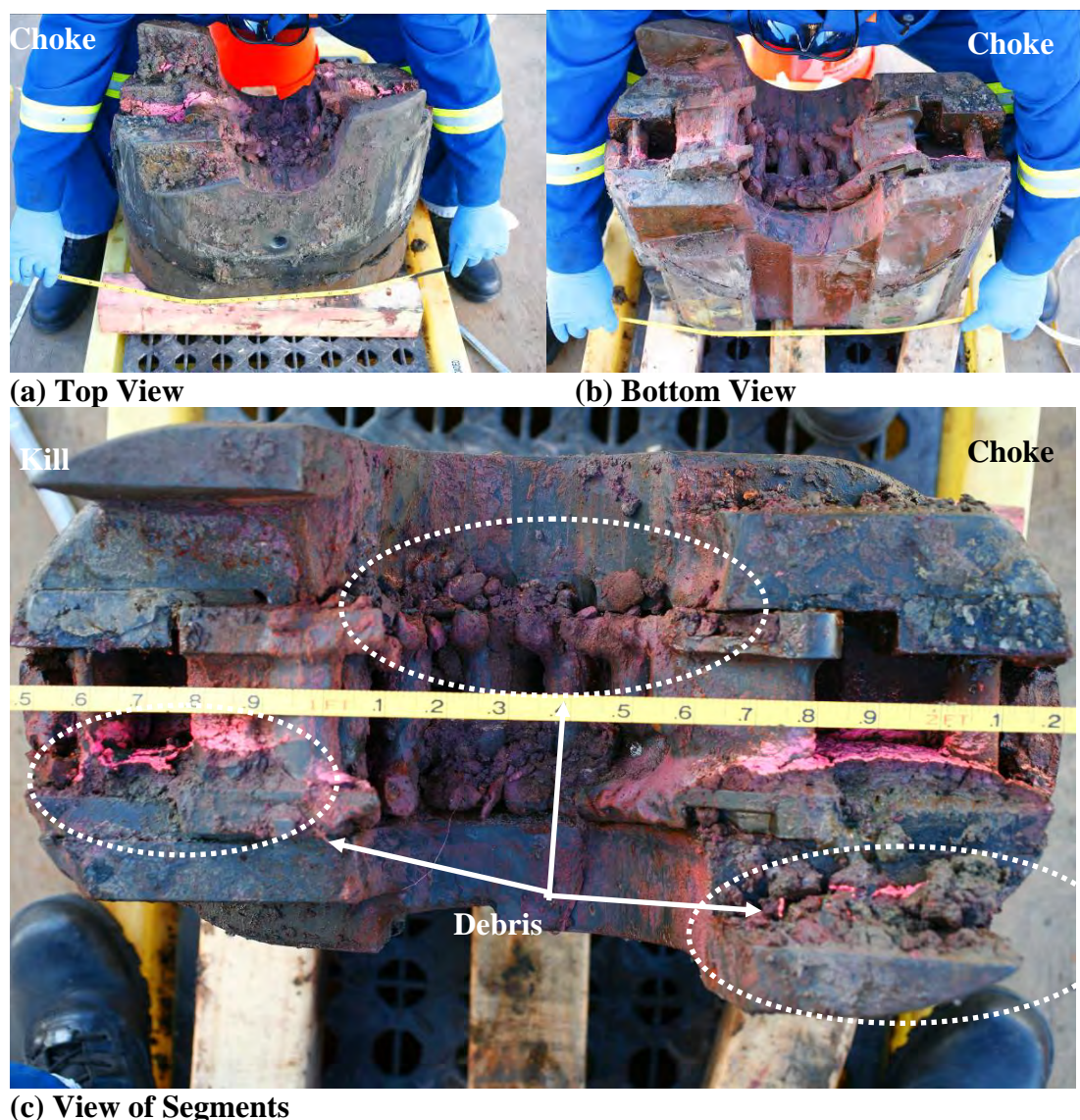


Figure 16 Starboard Side Upper VBR in the As-Recovered Condition

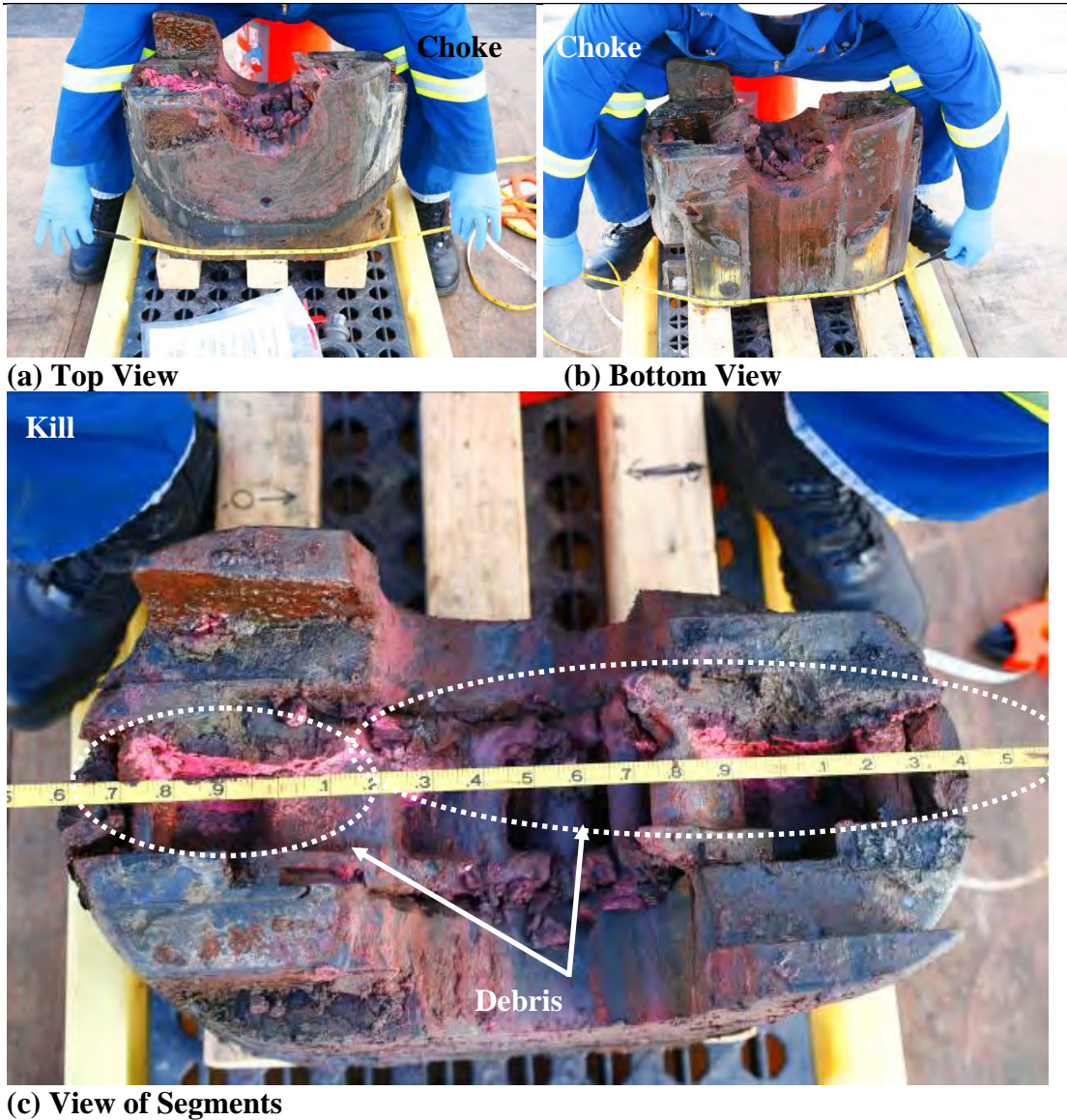


Figure 17 Port Side Upper VBR in the As Recovered Condition

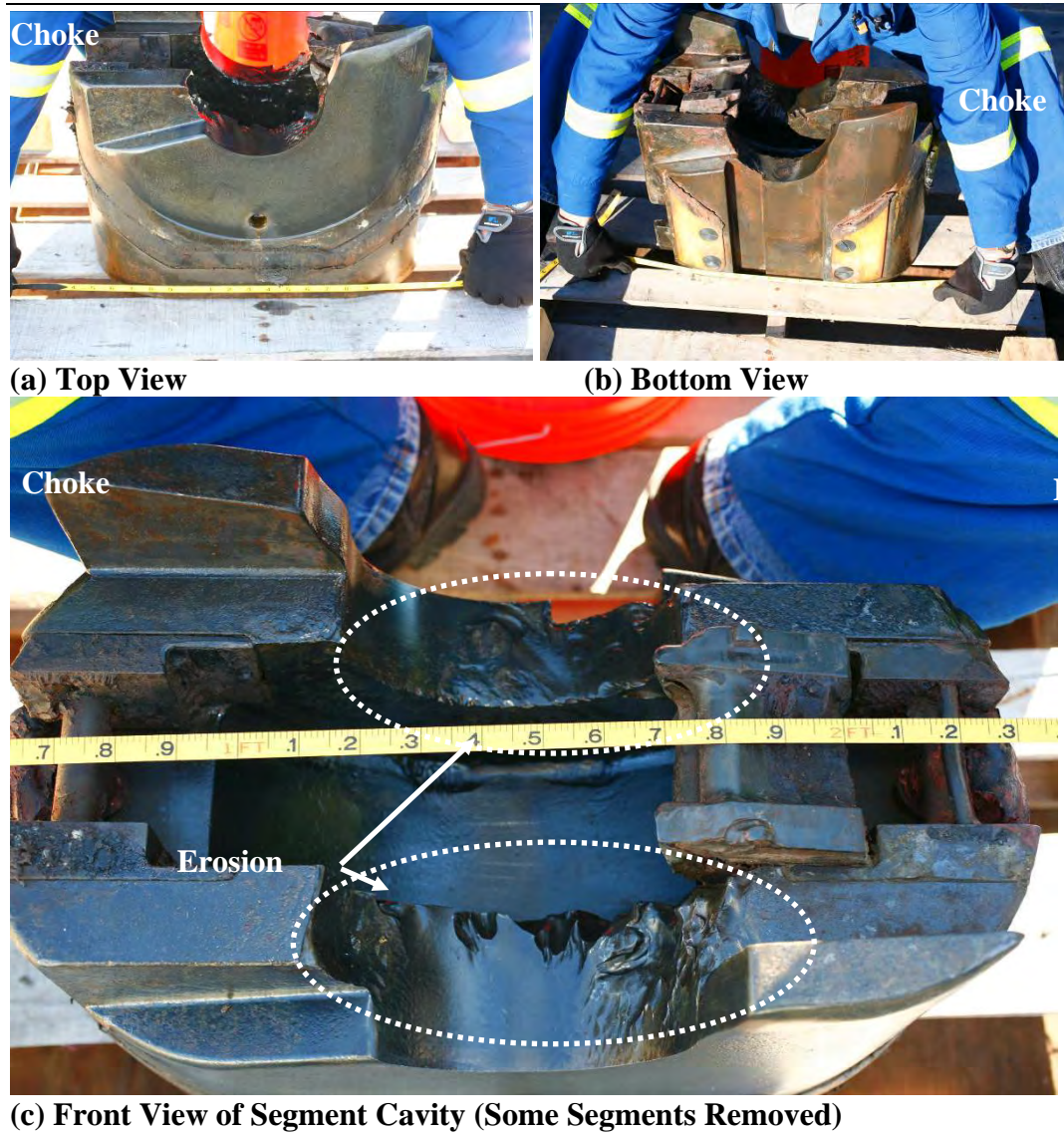


Figure 18 Starboard Side Upper VBR Following Cleaning (Segments Removed)



Figure 19 Starboard Segments from Upper VBRs Following Cleaning.

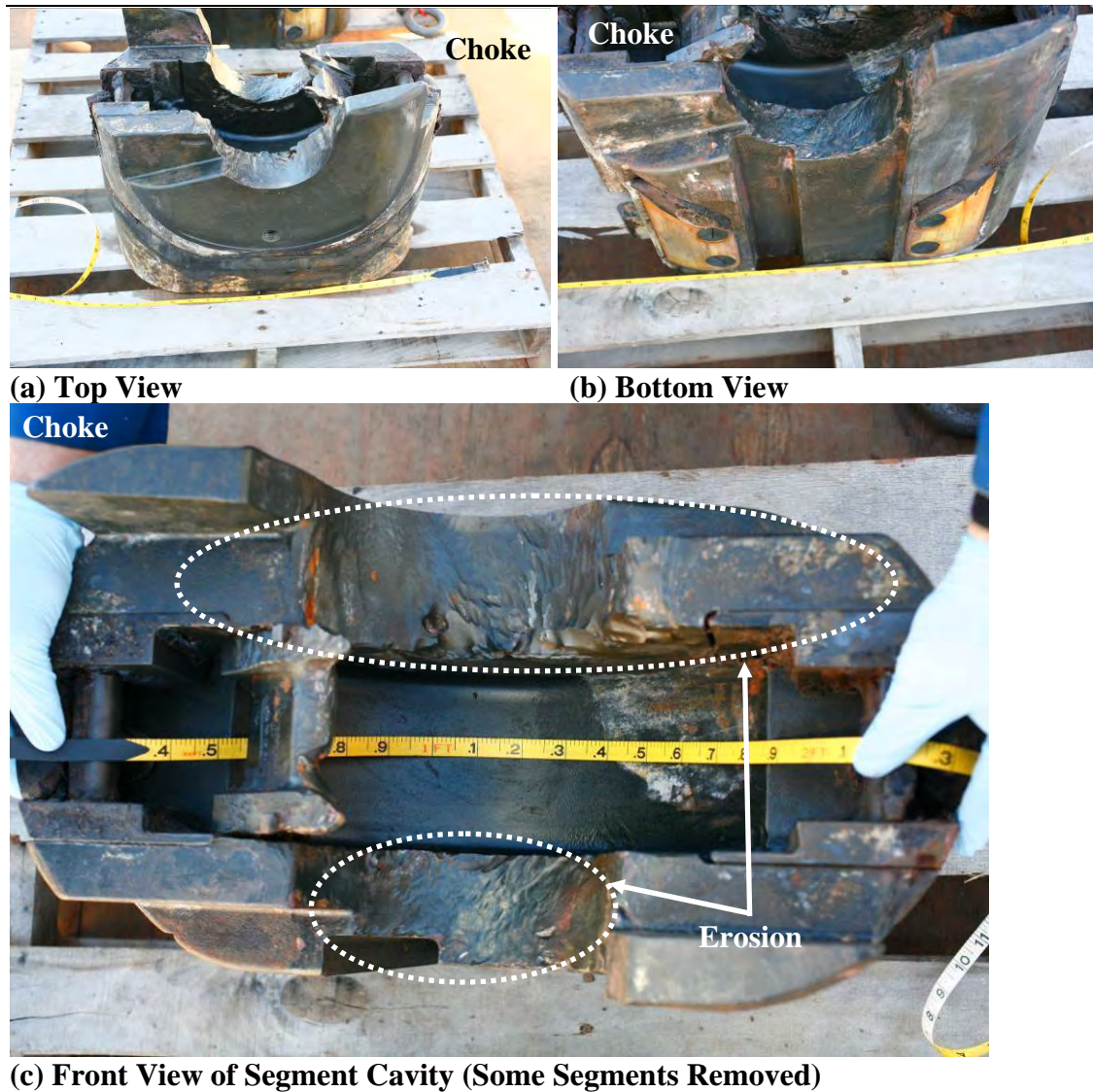


Figure 20 Port Side Upper VBR Following Cleaning



Figure 21 Port Segments from Upper VBRs Following Cleaning. (Segment 1 Remained in Ram)

Both the starboard and port side upper VBR blocks exhibited erosion on the block surfaces and the segments. The erosion on the blocks occurred predominantly in the portion of the ram packer cavity where the segments fit and on the front block face directly above and below the segments. The elastomer on the side packers was approximately 60% missing on the starboard side VBR block and 25% missing on the port side VBR block. All of the elastomer associated with the segments was missing.

6.2.1.4 Middle Variable Bore Ram Blocks

The Middle Variable Bore Ram Blocks (VBRs) in the as-recovered condition are shown in Figure 22 and Figure 23. Figure 24 and Figure 26 show the Middle VBRs following collection of viscous materials and any solid materials/objects and cleaning. Figure 25 and Figure 27 show the segments from the starboard and port side upper VBR, respectively.

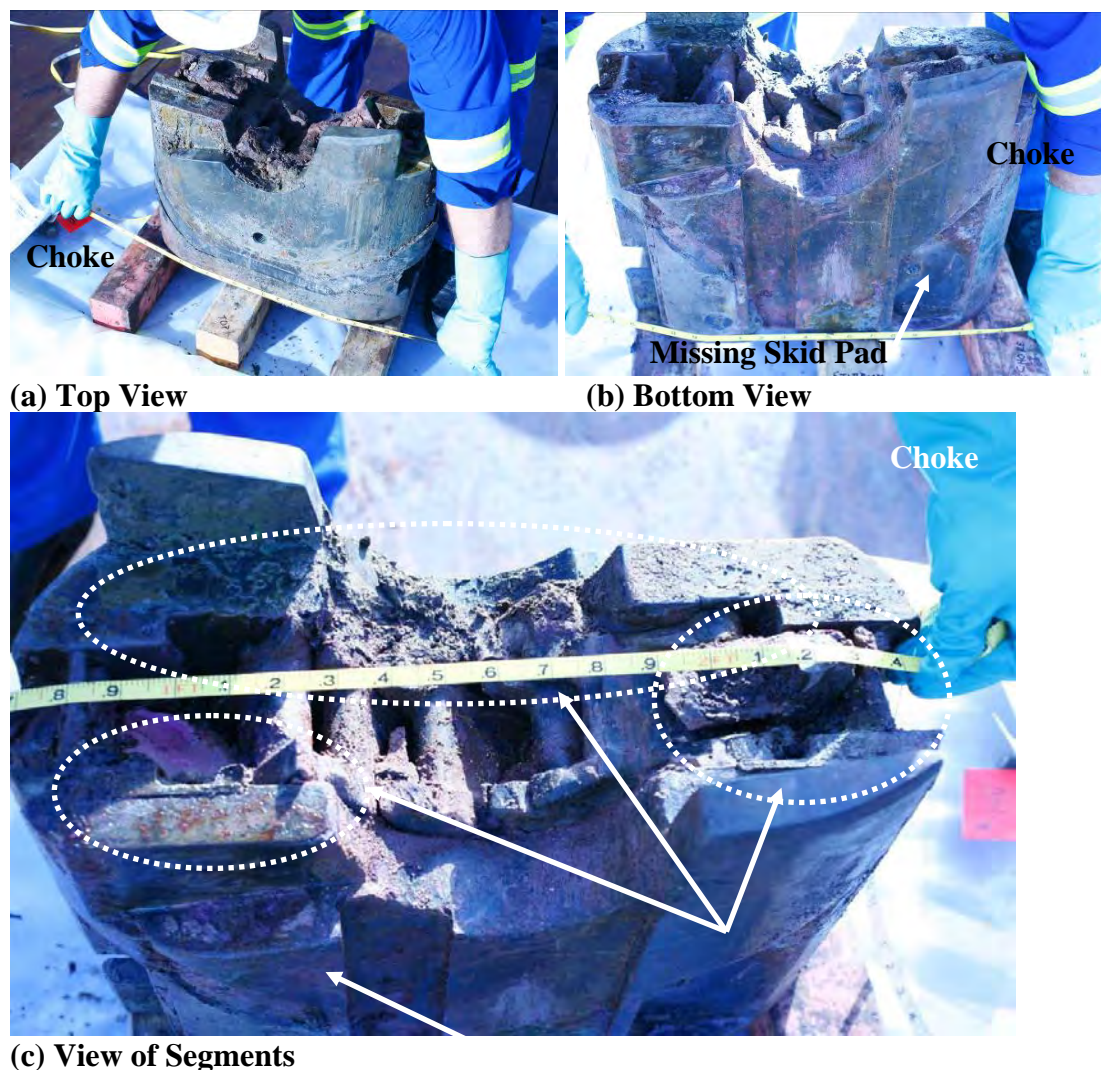


Figure 22 Starboard Side Middle VBR As-Recovered Condition

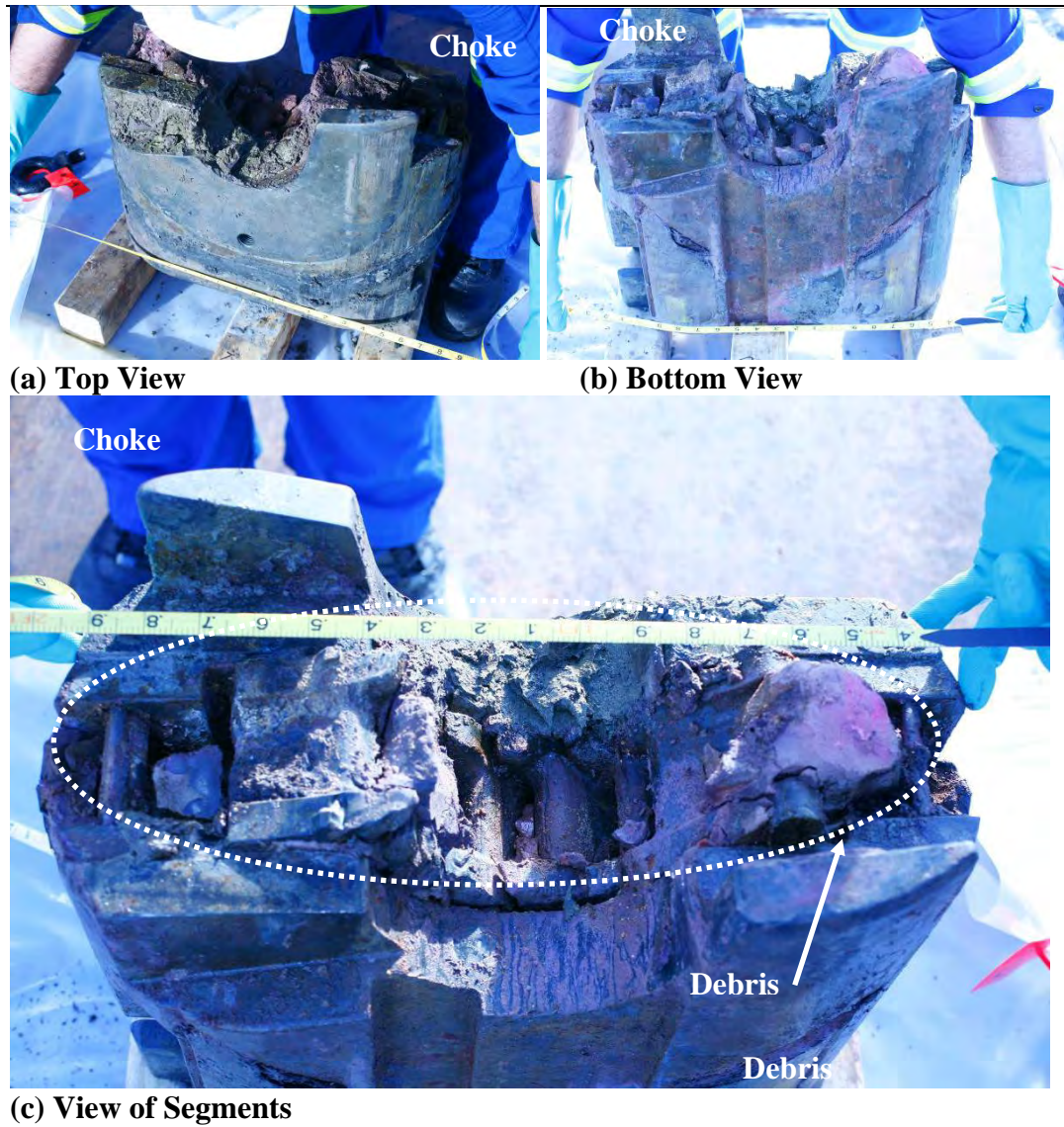


Figure 23 Port Side Middle VBR As-Recovered Condition

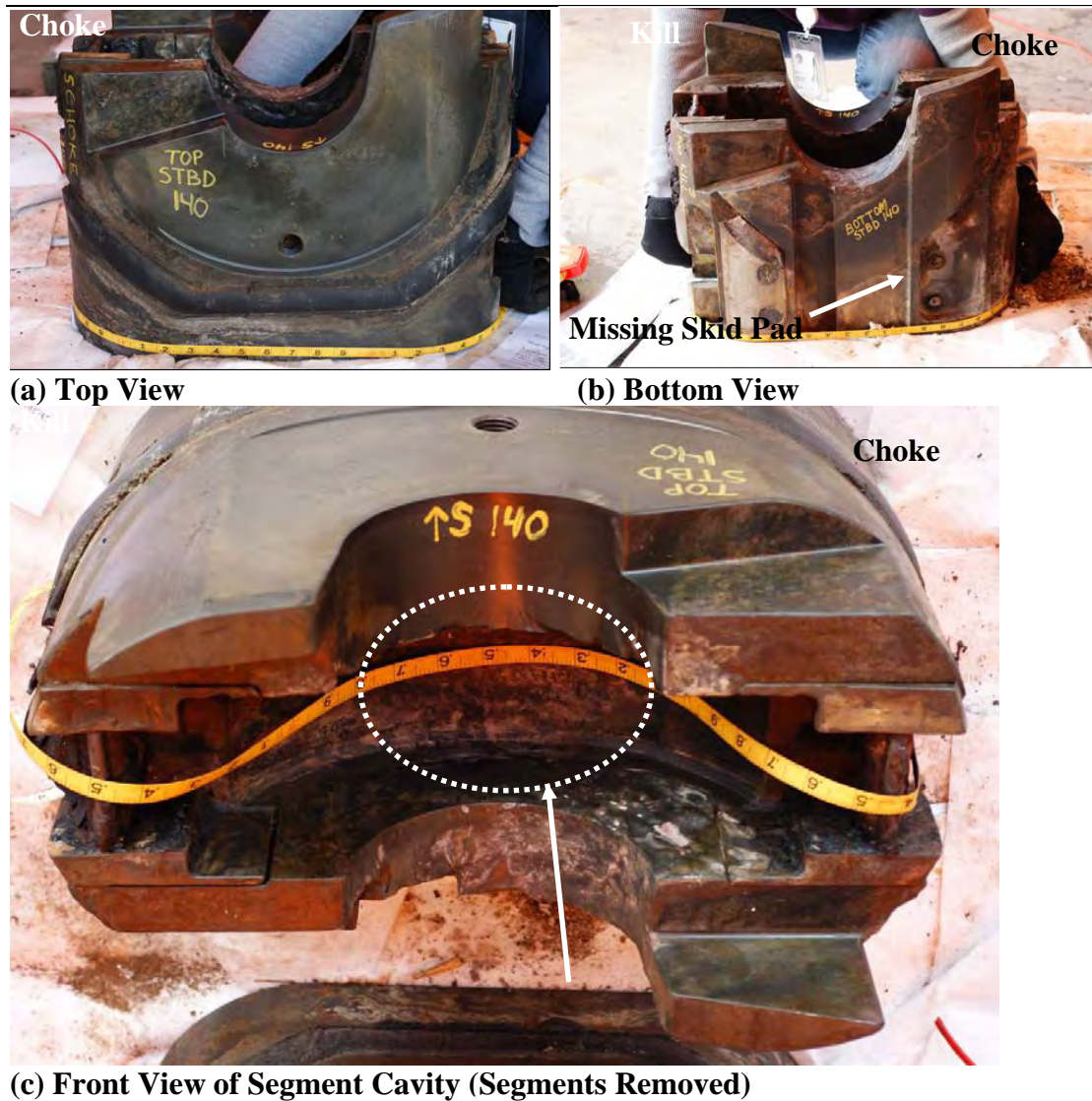


Figure 24 Starboard Side Middle VBR Following Cleaning

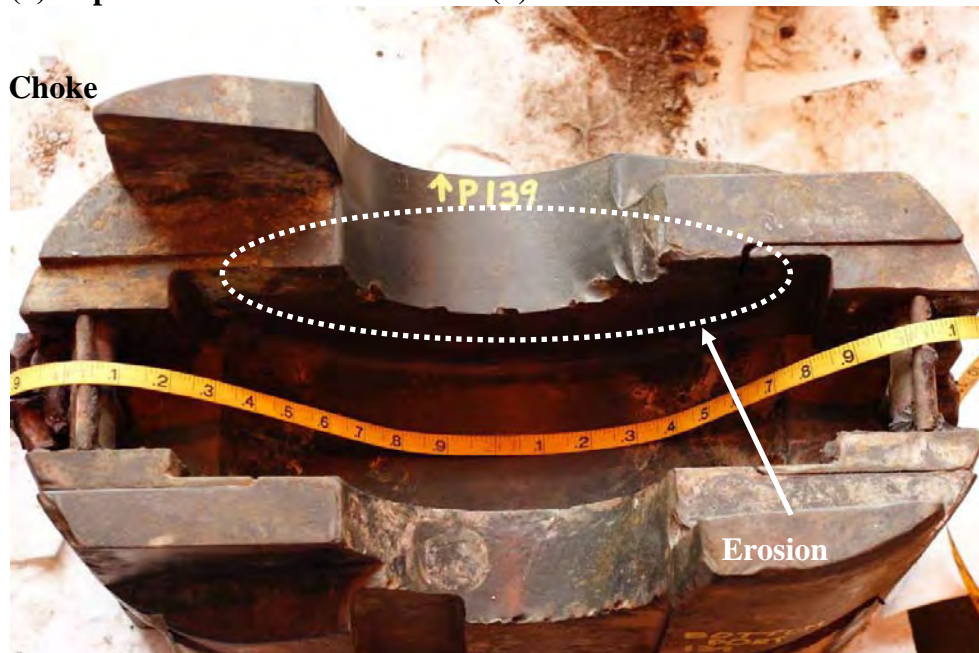


Figure 25 Starboard Segments from the Middle VBRs Following Cleaning



(a) Top View

(b) Bottom View



(c) Front View of Segment Cavity (Segments Removed)

Figure 26 Port Side Middle VBR Following Cleaning



Figure 27 Port Segments from the Upper VBRs Following Cleaning

Both the starboard and port side middle VBR blocks exhibited erosion on the block surfaces and the segments. The erosion on the blocks occurred predominantly in the portion of the ram packer cavity where the segments fit and on the front block face directly above and below the segments. The degree of erosion on the block face was less than on the upper VBR block. The elastomer on the side packers was approximately 90% missing on the starboard side VBR and 75% missing on the port side VBR. All of the elastomer associated with the segments was missing. The skid pad from the port block kill side is missing. The screws holding the pad in place appear to have been sheared.

6.2.1.5 Lower Variable Bore Ram Blocks

The Lower Variable Bore Ram Blocks (VBRs) in the as-recovered condition are shown in Figure 28 and Figure 29. Figure 30 and Figure 32 show the Lower VBRs following collection of viscous materials and any solid materials/objects and cleaning. Only one segment was still present in the starboard ram block (Kill side).

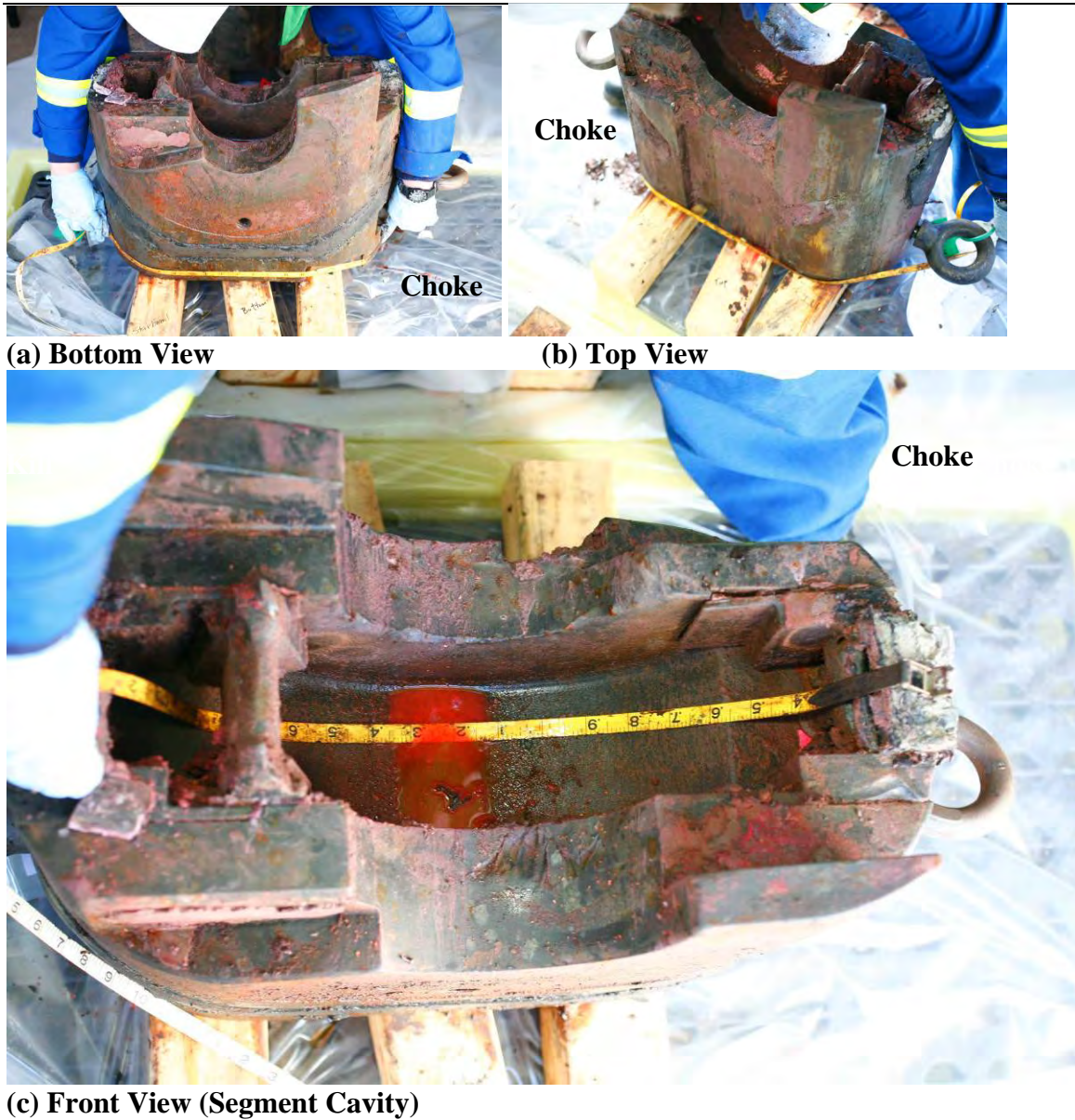


Figure 28 Starboard Side Lower VBR in the As-Recovered Condition

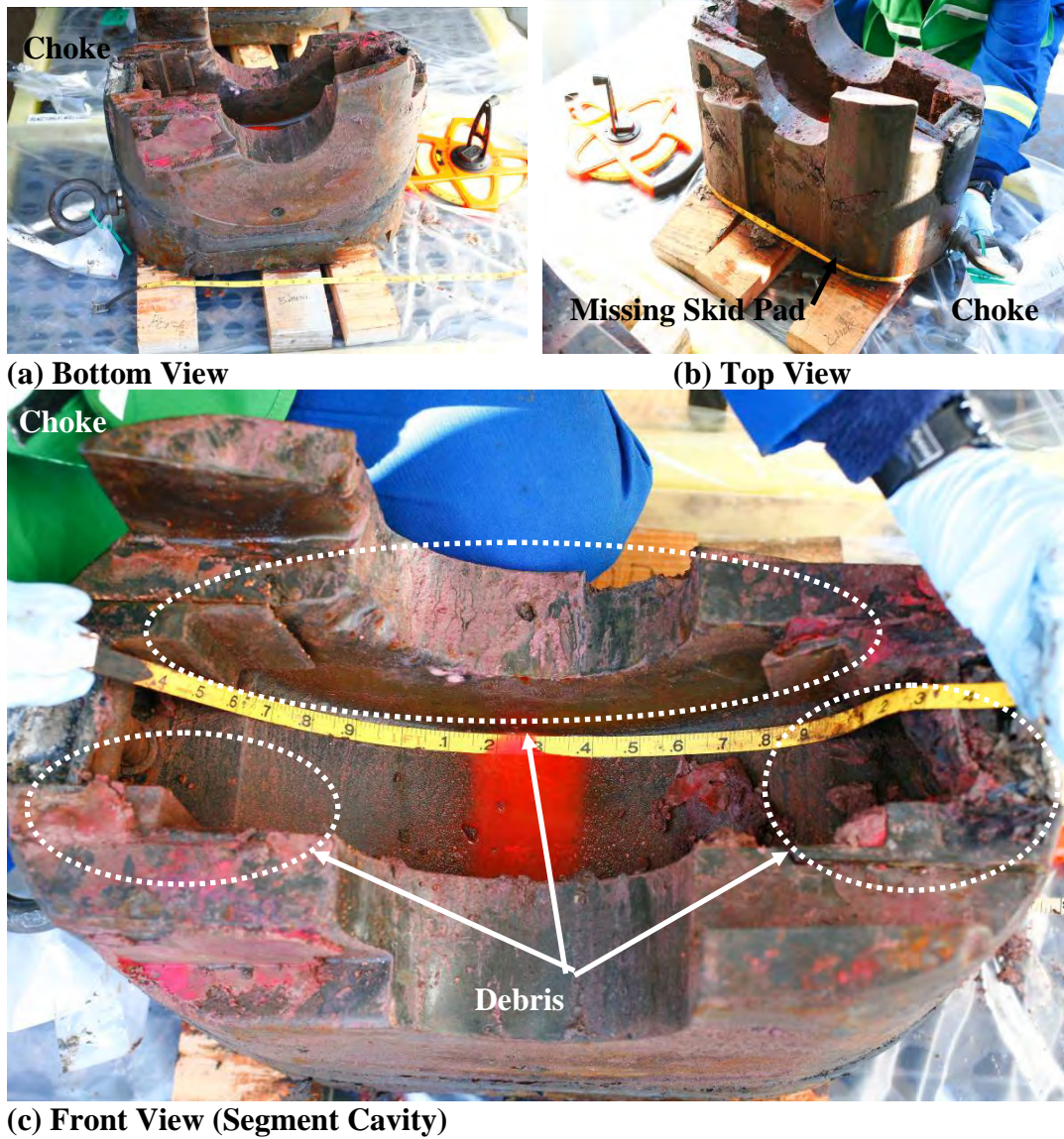


Figure 29 Port Side Lower VBR in the As-Recovered Condition

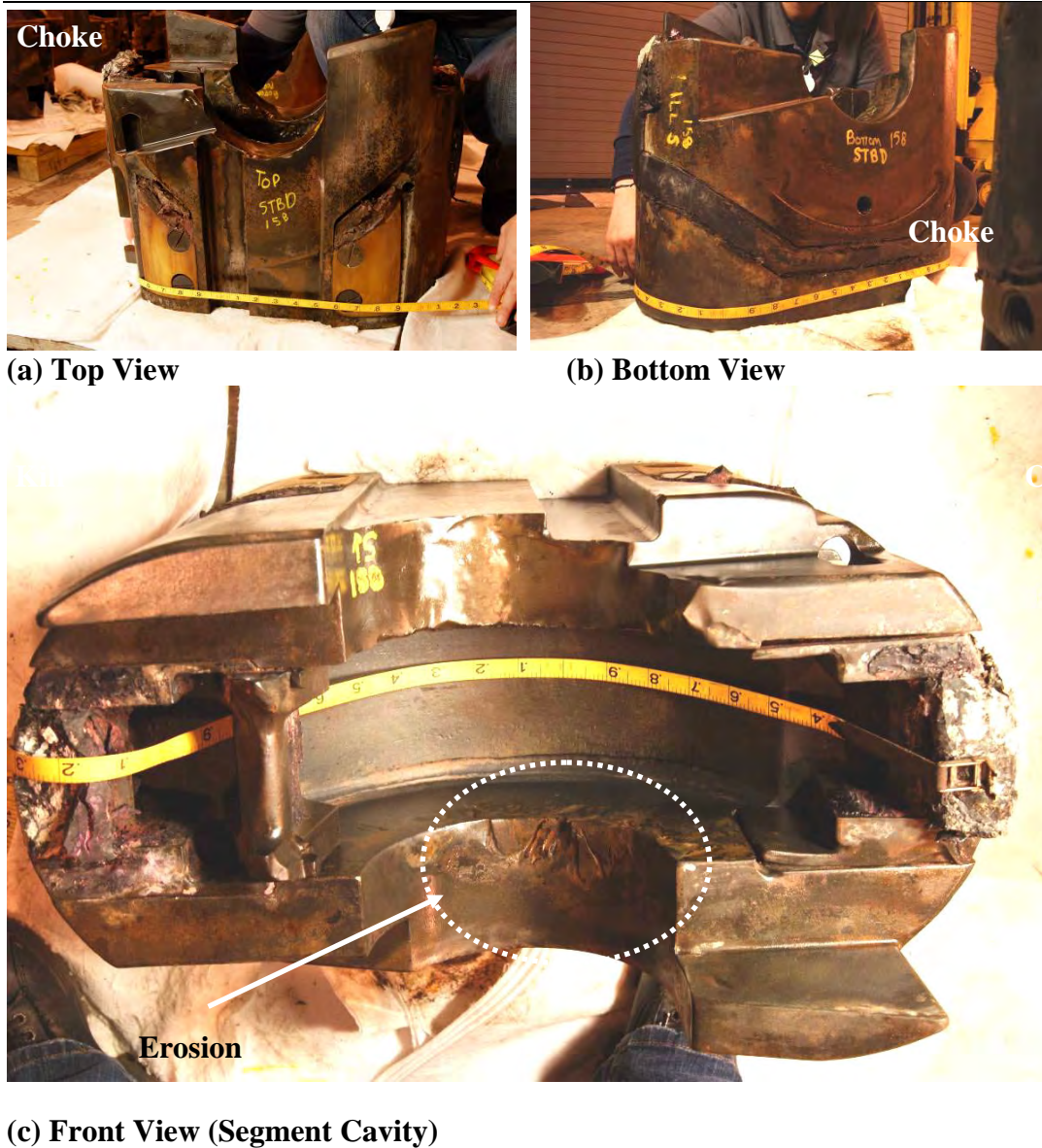


Figure 30 Starboard Side Lower VBR Following Cleaning



Figure 31 Starboard Segment from the Lower VBR Following Cleaning

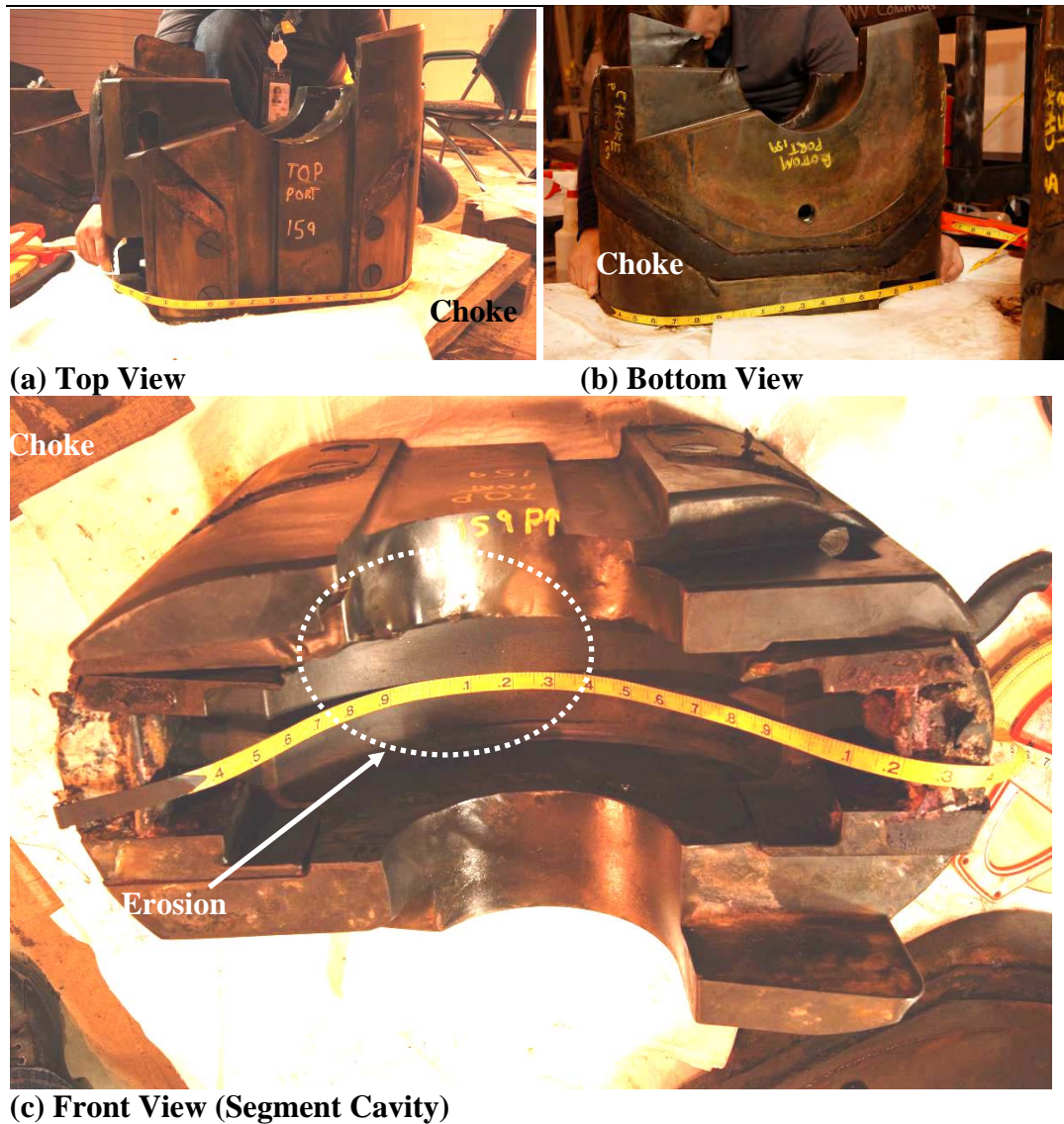


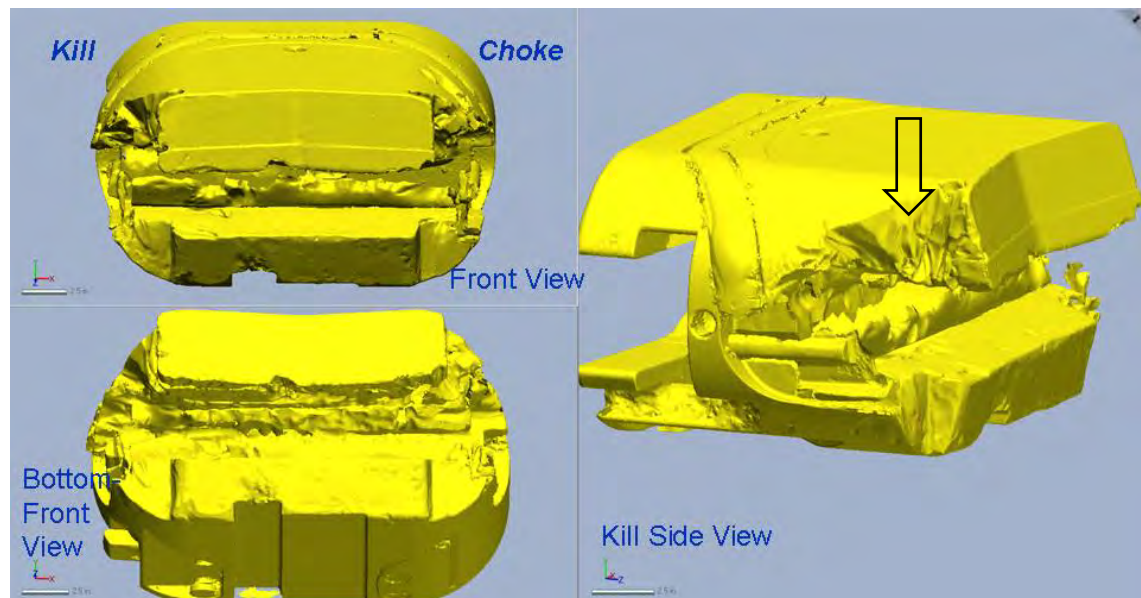
Figure 32 Port Side Lower VBR Following Cleaning

Both the starboard and port side lower VBR blocks exhibited erosion on the block surfaces. The erosion on the blocks occurred predominantly in the portion of the ram packer cavity where the segments fit and on the front block face directly above and below the segments. All segments were missing except one segment in the starboard side lower VBR block.. The elastomer on the side packers was approximately 10% missing on both the starboard side and port side middle VBR blocks. All of the elastomer associated with the segments was missing.

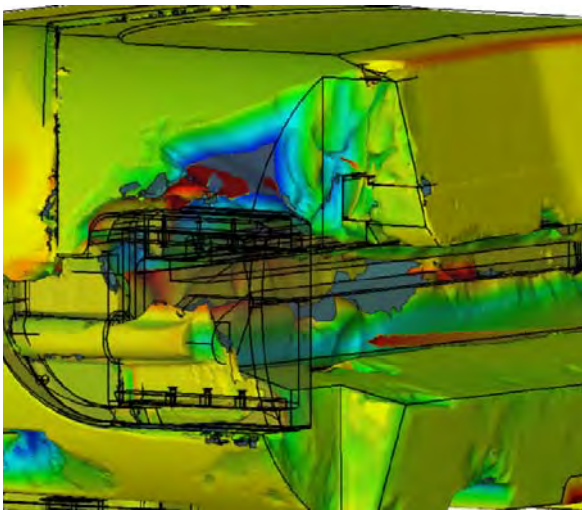
6.2.2 Three Dimensional Laser Scanning of Ram Blocks

Three dimensional laser scanning provided a means of characterizing surfaces in a quantitative manner and permitted ease of orientation of complex surfaces. Figure 33 and Figure 34 show that significant erosion occurred on the upper and lower BSR blocks. In order to quantify the erosion damage to the BSR blocks, the laser scan models were compared with generic CAD models depicting the unworn nominal geometry for the upper and lower BSR blocks. A contour surface plot of the deviation between the recovered blocks and the CAD model was developed.

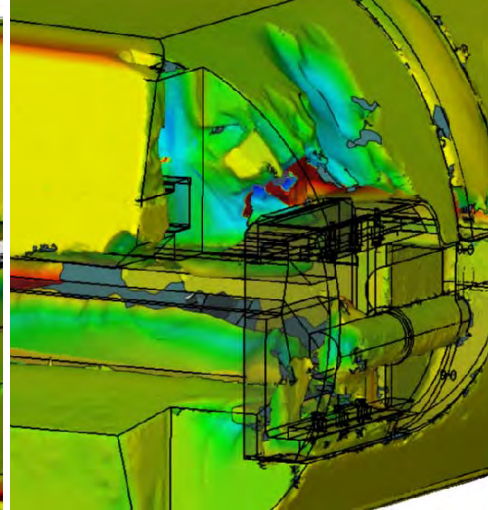
Figure 33 (b) and (c) show an overlay comparison for the upper BSR block with the laser scan model of the recovered BSR block shown as a deviation plot while the CAD model is overlaid as translucent and outlined. The blue color indicates material loss. Yellow indicates no material loss. Red indicates a positive deviation related to variations in recovered ram blocks associated with tolerances for the nominal geometry of the generic CAD model. There was more damage to the kill side of the upper BSR block than the choke side (Figure 33 (b) compared to (c)). The elastomer on the side packers was completely missing and much of the metallic side packer components was eroded away.



(a) Laser Scans of Upper BSR Block

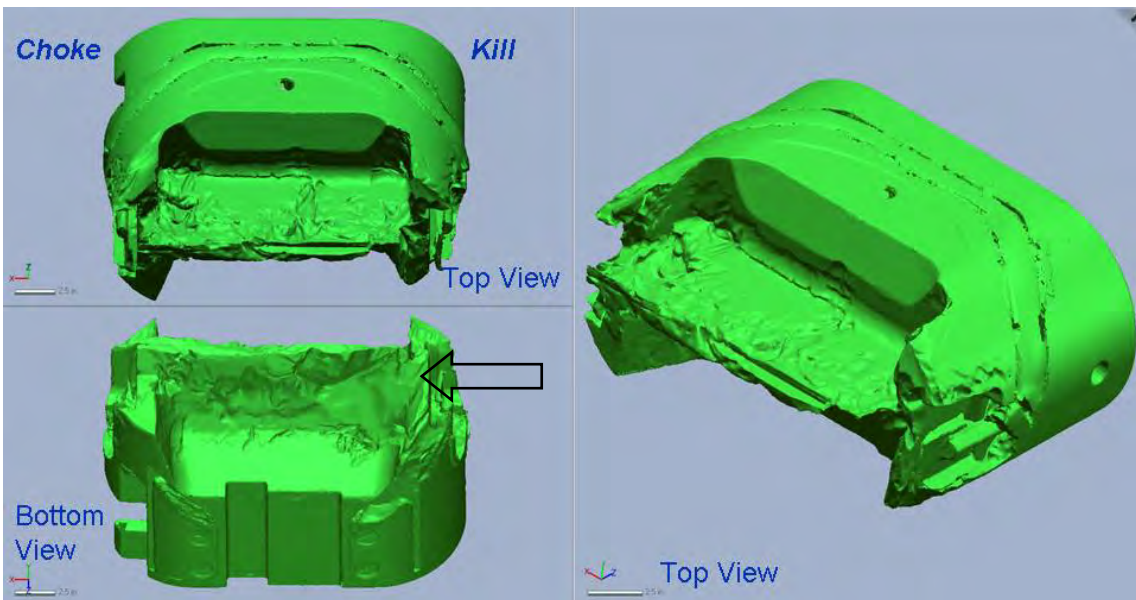


(b) Deviation Plot - Kill Side View



(c) Deviation Plot - Choke Side View

Figure 33 Three-Dimensional Laser Scan of Starboard-Side (Upper) BSR Block



(a) Laser Scan of Lower BSR Block

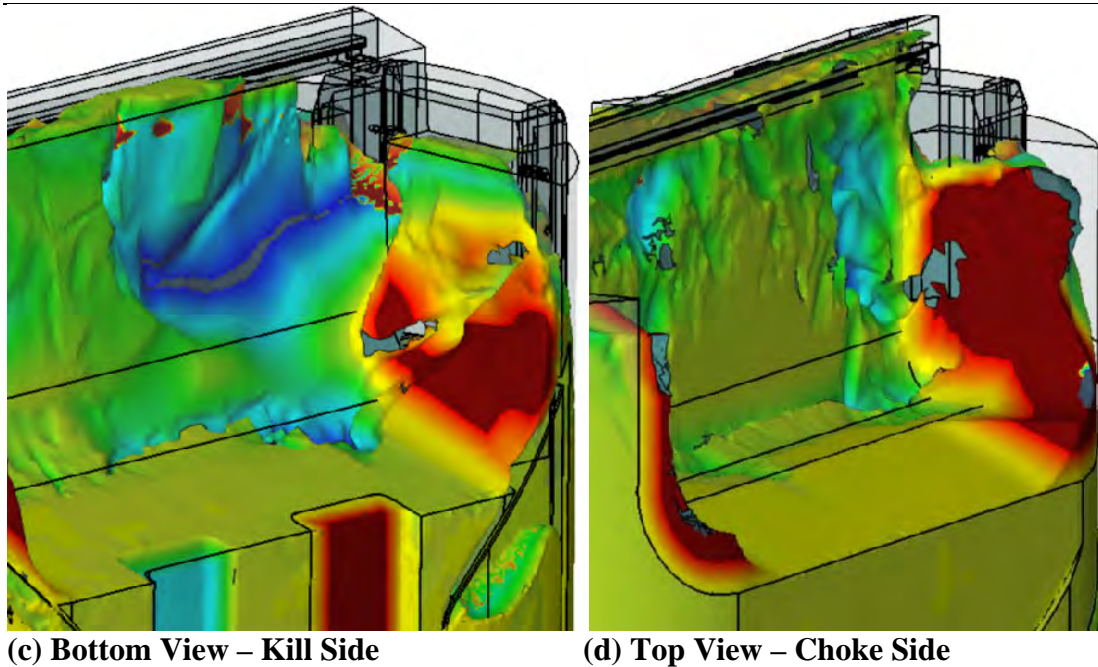
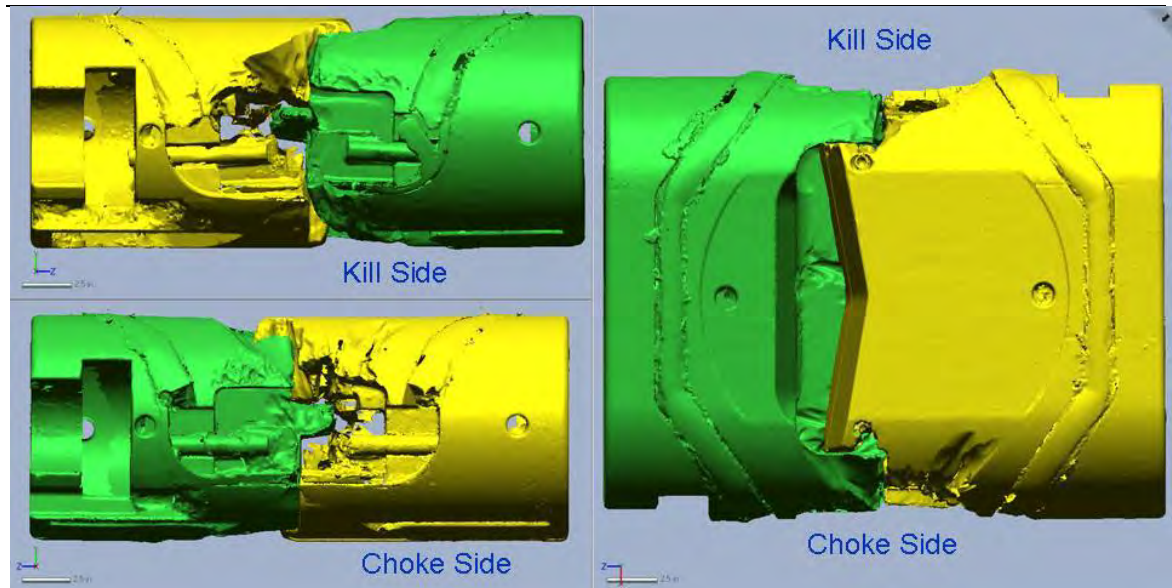


Figure 34 Three-Dimensional Laser Scan of Port-Side (Lower) BSR Block

Figure 34 shows that erosion occurred on both the top and bottom surfaces of the lower BSR blade. This erosion was particularly deep on the bottom surface on the kill-side of the blade (Figure 34 (b)) and on the top surface on the choke-side on the blade (Figure 34 (c)).

Figure 35 shows the upper and lower BSR blocks in the fully closed position. Based on the visual examination performed on site following recovery, the upper and lower BSR blocks exhibited metal-to-metal contact in multiple locations. As previously noted, the elastomer on the side packers and rear seals was missing allowing the metal-to-metal contact observed.



(a) Opaque



(b) Translucent

Figure 35 Three-Dimensional Laser Scan of BSRs Placed Together in the Closed Position

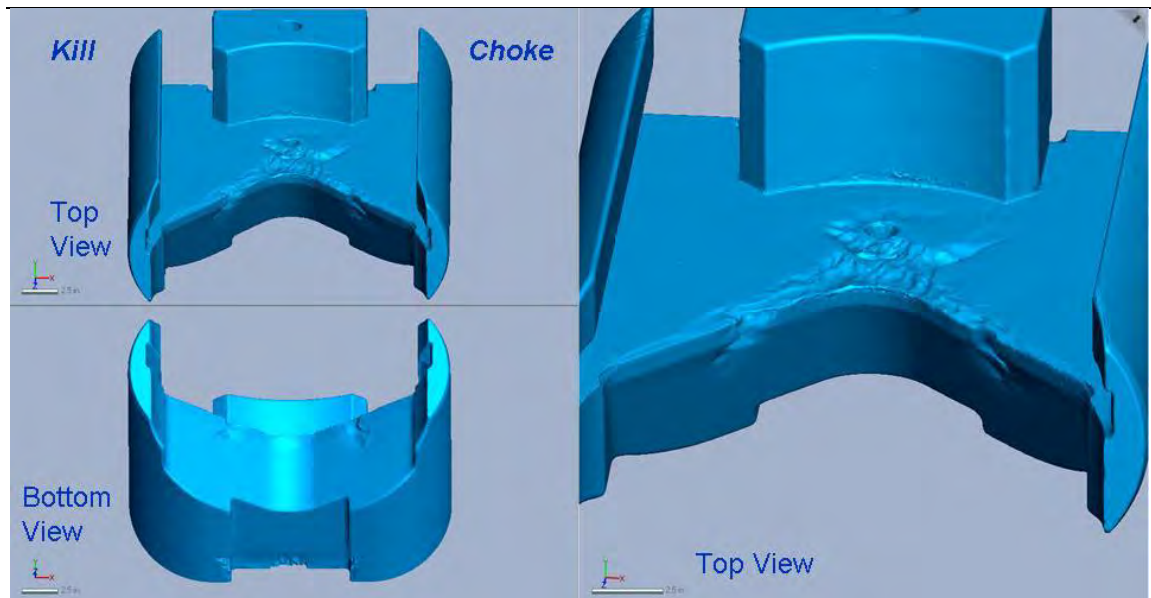


Figure 36 Three-Dimensional Laser Scan of Starboard-Side (Lower) CSR

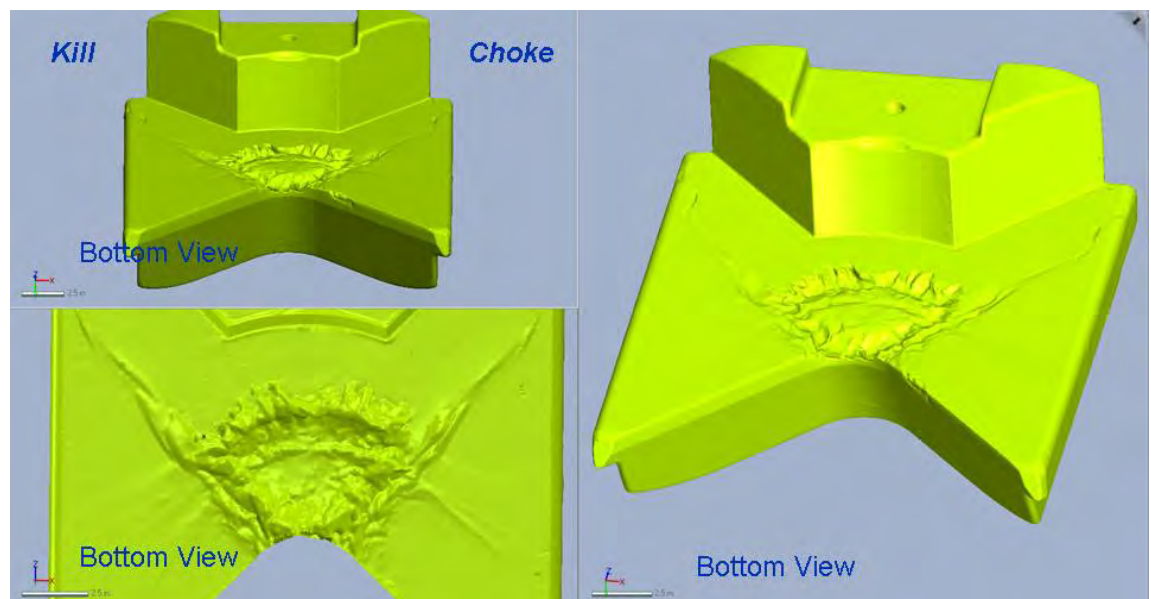


Figure 37 Three-Dimensional Laser Scan of Port-Side (Upper) CSR

Figure 36 and Figure 37 show the erosion on the CSRs. Significant erosion is observed on the bottom face of the upper CSR block (Figure 37). There is additional erosion on the top face of the Lower CSR (Figure 36) indicating the flow path out of the pipe impinging on the bottom face of the Upper CSR, flowing between the blades, and out across the top face of the Lower CSR. The CSR is not designed to seal (no side packers or seals for the blades) and there are relatively large gaps for fluid flow around the blades, ram cavities, and wellbore region of the CSR. Because there are not significant restrictions to fluid



flow, the total amount of erosion damage on the CSR is relatively small compared to the BSR.

6.2.3 Visual Examination of Drill Pipe

6.2.3.1 Location of Recovered Drill Pipe

Drill pipe was recovered from the LMRP, BOP, and Riser. Table 17 gives the length and description of the drill pipe segments recovered. Figure 38 shows a schematic diagram depicting the locations within the BOP stack and Riser from which the drill pipe segments were recovered.

Table 17 Evidence Item Numbers for Recovered Drill Pipe

Item No.	Length (inch)	Description of Segments of Drill Pipe
1-A-1	551.16	Recovered from the Riser at the USCG evidence yard above the kink.
39	137.25	Recovered from the LMRP at the Michoud Facility with the top end protruding ~6-inches above the UA
1-B-1	111.72	Recovered from the Riser at the USCG evidence yard above the kink (includes tool joint).
1-B-2	30.48	Recovered from the Riser at the USCG evidence yard between the kink and the intervention shear.
84	7.50	Recovered from the LMRP on the Q-4000 resting on top of the UA
83	111.60	Recovered from the LMRP on the Q-4000 inside the flex joint with the bottom end resting on the UA
94	42.00	Recovered from the BOP at the Michoud Facility between the BSR and CSR
148	142.25	Recovered from the BOP at the Michoud Facility between the CSR and Lower VBR

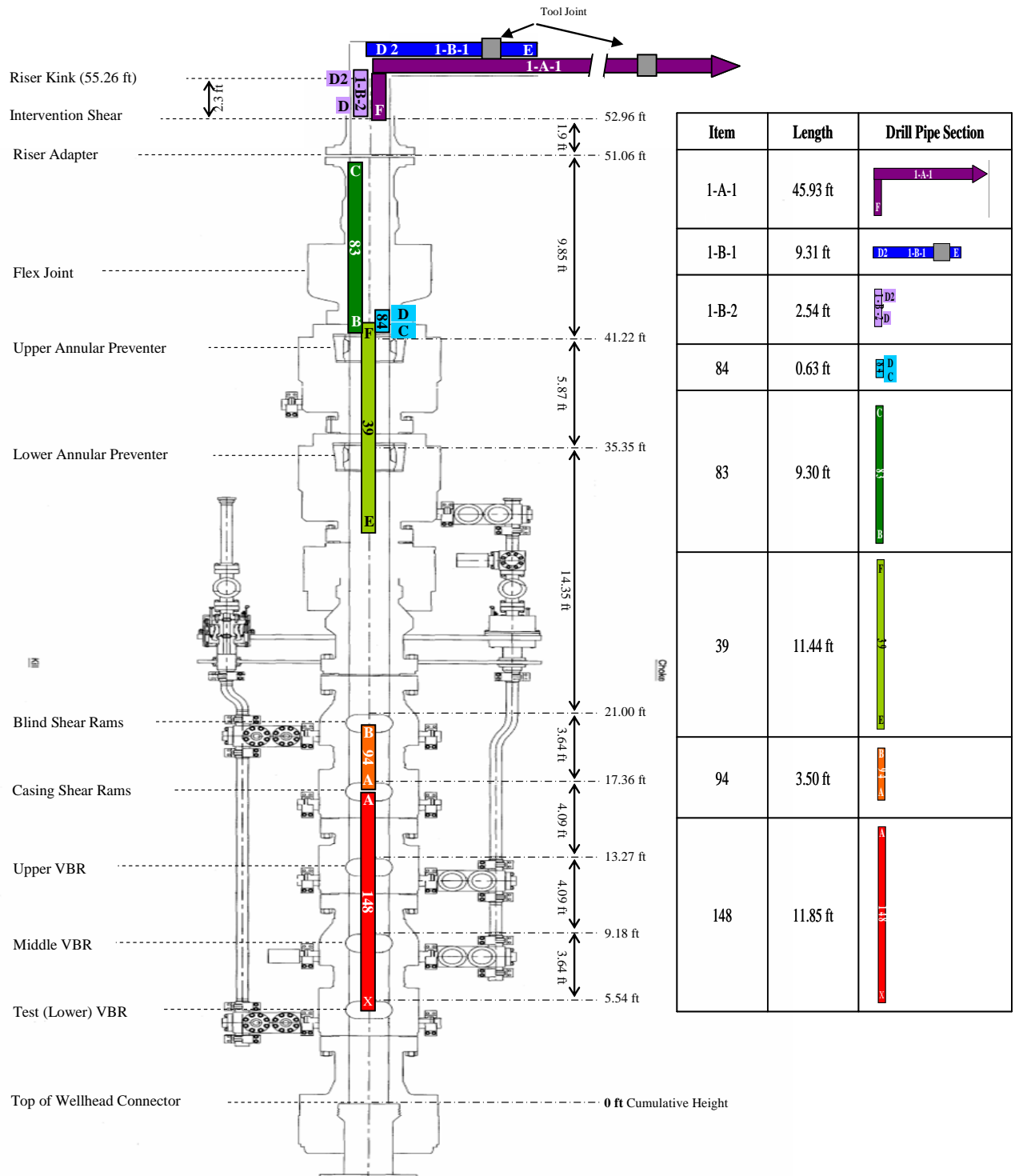
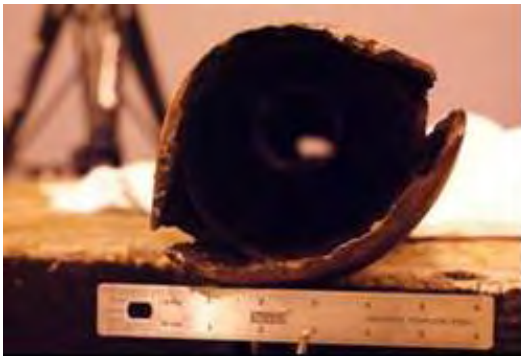


Figure 38 Schematic Diagram of Positions from which Drill Pipe was Recovered

6.2.3.2 Examination of the Drill Pipe

Figure 40 to Figure 54 show the individual drill pipe segments removed from the BOP, LMRP, and Riser. Figure 39 and Figure 40 show drill pipe segment 148 that was recovered from between the CSR and the Lower VBR. The top end exhibited a sheared surface representative of a CSR cut. The bottom end had significant erosion. The erosion is the most likely explanation for the separation of this segment from the rest of the drill pipe downhole. Significant erosion was also observed at areas where the segments of the Upper and Middle VBRs contact the drill pipe.



(a) Top End (148-A)



(b) Bottom End (148-X)

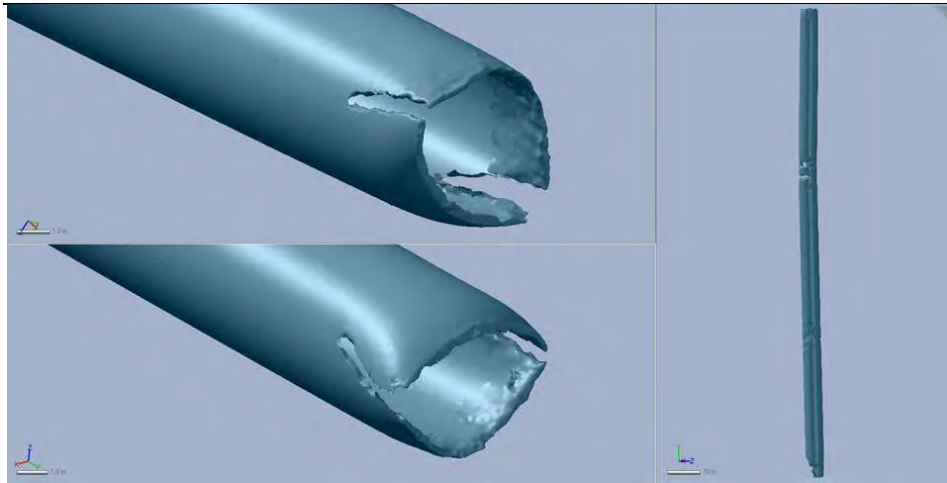


(c) Erosion at Upper VBR

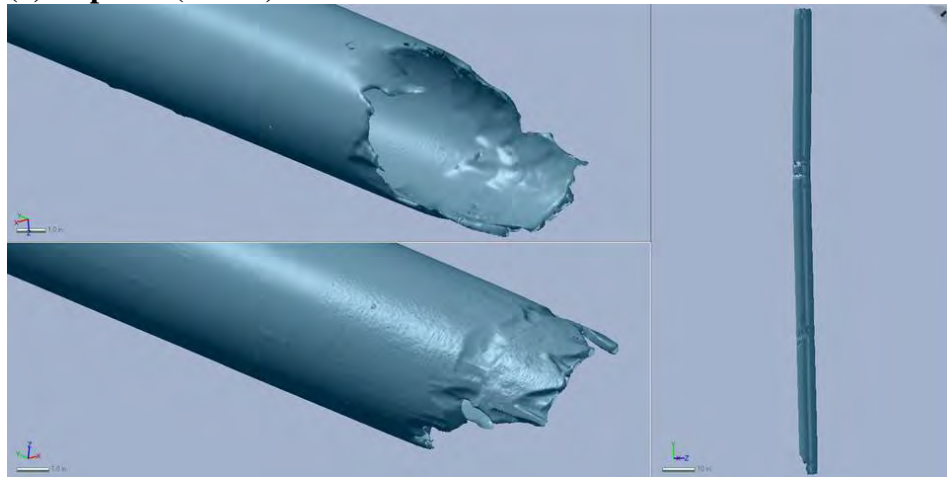


(d) Erosion at Middle VBR

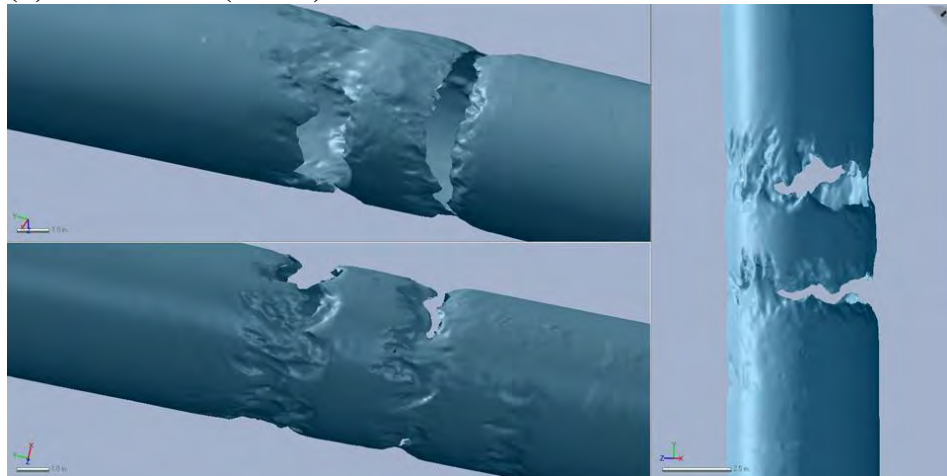
Figure 39 Photograph of Drill Pipe 148



(a) Top end (148-A)



(b) Bottom end (148-X)



(c) Erosion at the Upper VBR

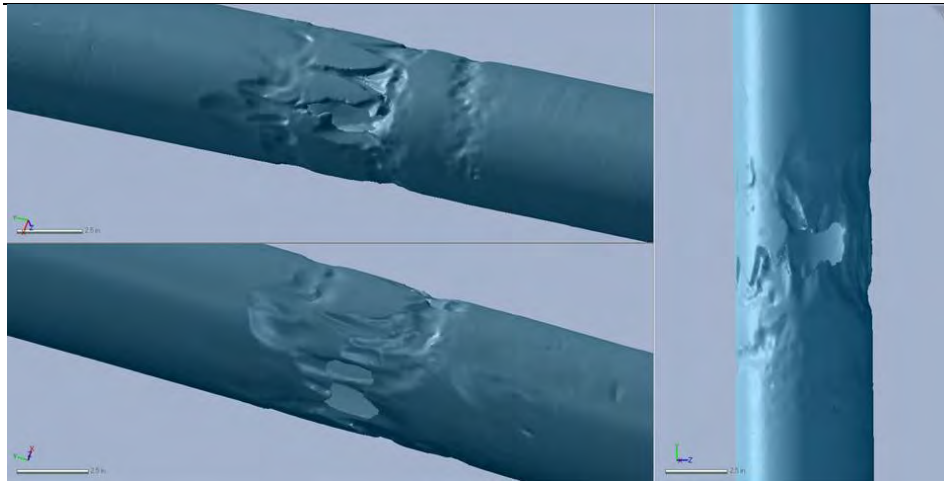
**(d) Erosion at the Middle VBR****Figure 40 Three-Dimensional Laser Scan of Drill Pipe Segment 148**

Figure 41 and Figure 42 show drill pipe segment 94 that was recovered from between the BSR and the CSR. The bottom end exhibits a sheared surface representative of a CSR cut and the top end has a surface that appears to be sheared (see a and b). One of the sides of the downstream end has a portion missing (see Figure 41 a [left side] and b [right side]).

**(a) Drill Pipe Segment 94****(b) Top end (94-B)****(c) Bottom end (94-A)****Figure 41 Photograph of Drill Pipe Segment 94**

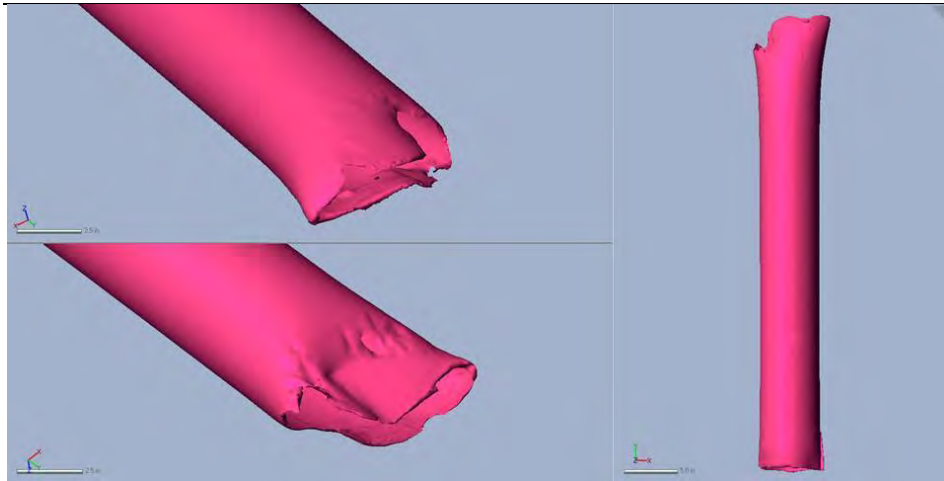
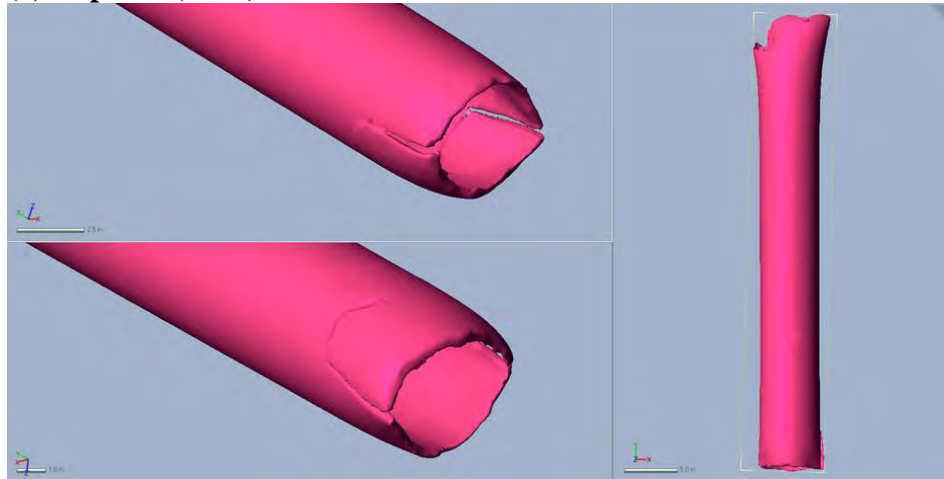
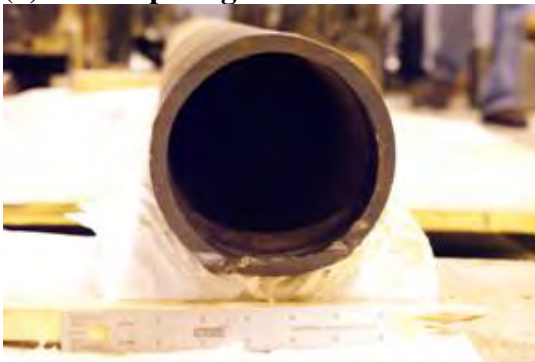
**(a) Top end (94-B)****(b) Bottom end (94-A)****Figure 42 Three-Dimensional Laser Scan of Drill Pipe Segment 94**

Figure 43 and Figure 44 show drill pipe segment 83 that was recovered from the wellbore of the Flex Joint and was resting on the UA. The bottom end is significantly deformed and approximately 1 inch of the end of the pipe is curled into the inside of the drill pipe with a flattened appearance on the end. The top end was cut (sawed) through for approximately 80 percent of the circumference and fractured the remainder.



(a) Drill Pipe Segment 83

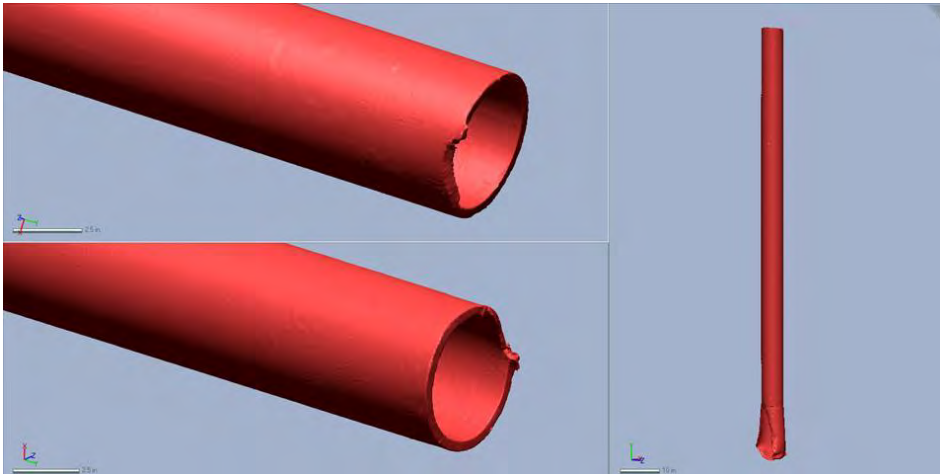


(b) Top end (83-C)

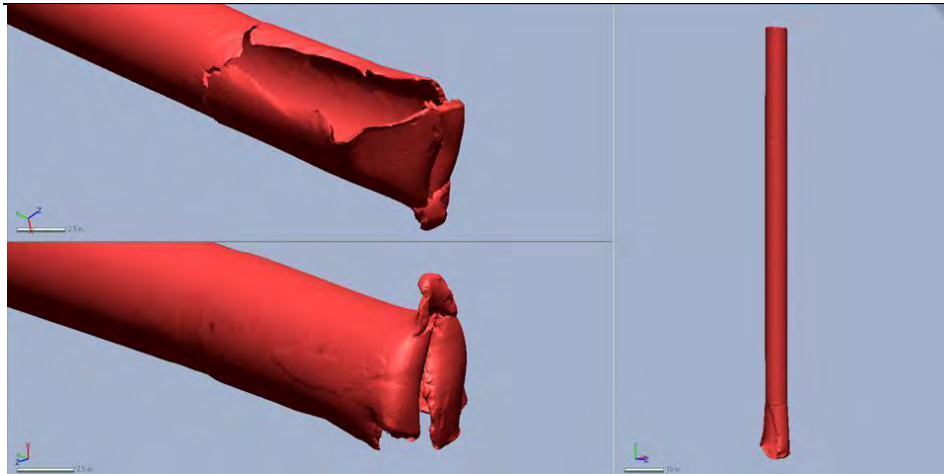


(c) Bottom end (83-B)

Figure 43 Photograph of Drill Pipe Segment 83



(a) Top end (83-C)



(b) Bottom end (83-B)

Figure 44 Three-Dimensional Laser Scan of Drill Pipe Segment 83

Figure 45 and Figure 46 show drill pipe segment 84 that was recovered from the top of the Upper Annular. Drill Pipe 84 had a saw cut on the bottom end (approximately 80% of circumference with the remaining exhibiting a fractured surface) and a shear cut on the top end.

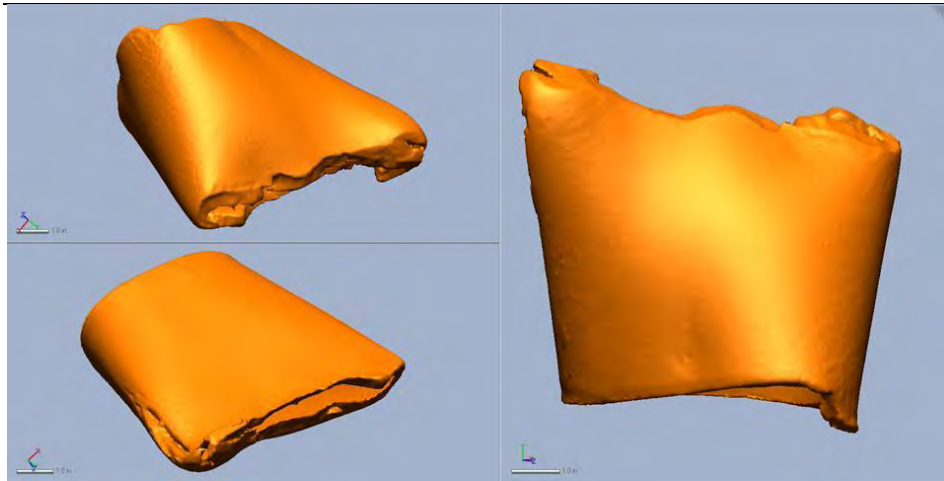


(a) Top end (84-D)

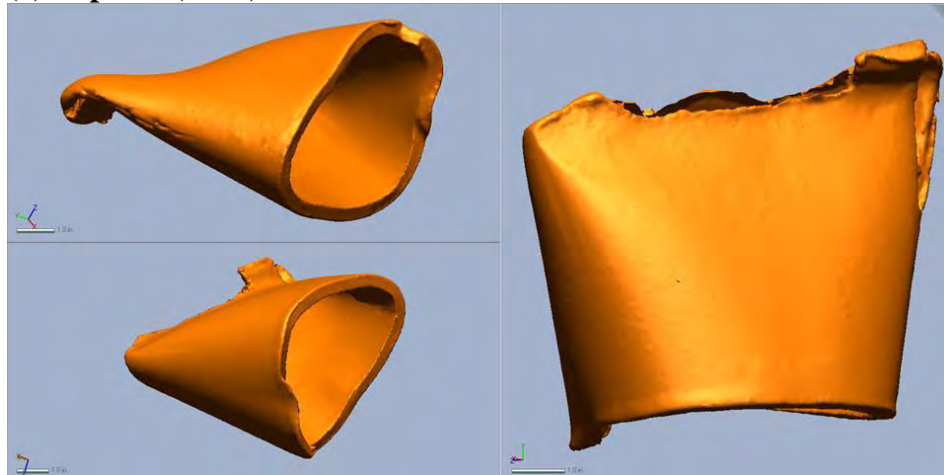


(b) Bottom end (84-C)

Figure 45 Photograph of Drill Pipe Segment 84



(a) Top end (84-D)



(b) Bottom end (84-C)

Figure 46 Three-Dimensional Laser Scan of Drill Pipe Segment 84

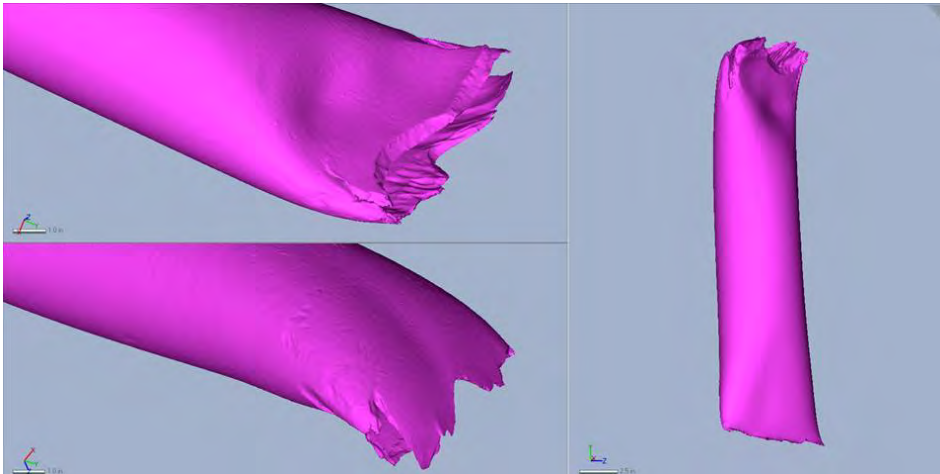
Figure 47 and Figure 48 show drill pipe segment 1-B-2 that was recovered from the Riser. Drill pipe segment 1-B-2 was recovered from below the kink in the Riser. The top end became separated from drill pipe segment 1-B-1 during removal from the Riser. The bottom end was an intervention shear cut.



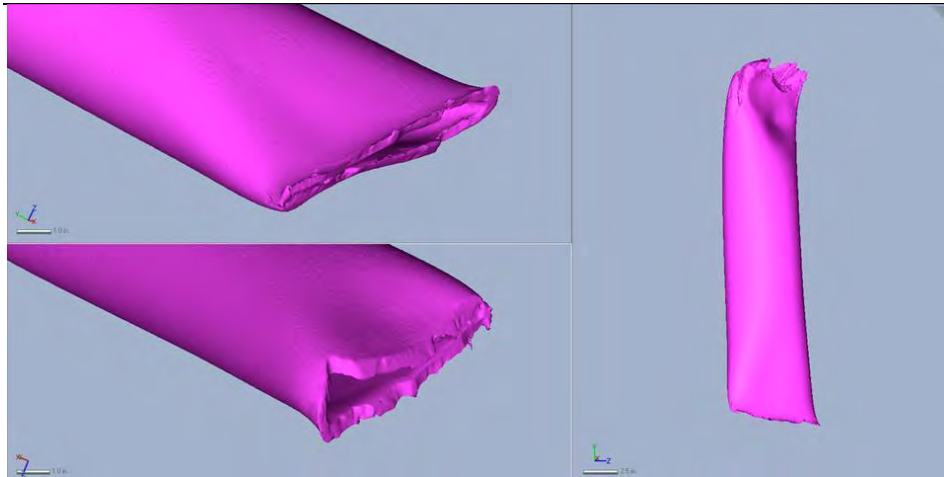
(a) Drill Pipe Segment 1-B-2

(b) Bottom end (1-B-2-D)

Figure 47 Photograph of Drill Pipe Segment 1-B-2



(a) Top end (1-B-2-D2)



(b) Bottom end (1-B-2-D)

Figure 48 Three-Dimensional Laser Scan of Drill Pipe Segment 1-B-2

Figure 49 and Figure 50 show drill pipe segment 1-B-1 that was recovered from the Riser. Drill pipe segment 1-B-1 was above the kink in the Riser and became separated from drill pipe segment 1-B-2 during removal. The bottom end of drill pipe segment 1-B-1 became separated from drill pipe segment 1-B-2 at the kink in the Riser. The top end was severely eroded with a fracture surface of approximately 30% of the circumference. The remainder of the circumference was too eroded to see the fracture surface.



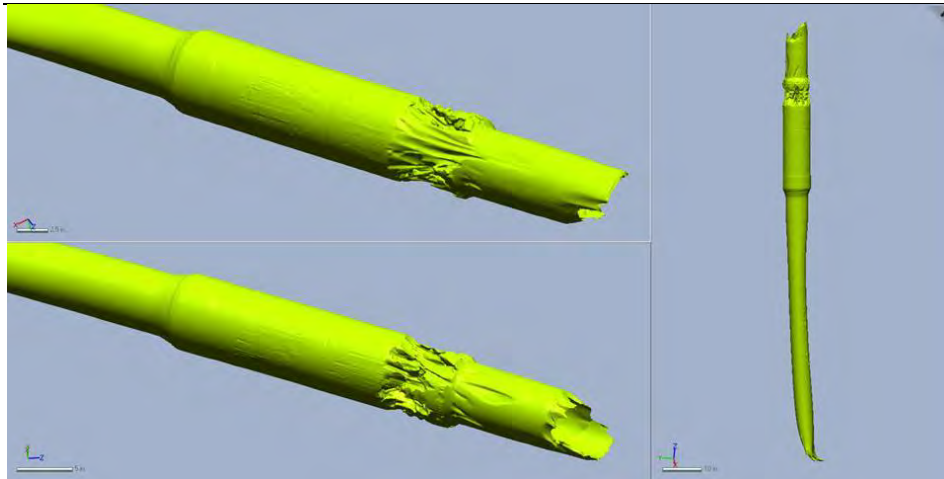
(a) Drill Pipe Segments 1-B-1 and 1-B-2



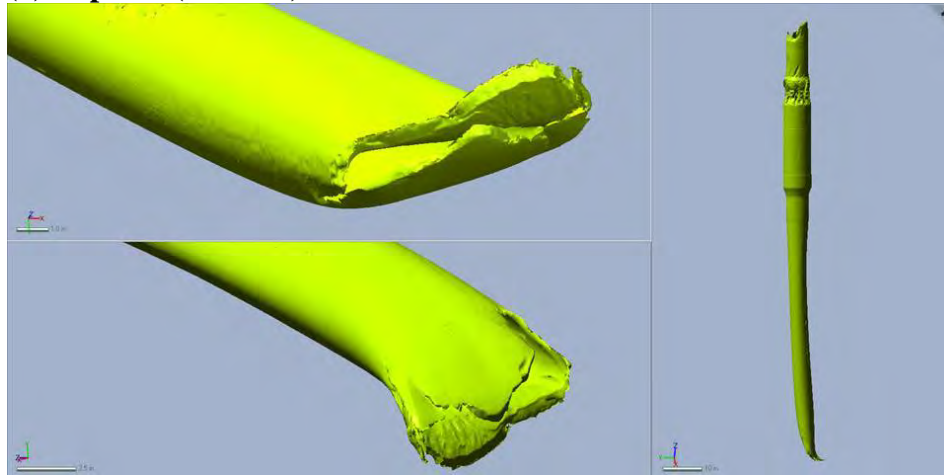
(b) Bottom End (1-B-1-D2)

(c) Top End (1-B-1-E)

Figure 49 Photograph of Drill Pipe Segment 1-B-1



(a) Top end (1-B-1-E)



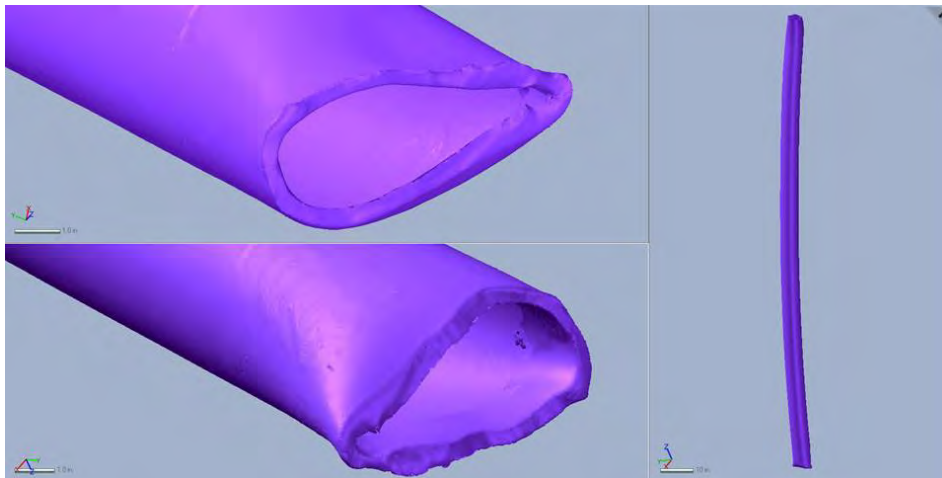
(b) Bottom end (1-B-1-D2)

Figure 50 Three-Dimensional Laser Scan of Drill Pipe Segment 1-B-1

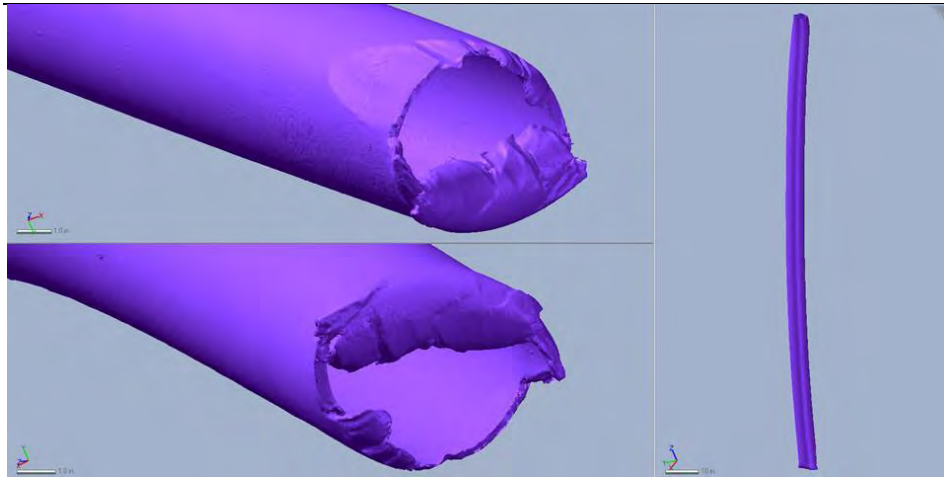
Figure 51 and Figure 52 show drill pipe segment 39 that was recovered from within the LMRP with a small portion above the UA. This segment of drill pipe had a curvature in its length. The top end was a shear cut and the bottom end was significantly deformed. The bottom end had approximately 1 inch of the end of the pipe curled into the inside of the drill pipe.



(a) Drill Pipe Segment 39 (b) Top End (39-E) (c) Bottom End (39-F)
Figure 51 Photograph of Drill Pipe Segment 39



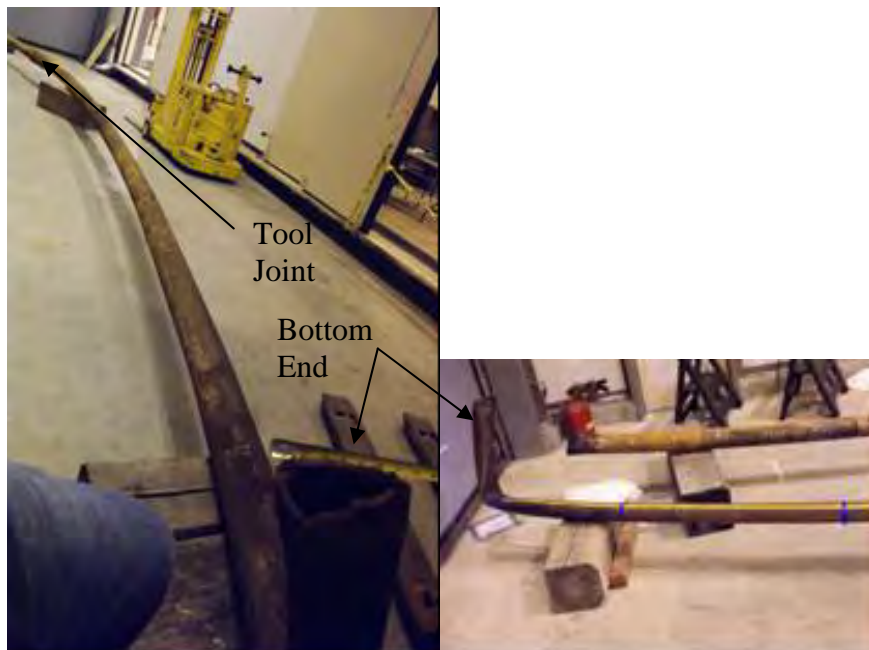
(a) Top End (39-F)



(b) Bottom end (39-E)

Figure 52 Three-Dimensional Laser Scan of Drill Pipe Segment 39

Figure 53 and Figure 54 show drill pipe segment 1-A-1 recovered from within the Riser. The bottom end of drill pipe segment 1-A-1 was an intervention shear cut and the top end was a shear cut that was made at the time of retrieval of this portion of the Riser from the sea floor. Drill Pipe 1-A-1 includes a tool joint towards the top end.

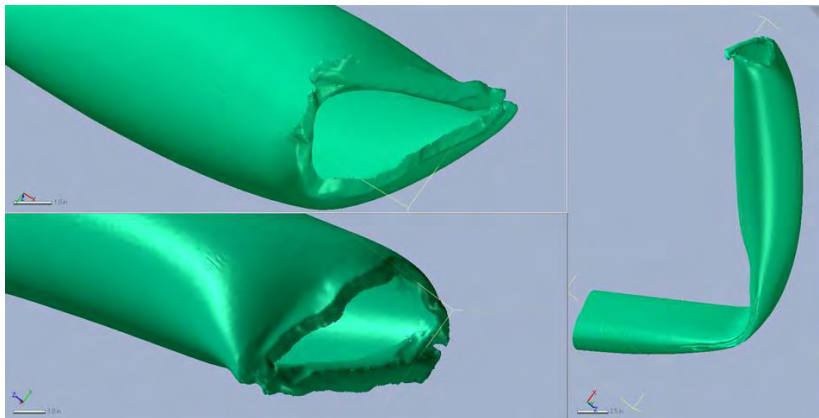


(a) Drill Pipe Segment 1-A-1



(b) Tool joint

(c) Bottom end (1-A-1-F)

Figure 53 Photograph of Drill Pipe Segment 1-A-1**Figure 54 Three-Dimensional Laser Scan of Drill Pipe Segment 1-A-1-F**

6.2.4 Matching Drill Pipe Segments

The ends of the recovered drill pipe segments were labeled U/S for bottom end and D/S for top end. Matching of drill pipe segment ends was initially performed by comparing locations recovered, surface end features and dimensions of pipe segments. The final analysis (presented below) provided the drill pipe end matching given in Table 18. Figure 55 (a) shows the drill pipe segments positioned in the BOP Stack based on this matching sequence.

Table 18 Detail for the Matching of the Drill Pipe Segment Ends

Top End	Bottom End	Method of Separation
39-F	1-A-1-F	Intervention Shear Cut of Riser above BOP
1-B-1-E	39-E	Separated at top of Upper Annular (tensile failure)
1-B-2-D2	1-B-1-E2	Separated at Kink in Riser during removal process at Michoud Facility
84-D	1-B-2-D	Intervention Shear Cut of Riser above BOP
83-C	84-C	Intervention Saw Cut of Riser above BOP
94-B	83-B	BSR Operation
148-A	94-A	CSR Operation

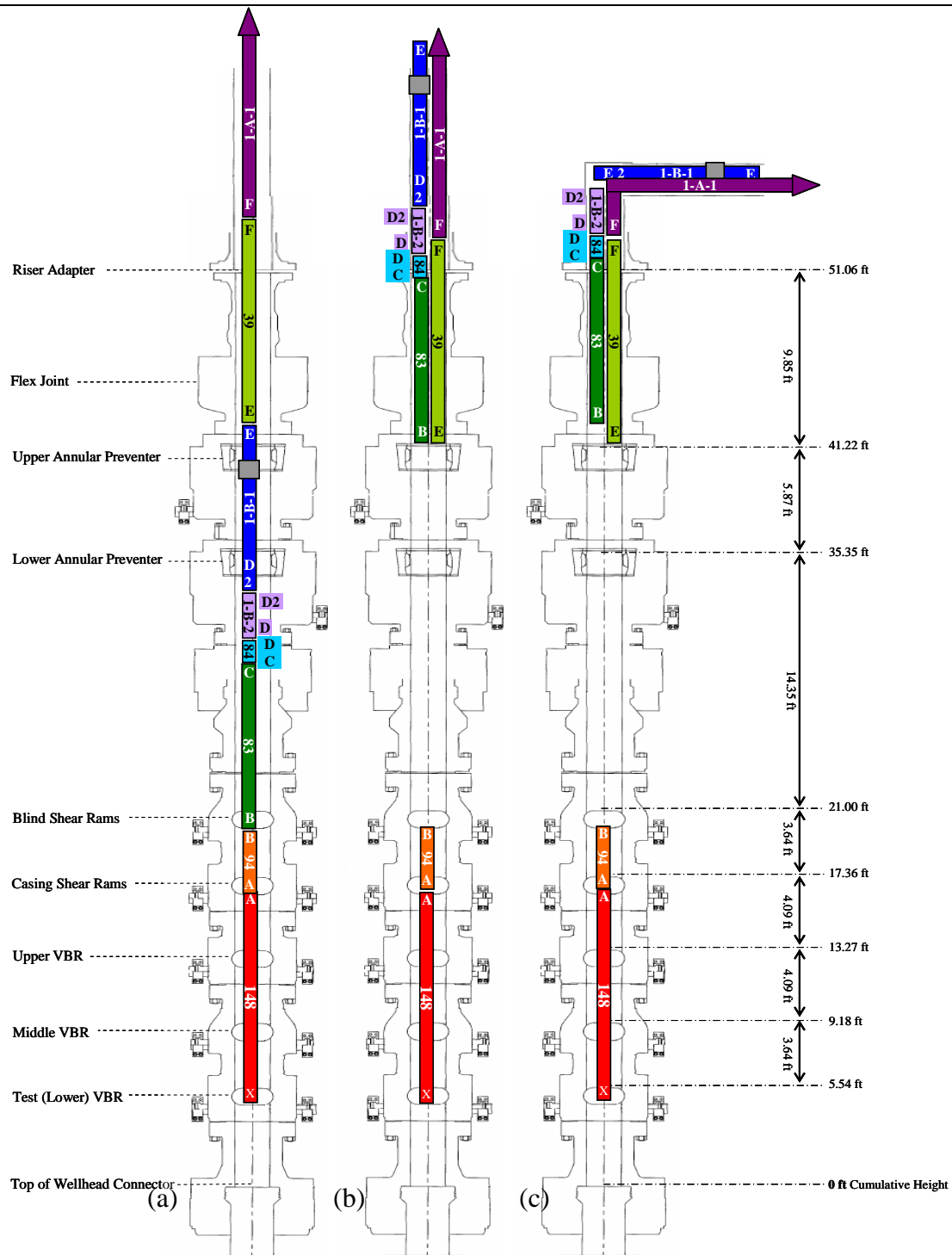


Figure 55 Schematic Diagram of Sequence of Drill Pipe Segment Movement

[Note: left to right (a) drill pipe prior to incident, (b) drill pipe following break at point E and point B, and (c) drill pipe following sinking of rig and kink in Riser above BOP stack.]

6.2.4.1 Matching 148-A to 94-A

The cut at 'A' was postulated to be the CSR cut and the ends 148-A and 94-A were representative of such a cut. Also, 148-A matched closely to 94-A (see Figure 56). Figure 56 also shows the pipe aligned with the CSRs prior to cutting. Figure 57 shows the positions of the drill pipe segment with respect to the CSRs following cutting. The erosion pattern on the bottom surface of the upper CSR block matched the shape of 148-A (Figure 37). Based on this analysis and the fact that the drill pipe segments were recovered with these ends facing toward the CSR, there is a high level of confidence that the cut at 'A' was due to the CSR.

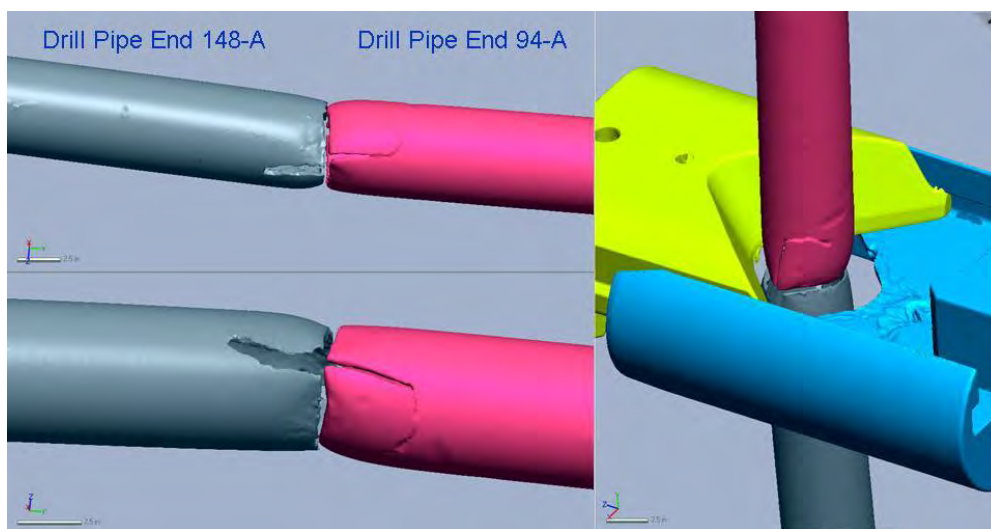


Figure 56 Three-Dimensional Laser Scan Comparing 148-A and 94-A

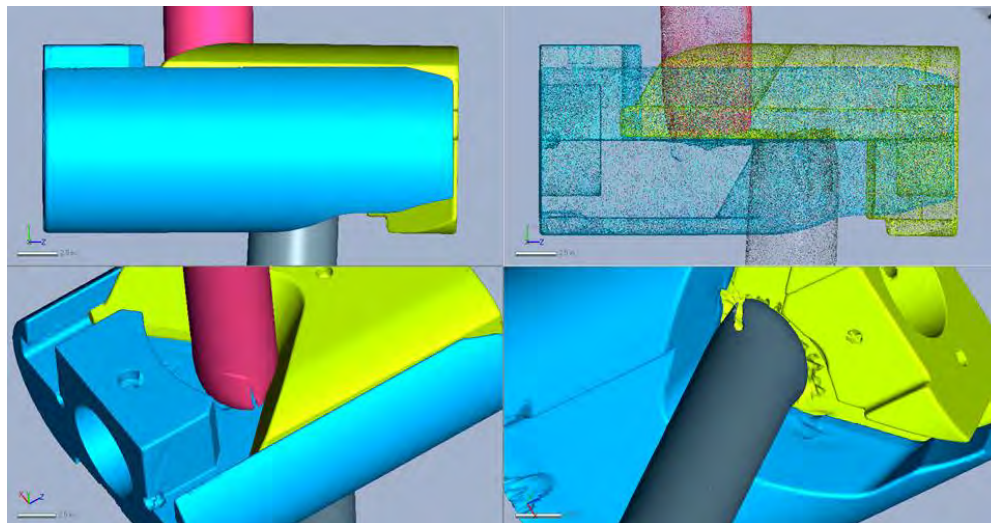


Figure 57 Three-Dimensional Laser Scan of 148-A and 94-A Following CSR Cutting

6.2.4.2 Matching 94-B to 83-B

The cut at 'B' is postulated to be the BSR cut and 94-B and 83-B are the matching ends of this cut. 83-B and 94-B are shown in Figure 58 and Figure 59, respectively. 83-B (Figure 58 (b)) was deformed, making matching of surface features to 94-B impossible. Figure 58 (c), (d), and (e)) shows the ends of the pipe curled inwards. The forces required to cause the deformation were probably responsible for the splitting and opening of the side wall of the pipe (Figure 58 (a), (c), and (d)). Erosion was also seen at the edges of the side wall of the pipe (Figure 58 (d)). Prominent at the end of the pipe was a missing "corner" of material (best seen in Figure 58 (a)) adjacent to the "flat" marked with the number 83.

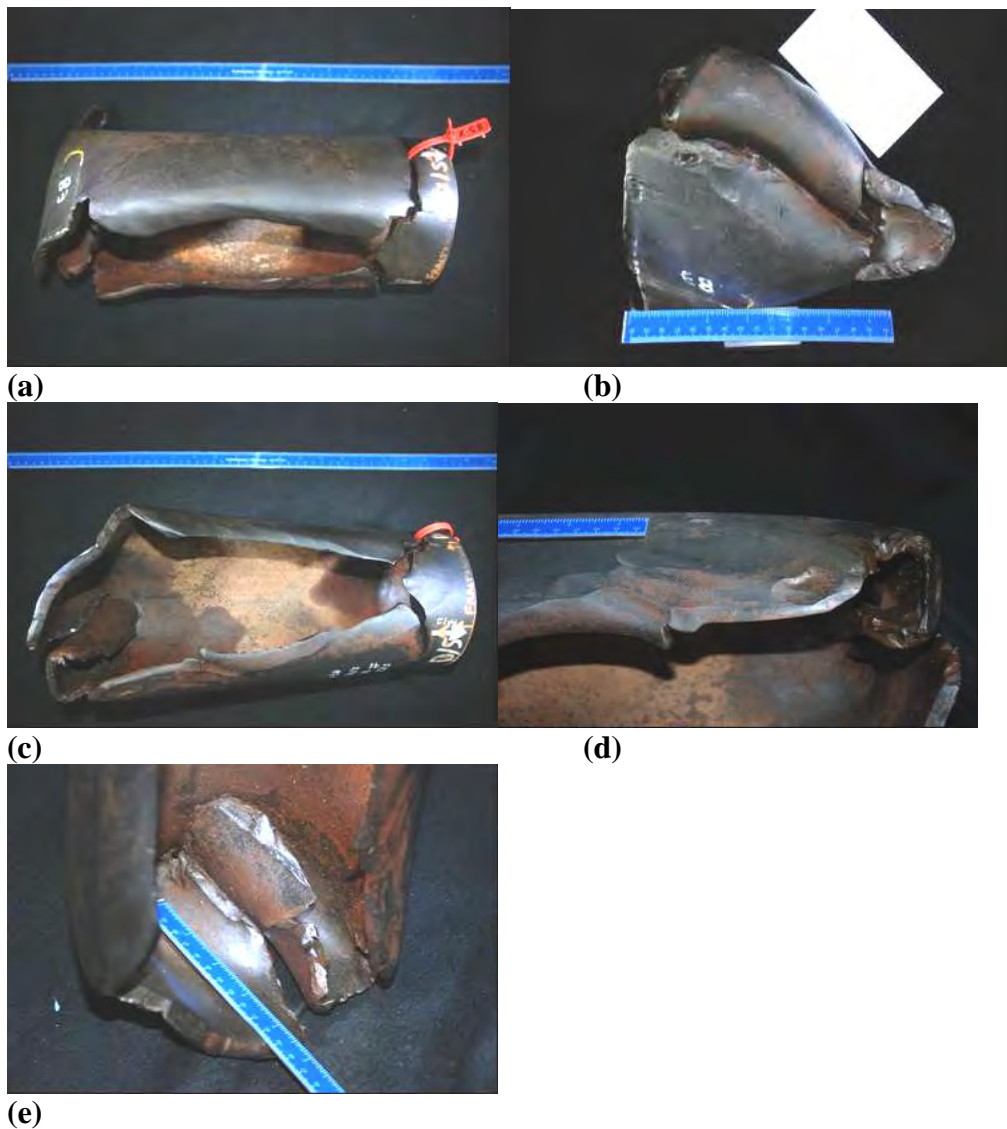


Figure 58 Photographs of 83-B

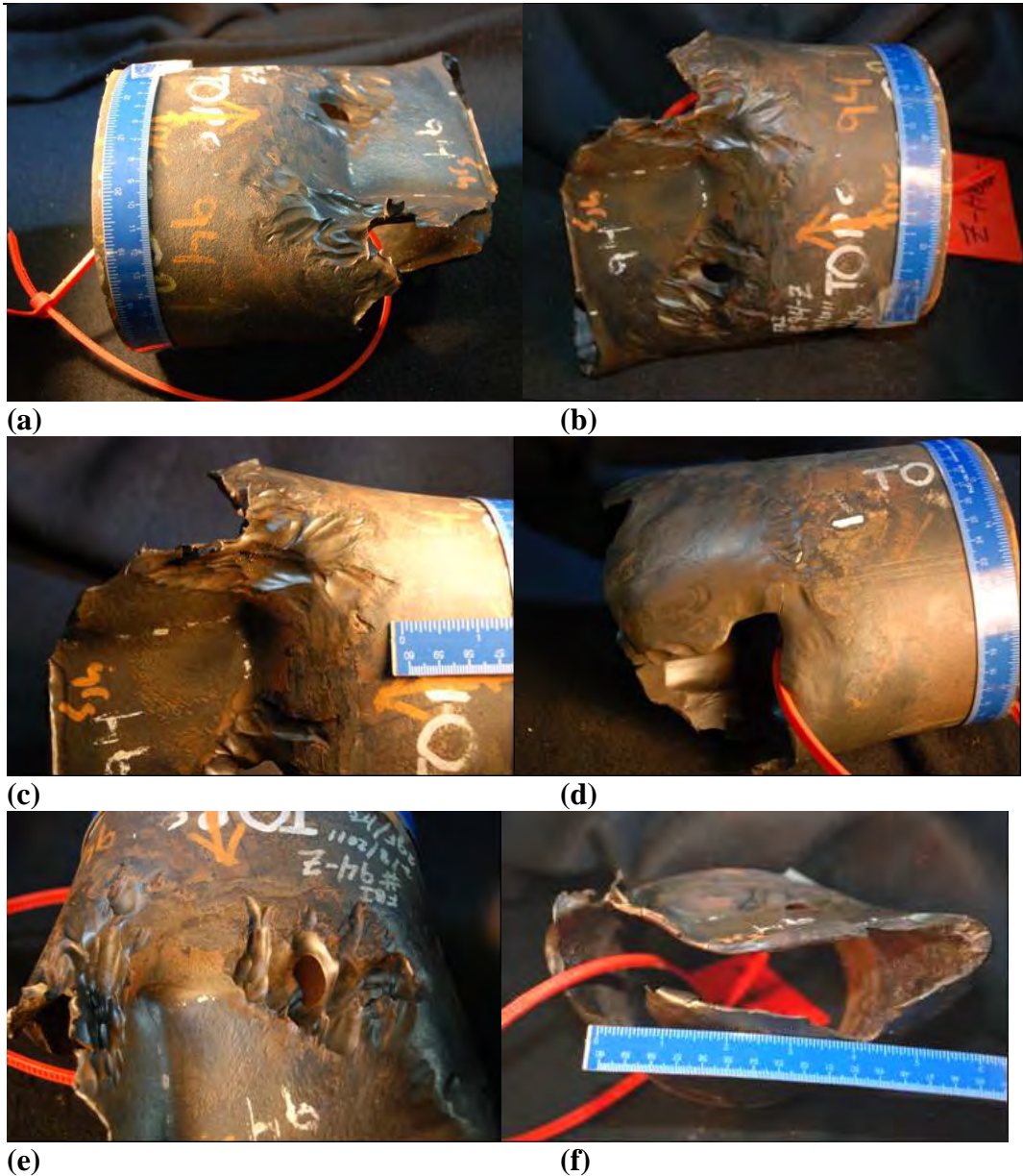


Figure 59 Photographs of 94-B

Figure 59 shows several views of 94-B. There was a prominent “flat” pressed into 94-B (Figure 59 (a), (b), and (c)). There was a missing corner of material as seen in Figure 59 (a), (b), (c), and (d). The erosion seen in the photographs resulted in a through-wall hole (Figure 59 (e)). The overall thinning of the drill pipe wall is seen in Figure 59 (f). In addition, 94-B may be missing a short (1.5 to 2-inch) length which may have been folded over during the BSR cut.

The common features of 83-B and 94-B are the flat areas that were pressed into their surfaces and the corners missing on one side of each. With 83-B and 94-B facing each other and the flats oriented to the same side, the missing corners match.

Figure 60 shows the laser scans for 83-B and 94-B. Figure 61 shows laser scans of 83-B and 94-B matched against the upper BSR block. The flats pressed into 83-B and 94-B matched against the kill side front face of the upper BSR block. The common features noted above for 83-B and 94-B and the matching to the upper BSR block provide a high level of confidence that 83-B and 94-B were the cut ends from the BSR.

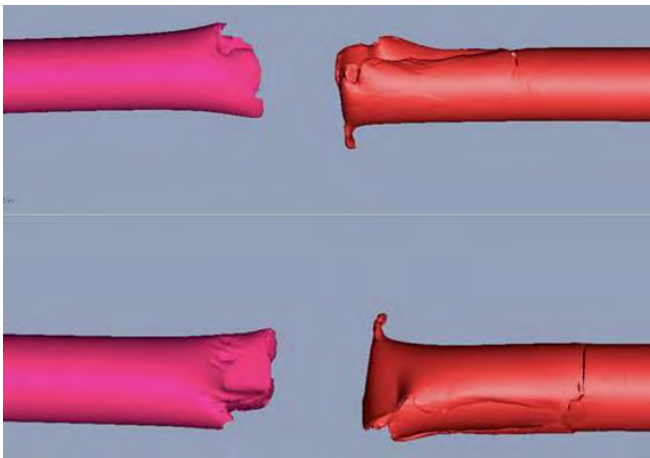


Figure 60 Laser Scans of 94-B and 83-B

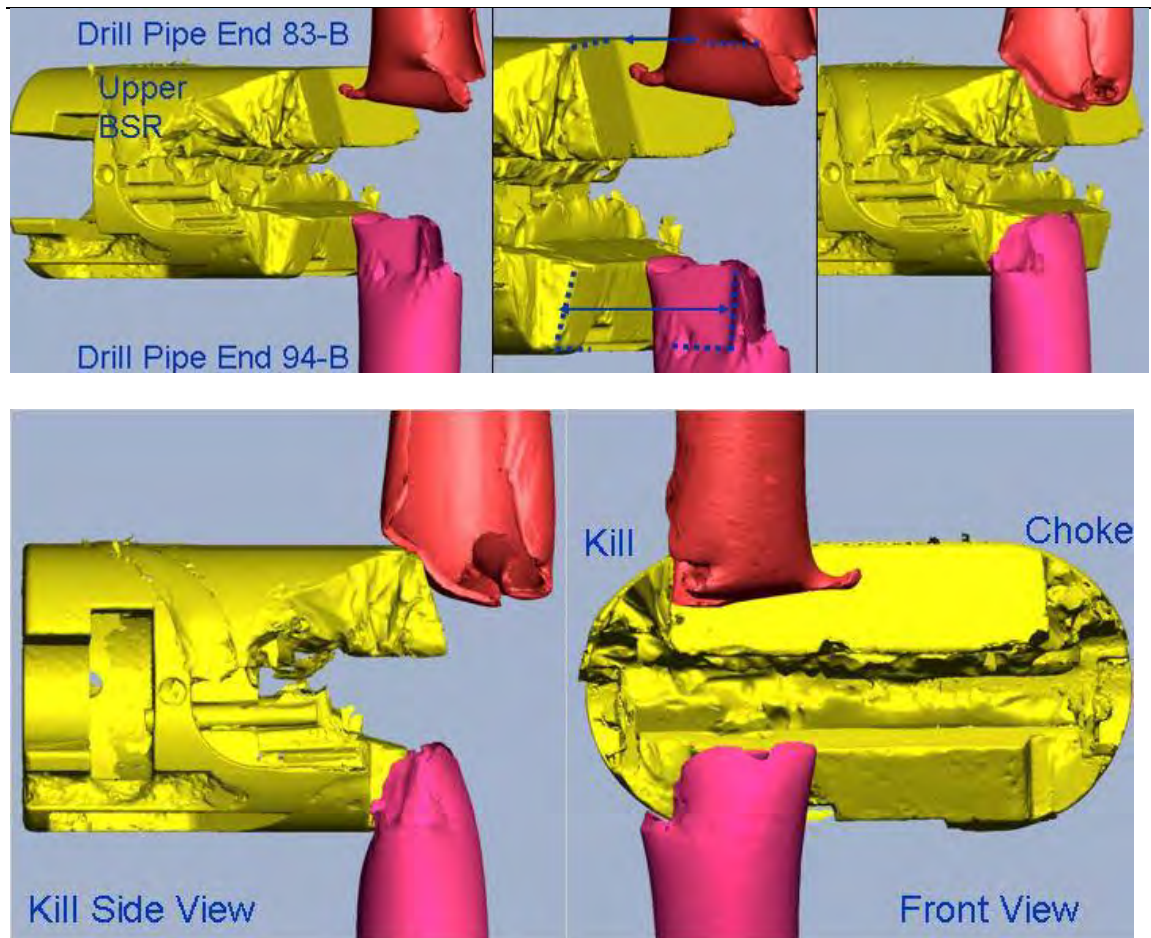


Figure 61 Laser Scans of 94-B and 83-B Matched Against the Upper BSR Block

6.2.4.3 Matching 83-C to 84-C

The cut at 'C' is postulated to be the intervention diamond blade saw cut of Riser above the BOP Stack. 83-C and 84-C were the matching ends of this cut (see Figure 62). Based on visual examination there is a high level of confidence that the cut at 'C' was due to the intervention diamond saw cut.

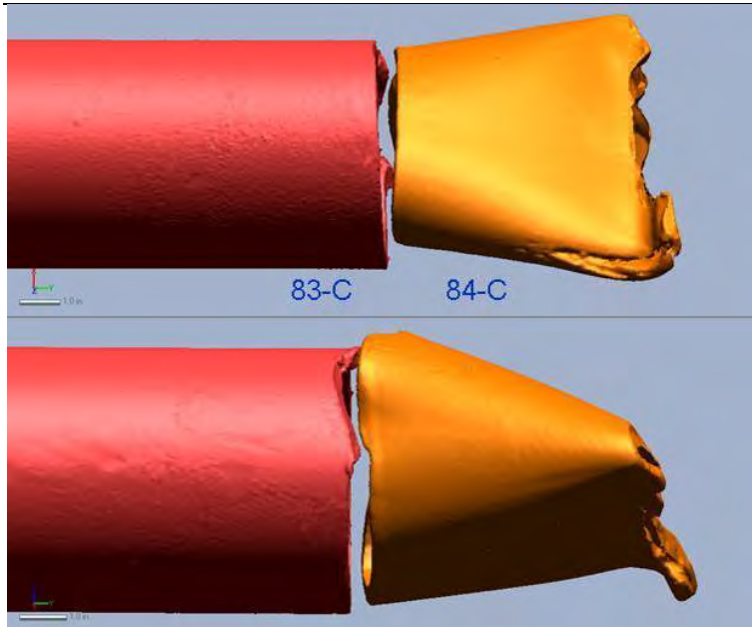


Figure 62 Laser Scans of 83-C and 84-C

6.2.4.4 Matching 84-D to 1-B-2-D

The cut at 'D' is postulated to be the intervention shear cut of Riser above the BOP Stack. 84-D and 1-B-2-D are the matching ends of this cut (see Figure 63). Based on this visual examination there is a high level of confidence that the cut at 'D' was due to the intervention shear cut.

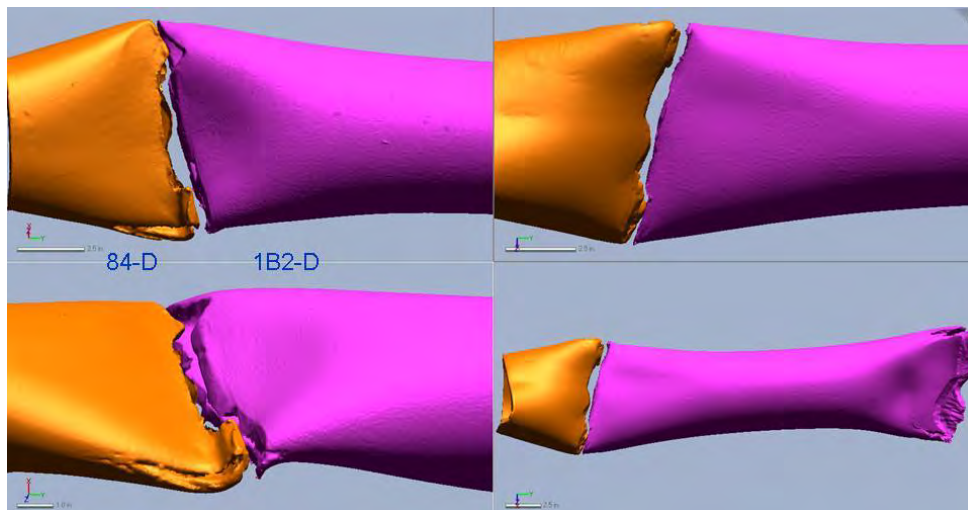


Figure 63 Laser Scans of 84-D and 1-B-2-D

6.2.4.5 Matching 1-B-2-D2 to 1-B-1-D2

The separation of drill pipe segment 1-B (resulting in 1-B-2 and 1-B-1) occurred at the kink in the Riser during the removal of the drill pipe segment from the Riser at the Michoud facility. Figure 64 shows the laser scans of these matching surfaces.

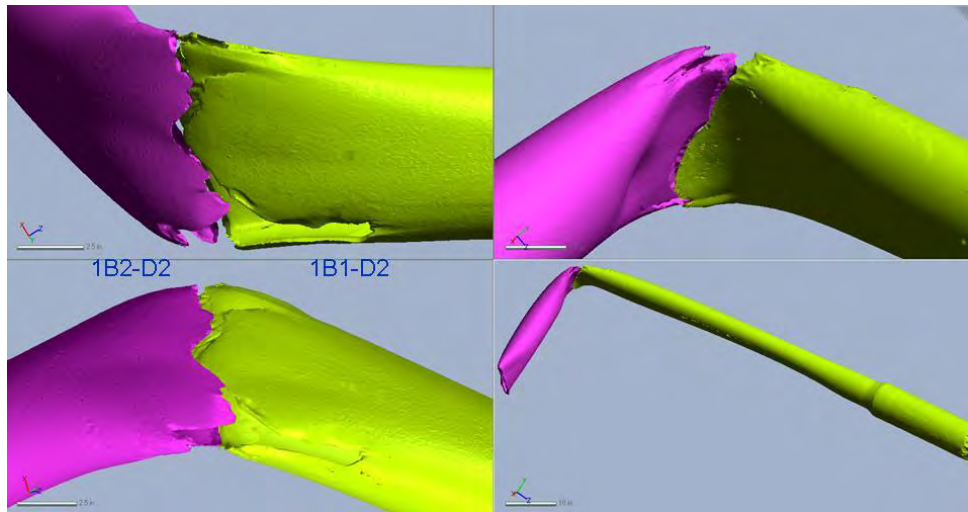


Figure 64 Laser Scans of 1-B-2-D2 and 1-B-1-D2

6.2.4.6 Matching 1-B-1-E to 39-E

The separation at 'E' is postulated to be a drill pipe tensile failure. 1-B-1-E and 39-E are matching ends of this failure. This failure of the drill pipe is postulated to have occurred in the top element of the UA (see location in Figure 55 (a)). 1-B-1-E and 39-E are shown in Figure 65 and Figure 68, respectively. The end of 39-E was deformed and the end of 1-B-1-E was eroded, making matching of surface features of the pipe ends difficult.

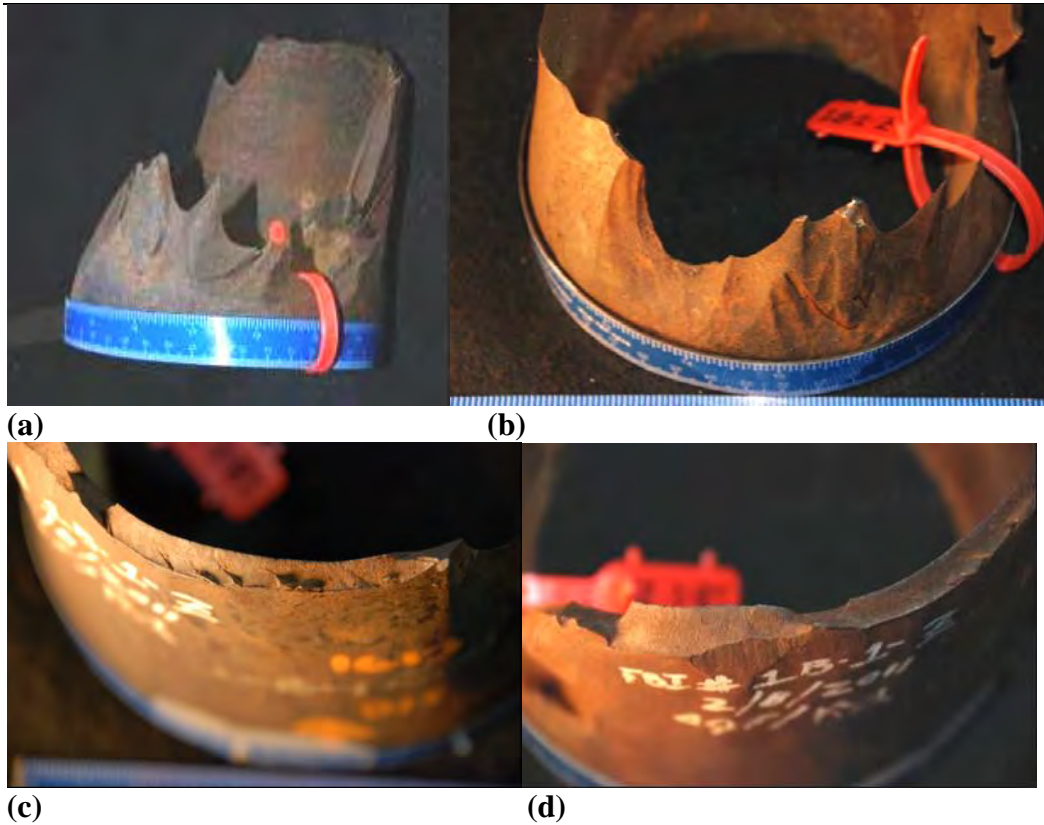


Figure 65 Photographs of 1-B-1-E

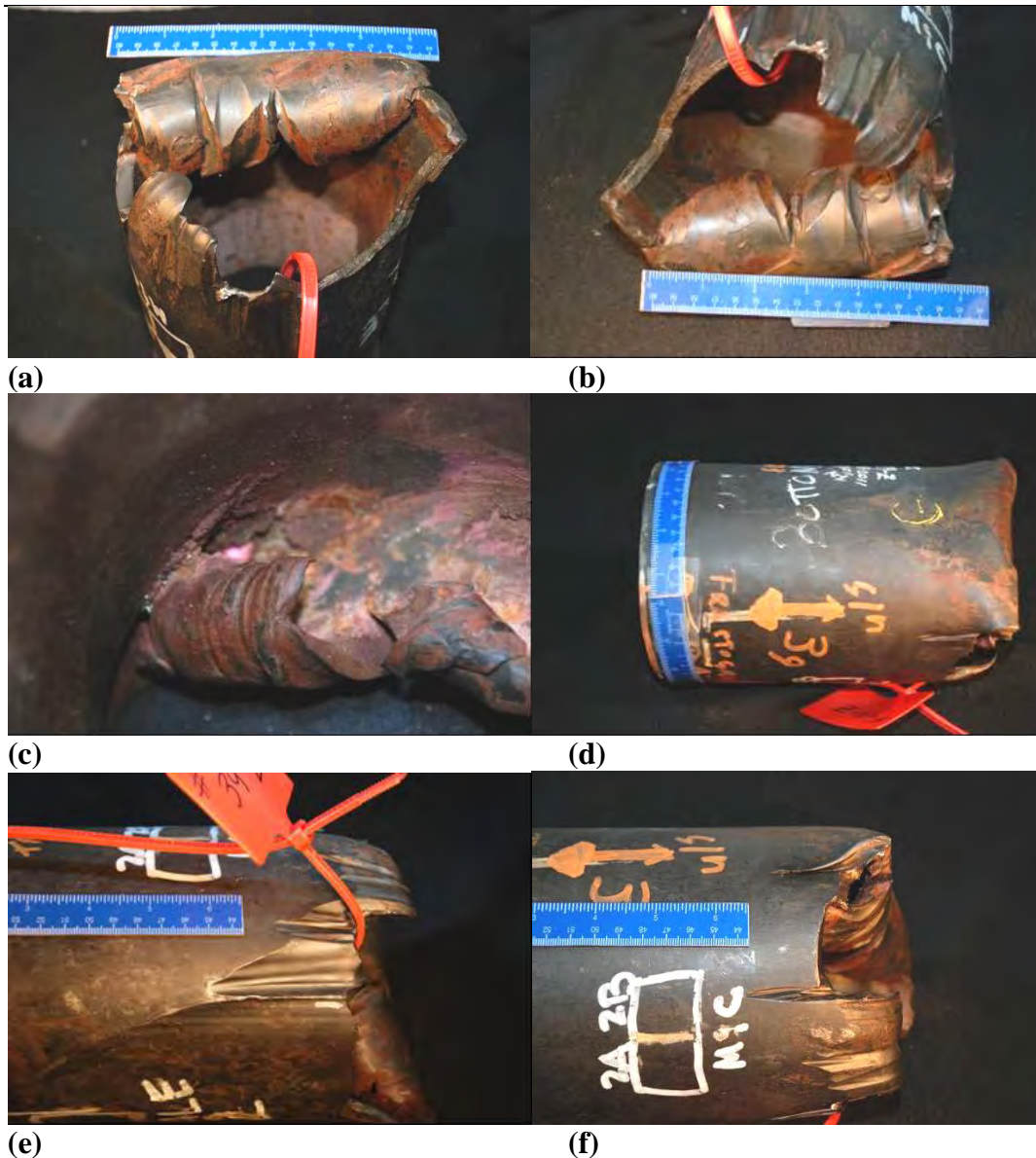


Figure 66 Photographs of 39-E

1-B-1-E was characterized by erosion that removed a portion of the drill pipe wall. There was an area of approximately 30% of the circumference (Figure 65 (a)) that exhibited only minor signs of erosion. This area was a fracture surface with a 45 degree shear angle (Figure 65 (c) and (d)). This is typical of a tensile failure of a high strength steel.

Figure 66 shows photographs of 39-E. The pipe end was characterized by deformation and erosion that had a regular spacing of 1 to 1.5 inches. The end of the pipe was curled inwards (Figure 66 (a), (b), and (c)). Figure 66 (c) shows the curled end as viewed from the inside of the pipe. The erosion pattern was along the entire length of the curled ends, indicating that the erosion most likely occurred prior to the deformation. There were

portions of the pipe wall that were missing. The flat portion of the end surface opposite of the ruler in Figure 66 (f) was presumed to have been broken off during the deformation event that caused the end to curl inward.

Figure 67 shows 1-B-1-E and 39-E with common features noted, namely a flat area on both surfaces and adjacent erosion feature (groove). Figure 68 shows the laser scan for 1-B-1-E and 39-E with common features aligned. The other and more compelling evidence for these drill pipe ends being matching ends is the overall length between the tool joint in 1-B-1 and the tool joint in 1-A-1. Using drill pipe segment 39 as the missing piece between the two (see Figure 55 (a)), this length is measured as 45.68 feet. This is in good agreement with the length of a joint of drill pipe. This length was determined with features like the curled-in ends of 39-E accounted for in the measurement. In addition, the top portion of 1-B-1 (above the tool joint), segments 39 and 1-A-1 were internally coated. The other recovered drill pipe segments were not internally coated.

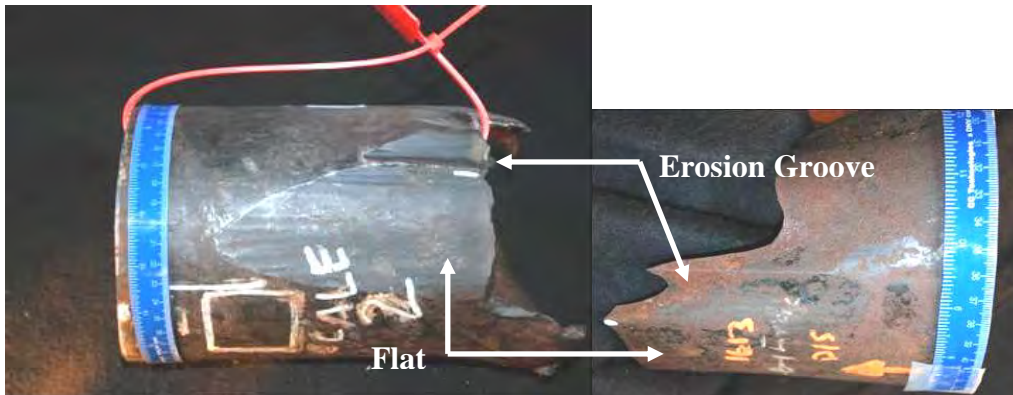


Figure 67 Photograph showing 1-B-1-E and 39-E

1-B-1-E and 39-E exhibited erosion features with regular spacing of 1 to 1.5 inches. This corresponded to the spacing of the element segment ends (fingers) in the UA element as shown in Figure 69. The erosion on 1-B-1-E and 39-E was due to their position at the top end of the UA element. Based on the above discussion, there is a high level of confidence that 1-B-1-E and 39-E were matching ends.

Erosion that occurred prior to tensile failure likely decreased the tensile strength of the drill pipe at this location. 1-B-1-E is postulated to have remained in the UA element while drill pipe segment 39 was free to move out of the primary flow path following tensile failure. Based on the above discussion, the majority of the erosion on 39-E is believed to have occurred prior to tensile failure of the drill pipe.

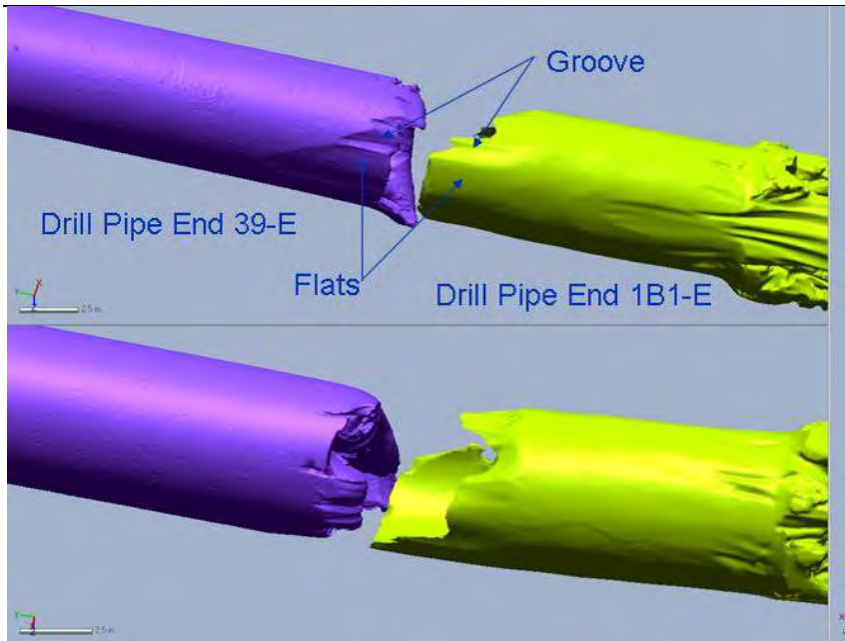
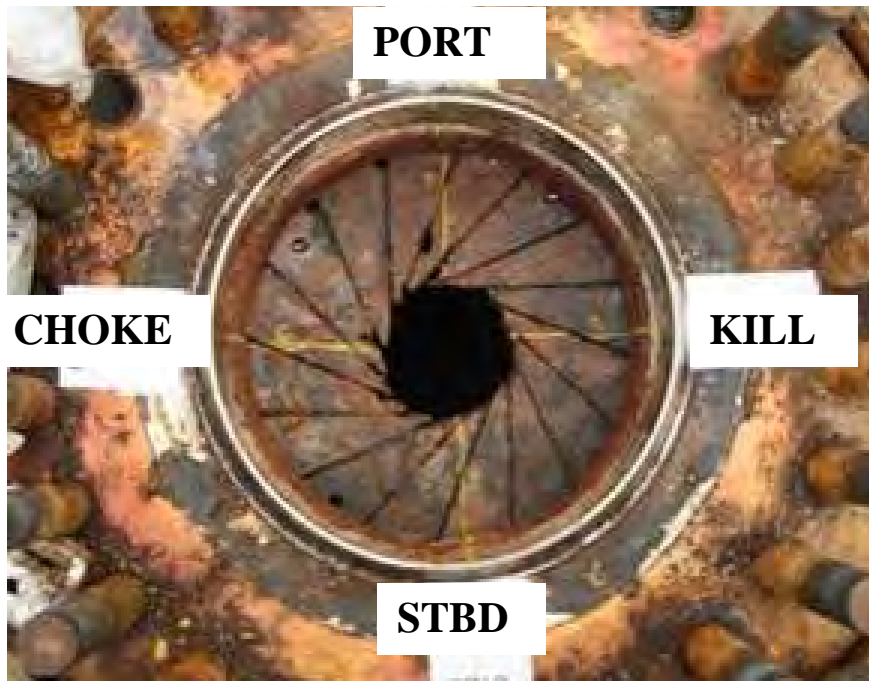
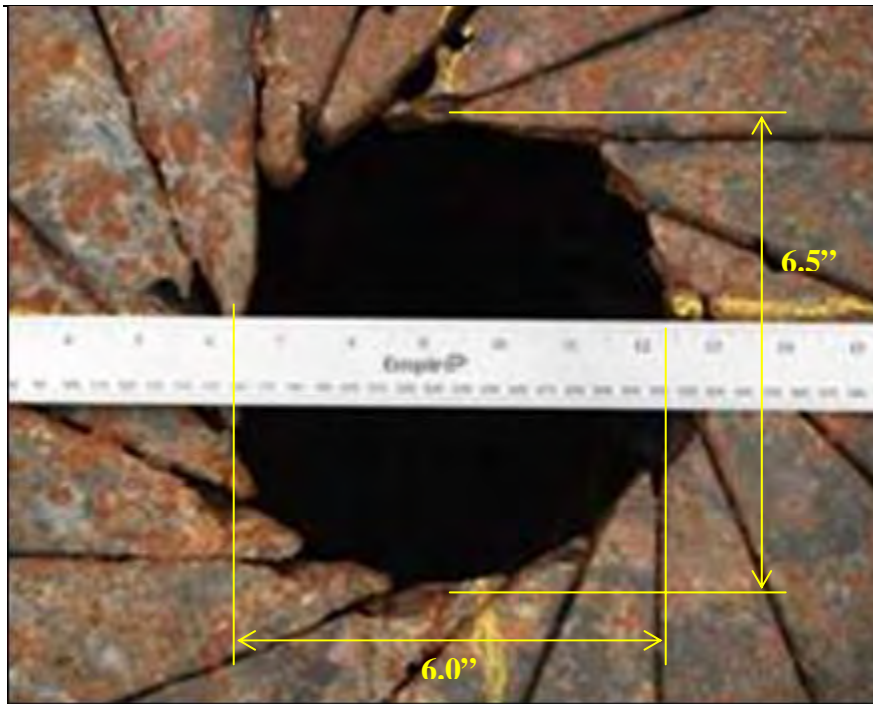


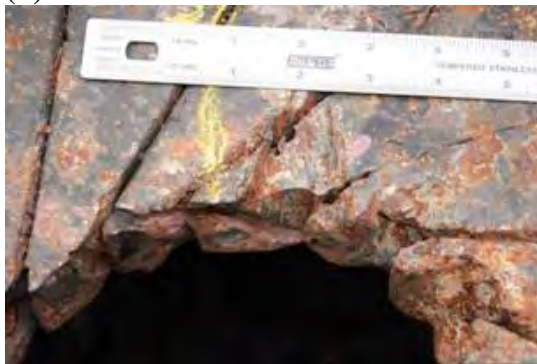
Figure 68 Laser Scans of 1-B-1-E and 39-E



(a)



(b)



(c)



(d)

Figure 69 Photographs of the Upper Annular Preventer

6.2.4.7 Matching 39-F to 1-A-1-F

The cut at 'F' is postulated to be the intervention shear cut of the Riser above the BOP Stack. 39-F and 1-A-1-F are the matching ends of this cut (see Figure 70). Based on visual examination, there is a high level of confidence that the cut at 'F' was due to the intervention shear cut.

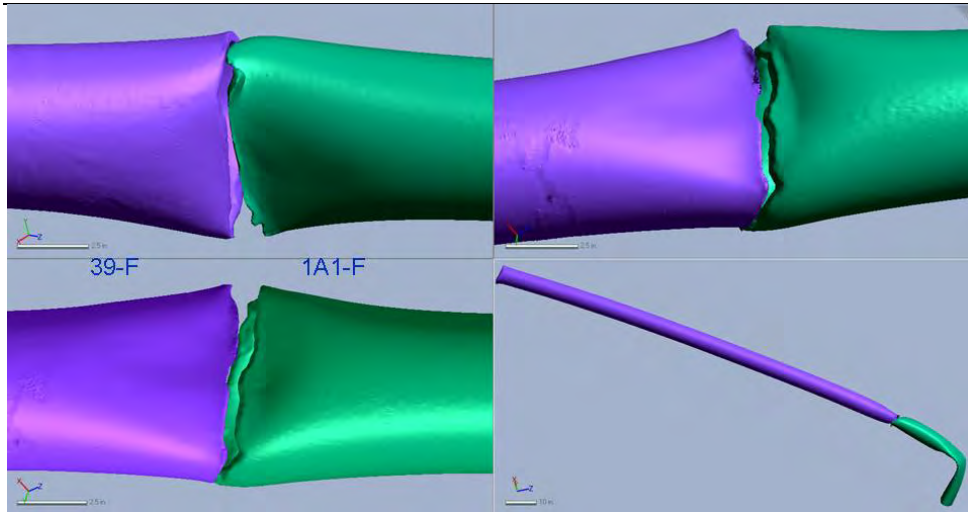


Figure 70 Laser Scans of 39-F and 1-A-1-F

6.2.5 Damage on Drill Pipe Segment in Variable Bore Rams

Drill pipe segment 148 was recovered from between the CSR and Lower VBR. The top end of drill pipe segment 148 (148-A) was cut by the CSR (Figure 56). Drill pipe segment 148 passed through the Upper and Middle VBRs and ended at the Lower VBR. Figure 72 shows the Upper VBR matched to segment 148. The two rings of erosion (see Figure 40 (c)) on segment 148 match to the packer segments in the Upper VBR. Figure 73 shows a similar match for the erosion on segment 148 (Figure 40 (d)) and the packer segments of the Middle VBR.

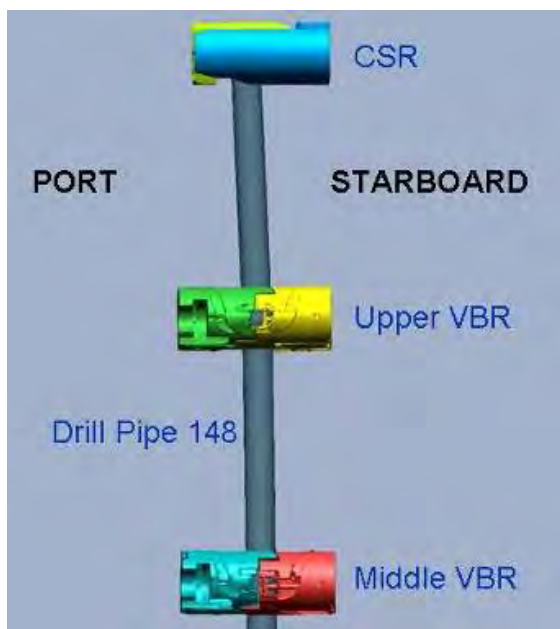


Figure 71 Laser Scans of Drill Pipe Segment 148 passing through the Upper and Middle VBRs

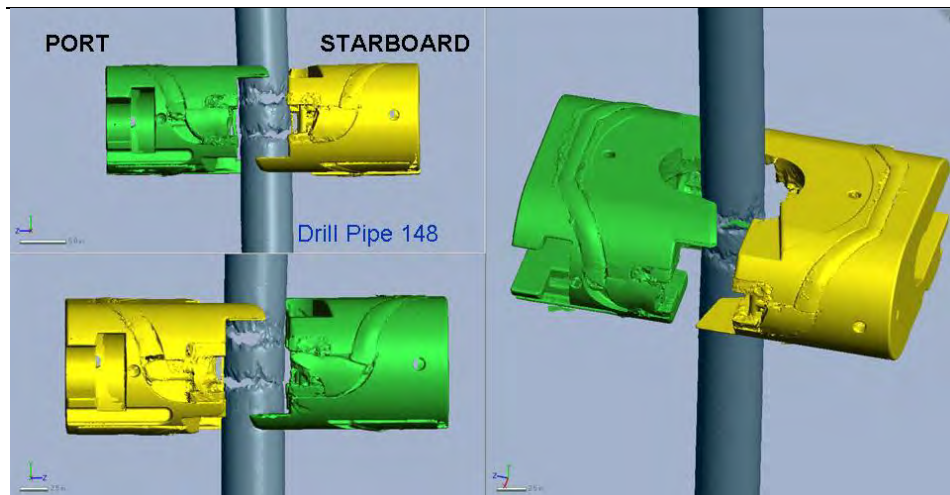


Figure 72 Laser Scan of the Upper VBR matched to Drill Pipe Segment 148

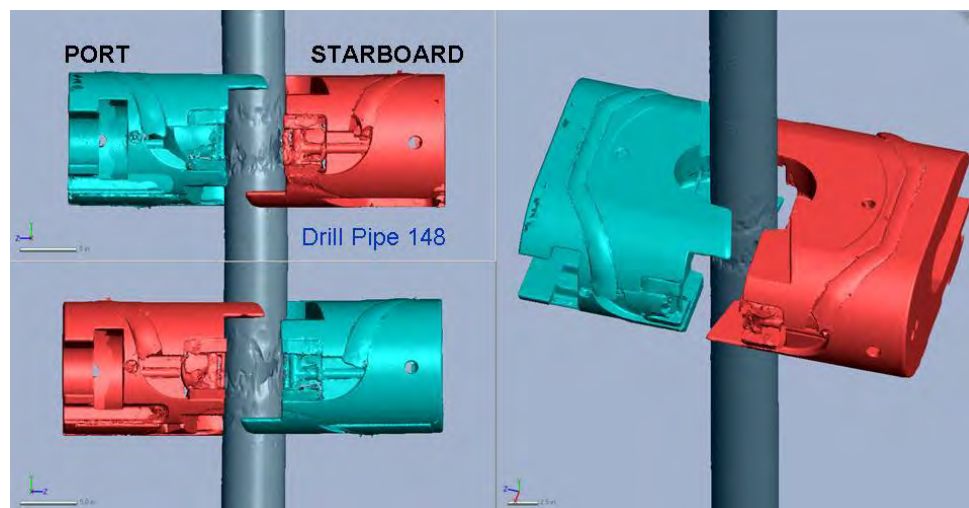


Figure 73 Laser Scan of the Middle VBR matched to Drill Pipe Segment 148

6.2.6 Damage to the Wellbore

During inspections of the wellbore, erosion damage was noted at the edges surrounding the BSR cavity. Although other areas of the wellbore exhibited some erosion damage, the most significant damage was associated with the BSR. Laser scanning was performed in this region to assess the erosion damage. The nominal wellbore geometry was modeled based on measurements of the undamaged locations of the scan models, and verified with known dimensions where possible. Figure 74 shows the laser scans for the upper and lower BSR blocks and the wellbore cavity. The damage in the wellbore was located in the area where the blocks meet (center of the wellbore). Figure 75 shows the overlay comparison for the wellbore surrounding the BSR cavity. The post damage scan model is given in green, while the nominal geometry is overlaid as translucent and outlined. Note

that the laser scanner was unable to capture all of the surface details due to line-of-sight and access limitations within the wellbore. The erosion damage was much greater on the kill side of the wellbore than the choke side.

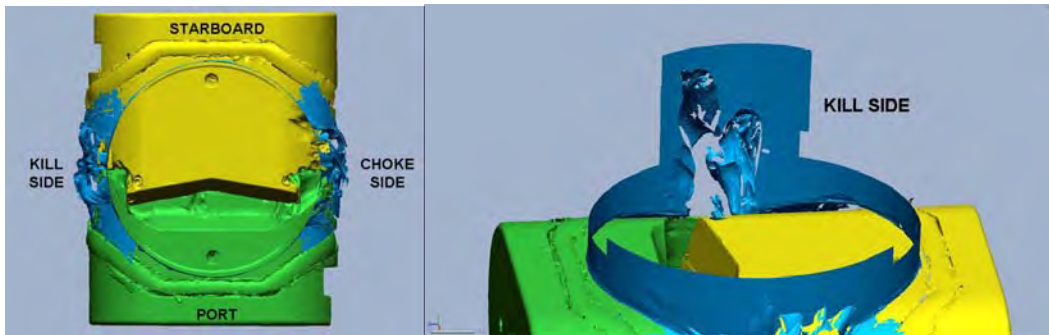


Figure 74 Laser Scan Showing Overhead View of BSR and Wellbore

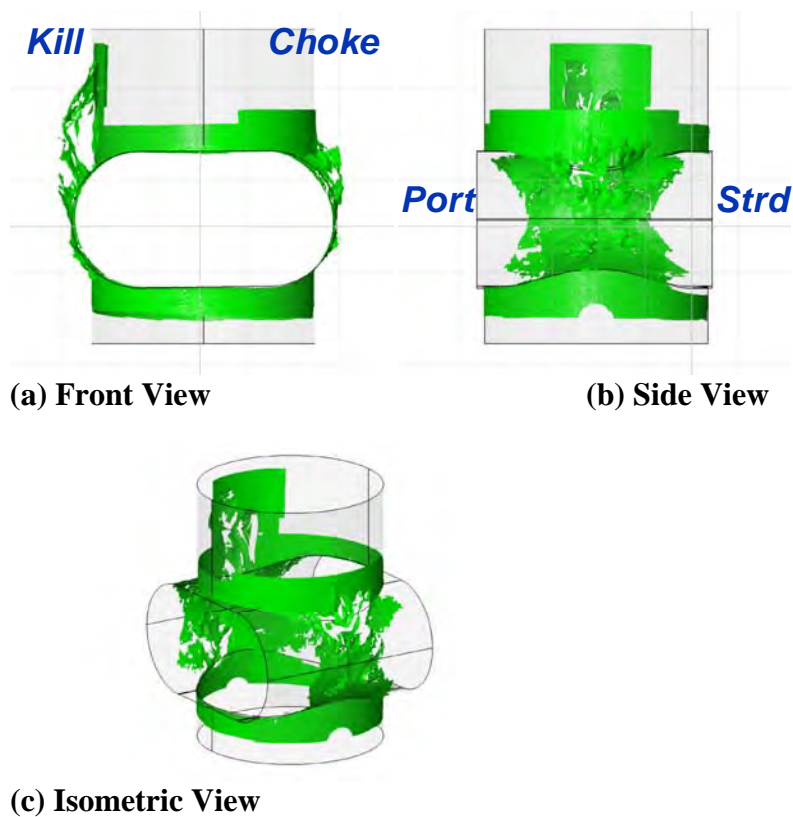


Figure 75 Laser Scan of Wellbore Damage

A comparative deviation plot for the wellbore damage is given in Figure 76 and Figure 77. Red indicates maximum material loss with an erosion depth of 2.75 inches on the kill side, and approximately 2.2 inches on the choke side. The kill side erosion channel extended approximately 9.5 inches up the wellbore from the BSR cavity, while the erosion damage on the choke side was limited to the first 4 inches above the BSR cavity.

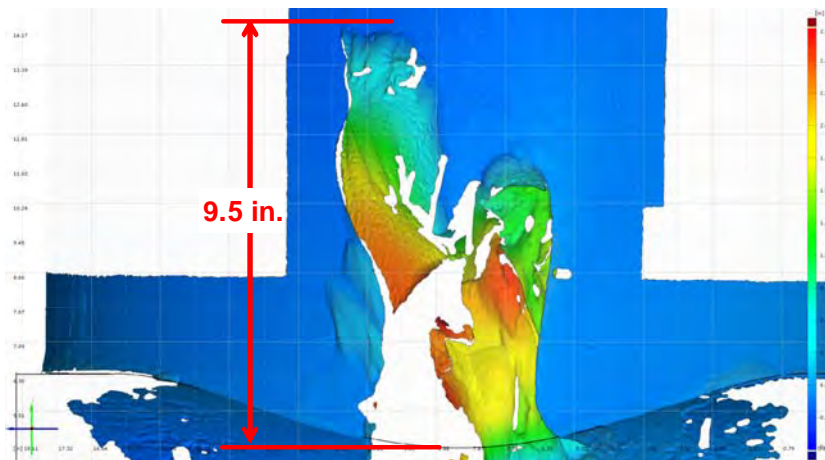


Figure 76 Laser Scan Deviation Plot of the Wellbore on the Kill Side of the BSR

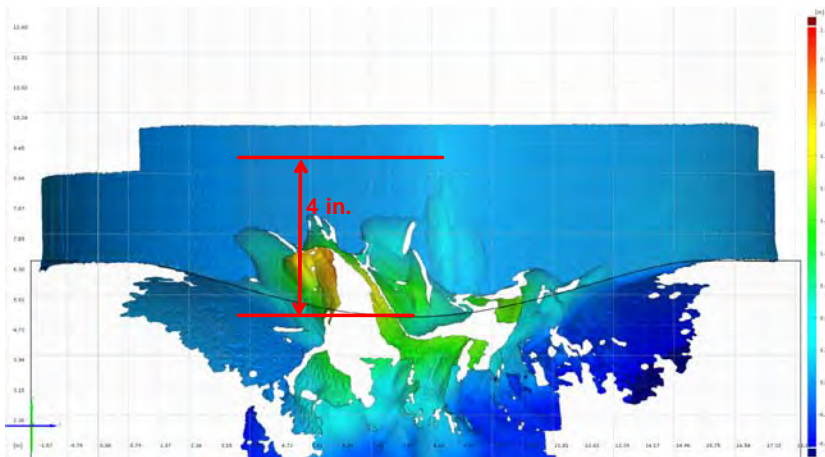


Figure 77 Laser Scan Deviation Plot of the Wellbore on the Choke Side of the BSR

6.2.7 Other Evidence Assessment

Appendix D is a list of all evidence. The numbering system is sequentially based on the discovery of the evidence and is based on the FBI ERT protocol. Additional evidence was recovered from viscous material and debris samples collected from the rams, within the ram cavities, and within the wellbore. This evidence was cleaned and photographed

according to protocol from the Forensic Testing Plan Protocol Section 5.14 (Appendix A).

Evidence retrieved from ram cavities and the wellbore was typically material from the well intervention effort, rubber, and metallic pieces. Figure 78 to Figure 81 show examples of retrieved evidence. Various quantities of well intervention material and other debris were discovered in all cavities and at different locations within the wellbore.



(a)



(b)

Figure 78 Photograph Illustrating Cementitious Pieces Discovered in Evidence



(a)



(b)

Figure 79 Photograph Illustrating Metal Discovered in Evidence



(a)



(b)

Figure 80 Photograph Illustrating Elastomeric Discovered in Evidence



Figure 81 Photograph Illustrating Polymeric Discovered in Evidence

6.2.8 Metallurgical, Mechanical, Chemical Property Assessment

6.2.8.1 Sample Preparation and Measurements

Table 19 summarizes the locations on the pipe segments from which test samples were removed for metallurgical, chemical and mechanical analyses. In total, four 3-inch ring specimens (Item 1-A-1-Q, Item 1-B-2-Q, Item 94-Q, and Item 148-Q), one 1-inch ring specimen (Item 1-B-1-Q), and two 21-inch specimens (Item 39-Q and Item 83-Q) were removed. Figure 82 through Figure 88 are photographs of the removed test samples (Item 1-A-1-Q, Item 1-B-1-Q, Item 1-B-2-Q, Item 39-Q, Item 83-Q, Item 94-Q, and Item 148-Q, respectively). Markings for flow direction, orientation, and item numbers were indicated on each test sample.

Table 19 Location and Identification of Types of Test Samples

Item Number	Length (inches)	Samples Removed for Analyses ⁽¹⁾	Distance from Top End of Pipe Segment (inches)
1-A-1-Q	3	M, C	341.28 to 344.28
39-Q	21	M, C, TC	59.19 to 81.19
1-B-2-Q ⁽³⁾	3	M,C	15.60 to 18.60
1-B-1-Q	1	M	5.38 to 6.38 ⁽⁴⁾
83-Q	21	M, C, TC	41.75 to 63.75
94-Q	3	M,C	19.25 to 22.25
94-Q	3	M,C	19.25 to 22.25
148-Q ⁽²⁾	3	M,C	114.84 to 117.84

(1) M = Metallurgical Samples, C = Chemical Samples, TC = Tensile and Charpy Samples (Mechanics)

(2) Sample taken toward the end, adjacent to debris recovered in the drill pipe.

(3) Sample removed toward the end away from undeformed end.

(4) Measured from the fractured surface, not the eroded area.



Figure 82 Photograph of 1-A-1-Q



Figure 83 Photograph of 1-B-1-Q



Figure 84 Photograph of 1-B-2-Q



Figure 85 Photograph 39-Q

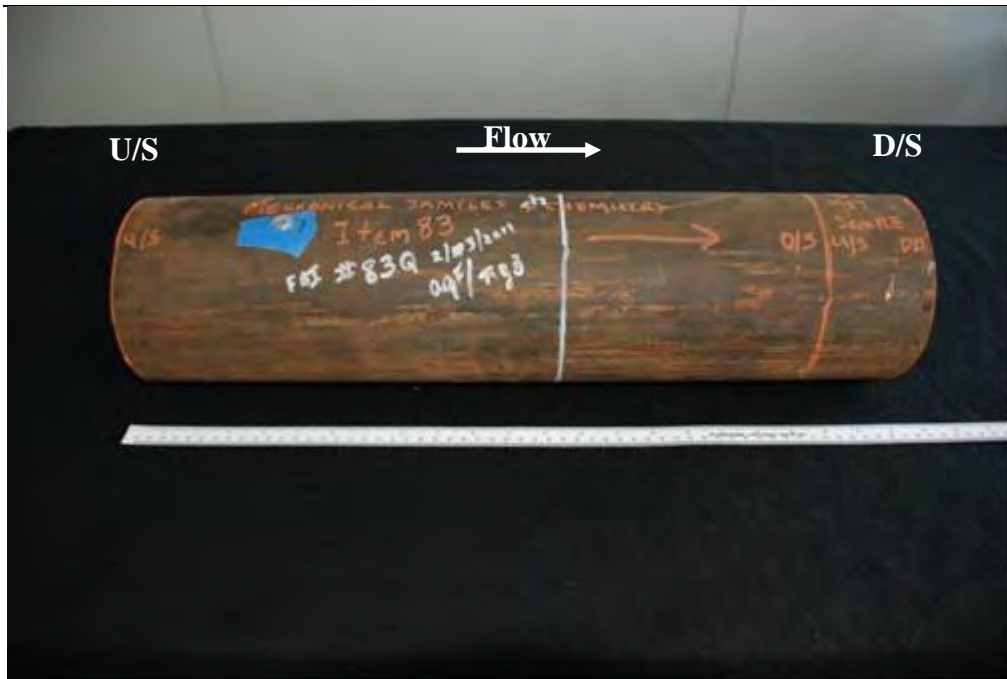


Figure 86 Photograph 83-Q



Figure 87 Photograph 94-Q



Figure 88 Photograph of 148-Q

The diameter of the bottom (U/S) end of each test sample was measured using Pi Tape (Serial Number 082510143). Measurements were performed in areas that were free of debris and undeformed. Table 20 summarizes the diameter measurements taken at the bottom end of each test sample. All measurements were consistent with 5.5-inch diameter drill pipe. The wall thicknesses were measured using a micrometer at four locations 90° from one another at the bottom end of the test samples. The results of the wall thickness measurements are summarized in Table 21. These values were consistent with 0.361-inch wall thickness drill pipe.

Table 20 Summary of Diameter Measurements Taken at Bottom End of 1-A-1-Q, 1-B-1-Q, 39-Q, 83-Q, 94-Q, and 148-Q

Item ID	Average Diameter Inches	API 5D ⁵	
		min*	max*
		inches	
1-B-2-Q	5.56	5.46	5.70
39-Q	5.56		
83-Q	5.55		
94-Q	5.56		
148-Q	5.55		

*Wall thickness tolerance was specified as +1/8 (max) and -0.75%D (min) in API 5D (5th Edition, 2001), where D is diameter.

⁵ API SPEC 5DP Specification for Drill Pipe, 5th Edition, 2001

Table 21 Wall Thickness Measurements Taken at Bottom End of 1-A-1-Q, 1-B-1-Q, 39-Q, 83-Q, 94-Q, 148-Q, and 1-B-2Q

Item ID	Wall Thickness on the Upstream End				Average	API 5D ⁵
	0°	90°	180°	270°		min *
	inches					
1-A-1-Q	0.401	0.404	0.408	0.377	0.398	0.316
1-B-1-Q**	0.788	0.689	0.772	0.778	0.757	
39-Q	0.376	0.385	0.398	0.382	0.385	
83-Q	0.385	0.381	0.386	0.393	0.386	
94-Q	0.392	0.393	0.382	0.391	0.390	
148-Q	0.330	0.353	0.330	0.317	0.333	
1-B-2-Q	0.378	0.396	0.405	0.400	0.395	

* Wall thickness tolerance was -12.5% in API 5D (5th Edition, 2001).

** Wall thickness was consistent with beginning of tool joint upset.

6.2.8.2 Hardness Testing

Prior to metallurgical examination, Rockwell C hardness measurements were performed on the external surfaces of the test samples. Figure 89 is a photograph of 148-Q showing the location of Rockwell C hardness measurements on the external surface. Before testing, the external surface was ground with a metal file. Hardness readings were taken 0.5-inches apart starting 0.5-inches from the bottom edge. Table 22 is a summary of the Rockwell C hardness testing for the specified test samples.

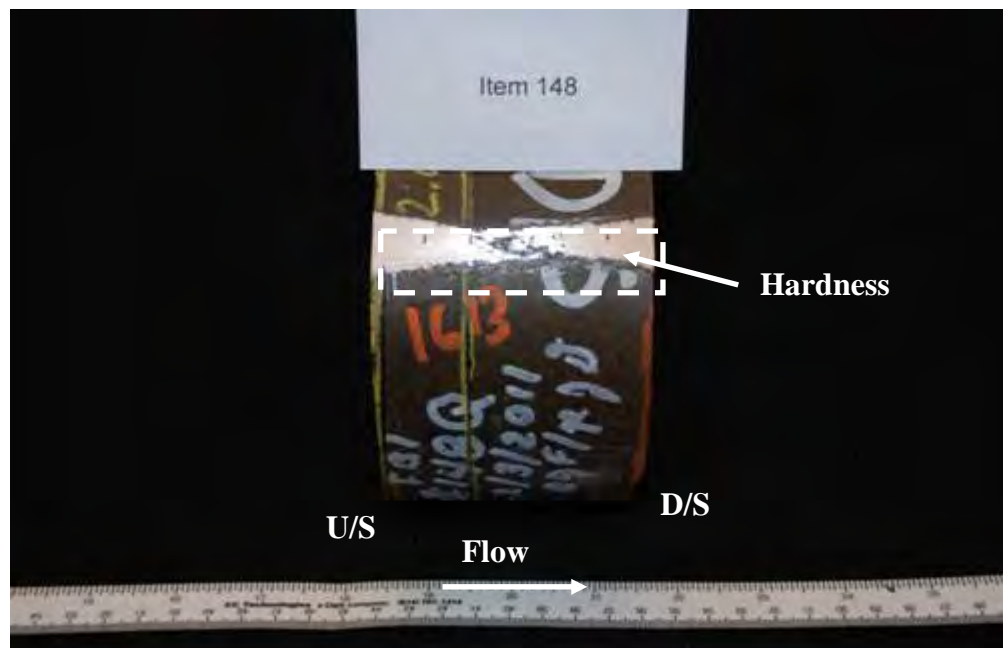


Figure 89 Photograph of 148-Q Showing the Locations of Rockwell C Hardness Measurements on the External Surface

Table 22 Results for Rockwell C hardness Tests Conducted on the External Surfaces on the Test Samples

Item ID	Hardness					Average	UTS
	1	2	3	4	5		
	HRC						ksi
1-A-1	27	32	32	30	30	30	138
1-B-1	32	28	28	30	28	29	131
1-B-2	30	33	29	31	34	31	141
39	34	33	32	22	35	31	141
83	35	33	34	31	31	33	149
94	33	34	34	32	34	33	149
148	26	32	32	33	31	31	141

Vickers hardness measurements were performed through thickness on the longitudinal cross-sections of selected test samples. Figure 90 is a photograph of 39-Q showing the location of Vickers hardness measurements.

Hardness readings were taken 0.6-mm apart starting 0.5-mm from the external surface proceeding to the internal surface. Table 23 is a summary of the Vickers hardness testing for selected test samples. The corresponding ultimate tensile strength (UTS) values met the criteria specified in API 5D for Grade S135, drill pipe (minimum 145 ksi).

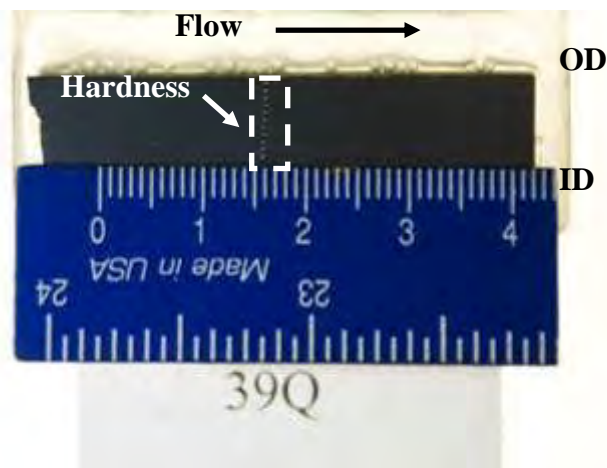


Figure 90 Photograph of Longitudinal Cross-Section of 39-Q

Table 23 Results for Vickers Hardness Tests Conducted Through Thickness on the Longitudinal Cross-Sections (see Figure 90)

Item ID	Hardness (Outside Diameter to Inside Diameter)										Average	UTS	API 5D ⁵
	1	2	3	4	5	6	7	8	9	10			
	HV											ksi	ksi
1-A-1	357	366	360	360	354	357	357	357	363	354	359	164	145
39	327	345	345	354	357	351	348	342	342	339	345	156	
83	342	342	342	339	336	339	342	339	345	345	341	154	
94	351	354	366	363	363	366	363	360	360	357	360	164	

Ultimate Tensile Strength (UTS) from Wilson Conversion Chart, 1968

6.2.8.3 Metallurgical Examination of Drill Pipe

Table 19 indicates the types of tests that were conducted on each test sample. Figure 91 is a photograph of 39-Q showing the locations for metallurgical, mechanical, and chemical samples. A 1-inch by 1-inch chemical coupon was removed from the upper most location on the test sample. A 1-inch by 2-inch longitudinal metallurgical coupon was removed from a location directly counter clockwise from the chemical coupon. A full ring for the transverse metallurgical coupon was located directly below the longitudinal coupon. Mechanical coupons were machined from the remaining test sample. Coupons for metallurgical, mechanical, and chemical analyses were removed from 83-Q in the same manner.

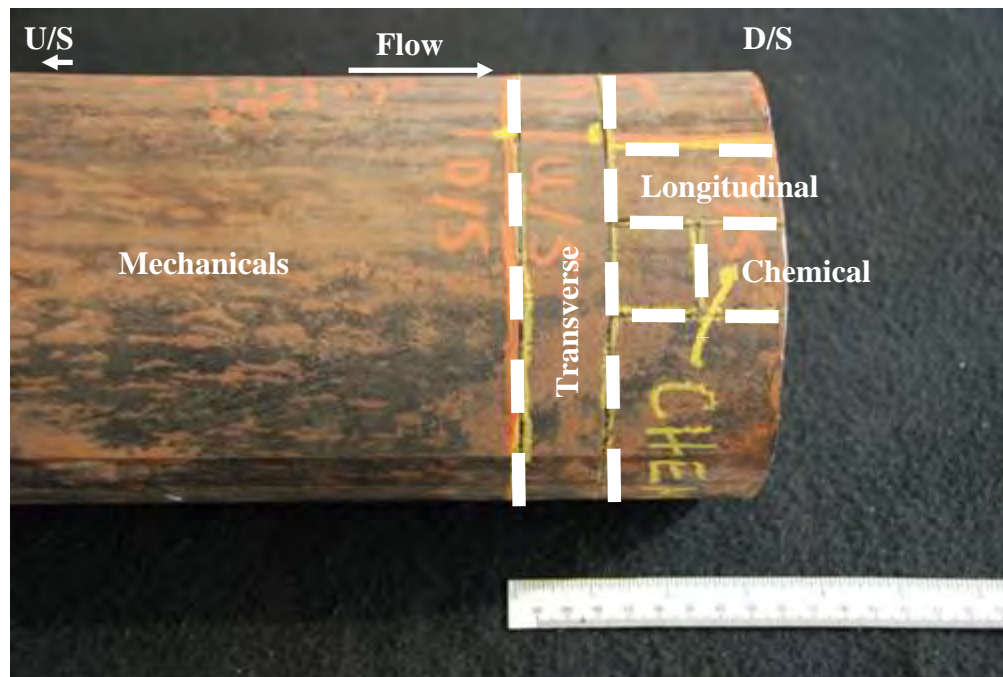


Figure 91 Photograph of 39-Q Showing the Locations for Metallurgical, Mechanical, and Chemical Coupons

Figure 92 is a photograph of 148-Q showing the locations for metallurgical and chemical coupons. The longitudinal metallurgical coupon, the transverse metallurgical coupon, and

the chemical coupons were removed in the same manner from 1-A-1-Q, 1-B-2-Q, and 94-Q.

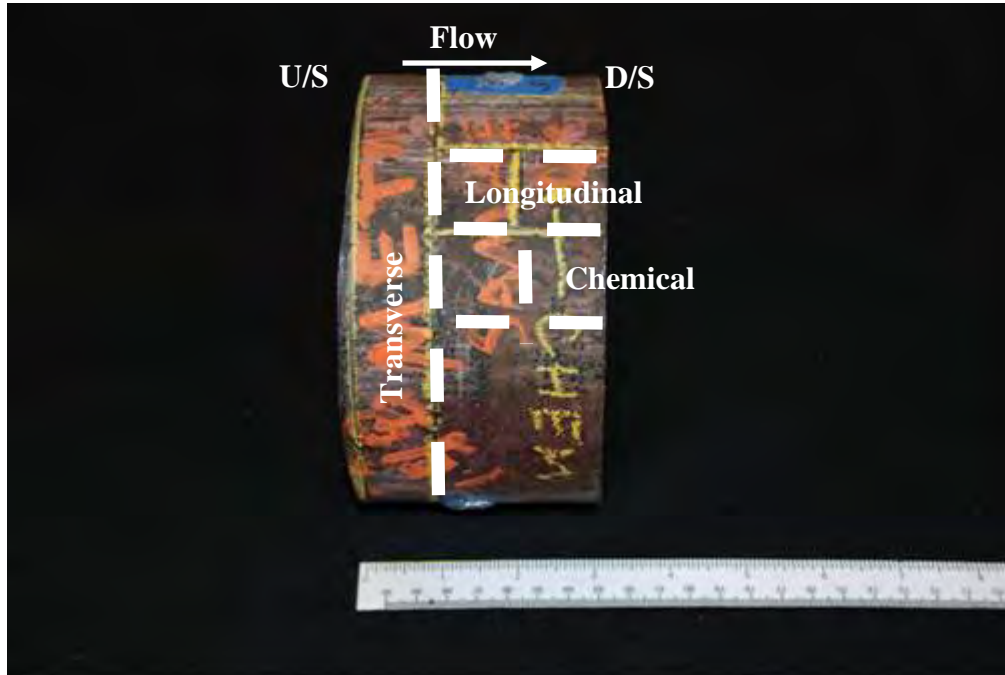


Figure 92 Photograph of 148-Q Showing the Locations for Metallurgical and Chemical Coupons

Figure 83 is a photograph of 1-B-1-Q that was prepared for metallurgical analyses. Only a transverse metallurgical coupon from the top end of the test sample was prepared for examination. With the exception of 1-B-1-Q, the bottom face of all other 1-inch ring transverse metallurgical coupons was polished and etched.

Figure 93 is a stereo light photograph near the inside diameter surface of 39-Q. The internal surface was coated (see yellow and green layer). The coating thickness was measured to be 8.3 mils (0.21-mm) at the location shown in Figure 93 for 39-Q. 1-A-1-Q and 1-B-1-Q (sample above tool joint) showed a similar coating on the internal surfaces. 1-B-2-Q, 83-Q, 94-Q, and 148-Q did not have an internal coating. The presence of the internal coating is indicative of 39-Q, 1-A-1-Q and 1-B-1-Q (above the tool joint) being from the same drill pipe joint. 1-B-2-Q, 83-Q, 94-Q, and 148-Q are all from a different drill pipe joint. This is consistent with the proposed stacking of the recovered drill pipe segments shown in Figure 55.

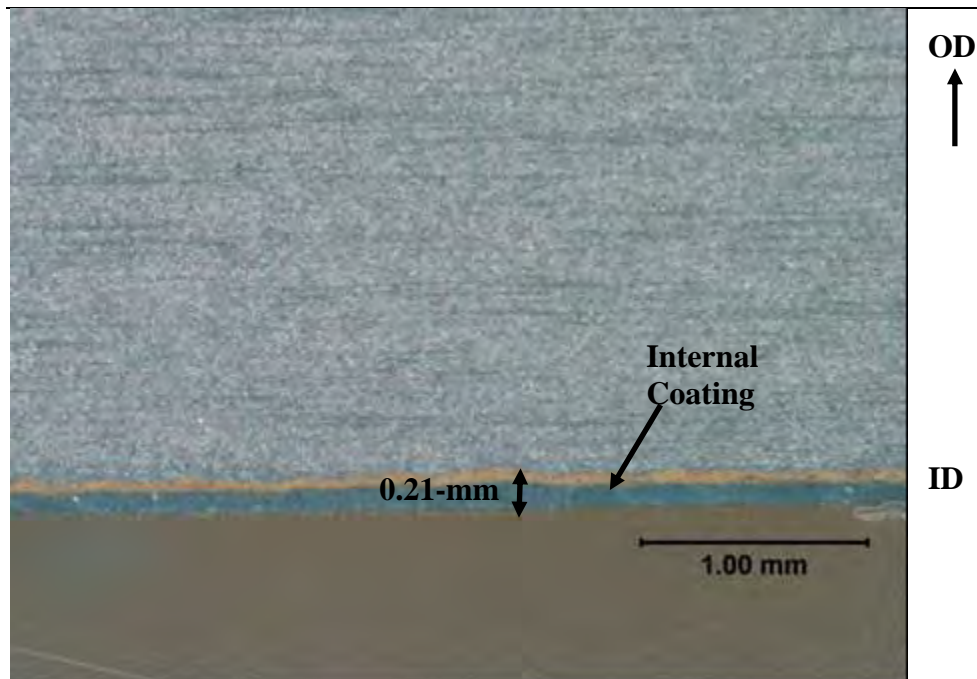


Figure 93 Stereo Light Photograph of Longitudinal Cross-Section of 39-Q

Figure 94 is a light photomicrograph showing the typical microstructure of the pipe steel in the longitudinal orientation for 39-Q. The microstructure of the pipe steel consisted primarily of tempered martensite, which is typical for quenched and tempered drill pipe. Figure 95 is a light photomicrograph showing the typical microstructure of the pipe steel in the transverse orientation of 39-Q. The microstructure of the pipe steel consisted primarily of tempered martensite, which is typical for quenched and tempered drill pipe. 1-A-1-Q had similar microstructures in both the longitudinal and transverse orientation.

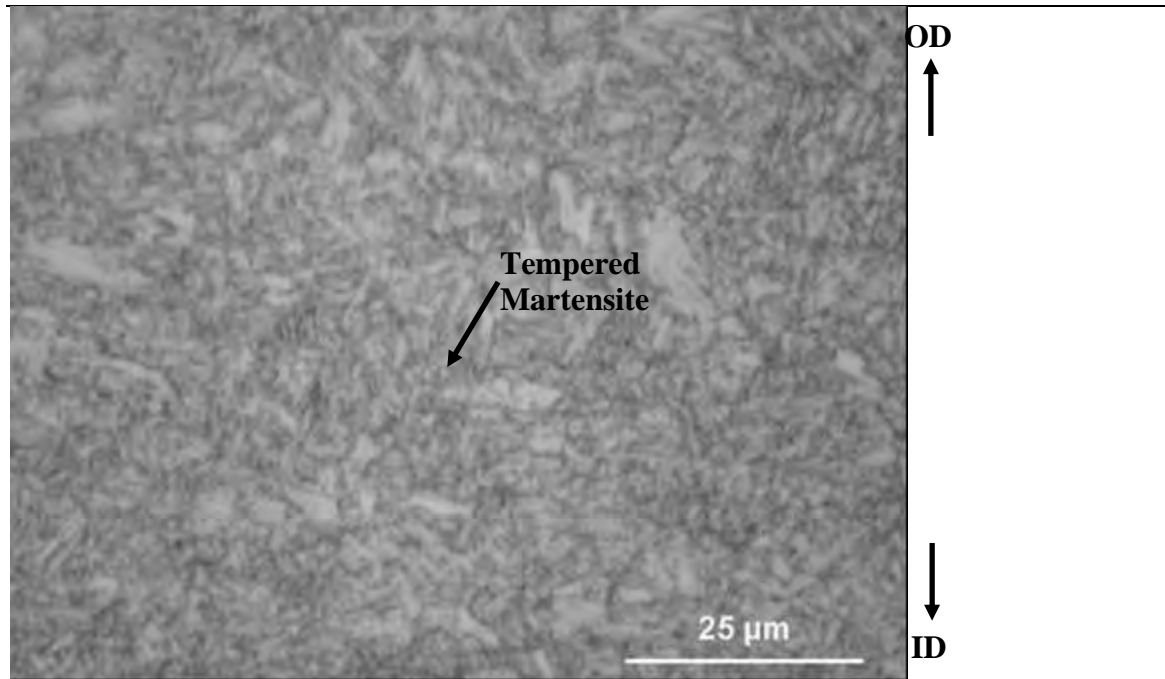


Figure 94 Light Photomicrograph Showing the Typical Microstructure of the Pipe Steel in the Longitudinal Orientation for 39-Q

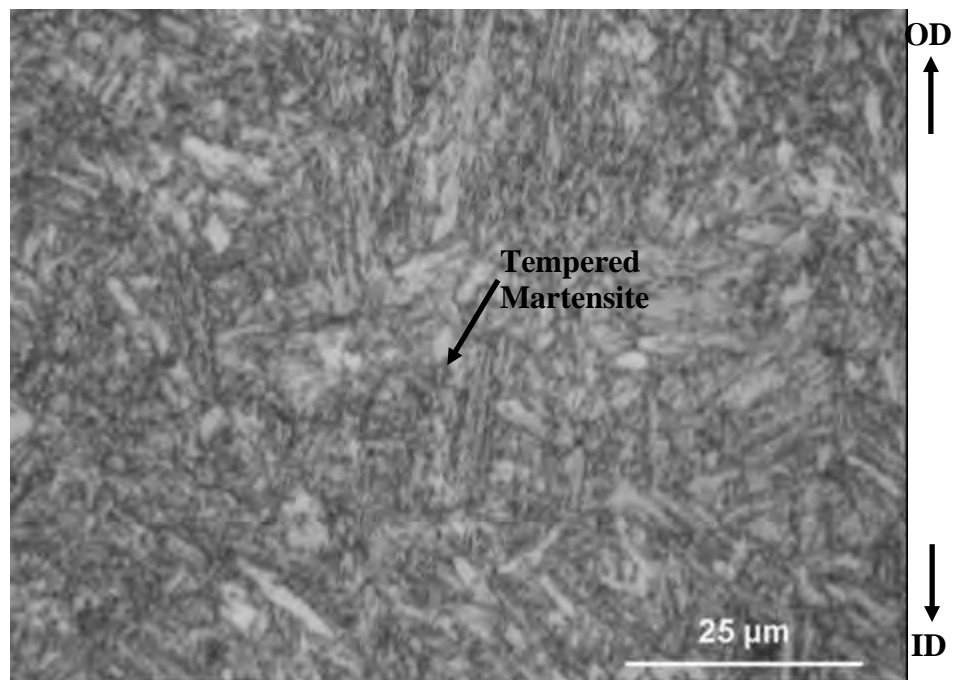


Figure 95 Light Photomicrograph Showing the Typical Microstructure of the Pipe Steel in the Transverse Orientation for 39-Q

Figure 96 is a light photomicrograph showing the typical microstructure of the pipe steel in the longitudinal orientation for 1-B-1-Q. The microstructure of the pipe steel consisted primarily of tempered martensite and some ferrite grains. The location from which this specimen was removed was located near the friction weld of the drill pipe to the tool joint. The ferrite grains are aligned as shown in Figure 96 (banded structure). The drill pipe wall thickness in this area was 0.69 to 0.79-inch. When compared to the other microstructures, the presence of ferrite could indicate either compositional variations or heat treating and quenching differences due to the increased wall thickness .

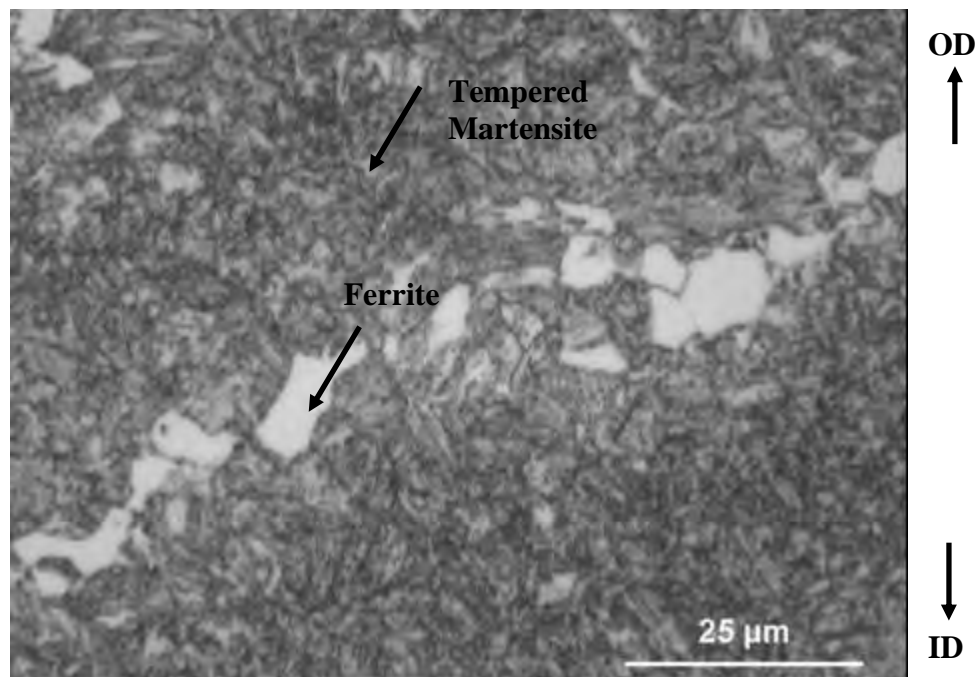


Figure 96 Light Photomicrograph Showing the Typical Microstructure of the Pipe Steel in the Transverse Orientation for 1-B-1-Q

Figure 97 is a light photomicrograph showing the typical microstructure of the pipe steel in the longitudinal orientation for 83-Q. The microstructure of the pipe steel consisted primarily of tempered martensite, which is typical for quenched and tempered drill pipe. Figure 98 is a light photomicrograph showing the typical microstructure of the pipe steel in the transverse orientation of 83-Q. The microstructure of the pipe steel consisted primarily of tempered martensite, which is typical for quenched and tempered drill pipe. 1-B-2-Q, 94-Q and 148-Q had similar microstructures in both the longitudinal and transverse orientation.

1-A-1-Q and 39-Q were from a drill pipe joint with an internal coating and 1-B-2-Q, 83-Q, 94-Q, and 148-Q were all from a drill pipe joint with no internal coating. Comparing these two groups, there is no discernable difference in metallurgy of the two drill pipe joints.

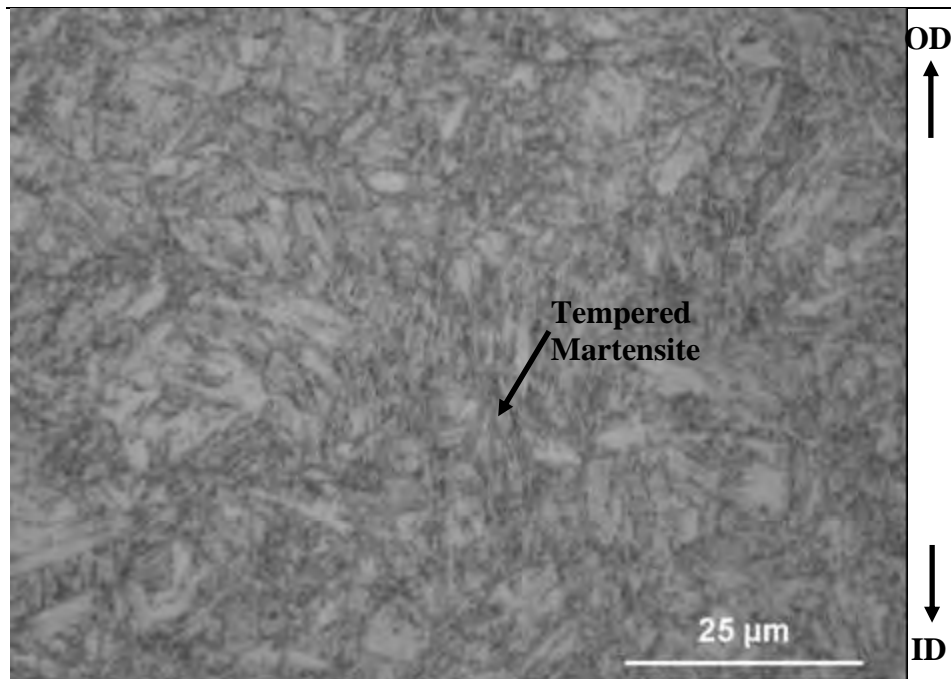


Figure 97 Light Photomicrograph Showing the Typical Microstructure of the Pipe Steel in the Longitudinal Orientation for 83-Q

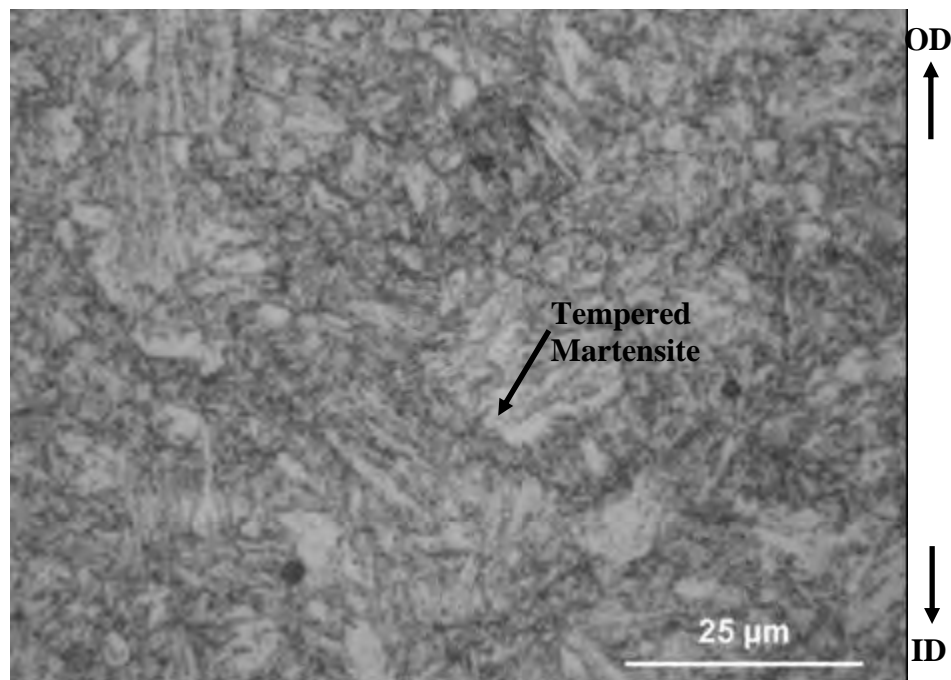


Figure 98 Light Photomicrograph Showing the Typical Microstructure of the Pipe Steel in the Transverse Orientation for 83-Q

6.2.8.4 Mechanical Testing of Drill Pipe

Figure 99 and Figure 100 show the locations from which coupons were removed from 39-Q and 83-Q, respectively, for mechanical testing. Charpy V-notch coupons were removed from the top end of the test sample. Tensile samples were removed from a location approximately 1-inch below the Charpy coupons. In total, four tensile coupons were removed (Coupons A, B, C, and D), but only two coupons were machined and tested. Coupons A and C were located 180° from Coupons B and D.

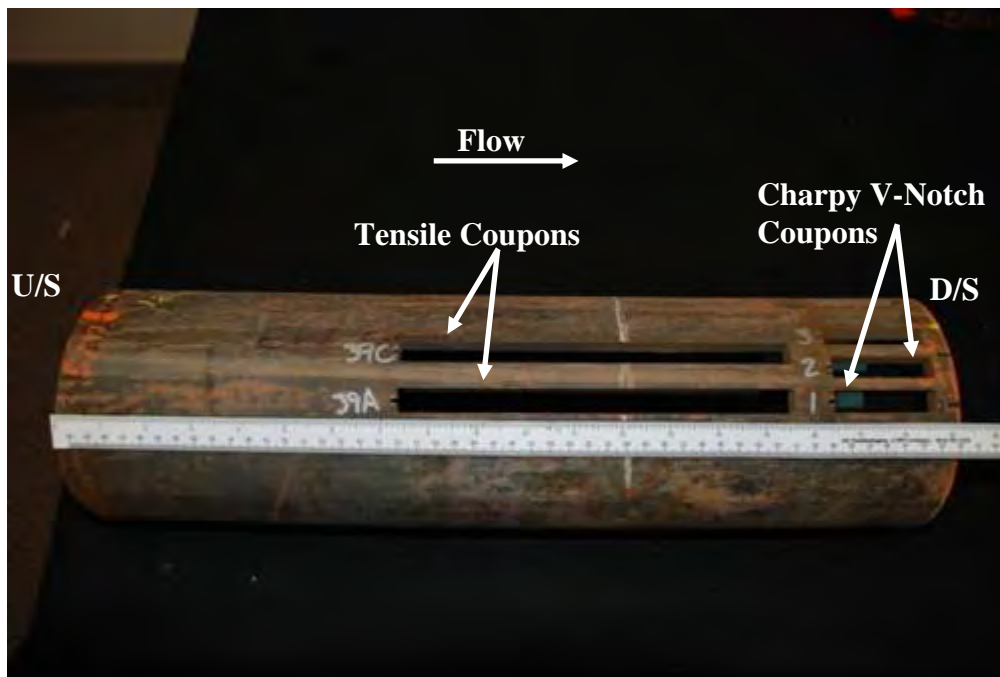


Figure 99 Photograph of 39-Q Showing the Locations for Mechanical Coupon Removal

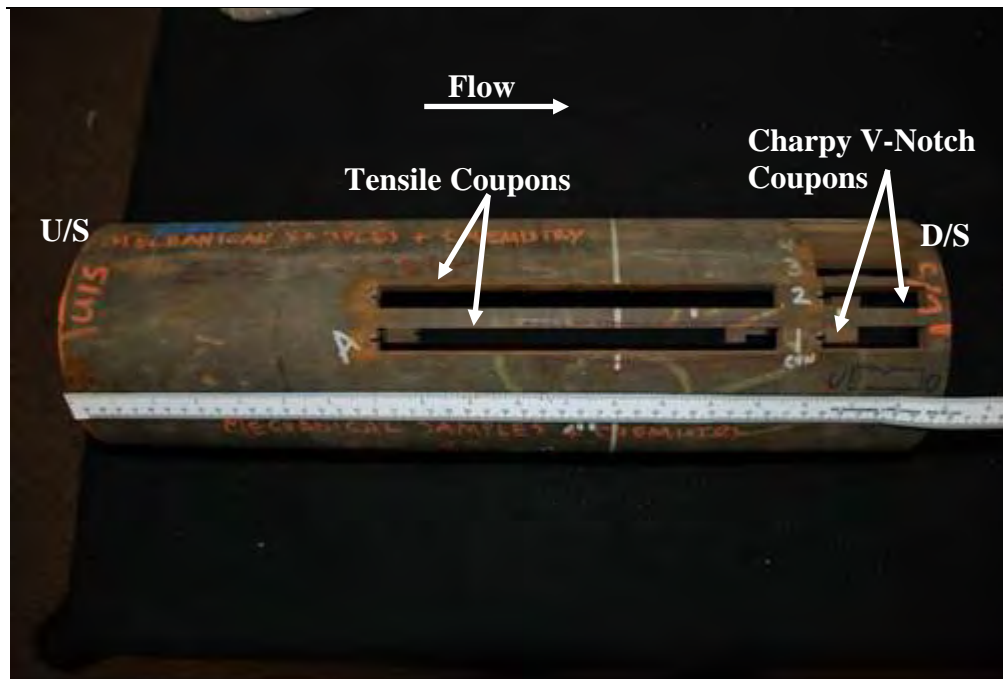


Figure 100 Photograph of 83-Q Showing the Locations for Mechanical Coupon Removal

6.2.8.4.1 Tensile Tests

The results of the tensile tests for 39-Q are shown in Table 24. The average yield strength (YS) and ultimate tensile strength (UTS) of the test coupons were 124.8 ksi and 160.5 ksi, respectively. The UTS values for Coupons 39-C and 39-D met the specified minimum value in API 5D (minimum 145 ksi). The range for the specified minimum yield strength (SMYS) in API 5D (135 to 165 ksi) was met for Coupon 39-D, but was not met for Coupon 39-C. The YS for Coupon 39-C was likely low because the coupon came from an area that had experienced compressive deformation (i.e., drill pipe segment 39 was bowed and 39-C was from the inside of the bow).

Table 24 Summary of Tensile Test Data for 39-Q

Item ID	Orientation	Diameter	UTS		0.7 YS		Elongation	Reduced Area
		inches	ksi	MPa	ksi	MPa	%	%
39-C	Longitudinal	0.349	160.5	1107	110.6	763	26.0	66.8
39-D	Longitudinal	0.353	160.5	1107	139	958	30.7	68.5
API 5D ⁵	Specification	0.350 ± 0.007						
	min	0.343	145	1000	135	931	8.9	
	max	0.357			165	1138		

The results of the tensile tests for Coupon 83-Q are shown in Table 25. The average yield strength (YS) and ultimate tensile strength (UTS) of the test coupons were 135.3 ksi and 156.8 ksi, respectively. The UTS values for Coupons 83-C and 83-D met the specified



minimum value in API 5D (minimum 145 ksi). The range for the specified minimum yield strength (SMYS) in API 5D (135 to 165 ksi) was met for Coupons 83-C and 83-D.

Table 25 Summary of Tensile Test Data for 83-Q

Specimen ID	Orientation	Diameter	UTS		0.7 YS		Elongation	Reduced Area
		(inches)	(ksi)	(MPa)	(ksi)	(MPa)	(%)	(%)
83-C	Longitudinal	0.354	158.2	1091	135.5	934	13.8	71.2
83-D	Longitudinal	0.355	155.3	1071	135.1	931	13	70.4
API 5D ⁵	Specification	0.350 ± 0.007						
	min	0.343	145	1000	135	931	8.9	
	max	0.357			165	1138		

6.2.8.4.2 Charpy Tests

Table 26 summarizes the results of the Charpy testing for 39-Q. Figure 101 and Figure 102 show the Charpy impact energy and percent shear curves for 39-Q, respectively. The upper shelf impact energy is approximately 72 ft-lbs (¾-size sample). The average Charpy value for the three 73°F temperature tests was 70 ft-lbs. API 5D specifies a minimum average of 32 ft-lbs and a minimum of specimen of 28 ft-lbs. The Charpy results for 39-Q exceeded the API 5D specifications.⁵

Table 26 Results of Charpy V-Notch Testing for 39-Q

Specimen ID	Test Temperature		Absorbed Energy		Lateral Expansion			Percent Shear
	(°C)	(°F)	(J)	(ft-lb)	(mm)	(inches)	(mils)	(%)
39-1	23	73	92	68.0	1.32	0.052	52	81
39-2	0	32	95	70.0	1.14	0.045	45	78
39-3	40	104	95	70.0	1.40	0.055	55	82
39-4	-60	-76	64	47.0	0.80	0.031	31	77
39-5	-90	-130	53	39.0	0.66	0.026	26	40
39-6	23	73	98	72.0	1.43	0.056	56	81
39-7	-196	-321	14	10.0	0.10	0.004	4	18
39-8	-160	-256	26	19.5	0.25	0.010	10	18
39-9	-175	-283	19	14.0	0.17	0.007	7	12
39-10	-140	-220	30	22.0	0.34	0.013	13	12
39-11	100	212	98	72.0	1.44	0.351	351	100
39-12	23	73	96	71.0	1.35	0.053	53	82
39-13	80	176	92	68.0	1.40	0.055	55	100

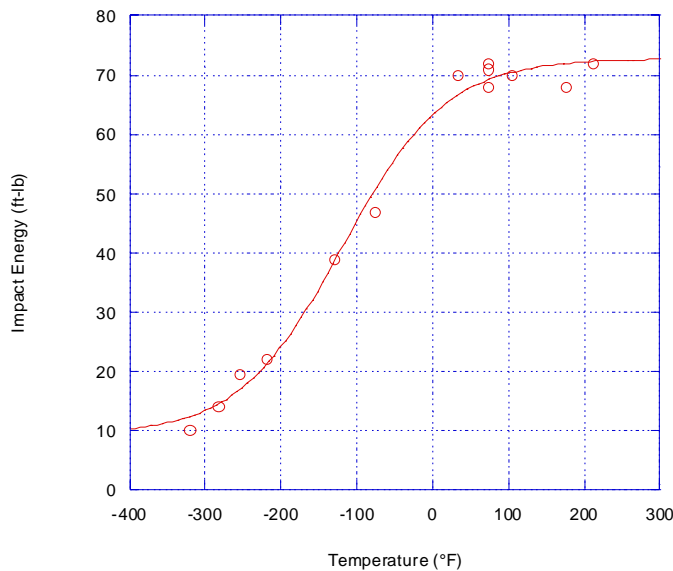


Figure 101 Charpy V-Notch Impact Energy Plot as a Function of Temperature for 39-Q (Plot of 3/4-size samples)

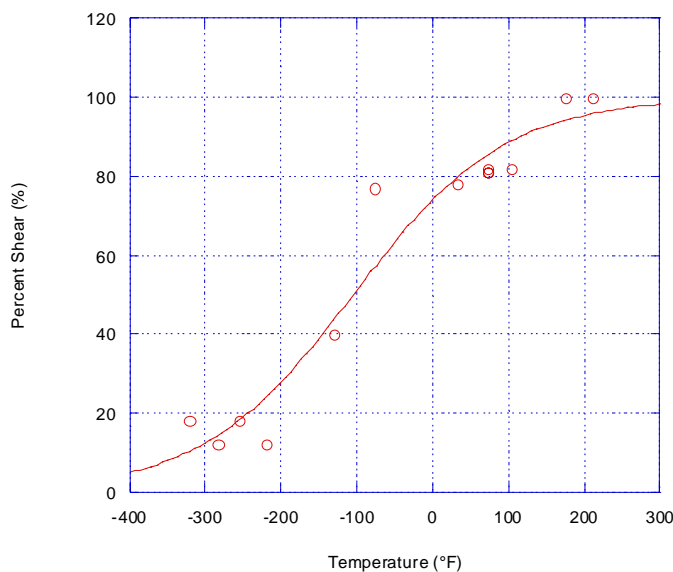


Figure 102 Percent Shear Plot from Charpy V-Notch Tests as a Function of Temperature for 39-Q

Table 27 summarizes the results of the Charpy testing for 83-Q. Figure 103 and Figure 104 show the Charpy impact energy and percent shear curves for 83-Q, respectively. The upper shelf impact energy was approximately 72 ft-lbs ($\frac{3}{4}$ -size sample). The average Charpy value for the three 73°F temperature tests was 72 ft-lbs. API 5D specifies a

minimum average of 32 ft-lbs and a minimum of specimen of 28 ft-lbs. The Charpy results for 83-Q exceeded the API 5D specifications.⁵

Table 27 Results of Charpy V-Notch Testing for 83-Q

Specimen ID	Test Temperature		Absorbed Energy		Lateral Expansion			Percent Shear
	(°C)	(°F)	(J)	(ft-lb)	(mm)	(inches)	(mils)	
83-1	23	73	98	72.0	1.05	0.041	41	81
83-2	0	32	91	67.0	1.27	0.050	50	77
83-3	40	104	92	68.0	1.32	0.052	52	82
83-4	-60	-76	71	52.0	0.82	0.032	32	83
83-5	-90	-130	53	39.0	0.69	0.027	27	54
83-6	23	73	98	72.0	1.07	0.042	42	82
83-7	-196	-321	2	1.5	0.10	0.004	4	29
83-8	-160	-256	25	18.5	0.24	0.009	9	30
83-9	-175	-283	25	18.5	0.22	0.009	9	19
83-10	-140	-220	27	20.0	0.28	0.011	11	24
83-11	100	212	95	70.0	1.40	0.055	55	100
83-12	23	73	96	71.0	1.38	0.054	54	81
83-13	80	176	95	70.0	1.45	0.057	57	100

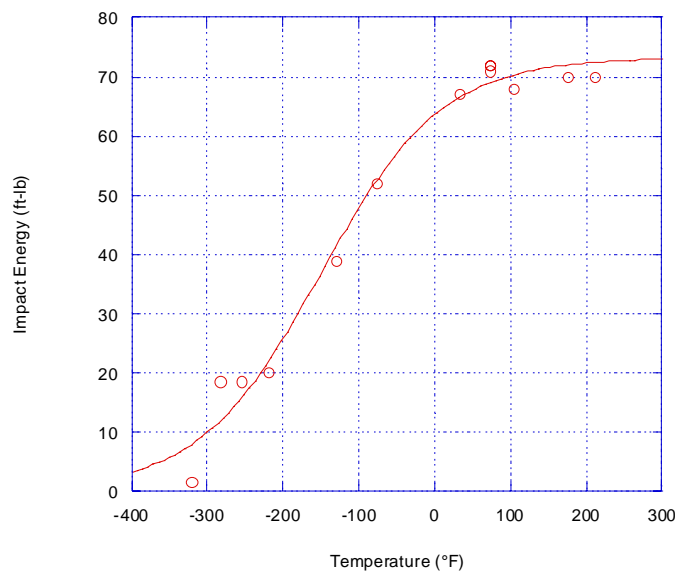


Figure 103 Charpy V-Notch Impact Energy Plot as a Function of Temperature for 83-Q (Plot of 3/4-size samples)

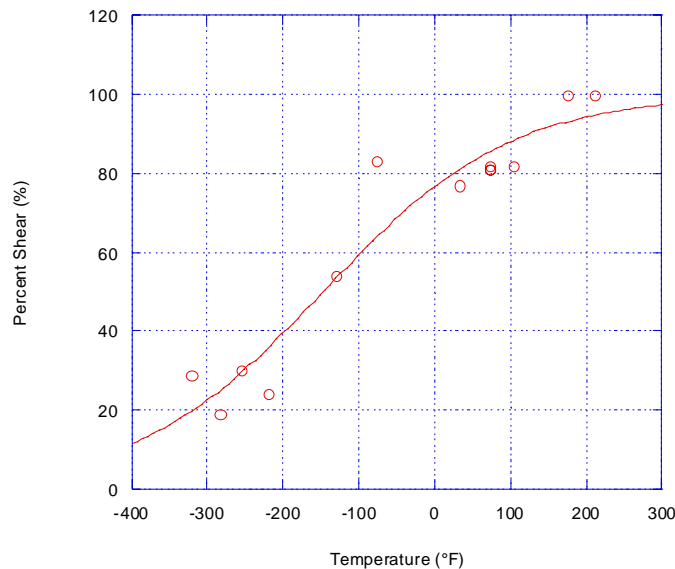


Figure 104 Percent Shear Plot from Charpy V-Notch Tests as a Function of Temperature for 83-Q

6.2.8.5 Chemical Analysis of Drill Pipe

Chemical analysis was conducted on coupons removed from 1-A-1-Q, 1-B-2-Q, 39-Q, 83-Q, 93-Q, and 148-Q. The results of the chemical analysis are summarized in Table 28. The results of the analysis indicate that the pipe steel meets the chemical composition specifications for API 5D Grade S135, seamless drill pipe.⁵

Items 1-A-1-G and 39-Q were from a drill pipe joint with an internal coating and 1-B-2-Q, 83-Q, 94-Q, and 148-Q were from a drill pipe joint with no internal coating. Comparing these two groups, there was no discernable difference in the chemistry of the two drill pipe joints.

Table 28 Results of Chemical Analysis Compared with Specification for API 5D Grade S135, Seamless Drill Pipe

Element	1-A-1-Q	39-Q	1-B-2-Q	83-Q	94-Q	148-Q	API 5D
	wt%	wt%	wt%	wt%	wt%	wt%	wt%
Aluminum	0.022	0.022	0.023	0.023	0.023	0.023	-----
Boron	0.0006	0.0005	0.0006	0.0005	0.0006	0.0006	-----
Carbon	0.24	0.24	0.25	0.24	0.25	0.24	-----
Cobalt	0.002	0.001	0.004	0.001	-----	0.001	-----
Chromium	1.25	1.26	1.25	1.24	1.26	1.25	-----
Copper	0.10	0.10	0.10	0.10	0.10	0.10	-----
Iron	Balance	Balance	Balance	Balance	Balance	Balance	-----
Manganese	0.74	0.73	0.73	0.73	0.74	0.73	-----
Molybdenum	0.61	0.62	0.61	0.61	0.61	0.62	-----

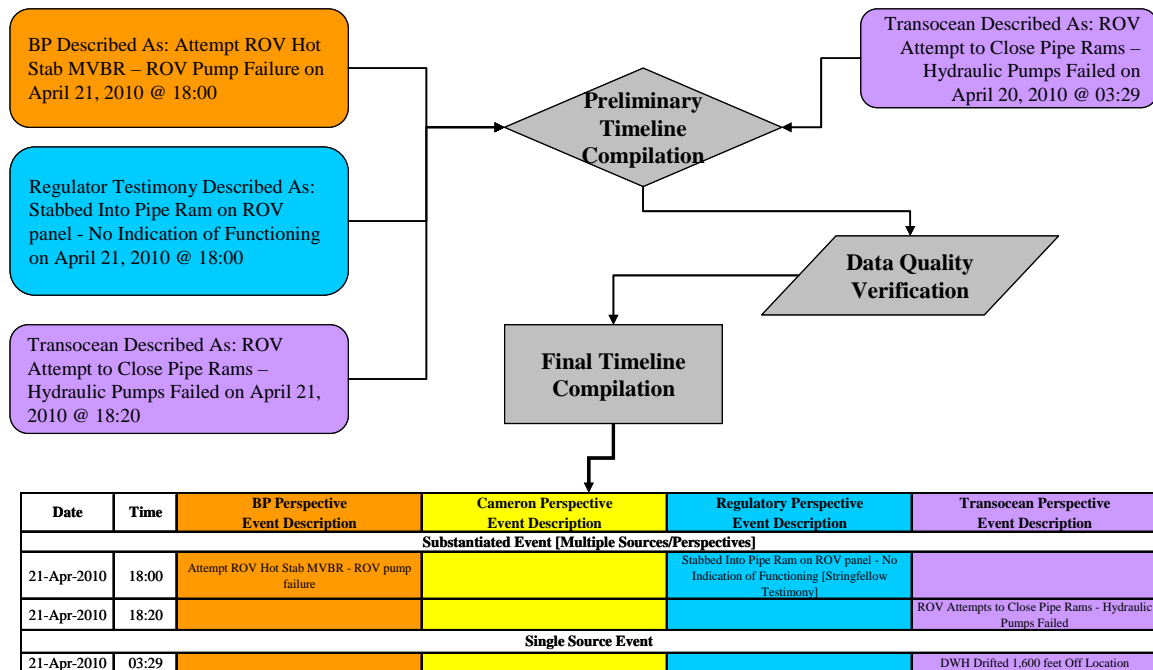


Element	1-A-1-Q	39-Q	1-B-2-Q	83-Q	94-Q	148-Q	API 5D
	wt%	wt%	wt%	wt%	wt%	wt%	wt%
Niobium	-----	-----	-----	-----	-----	-----	-----
Nickel	0.12	0.12	0.12	0.12	0.12	0.12	-----
Phosphorus	0.006	0.006	0.006	0.006	0.006	0.006	0.030
Sulfur	0.003	0.002	0.003	0.002	0.003	0.003	0.030
Silicon	0.26	0.25	0.26	0.25	0.25	0.25	-----
Tin	0.054	0.042	0.050	0.050	0.041	0.039	-----
Titanium	0.016	0.014	0.015	0.015	0.014	0.014	-----
Vanadium	0.006	0.006	0.007	0.007	0.007	0.006	-----
Zirconium	0.007	0.005	0.006	0.005	0.004	0.004	-----

6.3 Document Review

The publicly available and Government-provided documents and information, identified within Appendix C, were reviewed for the purpose of capturing and verifying where possible, the time of occurrence and descriptions of events that took place relevant to the BOP, prior to, during, and subsequent to the incident. Event descriptions and corresponding time occurrences were considered verified if derived from multiple sources and substantiated based upon consistent information. In only one case was an event (identified by two information sources and two perspectives) considered non-verifiable. DNV determined the event to be non-critical and conducted no further review.

Captured events were used to populate a comprehensive timeline for the purpose of illustrating the sequence of events. It was organized according to perspective or various original sources of information. The comprehensive timeline is provided within Appendix F. An illustration of the process used to create the comprehensive timeline is shown in Figure 105. The timeline was developed as an initial first step within the forensic investigation process and contains events considered by DNV to represent key data points. ROV footage was utilized to further substantiate and provide clarification for specific events. Findings of the ROV footage review are described in Section 6.4.

Substantiated Event [Multiple Sources/Perspectives]***Single Source Event***

* Event descriptions were abbreviated for clarity of the illustration

Figure 105 Timeline Process

- Maintenance records, inspection results, and audit reports were reviewed as part of the Document Investigation. The events contained within the maintenance records, inspection results, and audit reports were incorporated into the timeline using the process described above. The events were also used to establish, to the extent possible, the condition of the BOP stack at the time of the incident. The information concerning the condition of the BOP stack provided guidance for the BOP Functionality testing and the Materials Evaluation and Damage Assessment.

A series of three secondary timelines were developed to assist with the Failure Cause Analysis:

- Blind Shear Ram Timeline, detailing the time span from the incident on April 20, 2010 until April 29, 2010, when it was concluded that the Blind Shear Rams were closed. See Figure 108.
- Variable Bore Rams Timeline, detailing the time span from February 1, 2010, until May 5, 2010, when a final attempt was made to close the VBRs. See Figure 107.
- Annular Preventer Timeline, detailing the time span from January 31, 2010, when the Deepwater Horizon arrived at the Macondo site, until May 3 2010, when a fourth ROV attempt was made to close the Lower AP. See Figure 106.

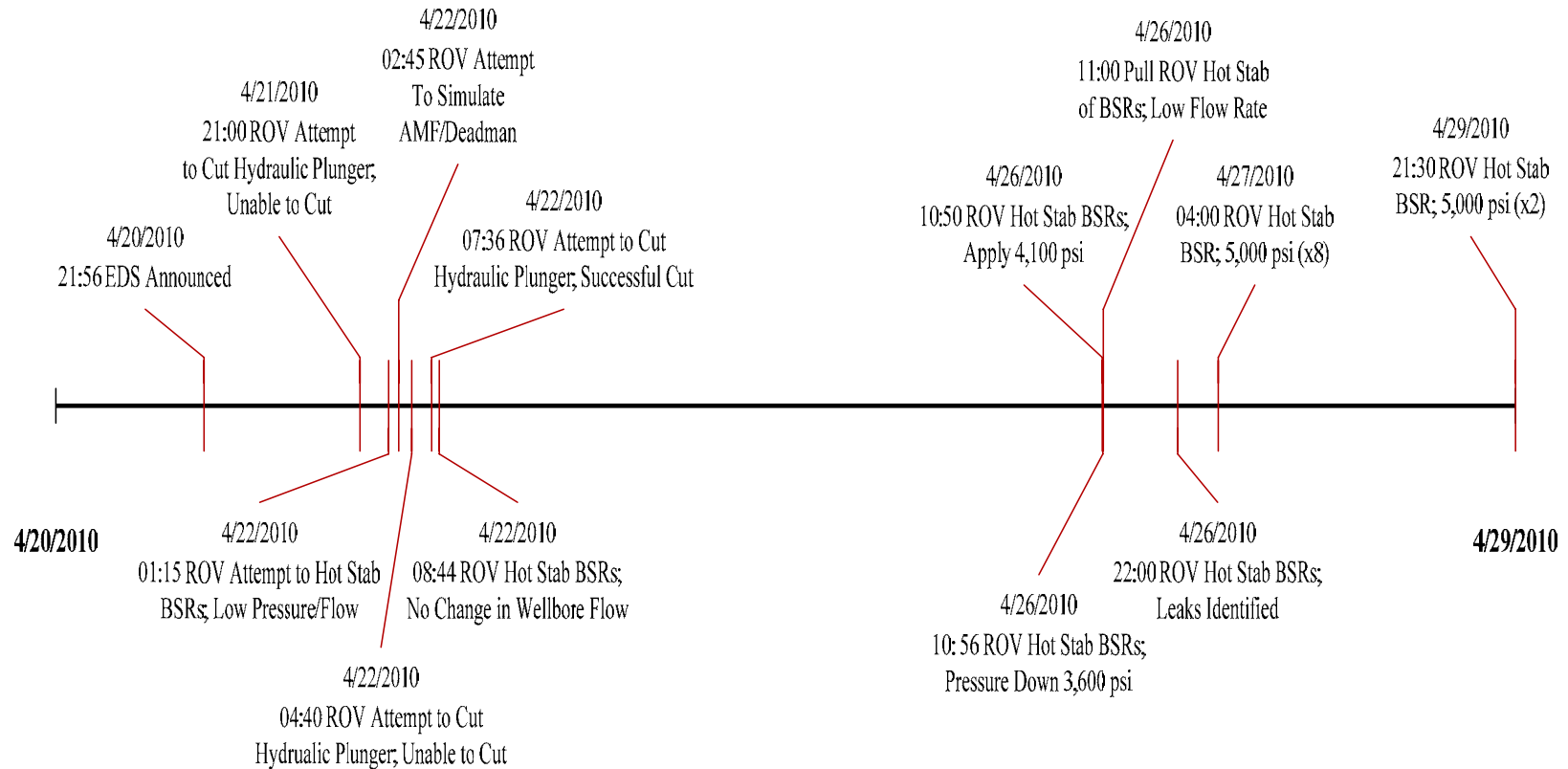


Figure 106 Illustration of the Events Pertaining to BSRs - April 20, 2010 to April 29, 2010

DET NORSKE VERITAS

United States Department of the Interior, Bureau of Ocean Energy
Management, Regulation, and Enforcement
Forensic Examination of Deepwater Horizon Blowout Preventer
Volume I Final Report

MANAGING RISK

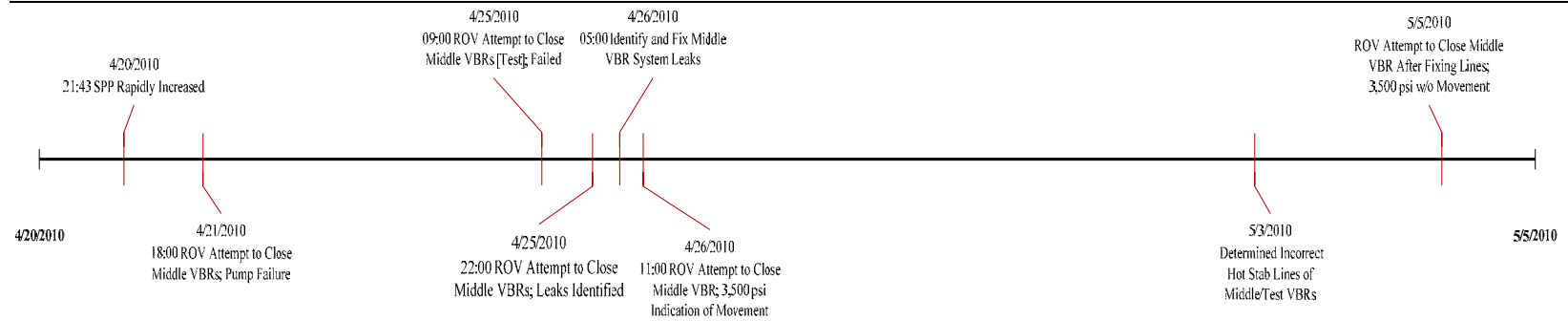


Figure 107 Illustration of Events Pertaining to VBRs - April 20, 2010 to May 5, 2010.

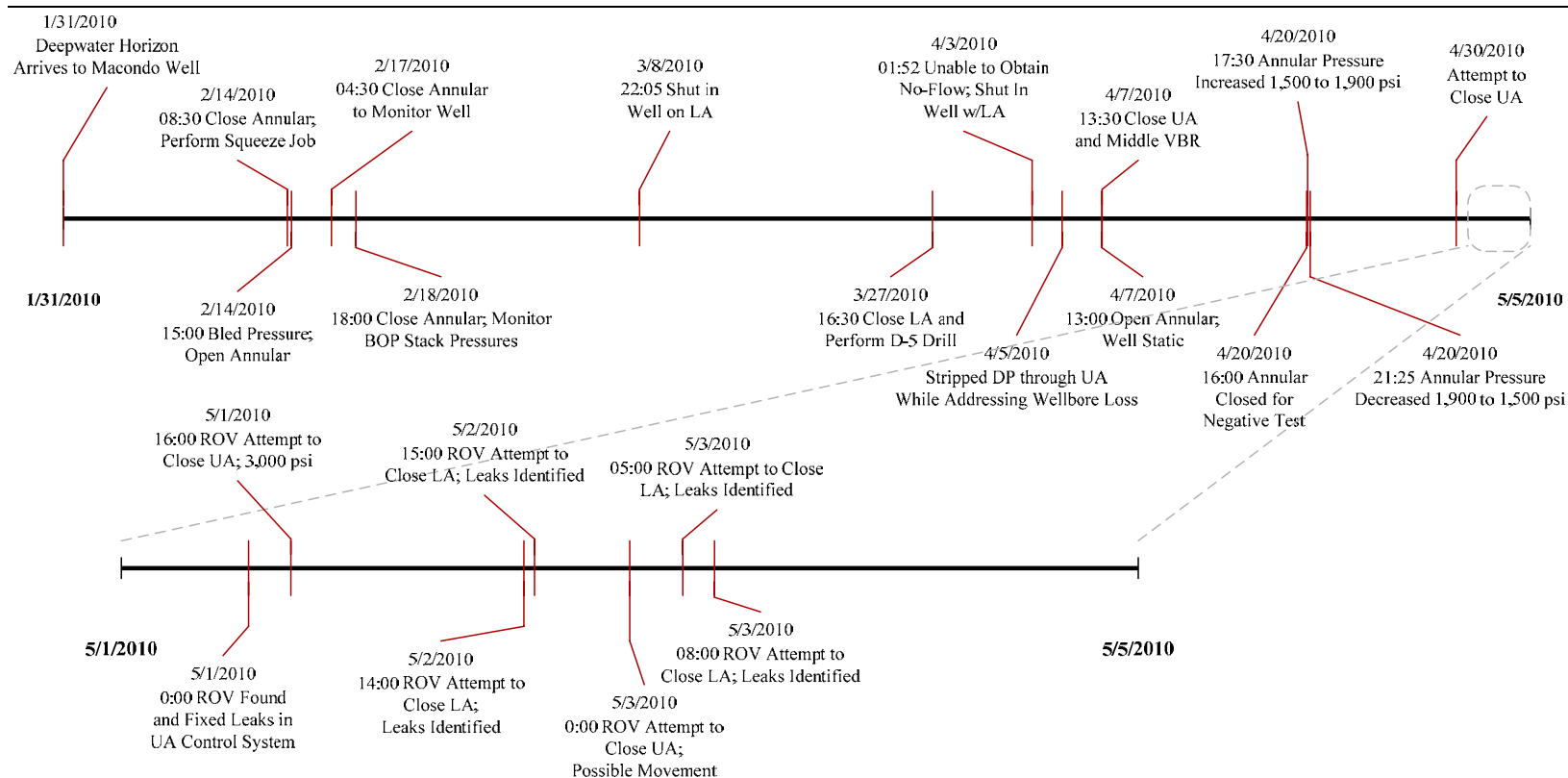


Figure 108 Illustration of Events from the comprehensive timeline that pertain to the Annular Preventers which occurred between January 31, 2010 to May 5, 2010



6.4 Remotely Operated Vehicle Intervention Efforts

Following the incident, there were several attempts to function the rams on the BOP and to effect repairs to the BOP hydraulic circuits by ROV. In addition, there was continuous ROV inspection and monitoring of various BOP components. Video footage and still photographs taken by the ROVs were provided by BOEMRE as part of the incident investigation documentation. The video footage of particular interest was provided for the time period from late April 21 to May 4, 2010.

The ROVs were equipped to perform a range of intervention tasks. Each ROV had robotic arms and pinchers used to grasp tools, including cutting wheels, wrenches, hot stabs to transfer pressurized fluid, and hose insertion tools. These tools were lowered to the seabed by a basket and crane. Each ROV had a hydraulic fluid pump on board to assist with hot stabbing operations. Hydraulic fluid was supplied by lowering accumulators to the sea floor. During some intervention efforts the hydraulic fluid was dyed green for visibility, to assist in identifying leaks in the hydraulic circuit.

Video footage and/or photographic stills were provided from the following ROVs:

- C-Express – C-Innovation,
- Boa Sub C - Millennium 36
- Boa Sub C - Millennium 37
- Skandi Neptune - Hercules 6
- Skandi Neptune - Hercules 14

The ROV video footage was reviewed with two objectives:

- To confirm the times, dates and activities referenced by other sources for the purpose of substantiating and illustrating timeline events.
- To provide on going ROV video review support to confirm observations related to the BOP condition and the origin of leaks and modifications to the hydraulic circuitry.

The video footage of primary interest was from three ROVs: C-Innovation, Millennium 36 and Millennium 37. These ROVs performed intervention work and monitoring after the incident. The other ROVs (from which video footage was provided) were generally involved in monitoring activities. The ROV operators completed dive logs during the course of their intervention efforts. The logs were provided by BOEMRE as part of the documentation. The dive logs were reviewed and used as guidelines to navigate the extensive ROV footage. The relevant ROV intervention times and activities were cross-referenced to supporting documentation and verified activities were then included in the primary timeline.



6.4.1 Activation of the Blind Shear Rams

Three different interventions were performed to initiate closure of the BSRs:

- Forced activation of the AMF/Deadman sequence by severing the pressure balance oil filled (PBOF) cables severing the Pressure Balanced Oil Filled cable between the Yellow and Blue Control Pods and the pilot pressure lines from the rigid conduit manifold
- Forced activation of the Autoshear sequence by manually cutting the hydraulic plunger
- Closure of the BSRs by “hot stabbing” directly into the ROV panel located on the lower choke side of the BOP

During the course of these activities there were also efforts to close the Middle VBRs by hot stabbing. It was later determined, on May 3, 2010, that the hydraulic line from the ROV panel Middle VBR close port was incorrectly connected to the Lower VBRs.

Later ROV interventions involved initiating closure of the CSRs and the Annular Preventers.

Intervention efforts related to the closing of the BSRs were reviewed and documented in detail in the primary timeline (Appendix F). Table 29 is a summary of these efforts.

Table 29 Summary of ROV Interventions for BSRs

Date	Time	Activity	Documented Result
April 21, 2010	23:00	C-Innovation attempted to activate Autoshear	The hydraulic plunger was not cut
April 22, 2010	01:10	C-Innovation attempted to close BSR by hot stabbing into the “SHR RAM CLOSE” port on the ROV panel.	Unable to raise pressure.
	02:45	C-Innovation attempted to simulate the Automatic Mode Function (AMF/Deadman) by cutting rigid piping and the PBOF hydraulic lines	The hydraulic line was severed. Fluid release from the line was minimal and indicated the line was not under high pressure.
	04:40	Second attempt to activate the Autoshear by cutting the hydraulic plunger	Unable to cut hydraulic plunger
	07:30	Millennium 37 attempted activate the Autoshear by cutting the hydraulic plunger	Hydraulic plunger was successfully cut.



Date	Time	Activity	Documented Result
	08:00	Millennium 36 attempted to close the BSR by hot stabbing into the "SHR RAM CLOSE" port on the ROV panel	Unable to raise pressure. Flow test on mud indicated fluid is flowing.
	10:22	Deepwater Horizon sank	
April 23, 2010		(No active intervention efforts related to BSR)	
April 24, 2010		(No active intervention efforts related to BSR)	
April 25, 2010		(No active intervention efforts related to BSR)	
April 26, 2010	10:45	Millennium 37 attempted to close the BSR by hot stabbing into the "SHR RAM CLOSE" port on the ROV panel	Pressure reached 4,400 psig, but was not maintained.
April 26, 2010	21:45	Millennium 37 attempted to close the BSR by hot stabbing into the "SHR RAM CLOSE" port on the ROV panel	Pressure reached 4,500 psig, but was not maintained.
April 27, 2010	03:15	Millennium 37 attempted to close the BSR by hot stabbing into the "SHR RAM CLOSE" port on the ROV panel	Pressurized to 5,000 psig. Appeared to maintain pressure.
April 28, 2010		(No active intervention efforts related to BSR)	
April 29, 2010	21:30	Millennium 36 attempted to close the BSR by hot stabbing into the "SHR RAM CLOSE" port on the ROV panel	Pressurized to 5,500 psig. Appeared to maintain pressure.
May 10, 2010	-	Gamma rays indicated all but one of the ST locks were closed and locked	-
May 20, 2010	-	ROV intervention activities ceased	-

The first ROV intervention effort related to the closing of the BSRs was an attempt to cut the Autoshear hydraulic plunger. C-Innovation attempted the cut using a circular saw at approximately 23:30 hours on the evening of April 21, 2010. The cut was not successful. Figure 109 shows two images captured from the video footage provided, from before and after the failed attempt.



Figure 109 ROV C-Innovation video footage of the failed attempt to cut the Autoshear hydraulic plunger at 23:30 on April 21, 2010

The first attempt to close the BSRs by hot stabbing was performed by C-Innovation at approximately 01:15 hours on April 22, 2010. The ROV was unable to generate pressure using the on-board hydraulic pump. Figure 110 shows two images captured of the failed attempt. C-Innovation then successfully severed various rigid piping and the PBOF cable between the subsea transducer module (STM) and SEMs on the Control Pods. Figure 111 shows images of the severing of the PBOF cables.



Figure 110 ROV C-Innovation video footage of the failed attempt to raise pressure during hot stab of the blind shear ram at 01:15 on April 22, 2010

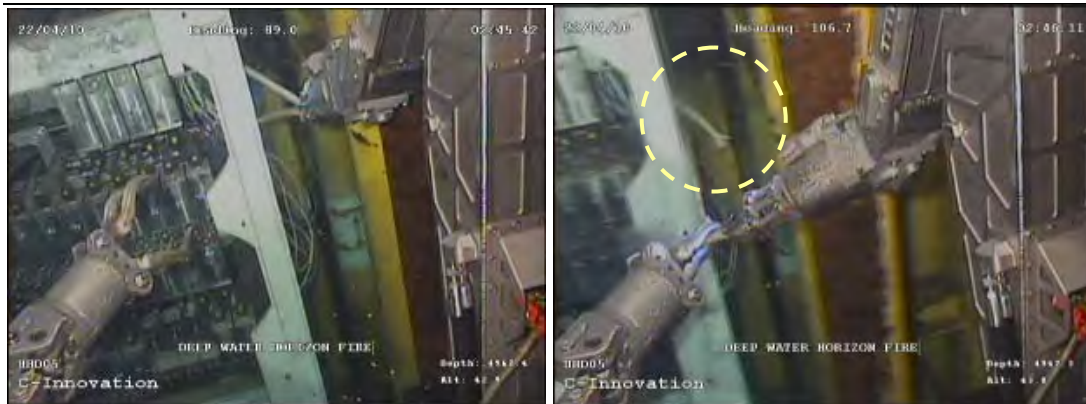


Figure 111 ROV C-Innovation video footage of the successful attempt to sever the PBOF cables 02:45 on April 22, 2010. The severed cable is highlighted with a yellow dashed circle.

The Autoshear hydraulic plunger was successfully cut using a circular saw by Millennium 37 at approximately 07:30 hours on April 22, 2010. Figure 112 shows images of the successful cut. Movement of the plunger (captured by the ROV footage) indicated that the Autoshear sequence was initiated.

Following the Autoshear hydraulic plunger cut, the ROV performed an inspection of the BOP stack. The inspection of the “LATCH/UNLATCH” indicator demonstrated that the LMRP had not unlatched (see Figure 113 and Figure 114).

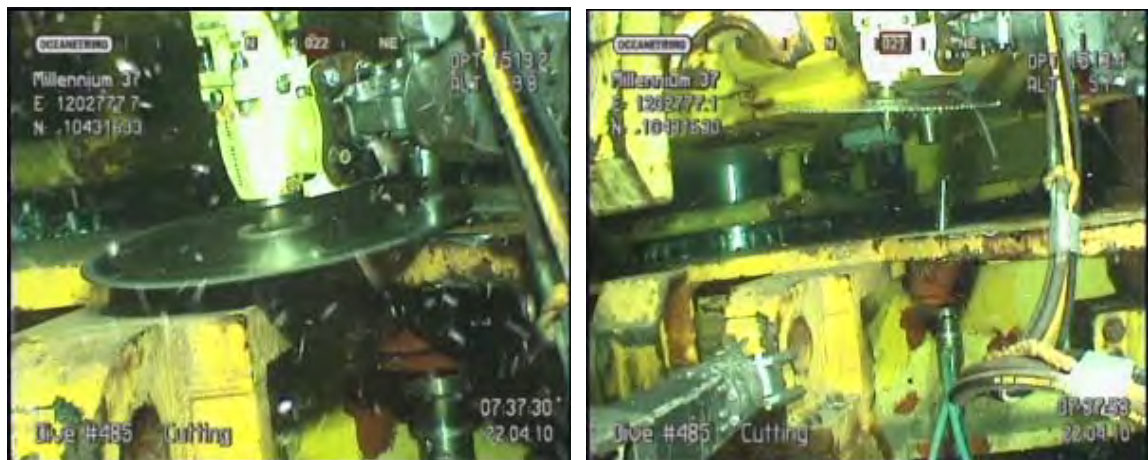


Figure 112 ROV Millennium 37 video footage of the successful attempt to cut the Autoshear hydraulic plunger at 07:30 on April 22, 2010



Figure 113 ROV Millennium 37 video footage of the LMRP/BOP stack connection shortly after cutting of the Autoshear hydraulic plunger at 07:30 on April 22, 2010



Figure 114 ROV Millennium 37 video footage of the LMRP “LATCH/UNLATCH” indicator shortly after cutting of the Autoshear hydraulic plunger at 07:30 on April 22, 2010

Millennium 36 made another unsuccessful attempt to hot stab into the BSR close port on the ROV panel at approximately 08:00 hours on April 22, 2010. The ROV was unable to generate pressure. Figure 115 is an image of the failed attempt. The ROV was pulled

back as the Deepwater Horizon sank. Figure 116 shows images of the LMRP Flex Joint before and after the riser kinked on April 22, 2010.



Figure 115 ROV Millennium 36 video footage of the failed attempt to raise pressure during hot stab of the blind shear ram at 08:00 on April 22, 2010

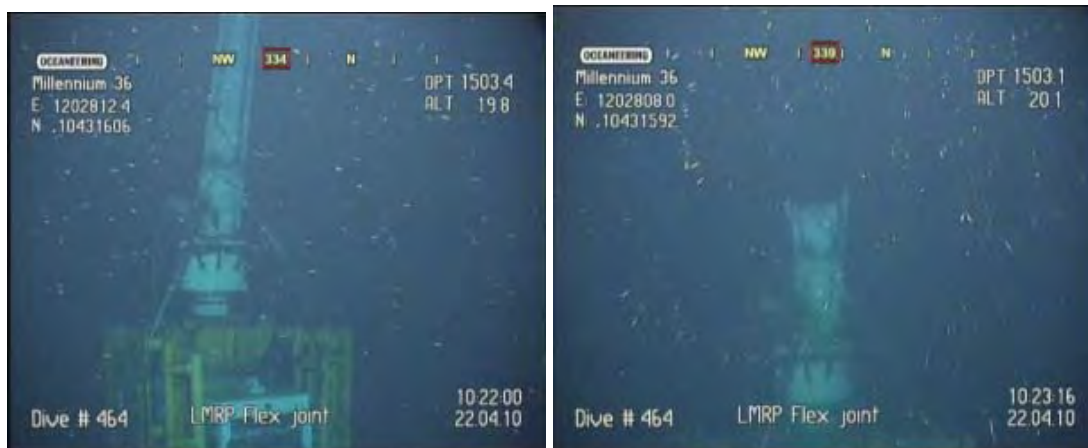


Figure 116 ROV Millennium 36 video footage of the LMRP Flex Joint before and after the kinking of the riser at 10:22 on April 22, 2010

Millennium 37 made two more attempts to hot stab the BSR close port on the ROV panel, at 10:45 and 21:45 hours on April 26, 2010. During both attempts the pressure was generated to over 4,000 psig, but could not be maintained. Figure 117 and Figure 118 show ROV images of the two attempts. The loss of pressure was attributed to leaks in the

ROV panel fittings, which were monitored and repaired before any further hot stabbing attempts.



Figure 117 ROV Millennium 37 video footage of a successful attempt to raise pressure during the hot stab of the blind shear ram at 10:45 on April 26, 2010



Figure 118 ROV Millennium 37 video footage of a successful attempt to raise pressure during the hot stab of the blind shear ram at 21:45 on April 26, 2010

Millennium 37 and Millennium 36 made two more attempts to hot stab the BSR close port on the ROV panel, at 03:15 on April 26, 2010 and 21:30 hours on April 29, 2010, respectively. During both attempts the pressure increased rapidly to over 5,000 psig, and was maintained. The maintained pressure indicated the leaks in the ROV panel had been successfully repaired.



Figure 119 ROV Millennium 37 video footage of a successful attempt to maintain pressure during hot stab of the blind shear ram at 3:15 on April 27, 2010

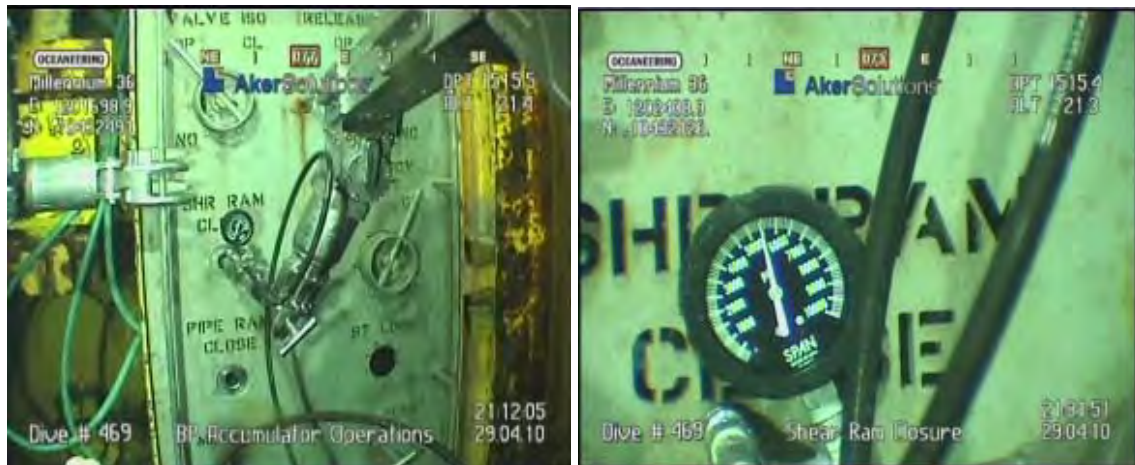


Figure 120 ROV Millennium 36 video footage of a successful attempt to maintain pressure during the hot stab of the blind shear ram at 21:30 on April 29, 2010

6.4.2 Repair Efforts

Leaks were identified in the hydraulic circuits while hot stabbing the BSRs. ROVs worked in tandem to identify leaks in the various components. One ROV would hot stab at the ROV panel, while another ROV monitored hoses and connections for leakage. Leaks were highlighted by injecting green dye into the hydraulic fluid prior to hot stabbing.

Intervention efforts related to the closing of the blind shear rams are shown in Figure 121 and Figure 122. Leaks were repaired by ROV using hand tools. Figure 123 and Figure 124 show images of the inspection and repair to the ST Lock shuttle valve above the

starboard side of the BSRs. Leaks were also identified in the fittings behind the port side ST Lock (see Figure 125).



Figure 121 ROV Millennium 37 video footage of an inspection of a fitting on the blind shear ram at 08:15 on April 22, 2010



Figure 122 ROV Millennium 37 video footage of a repair to a fitting on the blind shear ram at 08:20 on April 22, 2010



Figure 123 ROV Millennium 37 video footage of an inspection of the ST lock shuttle valve on the blind shear ram at 22:20 on April 25, 2010



Figure 124 ROV Millennium 37 video footage of a repair of the ST lock shuttle valve on the blind shear ram at 5:45 on April 26, 2010



Figure 125 ROV Millennium 36 video footage of a leak in the fittings behind the right side ST Lock on the blind shear rams

6.5 Modeling

Based on the examination of the damage to the BSR blocks and the drill pipe segments, the position of the drill pipe at the time of cutting by the BSR was not at the center of the wellbore. The evidence from the markings on the drill pipe indicated that the drill pipe was at the side of the wellbore. To explain the position of the drill pipe within the wellbore at the time of the BSR activation, buckling of the drill pipe within the well-bore between the UA and the Upper VBR was examined. The modeling described below was performed for different combinations of annular preventers and VBRs with only minor variations in results.

The scenario in which forces developed to produce buckling is discussed here. The UA was closed with either the tool joint directly below the element or with the element closing on the top portion of the tool joint (see erosion patterns on the tool joint in Figure 126). The closing force of the UA element restricted the drill pipe from upward movement. Upon closing the Upper VBR, the wellbore flow was directed only through the drill pipe, resulting in the pressure within the drill pipe rapidly increasing. The pressure increase produced an upward force (axial compression load pinned at the UA) on the drill pipe. This upward force provided the forces necessary for the drill pipe to elastically buckle, forcing the drill pipe to the side of the wellbore.

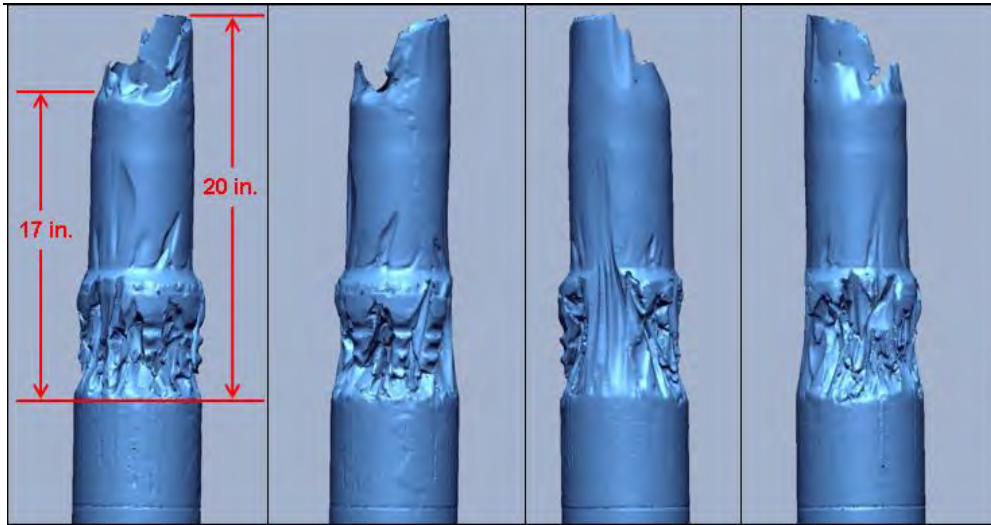


Figure 126 Laser Scan of Drill Pipe Segment 1-B-1 (Top End)

6.5.1 Buckling Model

Elastic buckling is characterized by a sudden instability of a structure subject to lateral loads or axial compressive loads. In the case of an axially loaded drill pipe, this instability would result in lateral displacement of the pipe within the wellbore. Finite element analysis (FEA) was performed to examine the possibility and effects of elastic buckling of the drill pipe within the wellbore between the UA and the Upper VBR.

Finite element modeling of a buckling event is typically handled as a two part analysis. An initial buckling analysis was run to calculate the critical buckling loads and predict the locations and manner that a structure will fail, and a post-buckling analysis was then run to calculate the pipe deformation response after the buckle initiates. For this model a linear eigenvalue buckling analysis was utilized to calculate the likely buckling modes and their corresponding critical loads.

The eigenvalue method is a numerical modeling technique to calculate the critical buckling loads of a given structure. For a drill pipe under axial load there are numerous ways in which the drill pipe can buckle (known as buckling modes). The buckling modes are affected by the loading conditions and sensitive to any stiffening elements in the structure. The tool joint and drill pipe were modeled in their entirety for the segment between the UA and the Upper VBR.

A three dimensional solid model was developed that included a drill pipe segment (including tool joint) that spanned from the UA down to the Upper VBR, the BSR cavity, and a section of the BOP wellbore, as shown in Figure 127. The drill pipe segment was modeled using the nominal geometry specified in API Specification 5D and API

Specification 7. The wellbore and the BSR cavity were modeled to simulate the displacement restrictions of the drill pipe within the wellbore.

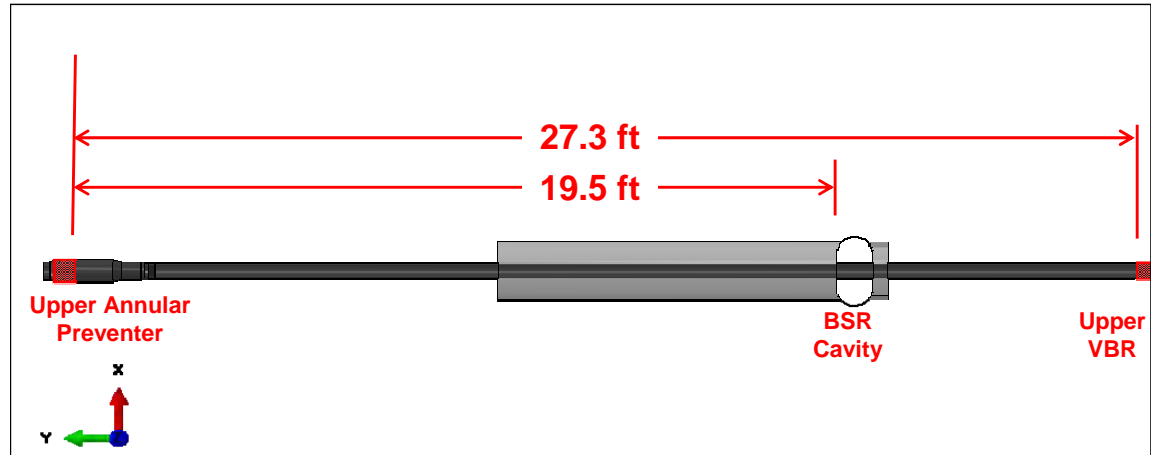


Figure 127 General Layout of Drill Pipe and Wellbore Section

The final drill pipe geometry was modeled with refined mesh of 27,520 elements, connected by 41,400 nodes. The elements used to construct the model were three-dimensional 8-noded hexahedral solid elements. Elements of this type and refinement ensured adequate mesh definition and solution accuracy. The wellbore and BSR cavity were modeled with rigid shell elements. These elements provided contact and displacement control. Elastic material properties were applied to the elements defining the behavior of the drill pipe using results from the mechanical testing (Section 6.2.8.4).

Boundary conditions were applied representing the constraints at the UA and the Upper VBR. An eigenvalue buckling analysis was then run to predict the buckling modes and calculate their respective critical loads. Critical loads were calculated by applying incremental axial loads to the bottom of the drill pipe until the point of instability was reached. The predicted buckling mode data was then utilized as input for the post-buckling deformation analysis.

The axial load components were added in a static Rik's type analysis to approximate the post-buckling deformation of the drill pipe. Rik's method is capable of varying the applied load components as the pipe deforms allowing the analysis to account for the non-linear effects expected as buckling progresses.

The models were solved using ABAQUSTM Standard. The initial buckling analysis predicted a single waveform buckling mode, at a critical axial load of 113,568 lbs. The predicted deformation and resulting stresses are shown in Figure 128 and Figure 129, and the calculated loads are given in Figure 130. The predicted deformation showed the peak curvature of the buckle would contact the wellbore above the BSR cavity, holding the pipe against the side of the wellbore.

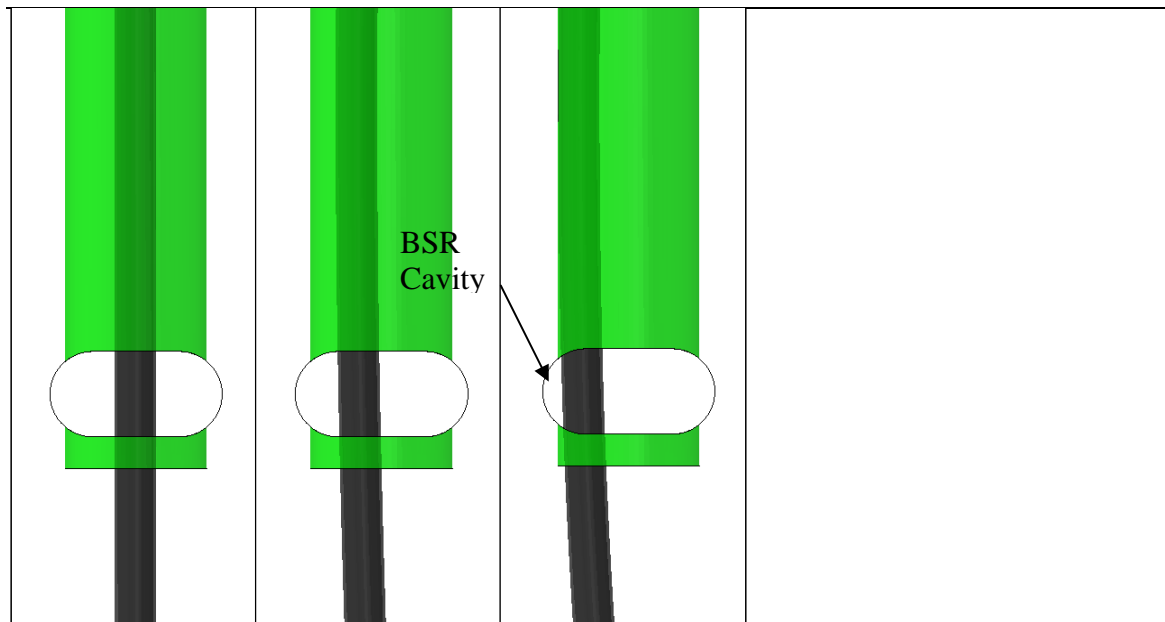


Figure 128 Progression of Pipe Displacement Under Buckling

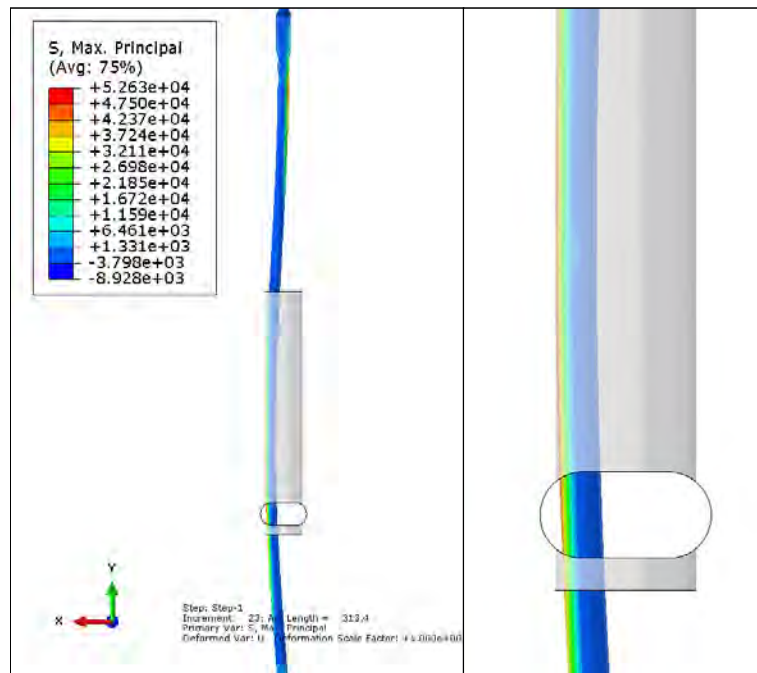


Figure 129 Predicted Deformation and Resulting Stresses Due to Buckling

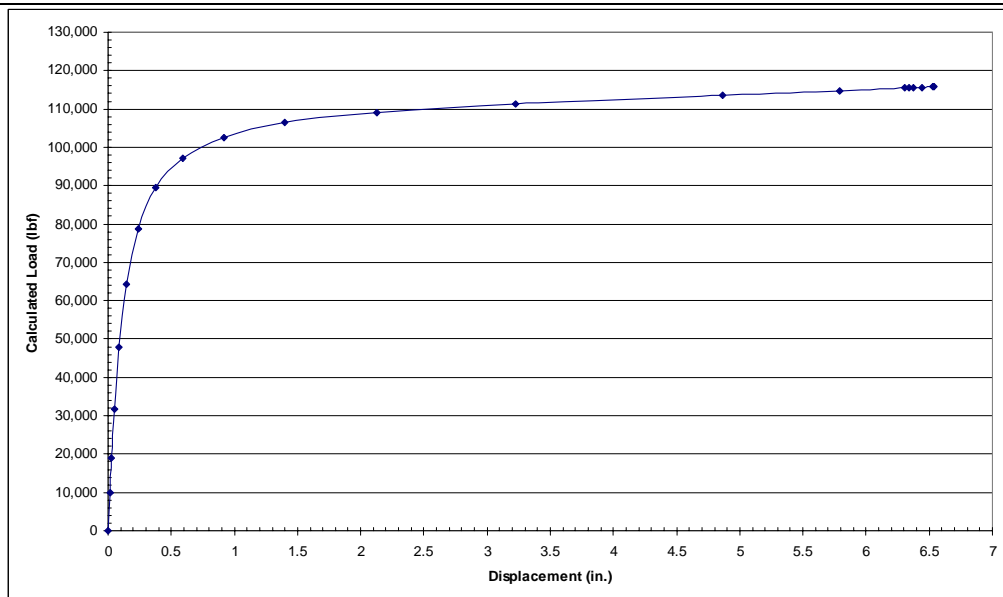


Figure 130 Calculated Loads as a Function of Drill Pipe Displacement

6.5.2 Buckling Considerations

It has been shown by finite element analysis (Section 6.5.1) that a compressive axial load of 113,568 lb on the drill pipe was necessary to cause buckling. The finite element analysis accounted for the specific geometry of the drill-pipe, tool joint and rams.

This result was validated by calculations based on Euler's equation. The drill pipe was assumed to be fully restricted from upward movement at the closed UA due to a tool joint positioned just below. At the upper VBR, the drill pipe was assumed to be fixed in the radial direction by the rams but unrestricted in the vertical direction (i.e. allowed to slide).

A compressive axial force that led to buckling of the drill pipe at the time the BSR was activated was the result of a combination of several components. These force components depend on the reservoir pressure, the fluid media in the drill pipe, the flow in the drill pipe, the friction between the fluid media and drill pipe and other factors.

The axial compressive force on the drill pipe that can cause buckling has a number of components including but not limited to:

- Upward friction force from the flow inside the drill pipe
- Upward buoyancy force on the drill pipe
- Upward force from reservoir pressure in excess of buoyancy acting on drill pipe
- Downward gravity force on the drill pipe
- Downward friction force on the outside of the drill pipe from seal at the VBR

Based on conditions likely present in the wellbore at the time of the incident, calculations indicate that the force needed to buckle the drill pipe was present. Detailed numerical simulations were not performed as part of this investigation.

6.5.3 Cutting of the Drill Pipe in the Blind Shear Ram

Physical evidence on the recovered drill pipe segments indicates that the drill pipe was not centered in the wellbore when the BSR was activated. Indications on drill pipe segment ends 94-B and 83-B were matched to the outer corners of the upper BSR block as discussed in (Section 6.2.4.2). These indications were aligned with the upper BSR block features to determine the position of the drill pipe. Figure 131 shows a comparison of the aligned pipe segments with the predicted drill pipe position from the buckling analysis.

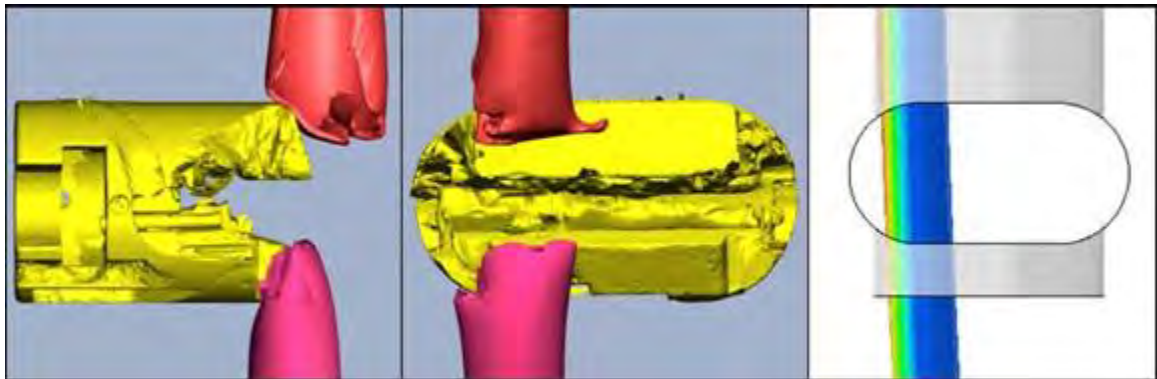


Figure 131 Alignment of Pipe Segments with BSR and Buckled Pipe Displacement Comparison

The BSR blades are designed with a face rake angle intended to impart tension on the drill pipe as the blades shear through it. Multiple numerical equations exist for approximating the shear forces necessary to shear drill pipe, however these only consider situations where the pipe is completely within the shearing blade surfaces of the BSR. A finite element analysis (FEA) was performed to simulate the effects of a non-centered drill pipe on the ability of the BSR to cut the drill pipe and seal the well.

Fracture of a ductile material is governed by two key mechanisms: ductile fracture due to the nucleation, growth, and coalescence of voids (ductile damage) and shear fracture due to shear band localization (shear damage).⁶ These two mechanisms call for different forms of the criteria for the onset of damage. FEA using Abaqus offers several mechanisms to accurately model material damage. For this analysis, ductile damage initiation was specified using the Johnson-Cook damage model and published damage

⁶ ABAQUS Analysis User's Manual, "21.2.2 Damage Initiation Criteria for Fracture of Metals"; (C) Dassault Systemes, 2010.

parameters for 4340 steel. The shear damage initiation was specified using shear criterion model within Abaqus and published damage parameters. This allowed for the model to consider material failure by ductile damage, shear damage, or a combination thereof.

Validation models were run to determine the forces necessary to cut the drill pipe when it is within the cutting blade surfaces (centered in the wellbore as illustrated in Figure 132). A three dimensional shell model was developed representing the BSR blades, block faces, and a section of 5.5 inch diameter drill pipe as shown in Figure 133. The final geometry was modeled with 20,030 elements connected by 20,183 Nodes. The blade surface models were developed from CAD models of the BSR provided by Cameron. The drill pipe was modeled with shell elements and a specified thickness of 0.386 inches, per measurements of pipe section 83-Q. The ram faces were modeled with rigid shell elements as they were assumed stiff relative to the deformable drill pipe. Elastic and plastic material properties were applied to the model defining the behavior of the drill pipe as determined by mechanical testing.

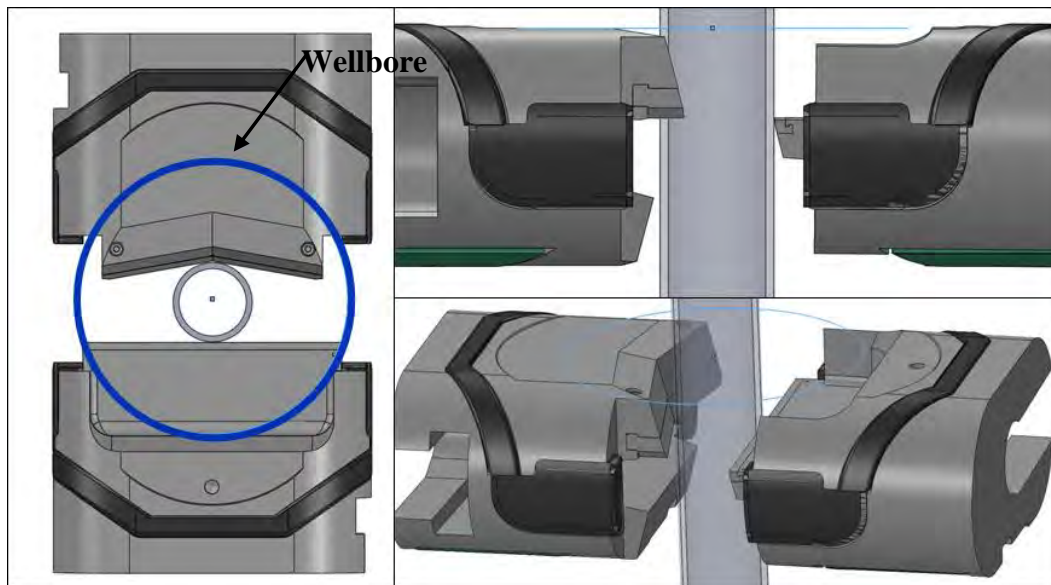


Figure 132 BSR Configuration

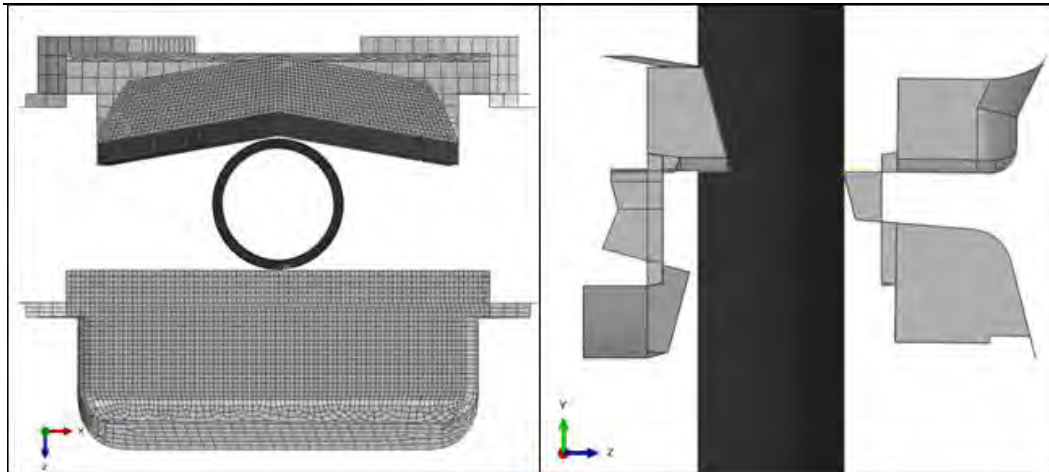


Figure 133 FEA Model of BSR Blade Surfaces and Drill Pipe

A second model was developed to analyze the effects of the drill pipe being off center in the wellbore (displaced to the far side of the wellbore as illustrated in Figure 134). The upper BSR block had a single “V” blade design, intended to create a progressive shear, thereby reducing the necessary cutting force. As shown in Figure 132, the upper BSR blade does not extend fully across the wellbore. The lateral forces due to buckling would likely have kept the drill pipe off center in the position illustrated in Figure 134.

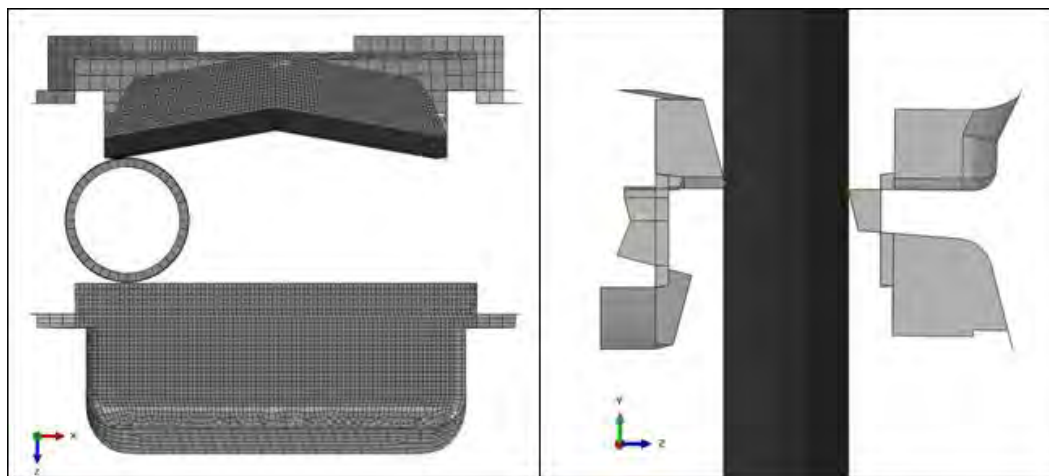


Figure 134 FEA Model of BSR Blade Surfaces and Off-Center Drill Pipe

The dynamic pipe shear models were solved using Abaqus Explicit. The progression of the shear cut for the model with centered drill pipe is shown in Figure 135 and Figure 136. The drill pipe was deformed initially (Frames 2 and 4). Frame 7 shows the step where the blade began to shear and penetrate the drill pipe. This was the point of highest calculated shear force (RF_{MAX}). As the shearing progressed and the drill pipe separated, the required force decreased (Frame 8). After full separation, the rams deformed the pipe

and folded over the lower sheared section (Frames 10 and 12). Figure 137 shows a BSR cut from Cameron Engineering Report 2613 with a very similar appearance as predicted by the FEA model.

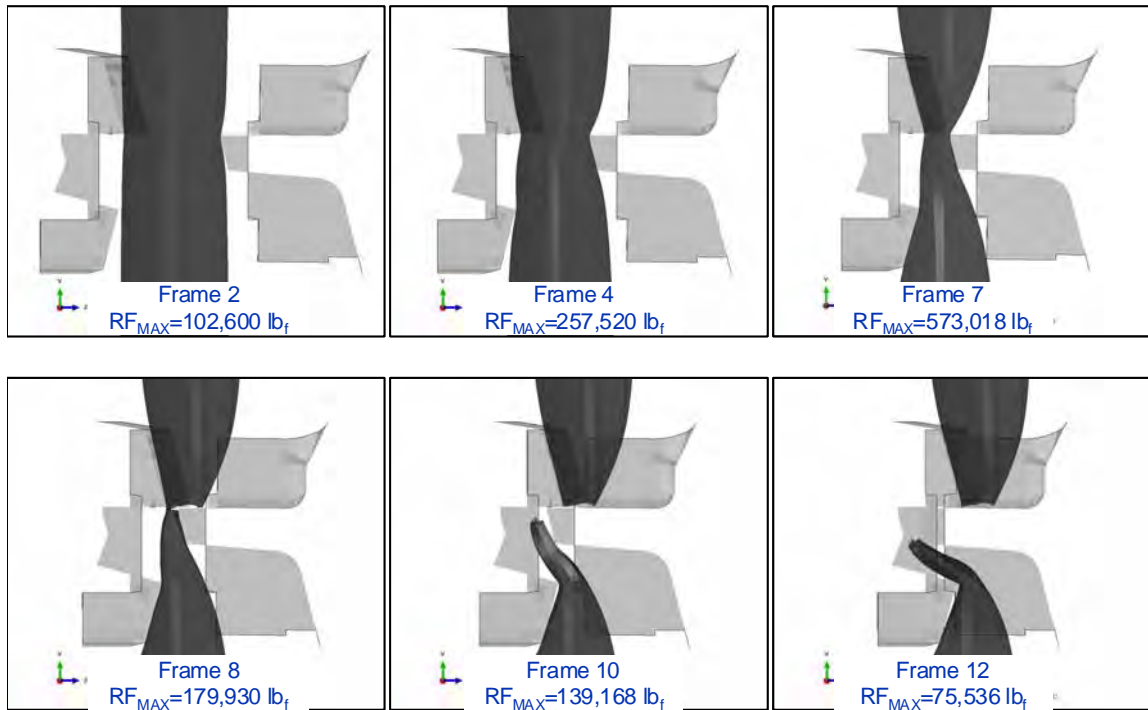


Figure 135 Progression of Centered BSR Shear Model - Side View

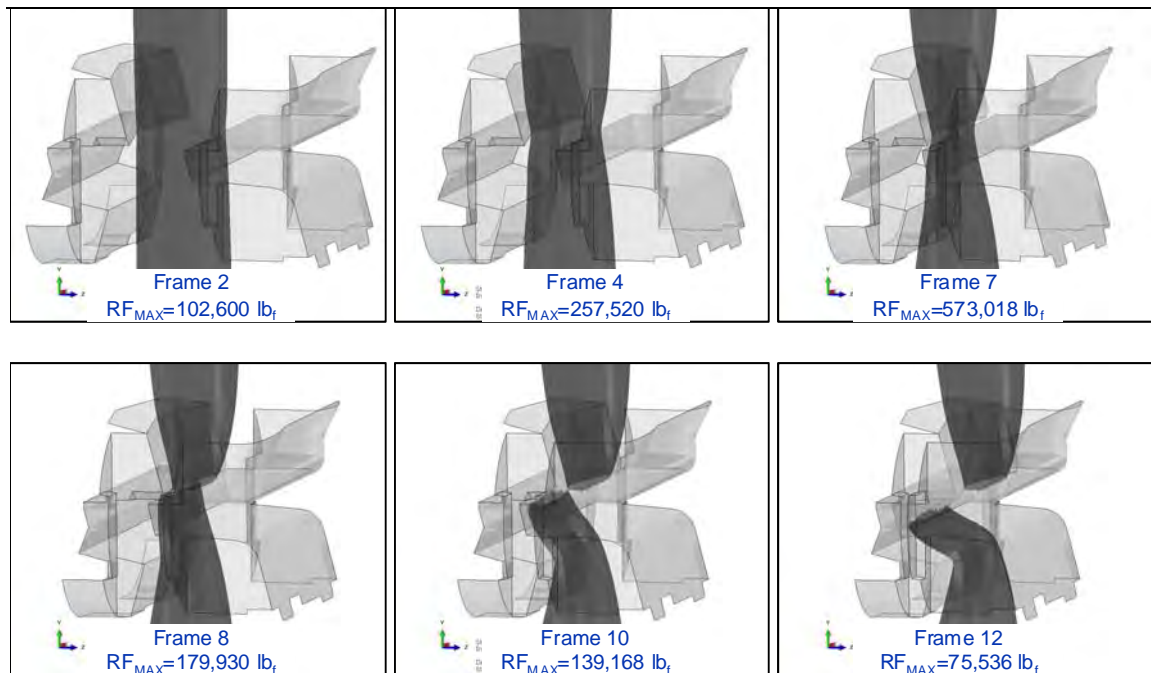


Figure 136 Progression of Centered BSR Shear Model - Isometric View



(a) Lower pipe with upper BSR block (b) Lower pipe with lower BSR block

Figure 137 Photographs of BSR Shear Samples.⁷

The model with centered drill pipe calculated a maximum required shear force of 573,018 lbs. Table 2 of Cameron Engineering Bulletin EB-702D provided the effective piston area for the BSR configuration (238 in²). The model-derived shear force, when divided by this effective piston area, equated to a maximum ram pressure of 2,408 psig. The FEA

⁷ Cameron Engineering Report 2613, Mach 3, 1999, 2nd Shear Test, Photo 8 and 9 of 16, p.22.

results were compared with shearing pressure results derived from methods proposed by Transocean⁸, West Engineering⁹, and Cameron¹⁰. The Transocean and West Engineering calculations were based on a modified distortion energy theory equation, while Cameron used an empirical formula developed from extensive testing. The calculated results for the given conditions are given in Table 30. The FEA model results showed good agreement with the calculated shear pressures.

Table 30 Comparison of Calculated BSR Pressures

Calculation Method	Calculated Shear Force	Shear Pressure
	(lbf _f)	(psi)
Transocean ⁸		2,378
West Engineering ⁹	504,805	2,121
Cameron ¹⁰		3,008
FEA Model	573,018	2,408

The BSR is designed to fold the end of the lower pipe segment over to prevent damage to the lateral sealing element behind the upper blade as it passes across. Testing has shown that the lower piece can fracture at the fold point (Figure 137). The centered pipe shear analysis calculated a strain concentration of 32% along the inner bend as seen in Figure 138, matching with the fracture area observed on physical tests.

⁸ TRN-USCG_MMS-00038805 Shear Pressure.xls.

⁹ West Engineering Report: Shear Ram Capabilities Study; Req. 3-4025-1001 for U.S. MMS, Sept. 2004.

¹⁰ ED-702 CAMCG 00003247 Page 5 – Table 2.

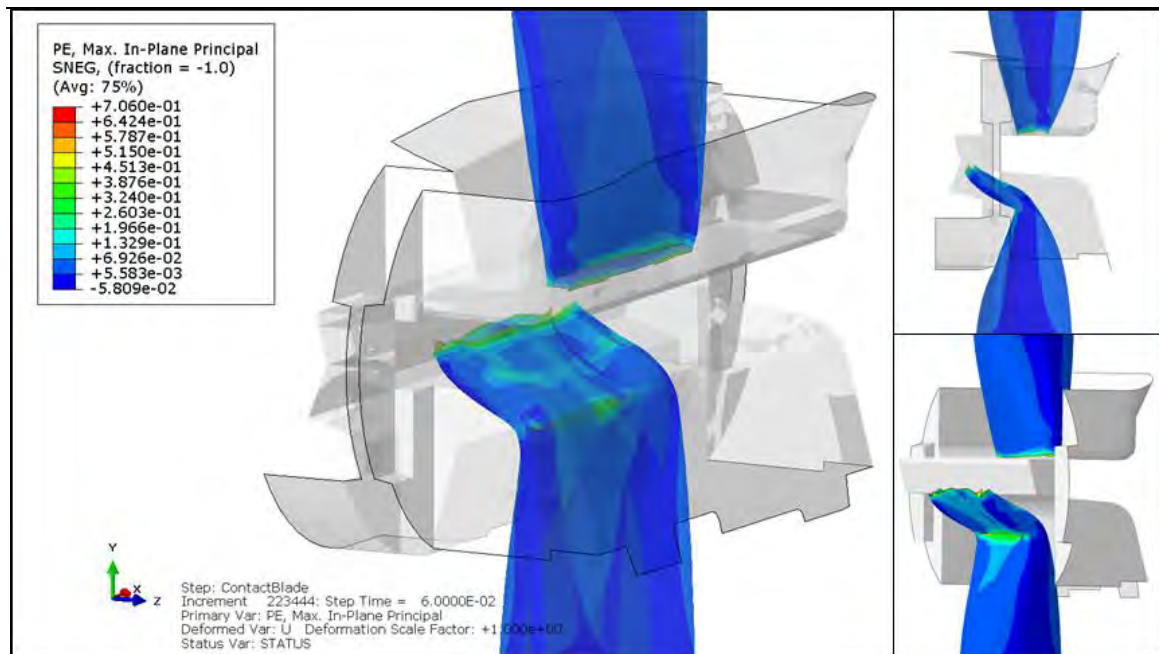


Figure 138 Final Deformed Configuration of Shear Cut Showing Strain Concentration at Inner Bend

The progression of the shear cut for the model with off-centered drill pipe is shown in Figure 139 and Figure 140. With the pipe displaced to the side of the wellbore, the corner of the upper blade made the initial contact with the drill pipe (Frame 2). In Frame 4, the corner of the upper blade has pierced the drill pipe and shearing has initiated. As part of the pipe is outside of the upper BSR blade surface, only 2/3 of the pipe is actually being sheared (Frame 7). Due to the earlier shear initiation at the blade point, and the fact that less of the pipe was sheared, the calculated shearing forces were less than those calculated for the centered pipe model. The remainder of the pipe was deformed outside of the upper blade surface (Frames 8, 10, and 11). This deformed portion was pinched and deformed between opposing side packers (Frames 10 and 11, and Figure 141).

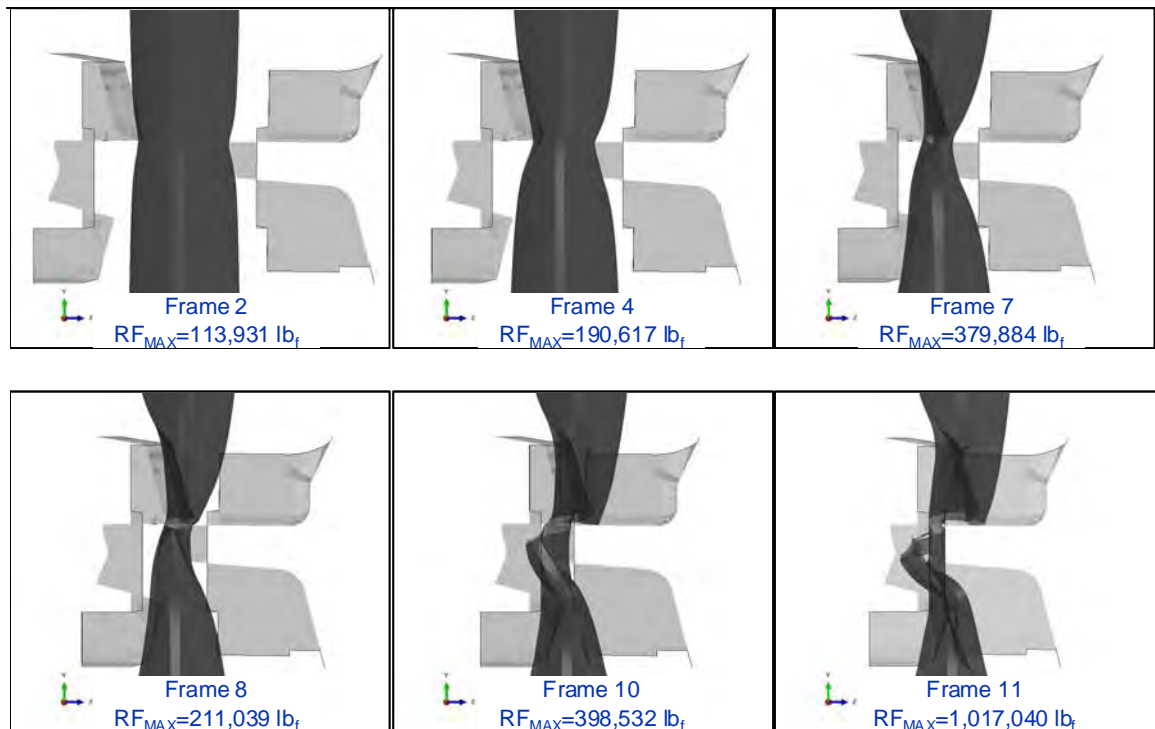


Figure 139 Progression of Off-Center BSR Shear Model - Side View

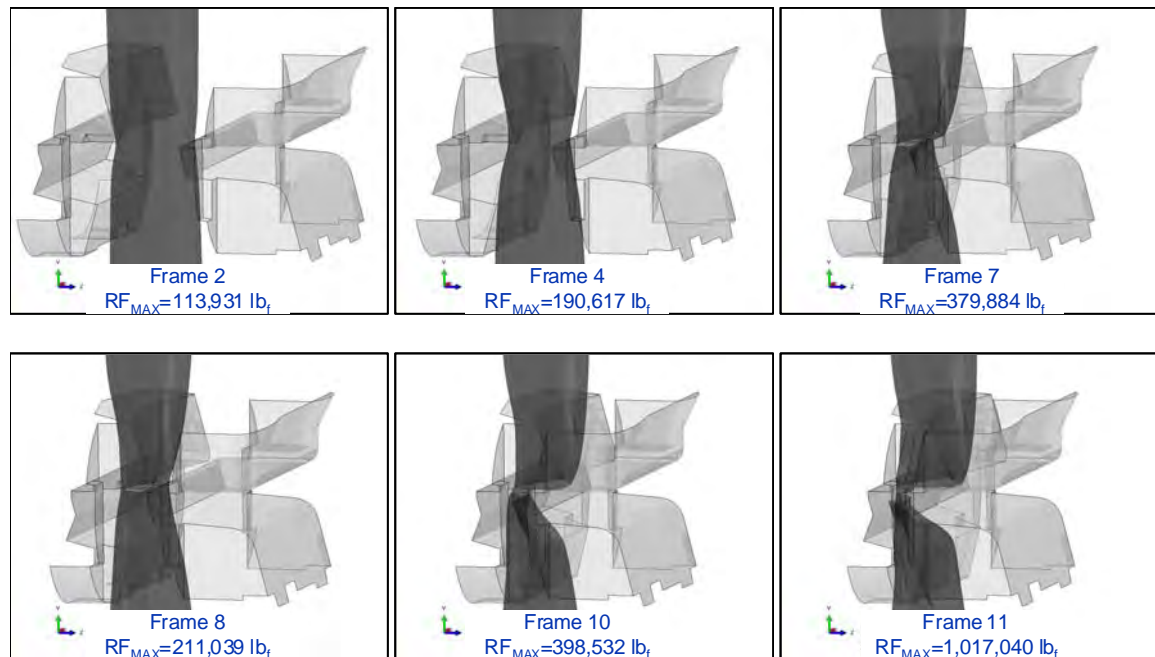


Figure 140 Progression of Off-Center BSR Shear Model - Isometric View

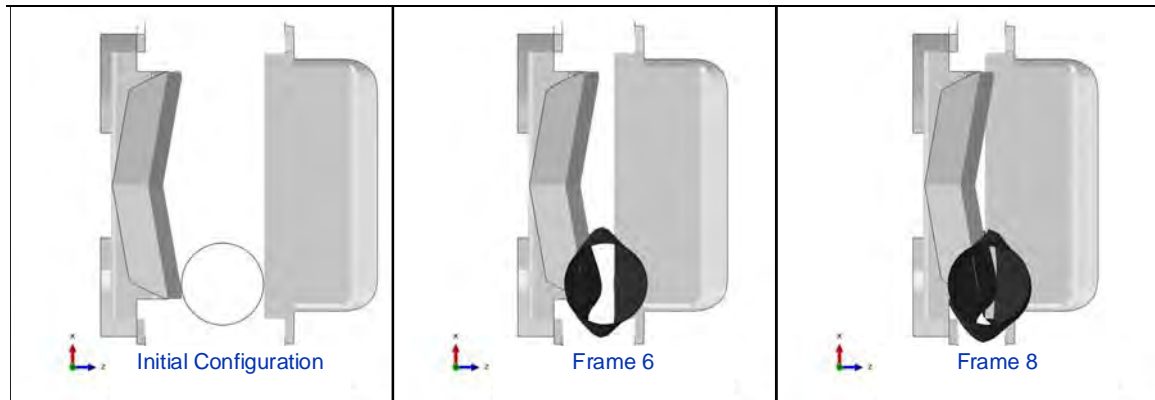


Figure 141 Top View Showing Deformation of Drill Pipe Outside of Shearing Blade Surfaces

The final deformed configuration of the drill pipe on the upper BSR block is shown in Figure 142 through Figure 144. The comparison between the aligned laser scanned sections with the final configuration predicted by the FEA model showed good agreement. The final deformed configuration of the drill pipe is given in Figure 145. Note that the ram block indentations on both the upper and lower segments of drill pipe were present and agreed with the recovered evidence. The fold over on the recovered lower pipe section was missing. This portion was removed from the center image in Figure 145 for visual comparison with 83-B and 94-B.

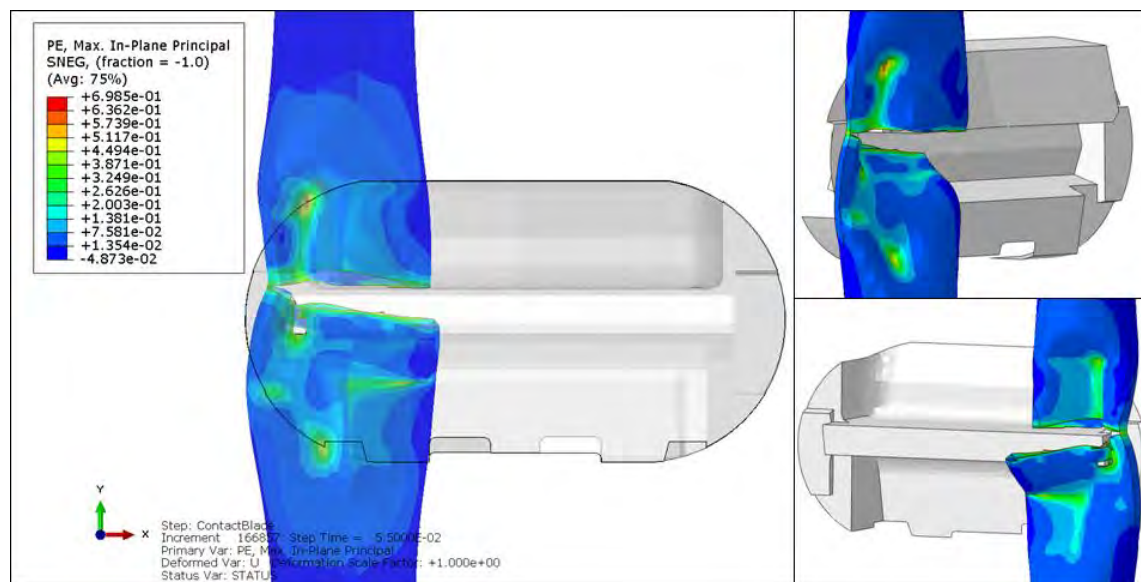


Figure 142 Final Deformed Configuration of Shear Cut Showing Strain Concentration at Inner Bend

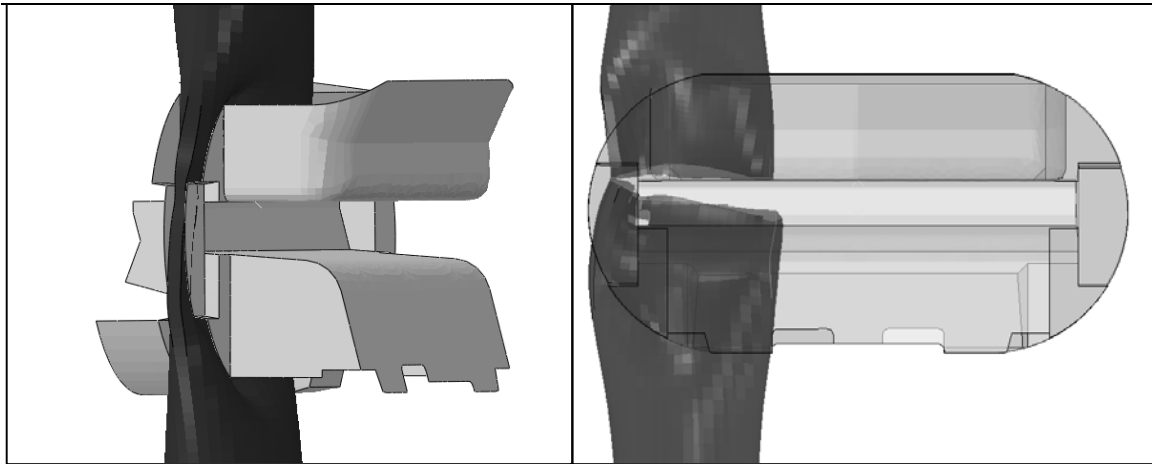


Figure 143 Final Deformation of the Drill Pipe as Predicted by the Off-Centered Pipe Model; Upper BSR Block Shown on the Right

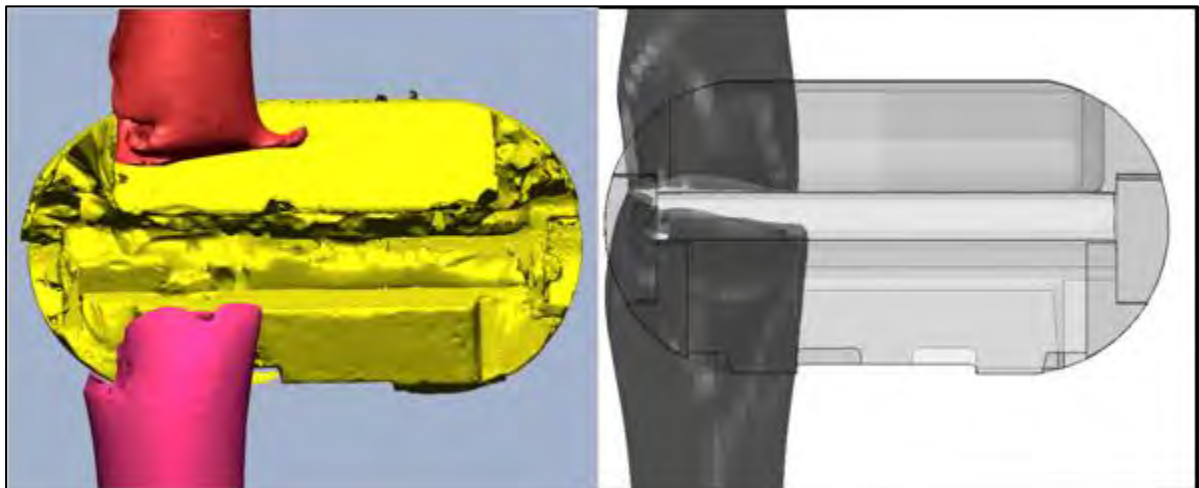


Figure 144 Comparison of Recovered Drill Pipe Segments and Final Model

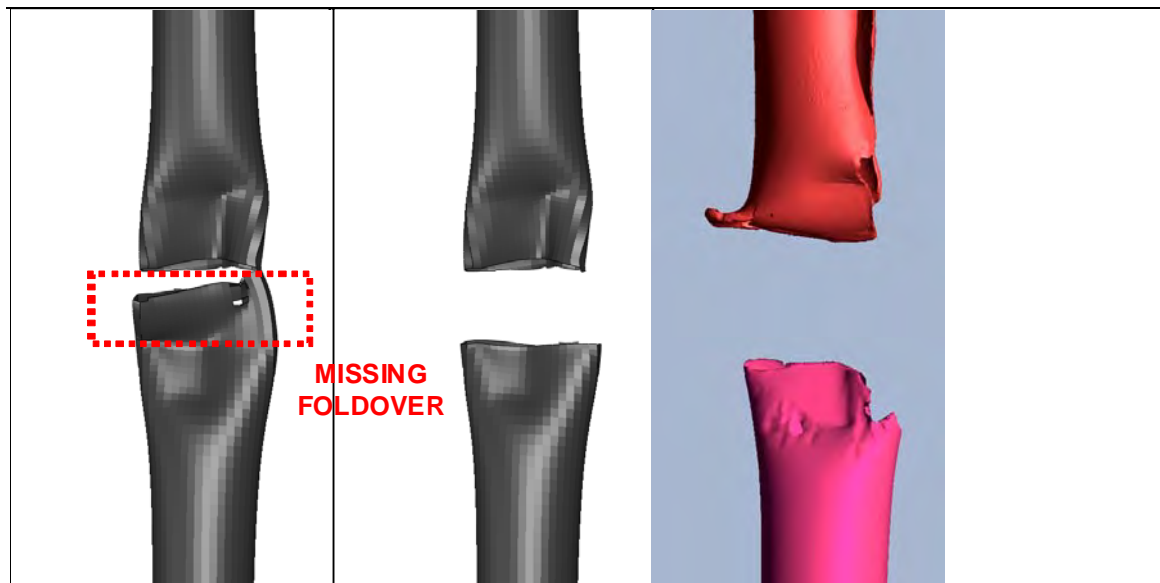


Figure 145 Final Model Deformation Compared with Recovered Drill Pipe Laser Scans - 83-B and 94-B

The shear model with off-centered drill pipe showed that the required shear force (RF_{MAX}) increased as the pipe was pressed between the flat outer faces of the ram blocks. A maximum shear force for the off-centered pipe analysis was calculated as 1,017,040 lb_f , which is equivalent to 4,273 psi for this BSR design. Based on this analysis, the BSR would likely stall at this point, if not prior to this, as the required pressure exceeded the available hydraulic system pressure (regulated to 4,000 psig).

With the drill pipe collapsed between the ram faces, the upper and lower BSR blocks were 2 inches from being fully closed (Figure 146). The side packers were 1 inch from making initial contact and sealing.

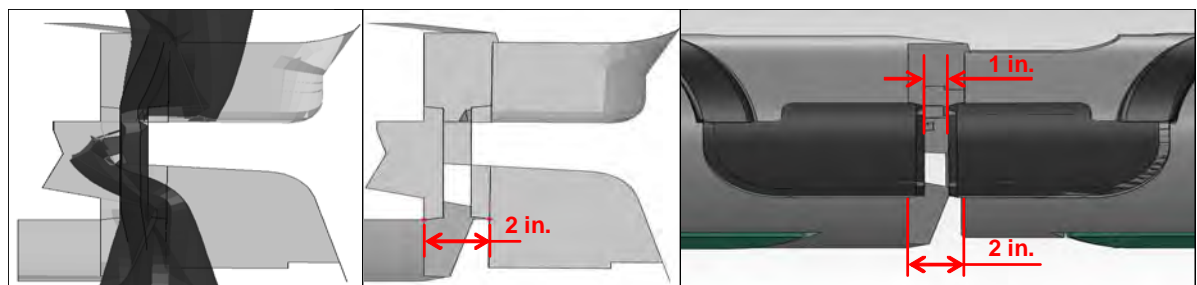


Figure 146 Spacing of Upper and Lower BSR Blocks in Partially Closed Position

Further investigation was performed using the laser scanned models. The models of the upper and lower BSR blocks, and drill pipe segment 94 were assembled with segment 94 contacting the upper block (deformation features aligned - Figure 147). With the blocks spaced 2 inches from fully closed, the lower block fit against segment 94. Figure 148 shows the BSR CAD models (side packers removed) in the same configuration and

demonstrates that the lower BSR blade was 1.4 inches from contacting the rear packers and sealing.

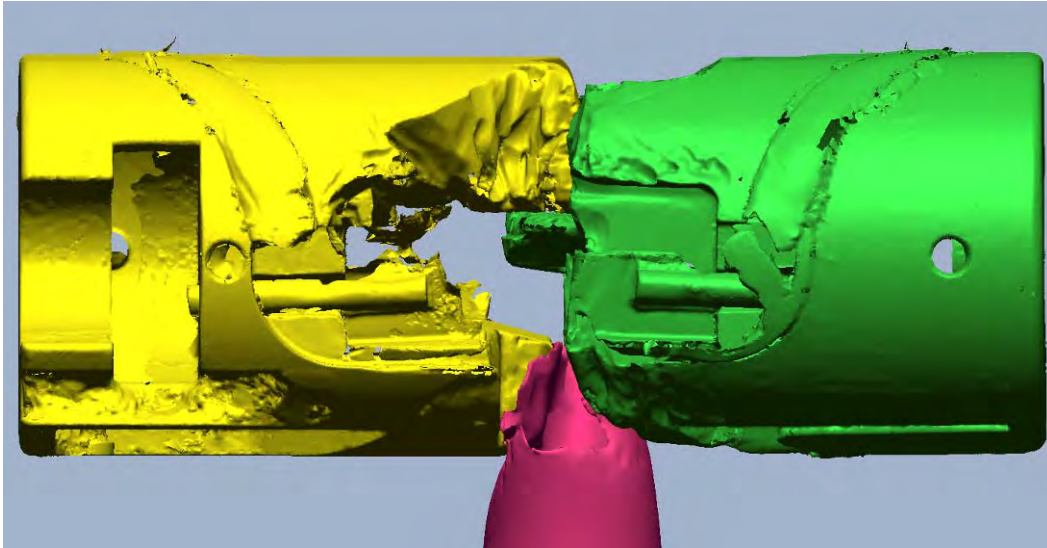


Figure 147 Alignment of Scan Models - 2 Inch Standoff Between Block

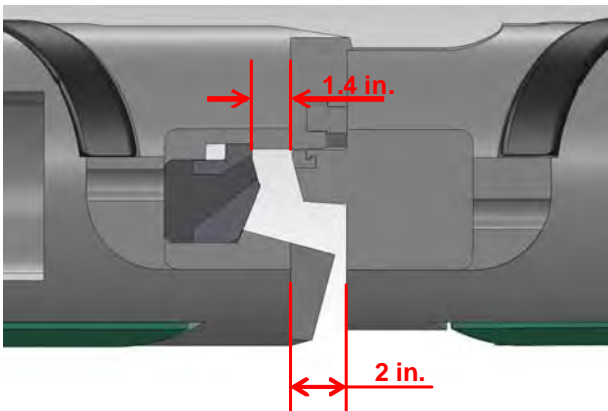
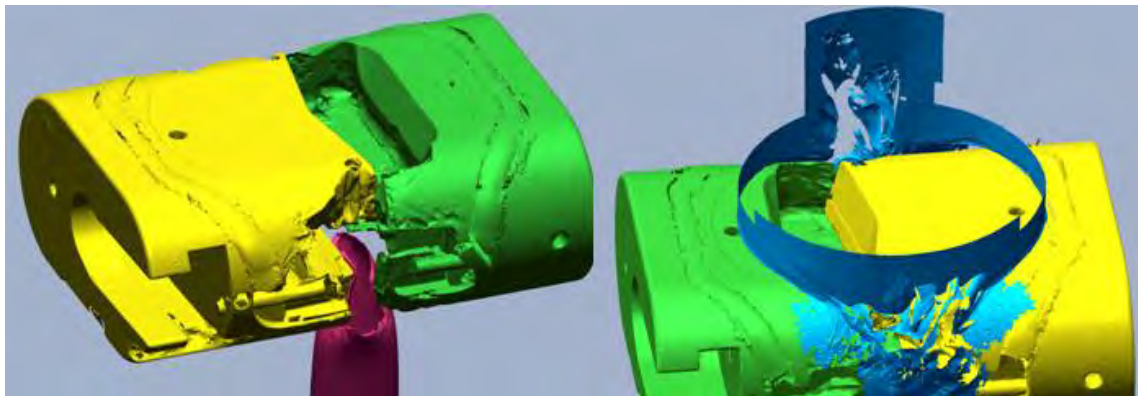


Figure 148 BSR CAD Models - 2 Inch Standoff Between Blocks

With the VBRs closed below the BSR, well flow was diverted through the inside of the drill pipe. After the BSR was activated and closed on the off-center drill pipe, the well flow was concentrated through the partially sheared drill pipe on the kill side of the BSR. The kill side of the blocks and wellbore experienced the most erosion damage. This concentrated flow condition remained until the CSRs were activated (April 29, 2010) shearing the drill pipe. This created a new flow condition that was no longer concentrated on the kill side of the BSR. Flow then exited the cut drill pipe below the CSR and impinged upon the bottom of the CSR blocks (evidenced by erosion pattern on recovered blocks). The CSR was intended only to cut tubulars. It was not designed to seal the

wellbore. Without a sealing mechanism in the CSRs, flow traveled around the CSR blocks and continued up the entire wellbore cross-section below the BSRs. Without contact between the lower blade and rear packer (forming a seal), flow occurred across the entire face of the blocks. This flow condition existed from April 29, 2010, until the well was brought under control.

Figure 149 shows the open cavity through the upper BSR block above the cut lower drill pipe segment. The image on the right shows the scan of the erosion in the wellbore along the kill side of the BSRs.



Note the image on the left is viewed from the kill side, while the image on the right is facing the kill side of the wellbore.

Figure 149 Erosion Damage - BSR Blocks and Wellbore

6.6 Failure Cause Analysis

Failure cause analysis was organized and conducted around a single top event and a secondary chain of events. For the purposes of this investigation the top event was defined as the failure of the BSRs to close and seal the well and the secondary chain was defined as the events responsible for the condition and location of the recovered drill pipe segments.

A fault tree was developed for the top event (Appendix G). Six different means were identified for initiating closure of the BSRs:

- Manual function via surface control through BSR Close
- Manual function via surface control through HP Shear Close
- Manual function via surface control of EDS
- Automated function via AMF/Deadman
- Manual initiation of Autoshear
- Manual function subsea via ROV

There were functions/components common to all six means:



- Port and starboard BSR hydraulic actuators (operators) on the BOP
- Port and starboard BSR Close shuttle valves
- Hydraulic lines

Testing of these components determined that they functioned as intended in the as-received condition. No further failure cause analysis was performed.

Manual function via surface control through BSR close is achieved through the activation of solenoid 66B/Y. However, the high-pressure BSR close function is achieved through solenoid 103 B/Y. High pressure close, EDS and AMF/Deadman all activate through the operation of solenoid 103B/Y. Specifics on solenoid 103 are discussed later in this section.

HP Shear Close, EDS, AMF/Deadman and Autoshear have a common reliance on the accumulator bottles (8 x 80 gallon) located on the BOP. Testing of these accumulators determined that they functioned as intended in the as-received condition. The analysis of the hydraulic fluid collected from the port side close operator of the BSR indicated the fluid was of a composition very similar in characteristics to the samples of Stack Guard and Aqualink provided by the manufacturer. This was the fluid that resided in the BOP accumulators at the time of the incident. This is further indication the BSR's were activated either by the Autoshear or possibly the AMF/Deadman functions. No further failure cause analysis was performed.

Each of these means are examined and discussed in further detail in the following sections.

6.6.1 Manual Function Blind Shear Ram Close and High Pressure Shear Close

Both of these manual functions required deliberate selection using a control interface on the Deepwater Horizon. Eyewitness accounts of the activities carried out during the loss of well control do not record any action carried out to close the BSRs independently using either the BSR Close function or the HP Shear Close function on the control interfaces from the rig. It was ruled as unlikely that either of these functions could have been accidentally pressed (instead of another intended function such as EDS) based on proximity to other functions on the control panel layouts. There was no evidence to support either of these means as possible. No further failure cause analysis was performed.

6.6.2 Manual Function of Emergency Disconnect Sequence

Eyewitness accounts record that the EDS function was initiated from the bridge of the Deepwater Horizon just before 21:56 on April 20, 2010. The initiation occurred approximately seven minutes after the first recorded explosion and power loss. There are



no corroborative eyewitness accounts regarding the status of the lights on the control panel. There is an account of lights flashing, indicating that the EDS function had initiated. There are no accounts of any specific lights going steady, which would have indicated a function had been completed and confirmed by the subsea control pods. The EDS function has two separate command sequences: (1) Blind Shear Ram Close, and (2) Casing Shear Ram Close. The latter sequence is used when casing is being run into the hole; otherwise the Blind Shear Ram Close is used as the default sequence. By design, the Blind Shear Ram Close sequence should have been completed within 25 seconds. Reviewed ROV video indicated no evidence that the sequence had initiated; the LMRP remained latched to the BOP, the Blue and Yellow Control Pod stingers were not retracted. Evidence supports that the EDS function was initiated but not successfully completed. Evidence indicates that the most probable reason for this failure was damage and loss of MUX communication to the BOP Stack due to and immediately after the first recorded explosion and loss of rig power. No further failure cause analysis was performed.

6.6.3 Automated Mode Function/Deadman

The AMF/Deadman sequence was designed to initiate from the control pods if electrical power, fiber-optic communication and hydraulic pressure to the control pods from the surface were lost. Regardless of which control pod was active or being used to control the BOP Stack, both the Yellow and Blue Control Pods continuously monitored the status of the power, communication and pressure. Both control pods communicated with each other regarding this status. One control pod had command (active) of the BOP Stack and monitored communication from the surface. The other control pod was on standby but it monitored communications from the active control pod. In the case of loss of all three inputs (power, communication and hydraulic pressure), both control pods required agreement on status in order to initiate the sequence. The AMF/Deadman sequence was required to be armed (command given after BOP Stack was installed) in order to function. At the time of the loss of well control, the Blue Control Pod was in command of the BOP stack.

Two scenarios were analyzed for the AMF/Deadman sequence: initiation after power, communication and hydraulic pressure loss caused by catastrophic failure at the surface, and initiation after ROV intervention.

As previously discussed in Section 6.6.2, evidence indicates that MUX cable transmission (power and communication) was lost due to and immediately after the first recorded explosion and loss of rig power. ROV intervention was completed at 02:45 on April 22, 2010 to remove hydraulic pressure by cutting the pilot lines from the rigid conduit manifold on the LMRP to both control pods and cutting the PBOF cables from the STM to the SEMs on both control pods. This intervention satisfied the three necessary conditions (power, communication and hydraulic pressure loss) for AMF/Deadman initiation.



Testing of the AMF/Deadman indicated the hydraulic circuit portion of the system functioned as intended. Testing of the original Solenoid 103Y yielded inconsistent results. Testing on the Blue Control Pod 27V battery bank indicated a low voltage that was incapable of actuating Solenoid 103B and therefore incapable of completing the AMF/Deadman sequence.

Evidence indicates that conditions necessary for AMF/Deadman (loss of power, communication and hydraulic pressure) existed immediately following the first explosion/loss of rig power and prior to ROV intervention. The function testing demonstrated that the AMF circuits within both the Blue and Yellow Control Pod SEMs activated when the loss conditions were simulated. Function testing on the Blue Control Pod proved that the 27V battery bank in the as-received condition could not carry the initiation from the AMF circuit in the SEM to completion. The function testing of the Yellow Control Pod circuits demonstrated that when both coils of original Solenoid 103Y were energized simultaneously, the solenoid functioned as intended. When only one coil was energized, the results were inconsistent.

While the conditions necessary for AMF/Deadman existed immediately following the first explosion/loss of rig power, because of the inconsistent behavior of original Solenoid 103Y and the state of the 27V battery bank on the Blue Control Pod, it is at best questionable whether the sequence was completed.

6.6.4 Autoshear

Autoshear is a hydro-mechanical system. Its functioning is not dependent on the state of the Control Pods. Testing of the Autoshear indicated the hydraulic circuit portion of the system functioned as intended. The Autoshear hydraulic plunger was successfully cut at approximately 07:30 hours on April 22, 2010. Movement of the plunger (visible on ROV footage) indicated that hydraulic pressure on the control valve was relieved allowing a spring return to shift the control valve, sending a pilot signal to open a high pressure shear control valve and send hydraulic supply from the high pressure shear circuit to the closing ports of the BSRs. Testing of the system resulted in functioning as intended. The evidence supports successful initiation of BSR close by Autoshear, if not previously by AMF/Deadman.

6.6.5 Manual Function via Remotely Operated Vehicle

Testing of the ROV Panel BSR port confirmed the panel functioned as intended. At the start of each test, connecting rod movement occurred at very low pressures for all three-flow rates. The pressure to the operators did not increase until the connecting rods had fully extended (fully closed).



The first attempt to close the BSRs using the ROV panel hot stab occurred prior to the successful cut of the Autoshear hydraulic plunger. The attempt was considered unsuccessful due to inability to generate pressure. There were continued attempts to close the BSRs following the initiation of Autoshear. The second attempt was similar to the first attempt; unsuccessful due to inability to generate pressure. In two subsequent attempts, pressure was generated to over 4,000 psig, but bled down due to leaks in the hydraulic circuit. In two final attempts, pressure was rapidly generated to over 5,000 psig and maintained.

The ability for the ROV to raise pressure to over 4,000 psig indicates that the reported leaks would have had little or no effect on closing the BSRs. The rapid generation of over 5,000 psig (on April 27, 2010 and again on April 29, 2010) when compared with the results from the function testing, indicated the BSRs were either fully closed or obstructed from closing further. No further failure cause analysis was performed.

6.6.6 Recovered Drill Pipe Segments

The recovery and examination of eight drill pipe segments from the BOP, LMRP and Riser was discussed in detail in Sections 6.1.4 and 6.2.3.

From the exercise to match segment ends it was determined that segments 1-B-1, 1-B-2, 84, and 83 (top to bottom) constituted a larger segment and segments 1-A-1 and 39 (top to bottom) constituted another larger segment. Both were located side by side above the UA when the riser kinking occurred. Segments 84 and 83 were nearly separated by the ROV saw cut intervention. Segments 1-A-1 and 39 were separated by the ROV shear cut intervention. Likewise, segments 1-B-2 and 84 were separated by the ROV shear cut. Segments 1-B-1 and 39 were determined to be from the same joint of pipe based on the presence of internal coating in both segments. Their separation was postulated to have been tensile failure based on the fracture surface of 1-B-1-E. Both the BSR shear (between segments 83 and 94) and the tensile failure above the tool joint (between segments 1-B-1 and 39) occurred before the riser kinking.

Two events were considered that were capable of producing sufficient force to part segments 1-B-1 and 39 in tension. The first event (chronologically) was the rig drift which occurred on the morning of April 21, 2010. The second event was the sinking of the Deepwater Horizon which occurred on the morning of April 22, 2010, and resulted in the kinking of the riser. In both events the drill pipe is postulated to have been captured or fixed at the drill floor. Tensile force was imparted to the drill pipe by the offset movement of the rig.

Segments 1-B-1, 1-B-2, 84, and 83 were measured, and their sum matched the distance between the BSRs and the UA. This evidence supports that the tool joint was at the level of the UA element prior to BSR closure.



In order to initiate tensile failure, the drill pipe was required to be captured or fixed at a point below the failure. For the second event (rig sinking), the BSR cut had already occurred. The fixed point was postulated to be the closed UA. For the first event (prior to Autoshear initiation), the BSR cut may not have occurred. Two fixed points were possible, the closed UA and one or both closed VBRs (Middle and Upper). Evidence indicates that the first event was the more likely source of tensile force required to part the drill pipe above the tool joint (between segments 1-B-1 and 39). No further failure cause analysis was performed.

Once the tensile failure between segments 1-B-1 and 39 had occurred, segments 1-B-1, 1-B-2, 84, and 83 would have moved upward as one segment after BSR closure, propelled by the force of the flowing well. It was postulated that the closed UA was unable to restrain this larger segment from moving upward and clearing the UA. The deformation on the bottom of segments 39 and 83 was postulated to have occurred when the riser kinked and forced both segments down onto the top of the closed UA.

6.6.7 Other Considerations

On trying to pressurize various hydraulic circuits during the ROV interventions, including those to the Blind Shear Rams, leaks were reported. Later interventions were reported to have fixed those leaks. However, DNV's review of the ROV videos raised questions on whether the leaks were on circuits that functioned the BSRs. In the tests of the hydraulic circuits performed at Michoud, other than the high-pressure casing shear regulator, the high-pressure shear circuits did not leak. Initial visual examination of the leak on the casing shear regulator led DNV to conclude that the conditions leading to the leak most likely developed after the time of the incident. Further, later ROV hot stab efforts were able to raise the pressure in one instance to 4,000 psig and then latterly to over 5,000 psig on the high pressure shear circuits. It is DNV's view that the evidence indicates the reported leaks in the hydraulic circuits were not a contributor to the blind shear rams being unable to close completely and seal the well.

In its review of various modifications made to the control logic or BOP stack, it is DNV's view that there is no evidence these modifications were a factor in the ability of the blind shear rams being able to close fully and seal the well.

The various tests of the performance of the solenoid 103Y at Michoud removed from the Yellow Pod in May 2010, gave inconsistent results when a single coil within the solenoid was activated by the PETU. When the Yellow Control Pod was removed from the BOP stack in May 2010 as part of the interventions a series of Factory Acceptance Tests (FATs) were run on the Pod. As part of those investigations the various solenoids mounted on the Pod were tested and it was determined that solenoid 103Y did not activate. The decision was taken on the Q-4000 to remove it and replace the solenoid 103Y with a new solenoid. The original solenoid 103Y was removed and taken into evidence by the FBI Evidence Response Team and a new solenoid was mounted to the



Yellow Pod. The original solenoid was then sent to the NASA-Michoud facility for secure storage. The bench tests and subsequent testing and activation of the solenoid at Michoud yielded inconsistent results, as noted earlier. When both coils were activated, as would be the case if the solenoid was activated by the AMF/Deadman circuits, the solenoid functioned as intended. However, in other tests when only one of the two coils of the solenoids was energized, the armature of the solenoid failed to activate. Two possible scenarios present themselves for explaining the inconsistent performance of solenoid 103Y. The first being the fact that the solenoid was removed in May 2010 and was not tested until March 2011. As a result it is possible deposits of seawater or hydraulic fluid built-up in the solenoid and were the cause of the inconsistent results. The second scenario is the possibility of a manufacturing defect. On the evidence to date, DNV is of the opinion that the explanation for the inconsistent results was due to the build-up of deposits or other factors resulting from storage of the solenoid.

DNV did not identify any other issues or evidence that manufacturing defects of one form or another contributed to the blind shear rams not closing completely and sealing the well.

Tests at Michoud of the AMF/Deadman circuits demonstrated that the 27 Volt battery in the Blue Pod had insufficient charge to activate solenoid 103B. Tests of the 27 Volt battery in July when the Blue Pod was raised and examined on the Q-4000 reported the battery level to be out of specification. There are indications that voltage, too, would have been insufficient to activate solenoid 103B. A Factory Acceptance Test and AMF/Deadman test was performed on the Blue Pod in June 2009. There are no records that the AMF/Deadman batteries were checked as part of this test. The review of available records could not confirm the date when the Yellow Pod AMF/Deadman last underwent a Factory Acceptance Test. To discern the state of the AMF/Deadman it is necessary to undertake further examination, investigation and tests of the Subsea Electronic Modules of both the Yellow and Blue Control Pods.



7 CONCLUSIONS

7.1 The Accident

The Deepwater Horizon was a semi-submersible, dynamically positioned mobile offshore drilling unit (MODU) that could operate in waters up to 8,000 feet deep and drill down to a maximum depth of 30,000 feet. The rig was built in South Korea by Hyundai Heavy Industries. The blowout preventer (BOP) stack, built by Cameron, was in use on the Deepwater Horizon since the commissioning of the rig in 2001.

The rig was owned by Transocean, operated under the Republic of the Marshall Islands flag, and was under lease to BP from March 2008 to September 2013. At the time of the incident, the rig was drilling an exploratory well at a water depth of approximately 5,000 feet in the Macondo Prospect. The well is located in the Mississippi Canyon Block 252 in the Gulf of Mexico.

On the evening of April 20, 2010 control of the well was lost, allowing hydrocarbons to enter the drilling riser and reach the Deepwater Horizon, resulting in explosions and subsequent fires. The fires continued to burn for approximately 36 hours. The rig sank on April 22, 2010. From shortly before the explosions until May 20, 2010, when all ROV intervention ceased, several efforts were made to seal the well. The well was permanently plugged with cement and “killed” on September 19, 2010.

7.2 What is Considered to have Happened

Prior to the loss of well control on the evening of April 20, 2010, the UA was closed as part of a series of two negative or leak-off tests. Approximately 30 minutes after the conclusion of the second leak-off (negative pressure) test, fluids from the well began spilling onto the rig floor. At 21:47 the standpipe manifold pressure rapidly increased from 1200 psig to 5730 psig. The first explosion was noted as having occurred at 21:49. At 21:56 the EDS was noted to have been activated from the bridge. This was the final recorded well control attempt from the surface before the rig was abandoned at 22:28.

The Upper VBRs were found in the closed position as-received at the Michoud facility. There was no documented means of ROV intervention to close the Upper VBRs. ROV gamma ray scans on May 10, 2010 confirmed that the ST Lock on the port side Upper VBR was closed. Scans of the starboard side ST Lock on the Upper VBRs were inconclusive. Measurements of the ST Lock positions performed at the Michoud facility confirmed that both ST Locks on the Upper VBRs were closed. Evidence supports that the Upper VBRs were closed prior to the EDS activation at 21:56 on April 20, 2010.

A drill pipe tool joint was located between the UA and the Upper VBRs. With both the UA and the Upper VBRs closed on the drill pipe, forces from the flow of the well pushed



the tool joint into the UA element. This created a fixed point arresting further upward movement of the drill pipe. The drill pipe was then fixed, but able to pivot at the UA, and horizontally constrained but able to move vertically at the Upper VBRs. Forces from the flow of the well induced a buckling condition on the portion of drill pipe between the UA and Upper VBRs. The drill pipe deflected until it contacted the wellbore just above the BSRs. This condition most likely would have occurred from the moment the well began flowing and would have remained until either the end conditions changed (change in UA or Upper VBR state) or the deflected drill pipe was physically altered (sheared). The portion of the drill pipe located in the between the shearing blade surfaces of the BSRs was off center and held in this position by buckling forces.

As the BSRs were closed, the drill pipe was positioned such that the outside corner of the upper BSR blade contacted the drill pipe slightly off center of the drill pipe cross section. A portion of the drill pipe was outside of the BSR shearing blade surfaces. As the BSRs closed, this portion of the drill pipe cross became trapped between the ram block faces, preventing the blocks from fully closing and sealing. The drill pipe most likely deflected to the side of the well from the moment the well began flowing. Trapping of the drill pipe between the ram faces would have taken place regardless of which means initiated BSR closure (AMF/Deadman or Autoshear).

Of the means available to close the BSRs, evidence indicates that trapping of the drill pipe occurred when the hydraulic plunger to the Autoshear valve was successfully cut on the morning of April 22, 2010 initiating activation of the Autoshear circuit. Albeit on the evidence available, closing of the BSRs through activation of the AMF/Deadman circuits cannot be ruled out.

In the partially closed position, flow would have continued through the drill pipe trapped between the ram block faces and subsequently through the gap between the ram blocks. When the drill pipe was sheared on April 29, 2010, using the CSRs, the well flow pattern changed to a new exit point through the open drill pipe at the CSRs expanded to flow up the entire wellbore to the BSRs and through the gap along the entire length of the block faces.

7.3 Discussion of Causes

7.3.1 Primary Cause

The BSRs failed to fully close and seal due to a portion of drill pipe trapped between the blocks.

On closure of the BSRs, a portions of the drill pipe cross section was outside of the BSR shearing surfaces. The portion of the drill pipe cross section outside the shear blade surfaces became trapped between the ram block faces, preventing the blocks from fully closing and sealing.



7.3.2 Contributing Cause

The BSRs were not able to move the entire pipe cross section completely into the shearing surfaces of the rams.

The drill pipe within the BOP stack was under a compressive load that elastically buckled the pipe between the Upper VBRs and the UA. This elastic buckling condition forced the drill pipe toward the sidewall of the wellbore and outside of the cutting blade surfaces of the BSRs. When the ram blocks closed they were not able to overcome the buckling forces holding the drill pipe against the sidewall of the wellbore. The blocks could not reposition the entire circumference of the drill pipe to within the shearing surfaces of the BSRs.

7.3.3 Contributing Cause

Drill pipe in process of shearing was deformed outside the shearing blade surfaces.

The portion of the drill pipe between the outside edge of the upper blade and wellbore sidewall was not sheared. As the ram blocks closed, a portion of the drill pipe was deformed (flattened) and trapped between the faces of the ram blocks preventing them from closing and sealing.

7.3.4 Contributing Cause

The drill pipe elastically buckled within the wellbore due to formation forces on loss of well control.

On loss of well control the drill pipe downhole of the UA was subjected to vertical forces from the flow of well fluids. These forces would have caused the drill pipe to move vertically upwards unless it was constrained.

7.3.5 Contributing Cause

The position of the tool joint at or below the closed UA prevented upward movement of the drill pipe.

The location of the tool joint pushing up against, or partially pushed into the UA element prevented the drill pipe from moving upwards in the BOP stack. This created a fixed point impeding further upward movement of the drill pipe.

7.3.6 Contributing Cause

The Upper VBRs were closed and sealed on the drill pipe



After the upper VBRs were closed, the drill pipe was centered at two locations within the BOP stack (at the UA and upper VBRs). In addition, with the upper VBRs closed, the drill pipe was then fixed at the UA (both horizontally and vertically) while being horizontally constrained at the upper VBRs but able to move vertically. The physical conditions and constraints were then in place to provide for the elastic buckling. Further the BSRs were vertically located at a position nearly midway between the UA and VBRs, coinciding with the center of the bow in the drill pipe.

7.3.7 Contributing Cause

Uncontrolled flow from downhole of the Upper VBRs

Forces from the flow of the well downhole of the VBRs induced a buckling condition on the portion of drill pipe between the fixed point (vertical) of the UA and Upper VBRs (horizontal constraint). The drill pipe bowed until it contacted the sidewall of the wellbore just above the BSRs.

8 RECOMMENDATIONS

8.1 Recommendations for Industry

The primary cause of failure was identified as the BSRs failing to close completely and seal the well due to a portion of drill pipe becoming trapped between the ram blocks. The position of the drill pipe between the Upper Annular and the upper VBRs led to buckling and bowing of the drill pipe within the wellbore. Once buckling occurred the BSRs would not have been able to completely close and seal the well. The buckling most likely occurred on loss of well control.

The recommendations are based on conclusions from the primary and contributing causes or on observations that arose during the course of DNV's investigations.

8.1.1 Study of Elastic Buckling

The elastic buckling of the drill pipe was a direct factor that prevented the BSRs from closing and sealing the well.

It is recommended the Industry examine and study the potential conditions that could arise in the event of the loss of well control and the effects those conditions would have on the state of any tubulars that might be present in the wellbore. These studies should examine the following:

- The effects of the flow of the well fluids on BOP components and various tubulars that might be present,
- The effects that could arise from the tubulars being fixed or constrained within the components of a Blowout Preventer,
- The ability of the Blowout Preventer components to complete their intended design or function under these conditions.

The findings of these studies should be considered and addressed in the design of future Blowout Preventers and the need for modifying current Blowout Preventers.

8.1.2 Study of the Shear Blade Surfaces of Shear Rams

The inability of the BSRs to shear the off-center drill pipe contributed to the BSRs being unable to close and seal the well.

It is recommended the industry examine and study the ability of the shear rams to complete their intended function of completely cutting tubulars regardless of their position within the wellbore, and sealing the well. The findings of these studies should be



considered and addressed in the design of future Blowout Preventers and the need for modifying current Blowout Preventers to address these findings.

8.1.3 Study of Well Control Procedures or Practices

The timing and sequence of closing of the UA and upper VBRs contributed to the drill pipe segment buckling and bowing between the two moving the drill pipe off center.

It is recommended the industry examine and study the potential effects or results that undertaking certain well control activities (e.g. closing of the annulars, or closing of the VBRs) could have on the BOP Stack. Examination and study should identify conditions, which could adversely affect the ability to regain control of the well (e.g. elastic buckling of tubulars). Industry practices, procedures and training should be reviewed and revised, as necessary, to address the prevention of these conditions.

8.1.4 Status of the Back-Up Control Systems

The BOP functionality testing indicated some back-up control system components did not perform as intended.

It is recommended the industry review and revise as necessary the practices, procedures and/or requirements for periodic testing and verification of the back-up control systems of a Blowout Preventer to assure they will function throughout the entire period of time the unit is required on a well.

8.1.5 Common Mode Failure of Back-Up Control Systems

The BOP functionality testing indicated not all back-up control systems had built in redundancy.

It is recommended the industry review and revise as necessary the practices, procedures and/or requirements for evaluating the vulnerability of the back-up control systems of a Blowout Preventer to assure they are not subject to an event or sequence of events that lead to common mode failure.

8.1.6 Study the Indication of Functions in an Emergency

The ROV intervention efforts reviewed indicated the ROVs were not capable of directly and rapidly determining the status of various ROV components.

It is recommended the industry examine and revise the current requirements for providing a means to verify the operation, state or position of various components of Blowout Preventers in the event of an emergency. The industry should require that it is possible to confirm positively the state or position of certain components such as the rams, annulars



and choke and kill valves either with the use of Remotely Operated Vehicles or by other means.

8.1.7 Study of the Effectiveness of Remotely Operated Vehicle Interventions

The ROV intervention efforts reviewed indicated initial ROV efforts were not capable of performing key intervention functions at a level equivalent to the primary control systems.

It is recommended the industry examine and study the conditions and equipment necessary for Remotely Operated Vehicles to perform various functions (e.g. the BSRs) at a performance level equivalent to the primary control systems. Make adequate provision to mobilize such equipment in the event of a well control emergency.

8.1.8 Stipulating Requirements for Back-Up Control System Performance

A review of industry standards indicated they do not stipulate performance requirements for back-up systems (e.g. closing response times) as they do for primary control systems.

It is recommended the industry review and revise the requirements for back-up control system performance to be equivalent to the requirements stipulated for primary control systems.

8.2 Recommendations for Further Testing

DNV's forensic examinations and testing were organized and conducted around the top event of the failure of the Blind Shear Rams to close and seal the well.

The recovery and examination of the eight segments of drill pipe and the five sets of rams shifted the focus from the question of whether the blind shear rams were activated to that of identifying the factors that would have caused or contributed to the blind shear rams failing to seal the well. As described in this report, DNV is of the view that the primary cause for the blind shear rams failing to close arose from conditions that led to the drill pipe being forced to one side of the wellbore at a position immediately above the Blind Shear Rams. DNV has investigated the conditions that could lead to such a buckling scenario developing. However, even here DNV recognizes there are additional studies and tests that could be undertaken to examine this scenario further.

In addition, DNV has identified a number of areas or issues associated with the overall performance of the BOP Stack that should be examined, investigated or tested further. As a result, DNV puts forward the following recommendations.



8.2.1 Additional Studies of Conditions Leading to Elastic Buckling

- Supplement the Finite Element Analysis buckling model with a Computational Fluid Dynamic simulation of the flow through the drill pipe.
- Run the Finite Element Analysis drill pipe-cutting model to include the buckling stresses that would have existed in the drill pipe.
- Field test the blind shear rams shearing a section of off-centered (buckled) 5-1/2 inch drill pipe.
- Field test the ability of a closed annular to restrain the upward movement of a 5-1/2 inch drill pipe tool joint at the forces calculated for buckling.
- Field test the conditions required to push a 5-1/2 inch tool-joint through a closed annular element.

8.2.2 Additional Tests or Studies of the Performance of the Blowout Preventer Stack

- It is suggested that the static pressure tests undertaken at Michoud on the high-pressure shear hydraulic circuits of the lower section of the BOP be supplemented with additional tests of the circuits of the Casing Shear Rams and the Variable Bore Rams.
- The tests at Michoud performed on the high-pressure blind shear close solenoid removed from the Yellow Pod in May 2010 gave inconsistent results. It is suggested this solenoid be further tested and possibly disassembled to discern the reason for its performance and whether it was likely to have functioned at the time of the incident.
- On pressuring the high-pressure shear ram circuit, the high-pressure casing shear regulator leaked. It is suggested the high-pressure casing shear regulator be further tested and disassembled to try and discern its state at the time of the incident.
- It is suggested that the behavior of the elastomeric elements of the rams and annulars be tested to assess their performance when exposed to well fluids at the temperatures that existed at the time of the blowout.
- The tests of the Subsea Electronic Modules (SEMs) undertaken at Michoud should be supplemented by removing the SEMs from the Control Pods, venting and then opening the SEMs to understand better their possible state at the time of the incident. The following tests or activities are suggested:
 - Collect and analyze samples of the SEMs gas/atmosphere prior to or as part of venting the SEMs.
 - Remove the batteries and record part numbers, serial numbers, date of manufacture and any other pertinent manufacturing data,
 - In place of the batteries connect a voltage generator and conduct a series of tests on the AMF/Deadman circuits at various voltages and record the results.



- The lower and upper annulars are well control components of the BOP stack. As a result the following tests or examinations of the lower and upper annulars are suggested:
 - Laser scanning of the upper annular in-situ and “as-is” condition,
 - Remove and examine the upper and lower annular elements,
 - Static pressure tests of the annular operating systems,
 - Function testing of the open and close operating systems of both the upper and lower annulars.
- The evidence from eyewitnesses was that the Emergency Disconnect Sequence was activated approximately seven minutes after the first explosion. It is suggested the hydraulic circuits and functioning of the LMRP HC collet connector and the choke and kill collet connectors be tested as a means to try and assess their state at the time of the incident.
- It is suggested the wellbore pressure-temperature sensor at the base of the lower section of the BOP be removed and its accuracy checked or tested.
- It is suggested the industry perform field tests on the ability of the BSRs to shear and seal a section of 5-1/2 inch drill pipe under internal flow conditions that existed at the time of the incident.

Det Norske Veritas

Det Norske Veritas (DNV) is a leading, independent provider of services for managing risk with a global presence and a network of 300 offices in 100 different countries. DNV's objective is to safeguard life, property and the environment.

DNV assists its customers in managing risk by providing three categories of service: classification, certification, and consultancy. Since establishment as an independent foundation in 1864, DNV has become an internationally recognized provider of technical and managerial consultancy services and one of the world's leading classification societies. This means continuously developing new approaches to health, safety, quality and environmental management, so businesses can run smoothly in a world full of surprises.

Global Impact for a Safe and Sustainable
Future